AD-A046 704 MCDONNELL AIRCRAFT CO ST LOUIS MO F/G 17/2

REMOTE VIEWING SYSTEM.(U)

JUN 77 R W FISHER N00014-75-C-0660

UNCLASSIFIED ONR-CR213-129-2F NL

1 OF 3
ADA
046704

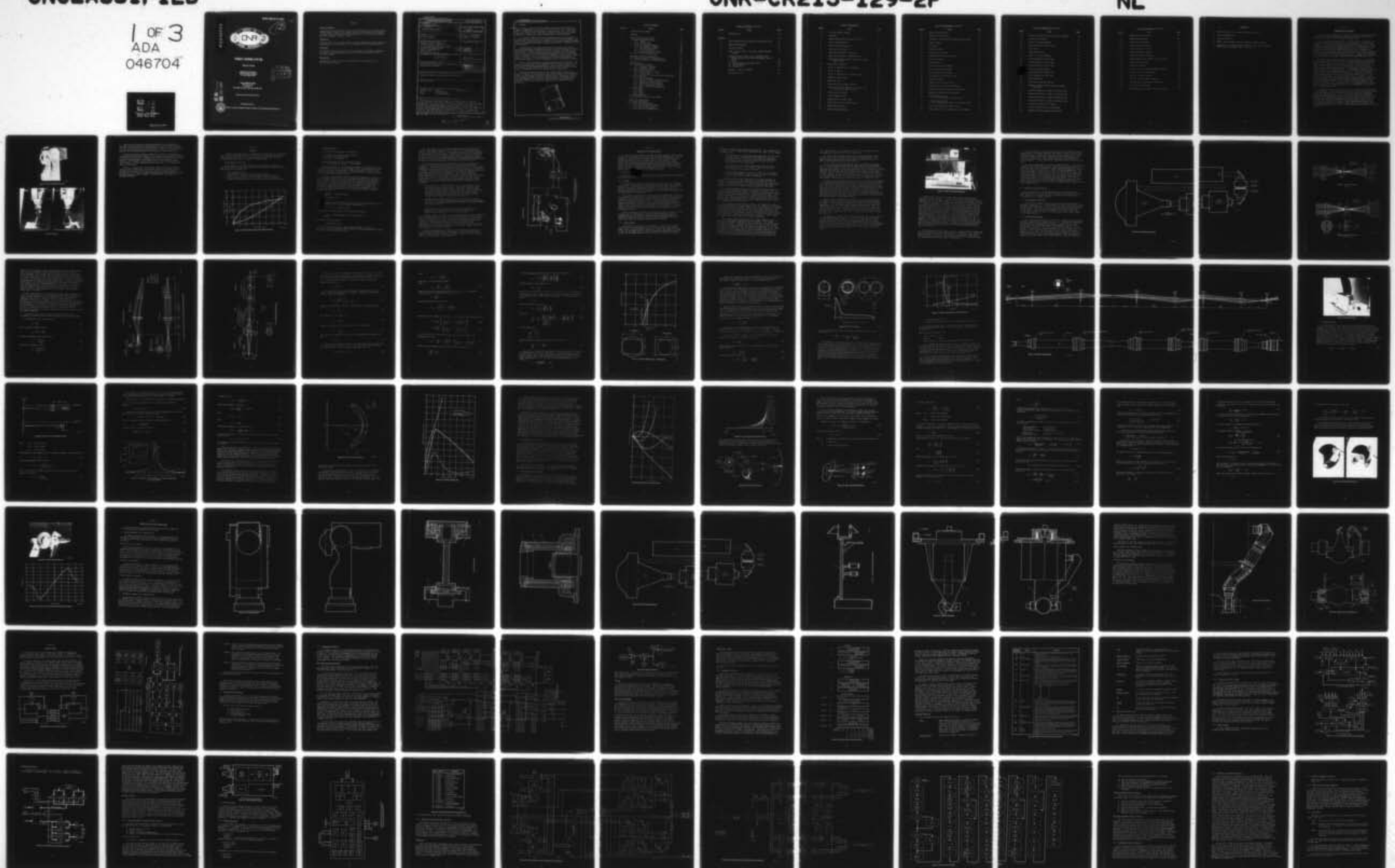

REPORT ONR-CR-213-129-2F

OFFICE OF NAVAL RESEARCH

REMOTE VIEWING SYSTEM

RALPH W. FISHER

McDonnell Aircraft Company
McDonnell Douglas Corporation
St. Louis, Missouri 63166

Contract N00014-75-C-0660
ONR Task 213-129
June 1977
Final Report for Period 1 July 1975 - 30 May 1977

PREPARED FOR THE

OFFICE OF NAVAL RESEARCH ● 800 N. QUINCY ST. ● ARLINGTON ● VA ● 22217

NOTICES

Change of Address

Organizations receiving reports on the initial distribution list should confirm correct address. This list is located at the end of the report. Any change of address or distribution should be conveyed to the Office of Naval Research, Code 221, Arlington, Virginia 22217.

Disposition

When this report is no longer needed, it may be transmitted to other authorized organizations. Do not return it to the originator or the monitoring office.

Disclaimer

The findings in this report are not to be construed as an official Department of Defense or Military Department position unless so designated by other official documents.

Reproduction

Reproduction in whole or in part is permitted for any purpose of the United States Government.

UNCLASSIFIED

SECURITY CLASSIFICATION OF THIS PAGE (When Data Entered)

(19) REPORT DOCUMENTATION PAGE

READ INSTRUCTIONS BEFORE COMPLETING FORM

1. REPORT NUMBER: (18) ONR-CR-213-129-2F
2. GOVT ACCESSION NO.:
3. RECIPIENT'S CATALOG NUMBER:

4. TITLE (and Subtitle): (6) REMOTE VIEWING SYSTEM .

5. TYPE OF REPORT & PERIOD COVERED: (9) Final Report, 1 Jul 75 - 30 May 77,

6. PERFORMING ORG. REPORT NUMBER:

7. AUTHOR(s): (10) Ralph W. Fisher

8. CONTRACT OR GRANT NUMBER(s): (15) N00014-75-C-0660

9. PERFORMING ORGANIZATION NAME AND ADDRESS:
McDonnell Aircraft Company
McDonnell Douglas Corporation
P.O. Box 516, St. Louis, Mo. 63166

10. PROGRAM ELEMENT, PROJECT, TASK AREA & WORK UNIT NUMBERS:

11. CONTROLLING OFFICE NAME AND ADDRESS:
Office of Naval Research
800 N. Quincy St.
Arlington, VA 22217

12. REPORT DATE: (11) June 1977

13. NUMBER OF PAGES: 196

14. MONITORING AGENCY NAME & ADDRESS (if different from Controlling Office): (12) 207p.

15. SECURITY CLASS. (of this report): UNCLASSIFIED

15a. DECLASSIFICATION DOWNGRADING SCHEDULE:

16. DISTRIBUTION STATEMENT (of this Report):
Reproduction in whole or part is permitted for any purpose of the United States Government.

DISTRIBUTION STATEMENT A
Approved for public release;
Distribution Unlimited

17. DISTRIBUTION STATEMENT (of the abstract entered in Block 20, if different from Report):
"Approved for public release distribution unlimited"

18. SUPPLEMENTARY NOTES

19. KEY WORDS (Continue on reverse side if necessary and identify by block number)

Variable Acuity, Optics, Vision, Displays, Remote Sensing, Television Systems, Optical Detection

20. ABSTRACT (Continue on reverse side if necessary and identify by block number)

A fully operable laboratory model of the Remote Viewing System was designed and built. The system consists of a TV camera and TV projector both equipped with a non-linear lens, i.e. a lens that matches the human eye acuity function with excellent resolution capability near the optical axis, but greatly reduced resolution capability in the peripheral areas. The camera and projector are slaved together by a digital servo system. An operator can steer the camera and thus the projector by use of a helmet mounted tracker. → next page

DD FORM 1 JAN 73 1473 EDITION OF 1 NOV 65 IS OBSOLETE

UNCLASSIFIED

SECURITY CLASSIFICATION OF THIS PAGE (When Data Entered)

403 111

LB

20. ABSTRACT.

As the operator rotates his head to observe off axis display detail, the camera is commanded to rotate and the projector follows. Thus, high acuity detail is retained on the foveal axis of the observer's eyes. This system allows wide field-of-view (160°) remote viewing of scenes, with resolution comparable to human vision, using conventional TV system bandwidths.

The gimballed camera and projector mechanical and optical designs are presented along with the method of relaying the optics thru the gimbals. The digital servo system is described along with the associated computer programs. The head tracking system includes sections on the tracker, illuminator, optics and electronics.

Considering that the system is the first of this type, the results were very encouraging. Equipment developed to perform conventional functions worked perfectly including the servo control, TV camera, TV projector, and Head Tracker. The most challenging problem encountered in the development were associated with the state-of-the-art advancement required in non-linear optics. Problems were also encountered in maintaining optical quality in the camera and display. The maximum resolution attained is approximately 1.5 milliradians compared to the 0.5 milliradians that is theoretically possible.

Even with this limitation, system performance was very impressive. The value of the wide field in maintaining observer orientation within the full 160° field-of-regard was readily apparent. Target tracking capability by head control was very good and peripheral cueing by motion and glints proved to be of significant value in the acquisition and tracking task.

Detailed performance analyses of the current design indicate better acuity is possible by fabricating new rear spline elements for the non-linear lenses and redesigning the projector optical relay. Through these efforts, 1 milliradian performance should be readily obtained. Performance better than this appears to be limited by a diffraction problem inherent in the projector Schlierin optics and would require use of a different type of projector.

TABLE OF CONTENTS

Section	Title	Page
1	INTRODUCTION AND SUMMARY	1
2	APPROACH	4
3	ELECTRO-OPTICAL SYSTEM DESIGN	8
	3.1 Camera Subsystem Design	8
	3.1.1 Camera	8
	3.1.2 Optical Relay	8
	3.2 Projector Sub-System Design	12
	3.2.1 The Projector Selection	12
	3.2.2 Optical Relay Design	12
	3.2.3 Focus Correction	26
	3.2.4 Projection Surface Design	32
	3.3 Head Tracking System Design	32
4	MECHANICAL DESIGN AND FABRICATION	42
	4.1 Camera Assembly (P/N 71A050002-1001)	42
	4.2 Projector Assembly (P/N 71A050003-1001)	42
5	CONTROL SYSTEM	52
	5.1 Microprocessor Hardware	54
	5.1.1 Diagnostic Hardware	55
	5.1.2 Diagnostic Software	58
	5.2 Camera Electronics Box	62
	5.2.1 System Clocks and Timing	63
	5.2.2 Control Logic	63
	5.2.3 Camera Box Electro Mechanical Description	66
	5.3 System Software	67
	5.3.1 PROM Programming	67
	5.3.2 PROM #1, Interrupt Handler Software	69
	5.3.3 Transmitter Service Routine	73
	5.3.4 PROM #2 Yaw Control Equations	74
	5.3.5 PROM #3 Diagnostic Software	75
	5.3.6 PROM #4 Pitch Control Equations	75
	5.4 Math Models	75
	5.4.1 Mode 1	76
	5.4.2 Mode 2	79
	5.4.3 Mode 3	84
	5.5 System Operation	84
	5.6 Head Tracker Interface Electronics	91
6	RESULTS AND CONCLUSIONS	94
	6.1 Camera Performance	98
	6.2 Total System Performance	98
	6.2.1 Low Contrast Performance	103
	6.2.2 Demonstration Results	107
	6.3 Conclusions and Recommendations	107

TABLE OF CONTENTS (Continued)

Section	Title	Page
7	REFERENCE LIST	109
Appendix		110
A	BRIEF DESCRIPTION OF THE REMOTE VIEWING SYSTEM (RVS)	110
B	CAMERA CONSIDERATIONS	113
C	PROJECTOR STUDIES	116
D	PROM 1, PROM 2, PROM 3, AND PROM 4 COMPUTER PROGRAM LISTINGS	129
E	APPLICATION OF THE NIGHT VISION LABORATORY (NVL) THERMAL VIEWING SYSTEM STATIC PERFORMANCE MODEL TO THE RVS	176
	E.1 MTF's	176
	E.2 Noise Equivalent Modulation (NEM)	181
	E.3 MRM Calculations	183
	E.4 Conclusions	184
	APPENDIX - LIST OF REFERENCES	186
	DISTRIBUTION LIST	187

LIST OF ILLUSTRATIONS

Figure	Title	Page
1	Two Axis Gimbaled Cameras	2
2	Projector	2
3	Remote Viewing System Optical Requirements	4
4	Control System Elements	7
5	Camera and Relay Brassboard	11
6	Camera Optical Elements	13
7	Light Valve Operation - No Output	14
8	Light Valve Operation - Maximum Oputput	14
9	Light Valve Nonlinear Lens Interface for Single Element Relay	16
10	Basic Relay Parameters	17
11	Effect of Magnification on Brightness	21
12	MTF of an Annulus	23
13	Effect of Magnification on System Acuity	24
14	Projector Optical Relay	25
15	Relay Test Setup	26
16	Projection Lens Comjugate Geometry	27
17	Image Plane Position Relative to Infinity Focus for 54 In. Conjugate Distance	28
18	Focus Corrector Geometry	30
19	Corrector Agnular Blur	31
20	Display Error vs Actual Angle	33
21	Nodal Point Shift of Nonlinear Lens	34
22	Head Position Sensing	34
23	Head Tracking Radiometrics	35

LIST OF ILLUSTRATIONS (Continued)

Figure	Title	Page
24	Helmet Mounted Detector	40
25	Projector Mounted Source	41
26	Response of Infrared Head Tracking Detector System	41
27	Camera Assembly	43
28	Pitch Axis	44
29	Yaw Axis Assembly	45
30	Camera Optical Elements	46
31	Camera Optical Mounting Surfaces	47
32	Projector Assembly	48
33	Relay Assembly	50
34	Projector Pitch Axis Assembly	51
35	Servo Control Block Diagram	52
36	Block Diagram Control System	53
37	Wiring Diagram SBC-80 Front Panel	56
38	Interrupt Channel	57
39	Computer Input and Output Ports	59
40	Display Processor Keyboard Explanation	61
41	Universal Asynchronous Receiver/Transmitter	64
42	Camera Electronics Box Block Diagram	65
43	Camera Electronics Box (a) Top View Camera Electronics Box)	67
43	Camera Electronics Box (b) SBC-80/Remote Camera Data Transfer Board	68
44	Camera Electronics Box Component List	69
45	Camera Electronic Box Transmitter Circuit Diagram	70

LIST OF ILLUSTRATIONS (Continued)

Figure	Title	Page
46	Camera Electronics Box Receiver Circuit Diagram	71
47	Software Flow Diagram	72
48	Mode 1 Servo Block Diagram	76
49	System Response for Stick Input	77
50	Servo Gains	78
51	Camera Azimuth Axis	79
52	Mode 2 Servo Block Diagram	80
53	System Response for Stick Input	81
54	System Response for Stick Input	82
55	System Response for Stick Input	83
56	Pitch Servo Block Diagram	85
57	System Response for Ramp Input	86
58	System Response for Step Input	87
59	System Math Model	88
60	Head Control Detector Amplifier	93
61	Geometry to Convert Shaft Encoders Readings to True Angles	95
62	Threshold Resolution vs Angle from Optical Axis	99
63	Threshold Resolution vs Angle from Optical Axis	100
64	Threshold Resolution vs Angle from Optical Axis	101
65	Threshold Resolution vs Angle from Optical Axis	102
66	Horizontal Display Error vs Angle	104
67	Vertical Display Error vs Actual Angle	105
68	Minimum Resolvable Modulation Predictions	106

LIST OF ILLUSTRATIONS (Continued)

Figure	Title	Page
A-1	Human Eye Characteristics	111
A-2	Bandwidth Requirements	111
A-3	Electro-Optical Schematic	112
A-4	Camera/Projector Interface	112
C-1	General Projection Geometry	117
C-2	Display Brightness Geometry	118
C-3	Normalized Display Brightness	121
C-4	Optimum Geometry for Specular Screen Coatings	122
C-5	Optimum Screen Coating	124
C-6	Light Valve Geometry	128
D-1	Prom No. 1 Service Interrupt Handler Software	130
D-2	Prom No. 2 Yaw Control Software	138
D-3	Prom No. 3 Monitor Program	151
D-4	Prom No. 4 Pitch Control Software	160
E-1	Scan Distortion Introduced by Foveal Lens	177
E-2	Optical Relay Parameters	179
E-3	NVL Model Adapted to VARVS for Visual Spectrum	185

APPENDICES

A Brief Description of the Remote Viewing System (RVS)

B Camera Considerations

C Projector Studies

D PROM 1, PROM 2, PROM 3 and PROM 4 Computer Program Listings

E Application of the Night Vision Laboratory (NVL) Thermal Viewing System Static Performance Model to the RVS

Section 1

INTRODUCTION AND SUMMARY

This final report documents the results of Contract No. N00014-75-C-0660. The objective of this contract was to design and build a fully operable laboratory brassboard of the MCAIR Remote Viewing System.

Under a previous ONR Contract (Ref. 1), MCAIR proved the feasibility of a unique non-linear lens which made this effort possible. This lens takes advantage of the "variable acuity" characteristics of human vision to reduce the amount of information (or bandwidth) that must be transmitted in a wide field-of-view high resolution imaging system. A brief description of the remote viewing system concept which utilizes this lens is presented in Appendix A. The brassboard system constructed under this contract represents a significant advancement in the state-of-the-art of remote viewing because for the first time a variable acuity picture that is designed to be compatible with human vision was recorded, transmitted, and displayed in real time.

The ONR Brassboard Remote viewing system consists of a two axis gimballed TV camera as shown in Figure 1 and a two axis gimballed TV projector as shown in Figure 2(a) and (b). A serial transmission link and low loss TV cable allow the camera to be located up to 400 ft. from the projector. The operator of the system can steer the camera under servo control using a helmet mounted tracker shown in Figure 2, approximately 90 degrees right and left and can look up and down $\pm 45°$. A microprocessor implements two axis servo control of the camera and projector servos. The system can track angular rates up to 1 rad/sec. It is capable of looking at the sun with no catastrophic failure. The projector subsystem consists of a 9 ft. dia sphere, a TV projector, and mounting support frame. It requires a floor area of 15 ft. by 15 ft. The lower portion of the sphere is cut away, thus an 8 foot ceiling is adequate. Interconnecting cables between the microprocessor and the operator allow the operator to position himself at the center of the sphere. He is required to be at the spherical center directly below the projector to realize the best optical performance of the system and for optimum head control.

Considering that the system is the first of this type, the results were very encouraging. As should be expected the only serious problems encountered in the development were associated with the state-of-the-art advancement required in non-linear optics. All conventional functions or equipment worked perfectly including the servo control, TV camera, TV projector, Head Tracker, etc. Problems were encountered in maintaining optical quality in the non-linear image when transmitted through the optical relays, both in the camera and display. While most of these problems were overcome, the resulting resolution was still about 3 times lower than anticipated, about 1.5 milliradians compared to the 0.5 milliradians that should be theoretically possible.

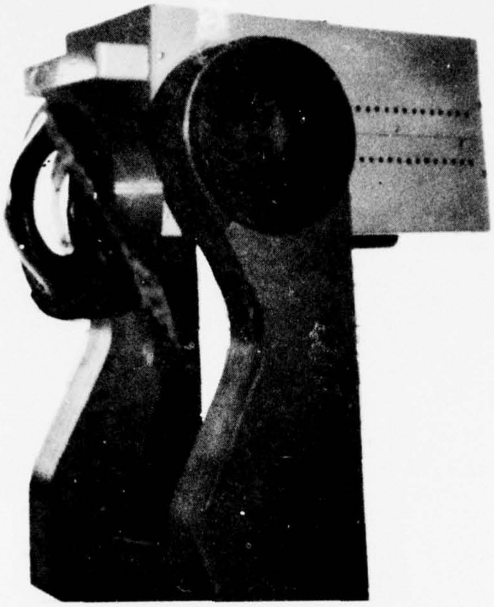

GP77-0549-71

Figure 1 Two Axis Gimbaled Camera

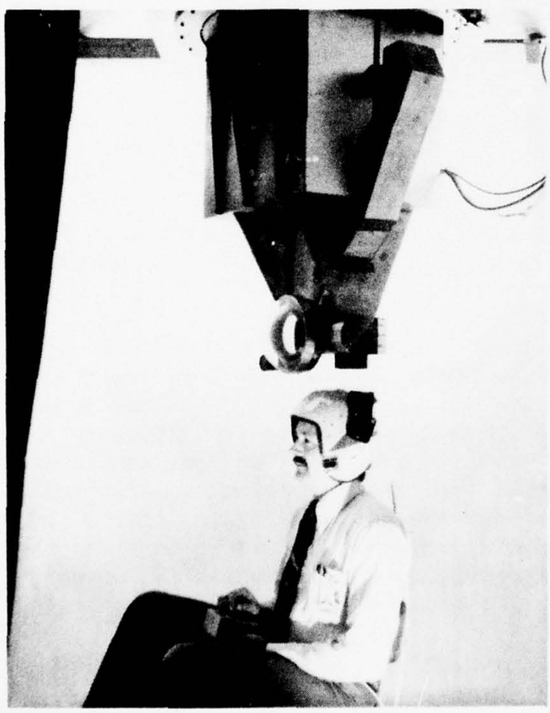

(a) Left Side Showing Detector Mounted on Helmet

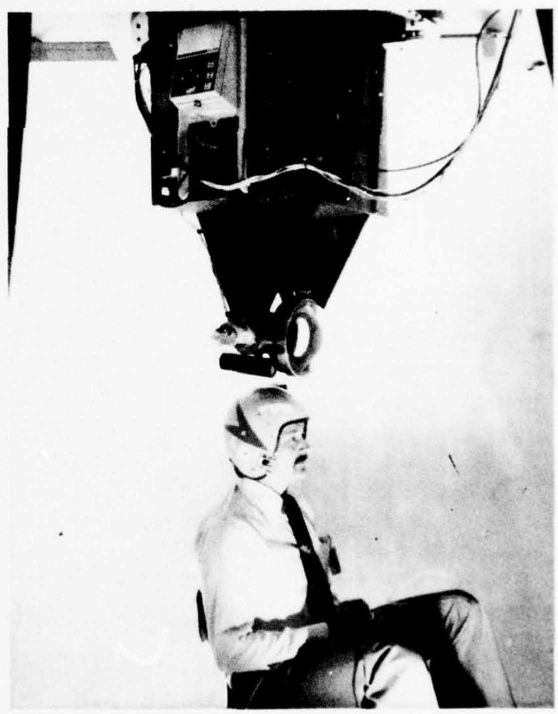

(b) Right Side Showing Source on Projector Assembly

GP77-0549-70

Figure 2 Projector

Even with this limitation, system performance was very impressive. The value of the wide field in maintaining observer orientation within the full 180° field-of-regard was readily apparent. Target tracking capability with head control was very good and peripherial cueing by motion and glints proved to be of significant value in the acquisition and tracking task.

Detailed performance analyses indicate better acuity is possible by fabricating new rear spline elements for the non-linear lenses and redesigning the projector optical relay. Through these efforts, 1 milliradian performance should be easily obtained. Performance better than this appears to be limited by a diffraction problem inherent in the light valve's Schlierin optical output. Further improvement would require use of a different type light valve projector.

Finally it appears that the laboratory demonstration which involved viewing a scene in which most of the spatial detail is stationary does not show the true potential of the system for the highly dynamic airborne application. It is therefore highly recommended that the brassboard hardware be flight tested in order to obtain a true performance assessment in a dynamic environment.

Section 2

APPROACH

The basic design philosophy is discussed and the rationale for the approach used is presented in this section. In subsequent sections detailed design of the equipment is developed. As a starting point for these discussions the original design goals from our proposal are listed below.

Electro-Optical Subsystem

The design goal of the video subsystems is to generate a projected display that fully supports human vision in both field-of-view and resolution. More specifically the goals are:

- 160° hemispherical FOV
- Image transfer characteristics as shown in Figure 3
- Resolution as a function of viewing angle as shown in Figure 3
- Display brightness greater than 1 ft-lambert over the entire FOV
- Standard TV bandwidth video transmission between camera and projector

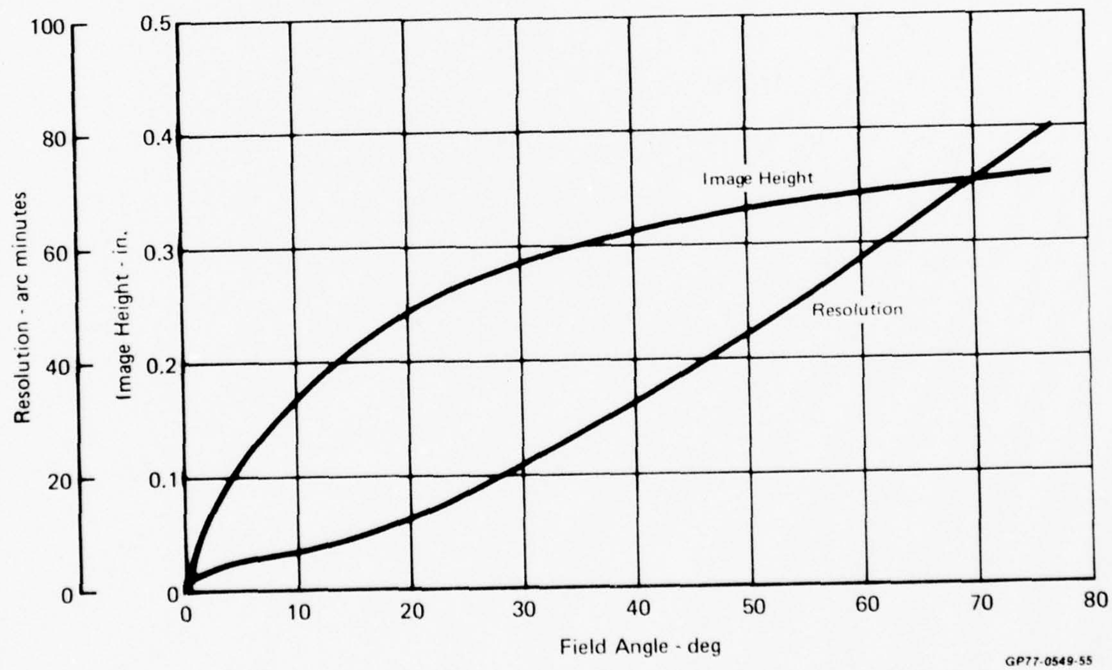

Figure 3 Remote Viewing System Optical Requirements

Control Subsystem

Camera platform with motion capabilities of:

- o Coverage - 360° azimuth, $\pm$60° elevation
- o Acceleration - 3000°/second^2
- o Slew rate - 300°/second

Projector platform with the same specifications
Servo static position accuracy - 30 arc minutes

The starting point for the design was presented in the proposal for this study (References 2 and 3). As this design evolved, considerable change was dictated by practical considerations. Salient differences occurred in the gimballing philosophy and electronic servo control system. The basic design and these changes are summarized below.

The camera electro-optical design followed the proposal very closely. A silicon vidicon camera was used for solar damage protection (See Appendix B). This necessitated use of an optical relay with a mechanical iris for light level control. A significant change from the proposal was the decision to utilize a 1023 line raster TV system which was selected to obtain greater resolution. The basic non-linear lens has an on-axis focal length of 2 inches and an image plane height of 0.72 inches (for maximum FOV of 160°). In a 525 line raster system (488 effective lines), the angular separation between scan lines is:

$$\frac{.72}{488 \times 2} = 0.738 \text{ milliradians}$$

2.5 minutes of arc

ngular resolution results when this separation is multiplied by the Kell r which is 1.4. Thus the angular resolution is:

$$2.5 \times 1.4 = 3.5 \text{ minutes of arc}$$

By utilizing a 1023 line system, the scan line separation is:

$$\frac{.72}{937 \times 2} = .384 \text{ milliradians} = 1.32 \text{ minutes of arc.}$$

The angular resolution then is:

1.85 minutes of arc

This value is much closer to the desired performance. It will be shown later, however, that only a small fraction of this improvement was actually achieved for various technical reasons.

The camera gimbal approach changed somewhat from that outlined in the proposal. The azimuth gimbal axis was not at the lens nodal point but was offset as illustrated in Figure 4. The primary reason for this was simplicity of fabrication and the wide azimuth coverage available with this arrangement. The use of gimbal position encoders shown on Figure 4 reflects our decision to employ digital electronics wherever possible. This approach eliminated the need for rate and acceleration sensors on the camera platform because these functions can be derived digitally from the position encoder outputs.

The projector design deviated substantially from that outlined in the proposal, the difference being primarily in the mechanical gimballing arrangement. After consultation with General Electric Co. (G.E.) on mechanical constraints of the light valve projector, we decided to gimbal the projector in azimuth. This simplified the optical relay because it required articulation in one dimension only, the pitch direction. This could be handled by a simple half-angle mirror and eliminated the need for image derotation. Besides making the relay much simpler and easy to align, this approach assured a much higher level of light output, a critical concern with this system (See Appendix C). The resulting projector gimballing arrangement is shown in Figure 4. Other minor problems that impacted on the projector system design were:

- Focus correction is required because of the close proximity of the projection screen to the projector. This arises because the lens has a flat focal plane when focused at infinity. When the plane is shifted to obtain correct on-axis focus, the variable focal length makes this location incorrect for all other field angle points. An additional lens element was required to correct this problem. Design of this element is discussed in Section 3.2.3.

- Incompatibility between the projector Schlerin optics and the non-linear lens. This rather complex problem is described in Section 3.2 and caused inefficient optical relay performance for projection angles near the optical axis.

  This problem required refabrication of the rear element of the projection lens and relay design revision to obtain greater magnification between projector and non-linear lens.

A digital control system was selected primarily because of its flexibility. Since a control system for a variable acuity optical link of this type had never been constructed, we felt a great number of changes in control system dynamics and modes would be required before successful operation would be achieved. A digital system with microprocessor control met these requirements. In addition, this approach will make future additions of more sophisticated control modes possible e.g., eye control. Figure 4 shows the basic elements of this control system.

Head position sensing was as outlined in the proposal except that the souce and detector locations were interchanged. The IR source had to be mounted on the projector instead of the helmet so that it would be additive with the infrared output from the projector.

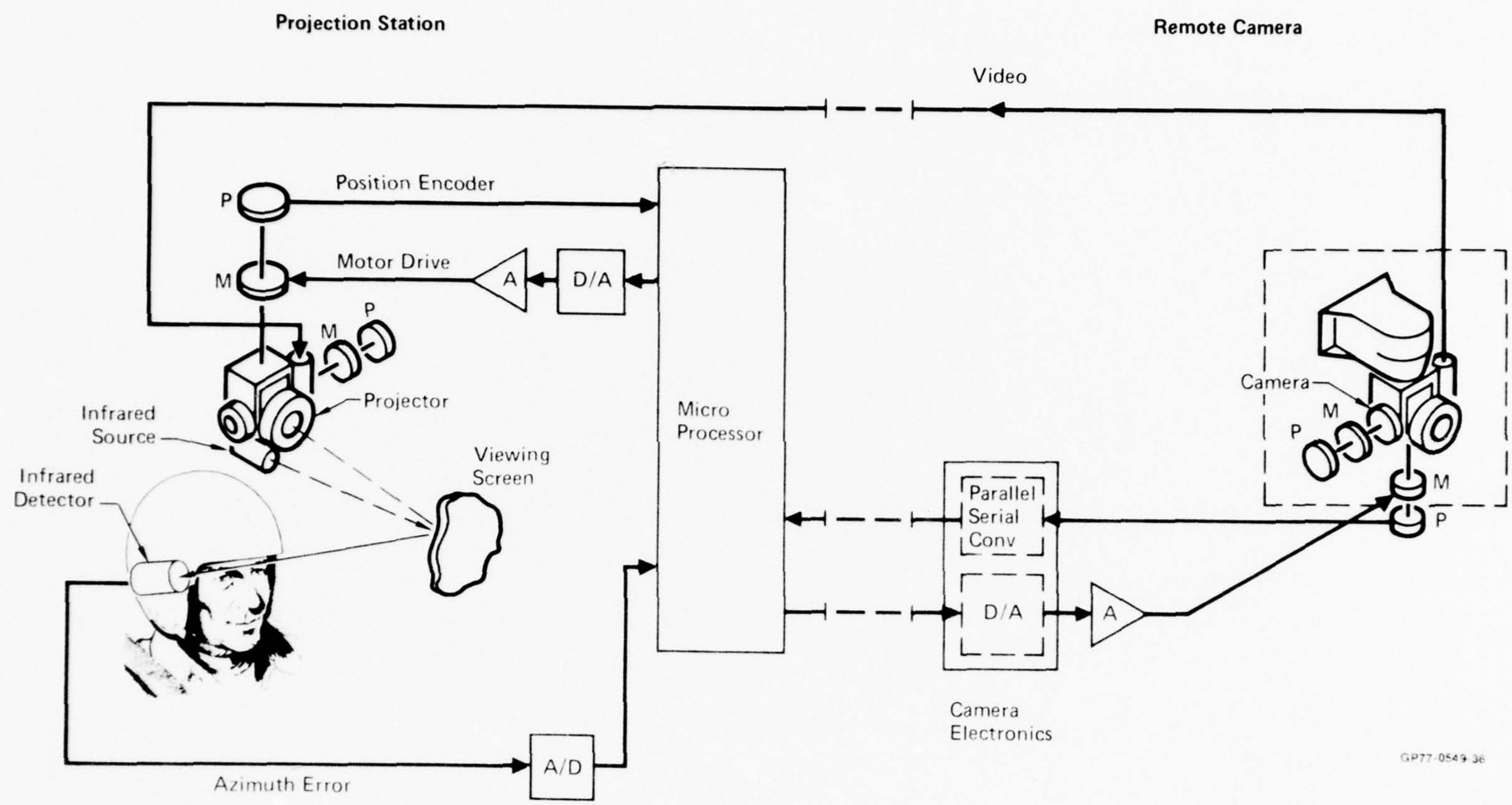

Figure 4 Control System Elements
Azimuth Axis Shown Only

Section 3

ELECTRO-OPTICAL SYSTEM DESIGN

The electro-optical design is divided into three separate efforts, those relating to the camera, the projector, and the head tracking system. For the camera, this effort includes TV camera selection and optical relay design to mate the camera with the non-linear lens. For the projector, this effort covers TV projector selection, relay design, and focus corrector design. The head tracking system design uses an infrared source boresighted with the projector and a detector assembly mounted on the helmet and is a part of the control system which is described in Section 5. Each of these items is discus[illegible] detail in the following sections.

3.1 CAMERA SUB[illegible]

The camera su[illegible] design consisted of the camera subsystem integration and optical relay design.

3.1.1 Camera

The camera electro-optical configuration followed that of the proposal very closely. The original TV camera purchased as the sensor was a GE model 4TE33A1. This camera was selected because it utilized a silicon vidicon which is necessary for solar burn protection. It was compact and self contained and was believed to be compatible with the GE light valve projector which was selected for the display.

During early evaluation of the camera/projector combination, a vertical jitter was noted on the display. This problem was traced to the random scan interlace of the GE camera. The projector however, requires a precise 2/1 interlace to maintain a stable picture. This problem was corrected by using an external sync generator. Later in the systems integration effort, numerous intermittent electrical connections were encountered in the TV camera. This, plus poor optical performance of the automatic iris assembly caused us to conclude that the GE camera would not be suitable for the demonstration system.

Therefore, another camera was selected and we elected to choose one with a higher line rate capability to obtain greater resolution. After a thorough search of available TV cameras, a General Electrodynamics Co. Model 6073B camera was selected. This system had the desired 1023 line rate and a stable 2/1 interlace required by the projector.

3.1.2 Optical Relay

The function of the optical relay system is to relay a good quality image from the non-linear lens to the TV camera vidicon with no loss of field-of-view or any noticeable vignetting. It must also magnify the image to the size compatible with the vidicon requirements and provide exposure control for the camera system. Exposure control is obtained by using an electronic controlled iris on one of the relay lens. For convenience and to reduce cost, this element was purchased with the camera. Relay design requirements are:

- Its input must be the non-linear lens image which is 0.72 inches in diameter and is located about 0.070 inches from the last (aft) lens element. An F/5.6 ray bundle must be accommodated and imaging is nearly telecentric where all chief rays are nearly parallel to the optical axis.

- Its output must be to vidicon faceplate which has an active scanning area of 0.5 X 0.375 inches. Later this was found to be a circular area 0.7 inches in diameter.

- One relay element must be a 50 mm F/1.4 lens with an installed automatic iris assembly. This iris must be properly integrated to form an aperture stop without vignetting.

Using these optical relay requirements, the design progressed as follows. The relay optics were designed to use lenses that could be purchased off-the-shelf rather than custom designed and fabricated special lenses. The lenses were chosen with sufficient aperture and format to transmit the F/5.6 cone of light forming the non-linear lens image.

Use of the available automatic iris/lens assembly dictated that the relay use lenses operating at infinity conjugates. A pair of lenses are therefore required to relay an image. The first lens collimates the image and the second forms an image from the collimated bundle of light. The lens speed required is the same as the speed of the cone of light to be relayed. The image-to-image distance is approximately the sum of the two focal lengths. Magnification of the relayed image is equal to the ratio of the focal lengths of the two lenses.

If the purchased camera with the automatic iris assembly is used as the second relay lens, the focal length of the first relay can be calculated if the final image size is known. Selection of a final image size, requires a tradeoff of resolution and field-of-view. The problem is that a 4 X 3 aspect raster is used to scan the circular image from the non-linear lens. The aspect ratio of the TV raster must be 4 X 3 because the projector system uses a light valve television projector with a fixed 4 X 3 raster format. The image should cover as much of the raster as possible.

If the raster height is made equal to the image diameter, no FOV is lost but it does waste a large part of the TV format. If the image is larger, the angular resolution would be improved but the top and bottom of the FOV is cutoff. A compromise solution is to let the raster height cover 90% of the image diameter. The part of the image that is lost lies in an area of low interest. The non-linear lens image which is 0.72 inches in diameter should be demagnified to be 0.417 inches in diameter for a standard 1/2 by 3/8 inch television raster. An 86 mm focal length lens when paired with the 55 mm Vicon lens will give the desired image size. An 85 mm F/2.0 Olympus lens was selected for the first relay lens which has an aperture that is large enough to collect all the light from the non-linear lens without the need for a field lens.

The second relay lens has an auto-iris to provide exposure control. However, this is the case only if the iris is the aperture stop. The aperture stop is defined to be the stop that effectively restricts the cone of rays passing through the lens system.

The following analysis shows how the auto-iris becomes the aperture stop. The first element restricting the light bundle is the non-linear lens which has a speed of F/5.6. The non-linear lens is telecentric in the image plane which means the non-linear lens' exit pupil is located at infinity. Therefore, the next lens, the 85 mm Olympus, will reimage the non-linear lens exit pupil in it's back focal plane. The 85 mm lens is fast enough so that it doesn't restrict the F/5.6 light bundle. Therefore, if the 50 mm lens is positioned so that it's entrance pupil is coincident with the back focal plane of the 85 mm lens, the auto-iris will be the aperture stop.

The relay system described above fulfills all of the optical requirements but is mechanically awkward when coupled to the camera and non-linear lens. It is about three feet long and the two heavy elements are located on the ends. It can't be folded into a more compact package without severe vignetting unless a second relay is added. Therefore, an additional pair of relay lenses are used to fold the optical system 180° so that the vidicon is located directly above the first relay. The back focal distances of the second pair of relay lenses are large enough to accommodate folding mirrors. Each mirror folds the system 90°. Two 80 mm F/2.8 Xenotars are used for the second relay giving it unity magnification.

Adding a second relay makes it necessary to use a field lens to keep the auto-iris as the aperture stop and to keep vignetting from becoming noticeable. The field lens is a double convex lens located in the second image plane. With the image actually being formed inside the lens, the field lens doesn't affect the image and dust particles on the field lens surface are not in focus. The focal length of the lens is chosen to form an image of the exit pupil of the 50 mm relay lens onto the iris of the last relay lens. Using the lens maker's formula the focal length is found to be 52 mm.

The vidicon has typical silicon detector response and is very sensitive to near-infrared energy. However, the non-linear lens and relay optics are not optimized for this spectral band and the image suffers if the infrared is not filtered out. Various narrow band and low pass filters were tried and the one that worked best was a Schott KG-3 infrared absorbing glass. It is placed in the collimated region of the relay. A brassboard of this system was constructed and evaluated. This setup is shown in Figure 5.

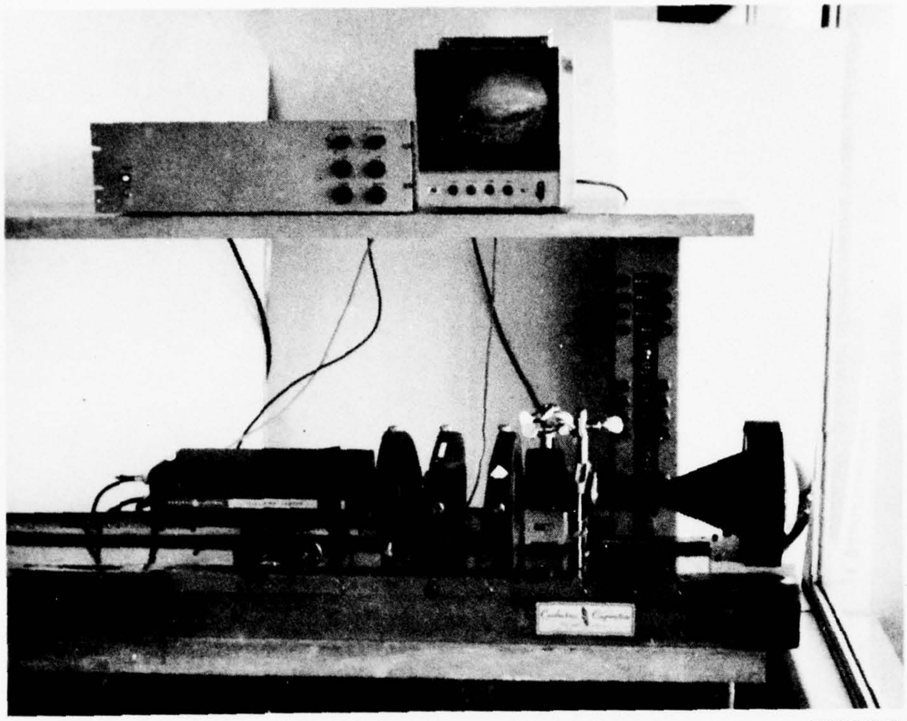

GP77-0549-67

Figure 5 Camera and Relay Brassboard

After initial testing of the camera and projector systems, some modifications were necessary. First the camera vidicon was rotated 90° to compensate for the 90° image rotation which occurs in the projector system. This gave more vertical FOV coverage than horizontal FOV coverage due to the 4 X 3 raster. Previously, the image size was chosen so that the part of the image falling outside of the raster was the top and bottom of the FOV. Now the 10% image loss occurs in the horizontal direction where the full FOV is desired. To get full coverage of the horizontal FOV, the circular image from the non-linear lens must fit within the rectangular raster but the system resolution must not suffer. The solution was to magnify the image and increase the raster size so that the image would cover as many of the discrete diodes that makeup the sensitive surface area of the vidicon as possible. The vidicon has a sensitive area about 0.7 inch in diameter. The image which is also circular is made slightly smaller. The raster size is increased to 0.93 X 0.70 inches so that the raster height is about the same as the image diameter. Consequently the image covers more discrete sensitive elements than before and the resolution is improved with no loss of FOV.

The relative size of the image to the 4 X 3 aspect raster is smaller now than it was because the full image lies within the raster. This causes the projected image to be smaller. Consequently, the projector relay optics must be altered to provide increased magnification of the television image. This modification is described later in Section 3.2.

As in the projector, the camera relay optics had to provide increased magnification. The second relay pair which before operated at unity magnification was made to magnify the 0.417 inch diameter image to 0.703 inches. The larger image was obtained by replacing the last 80 mm Xenotar with a 135 mm, F/4.7 Xenar lens. This required only mirror modifications in mouting hardware. The other optics were unchanged with the same field lens used.

The optical components are located as shown in Figure 6. The television image is formed in the following way. Light from the object enters the non-linear lens from the left and is imaged immediately behind the non-linear lens. This image is collimated by a 85 mm F/2.0 Zuiko Olympus lens. The collimated bundle is imaged a second time by a Vicon 50 mm F/1.4 lens that contains the aperture stop for the system. A field lens is located in the second image plane. The first mirror folds the optical axis up 90° where a 80 mm F/2.8 Xenotar lens collimates the second image. A 135 mm F/4.7 Xenar lens picks up the collimated bundle and the final image. The second mirror folds the optical axis 90° to make the image hit the vidicon. An infrared absorbing filter is placed in the collimated bundle between the last pair of relay lenses.

3.2 PROJECTOR SUB-SYSTEM DESIGN

The second effort in the system design was the electro-optical subsystem design of the projector which consisted of projector selection, relay design, focus corrector design, and projection dome design and is detailed in the following sections.

3.2.1 The Projector Selection

Logic for the original selection of the GE light valve projector is presented in Appendix C. It was the lowest cost approach that could produce adequate display brightness. A PJ7000 light valve was originally purchased for the system. This unit had a 525 line raster and an optical output of 700 lumens. Later this unit was updated to a 1023 line raster for reasons stated earlier in Section 2 and 1000 lumen output thereby making it a PJ7150 projector.

3.2.2 Optical Relay Design

After receiving the projector from GE it was coupled to the non-linear lens with a simple single element optical relay. Problems were immediately encountered with the optical energy transfer. The problem was traced to the Schlieren optical technique used in the projector. This is shown schematically in Figure 7, for the no output case and Figure 8 for full output. The light output is proportional to the rate of change of oil film thickness. This rate of change is generated by an electron beam which writes on the oil film. As can be seen in these figures, the result is a centrally obscurred bundle of illuminated segments. When this bundle is coupled into the non-linear lens a problem results. This is illustrated

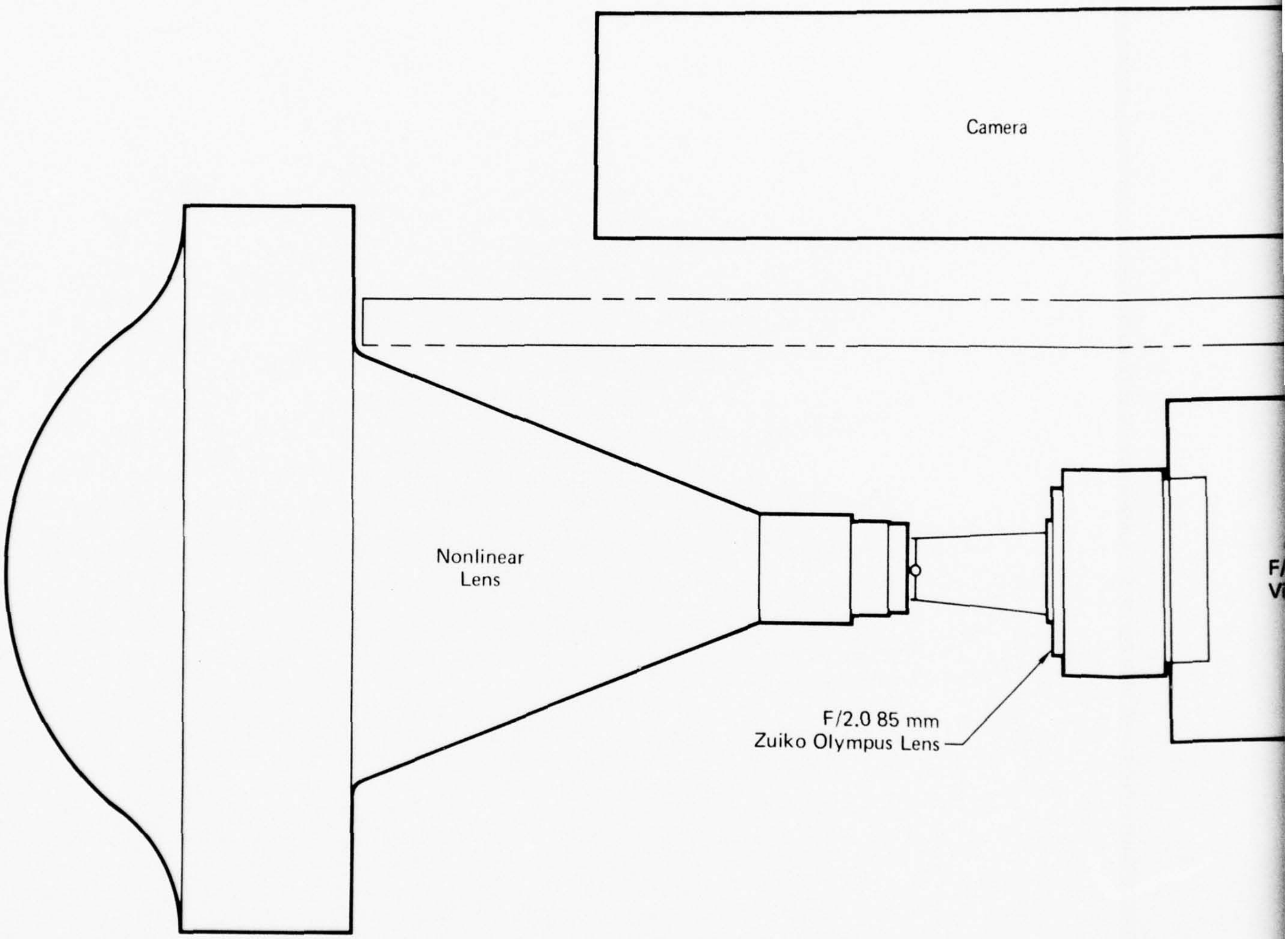

Figure 6 Camera Optical Elements

GP77-0549-51

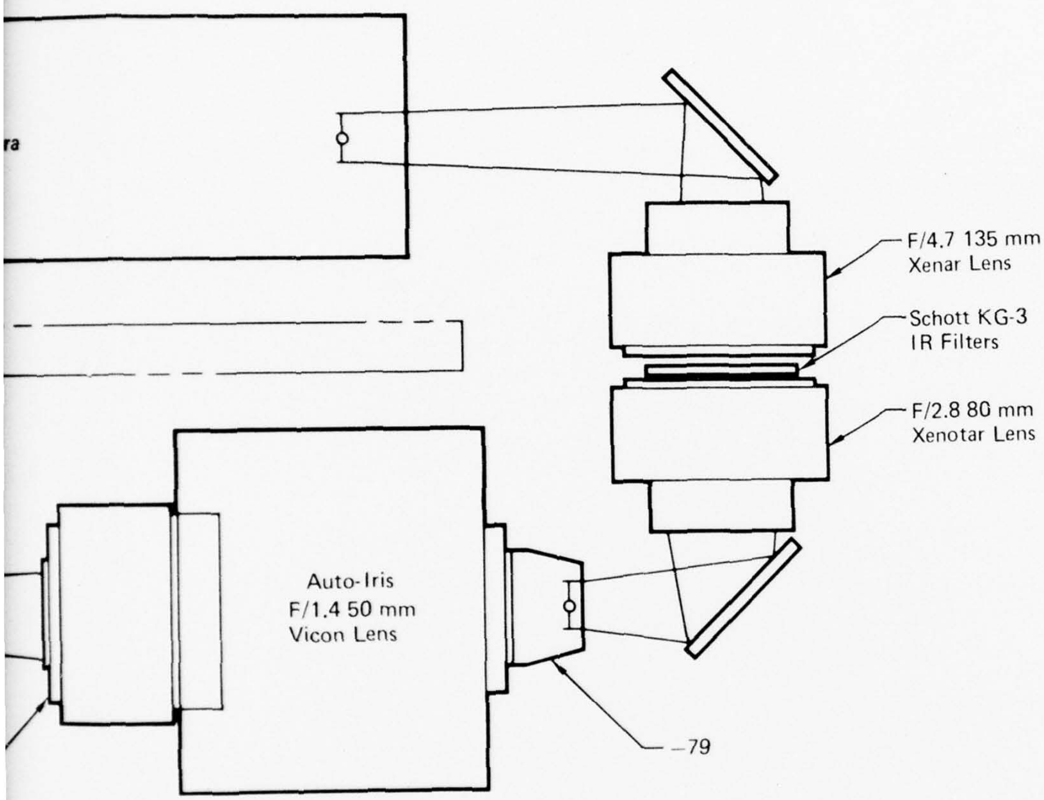
ra
F/4.7 135 mm
Xenar Lens
Schott KG-3
IR Filters
F/2.8 80 mm
Xenotar Lens
Auto-Iris
F/1.4 50 mm
Vicon Lens
—79

2

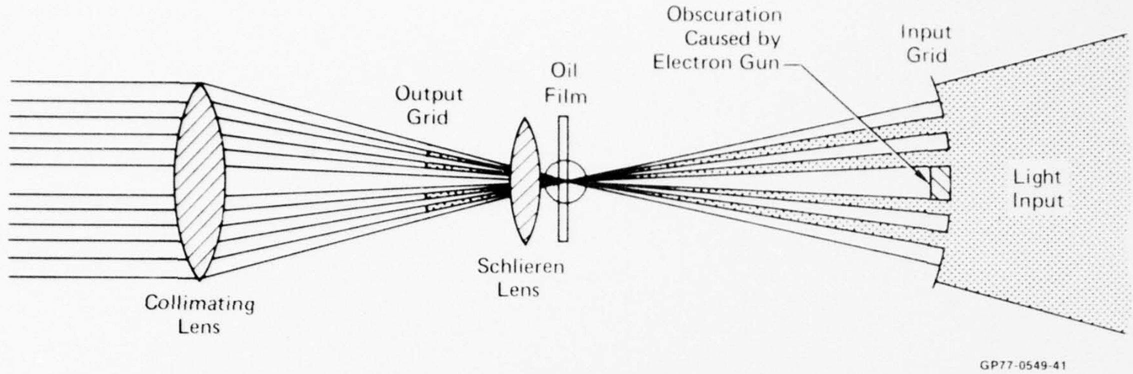

Figure 7 Light Valve Operation
No Output

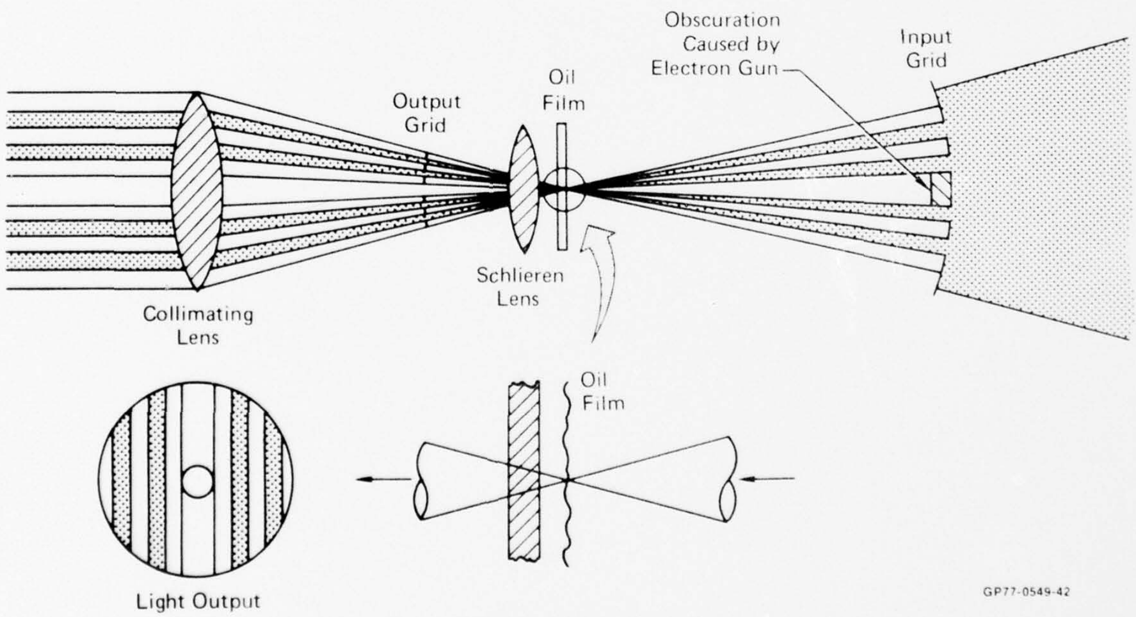

Figure 8 Light Valve Operation
Maximum Output

in Figure 9 for a simplistic one element relay used in our original experiment. In this experiment a dark spot was noted at the center of the projected image. In the on-axis case, the reason for this is that almost all of the energy from the light valve falls outside of the acceptance cone of the non-linear lens as can be seen in Figure 9. This causes two areas of concern. The low light in the central high acuity area of the image can seriously reduce the observer's visual capabilities. In addition, the annular shaped input to the lens provides energy in the worst possible portion of the acceptance ray cone if good image quality is desired. The latter is known from original ray trace data on the lens. In addition, the annular input by itself can cause serious diffraction problems. All of these problems can lead to low display acuity in the central region where the highest acuity is desired.

GE was consulted to see if the projector output could be modified to correct for this situation. After considerable study, they concluded that a major redesign would be required to make the light valve output more compatible with our lens. This left only the relay parameters as a possibility to effect an improvement. From an optical viewpoint, the only relay parameter that can be varied which affects the output ray cone geometry is magnification. This parameter can expand or compress the F/number cone from the projector. In our case, we need to reduce the cone size which requires more magnification within the relay. A derivation will be presented which relates the F/number and magnification to the ratio of source and display brightness.

The entire optical system is shown schematically on Figure 10. The symbols to be used in this derivation are also defined on this figure.

The illumination (E_s) of the source is:

$$E_s = \frac{F}{A_s} \tag{1}$$

Thus the source brightness (B_s) is:

$$B_s \cong \frac{E_s}{\omega_s} = \frac{F}{A_s \omega_s} \tag{2}$$

Now from cone geometry the solid angle is:

$$\omega_s = \frac{\pi}{4 \, FNO_s^2} \tag{3}$$

where FNO_s = F/number of source

$$B_s = \frac{4 \, FNO_s^2 \, F}{\pi A_s} \tag{4}$$

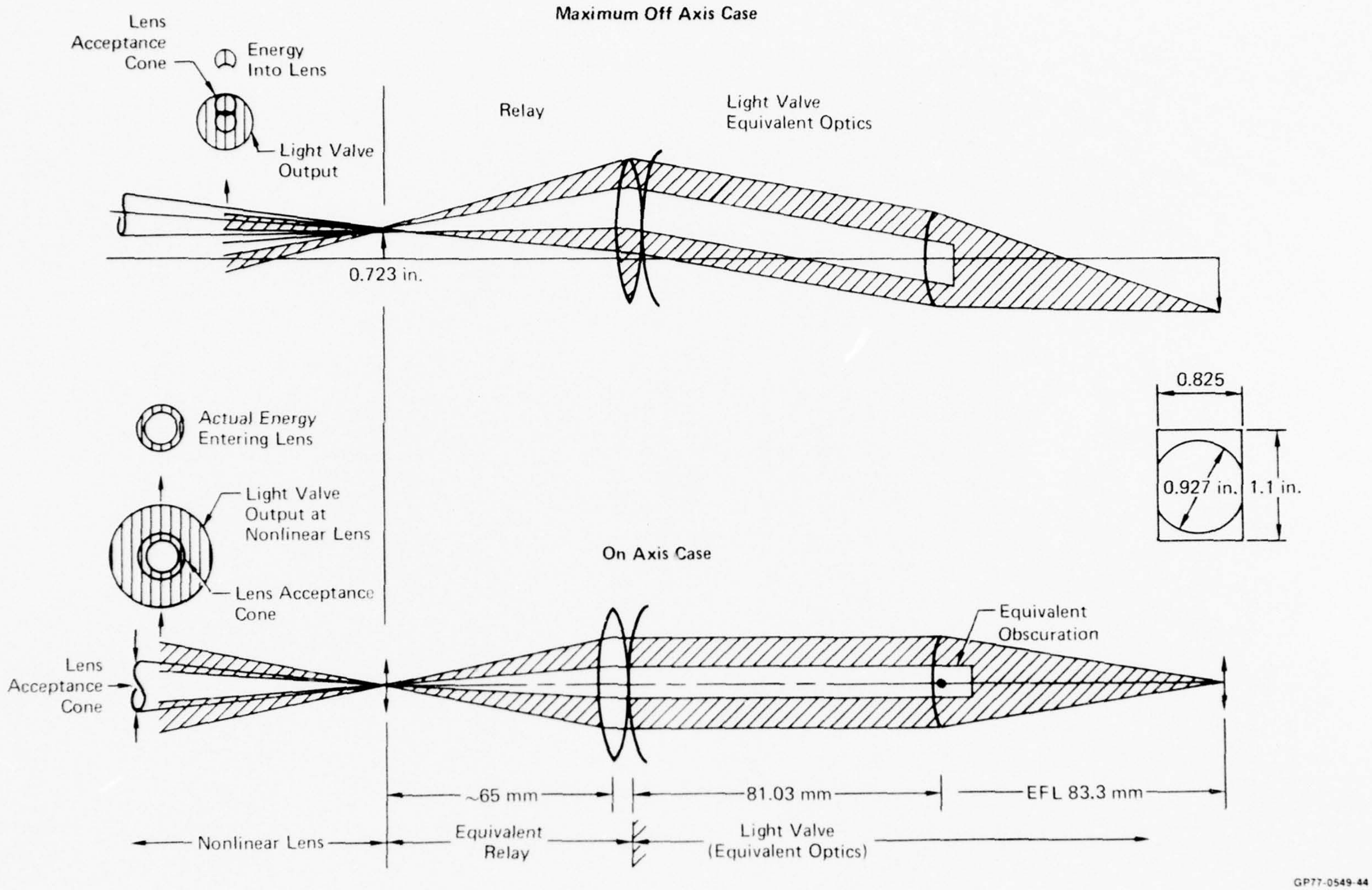

Figure 9 Light Valve Nonlinear Lens Interface for Single Element Relay

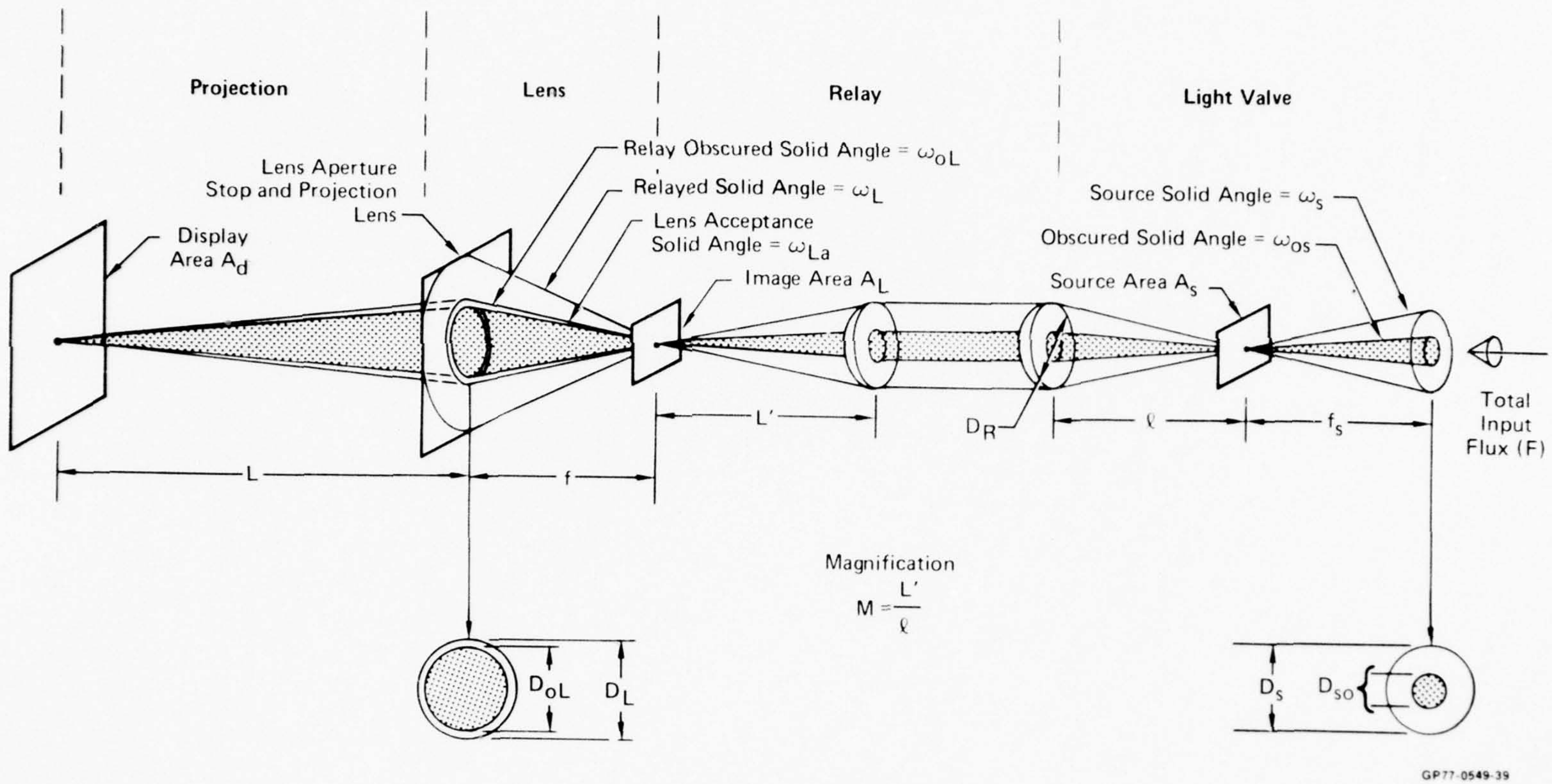

Figure 10 Basic Relay Parameters

This (B_s) is also the brightness of the image at the lens. For those who are not familiar with this fact it can be proven as follows: The total flux passing through the source area (A_s) will arrive at the lens area (A_L) assuming good relay design. The area A_L is related to A_s by the magnification (M), viz:

$$A_L = M^2 A_s \tag{5}$$

Since the output of relay is collimated as any good relay is, the output ray diameter equals the input diameter. Therefore, the ratio of output to input solid angle is

$$\frac{\omega_L}{\omega_s} = \frac{\pi D_R^2}{L^{1\,2}} \; \frac{1^2}{\pi D_R^2} = \frac{1}{M^2} \tag{6}$$

In addition, the areas A_L and A_s are also related by the magnification viz:

$$M^2 = \frac{A_L}{A_s} \tag{7}$$

The brightness of the image is:

$$B_L = \frac{F}{A_L \omega_L} \tag{8}$$

Substituting Equations (5), (6), and (7) into (8) results in:

$$B_L = \frac{F}{A_s \omega_s} \tag{9}$$

The right side of Equation (9) is equal to the right side of Equation (2), thus:

$$B_L = B_s \tag{10}$$

Now we will determine the effect of the lens obscuration, magnification, and F/number on the screen brightness. The light flux actually entering the projection lens from an incremental image area (dA_L) is:

$$F = B_L \, dA_L \, (\omega_{La} - \omega_{LO}) \tag{11}$$

where

$$\omega_{La} = \frac{\pi}{4\ FNO_L^{\ 2}}$$

where FNO_L = Lens acceptance F/Number

Also:

$$\omega_{Lo} = \frac{\omega_{so}}{M^2} = \frac{\pi\ D_{so}^{\ 2}}{M^2\ f_s^{\ 2}} \qquad (12)$$

Now if we define an obscuration factor (K) as the ratio of the obscured diameter (D_{so}) to the aperture diameter (D_s), viz:

$$K = \frac{D_{so}}{D_s} \qquad (13)$$

Substituting Equation (13) into (12)

$$\omega_{Lo} = \frac{\pi\ K^2\ D_s^{\ 2}}{M^2\ f_s^{\ 2}} = \frac{\pi\ K^2}{M^2\ FNO_s^{\ 2}} \qquad (14)$$

where FNO_s is the F/number of the source. Now substituting into Equation (11).

$$F = B_L\ dA_L \left[\frac{\pi}{4\ FNO_L^{\ 2}} - \frac{\pi\ K^2}{4\ FNO_s^{\ 2}\ M^2} \right] \qquad (15)$$

$$= \frac{\pi\ B_L\ dA_L}{4} \left[\frac{1}{FNO_L^{\ 2}} - \frac{K^2}{FNO_s^{\ 2}\ M^2} \right] \qquad (16)$$

All of this flux falls within area dA_d on the projection screen. The illumination is then:

$$E_d = \frac{F}{dA_d} = \frac{\pi\ B_L\ dA_L}{4\ dA_d} \left[\frac{1}{FNO_L^{\ 2}} - \frac{K^2}{FNO_s^{\ 2}\ M^2} \right] \qquad (17)$$

However the focal lengths and differential areas are related by:

$$\frac{dA_L}{dA_d} = \frac{f^2}{L^2} \qquad (18)$$

Substituting Equation (18), (3) and (2) into (17) results in:

$$E_d = \frac{F f^2}{L^2 A_s} \left[\left(\frac{FNO_s^{\ 2}}{FNO_L}\right) - \left(\frac{K^2}{M}\right)\right] \tag{19}$$

Now the display screen brightness is:

$$B_d = \frac{E_d}{\omega_d} \tag{20}$$

where ω_d is the solid angle over which E_d is reflected. For our purpose of studying the effects of magnification, the relative brightness referenced to an unobscured source will simplify the analysis. For an unobscured source:

$$K = 0$$

And then Equation (19) becomes:

$$E_r = \frac{F f^2}{L^2 A_s} \left(\frac{FNO_s^{\ 2}}{FNO_L}\right) \tag{21}$$

Therefore:

$$\frac{B_d}{B_r} = \frac{E_d}{E_r} = \frac{\left(\frac{FNO_s}{FNO_L}\right)^2 - \left(\frac{K}{M}\right)^2}{\left(\frac{FNO_s}{FNO_L}\right)^2} = 1 - \left(\frac{K\ FNO_L}{M\ FNO_s}\right)^2 \tag{22}$$

For our light valve

$$K = 0.36$$

$$FNO_s = 2.8$$

$$FNO_L = 5.6$$

Substituting these values into Equation (22) results in:

$$\frac{B_d}{B_r} = 1 - \frac{.518}{M^2} \tag{23}$$

This curve is plotted in Figure 11(a). This curve clearly illustrates the problem noted in our first experiments. During this exercise we had the full width of the light valve format filling the lens image plane as shown in Figure 11(b). Here the magnification was the ratio of the non-linear lens diameter of 0.72 inch to the camera scanning width of 1.1 inches, viz:

$$M = \frac{0.72 \text{ inch}}{1.1} = 0.65$$

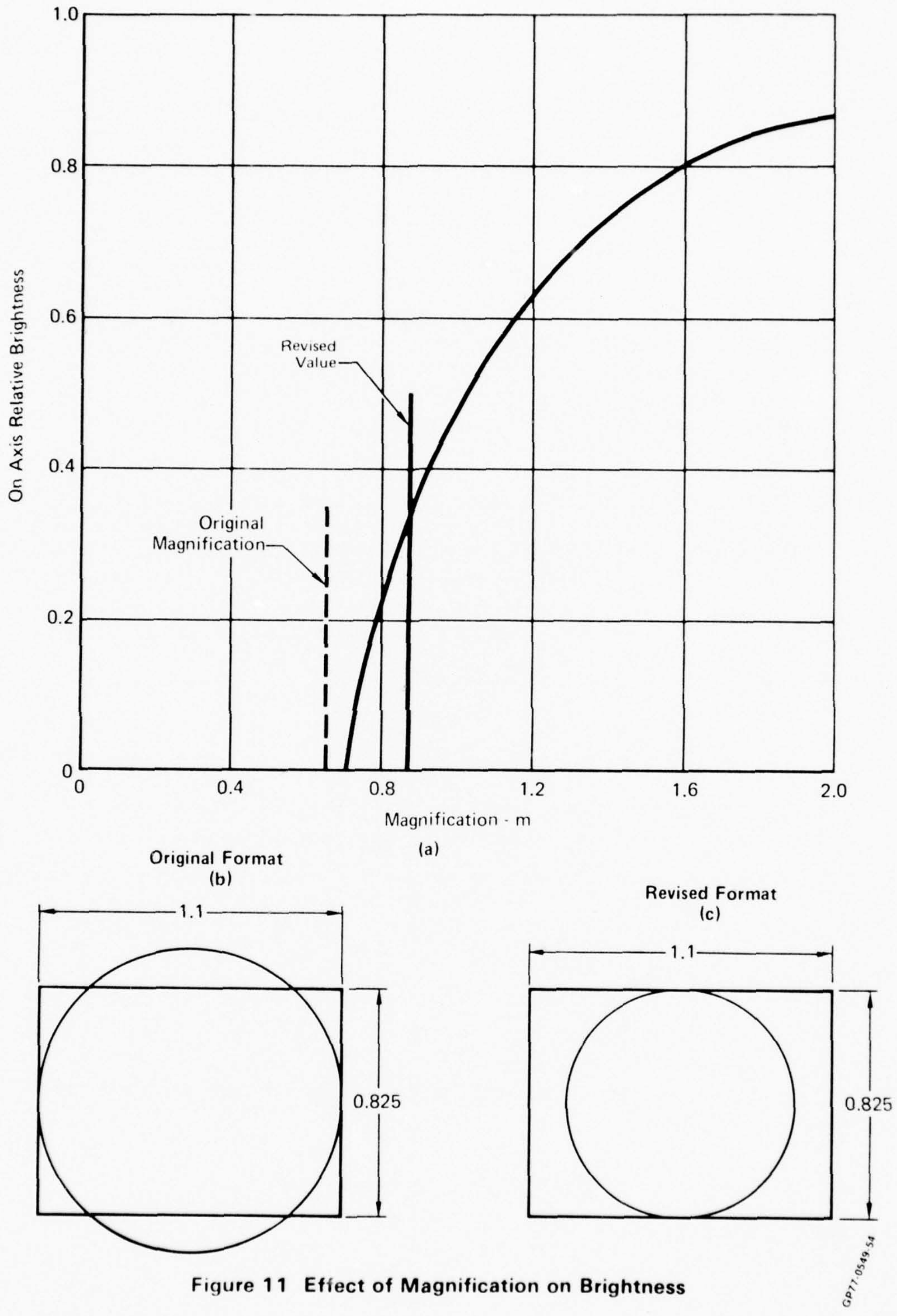

Figure 11 Effect of Magnification on Brightness

Under these conditions no light was entering the lens. The system was made useable by reducing the portion of the source area occupied by the lens image as shown on Figure 11(c). Thus, the magnification is:

$$M = \frac{0.72}{0.825} = 0.87$$

Now the display brightness is 0.3 that of an unobscured or conventional optical system. Since considerably more light is available in the central area of the display (See Appendix C), this is an acceptable situation. In fact it helps to make the display brightness more uniform if the relay is correctly designed. Such a design was shown on Figure 9. Note that for the edge ray bundle that the lens acceptance cone shifts to a more desirable portion of the light valve cone. The result is essentially an increase in output when compared to that of an unobscured system at the field edge. Since the above solution appears to be satisfactory from a brightness standpoint the question of acuity was then considered.

While the exact effect of an annular aperture function is very difficult to predict precisely, an approximation of its affect on resolution is rather easy. Figure 12 shows such an aperture and its associated diffraction MTF. For a thin annulus where the inner (D_{OL}) and outer (D_L) diameters are approximately the same, the MTF shows a pronounced drop in response at a spatial frequency (S_1) proportional to the difference in the diameters divided by twice the light wavelength (2λ), viz:

$$S_1 = \frac{D_L - D_{OL}}{2\lambda} \tag{24}$$

Therefore, a good approximation to the MTF is to assume that the spatial frequency (S_1) is the limiting factor in performance. For this reason this frequency was calculated in terms of the parameters of Figure 12.

At the projection lens output, the lens diameter (D_L) and focal length (f) are related to F/number (FNO_L) by:

$$D_L = \frac{f}{FNO_L} \tag{25}$$

Substituting Equation (13) into (25) and relating FNO_L to FNO_s by the magnification

$$D_{LO} = \frac{K\,f}{M\,FNO_s} \tag{26}$$

Substituting into Equation (24)

$$S_1 = \frac{f}{2\lambda}\left[\frac{1}{FNO_L} - \frac{K}{M\,FNO_s}\right] \tag{27}$$

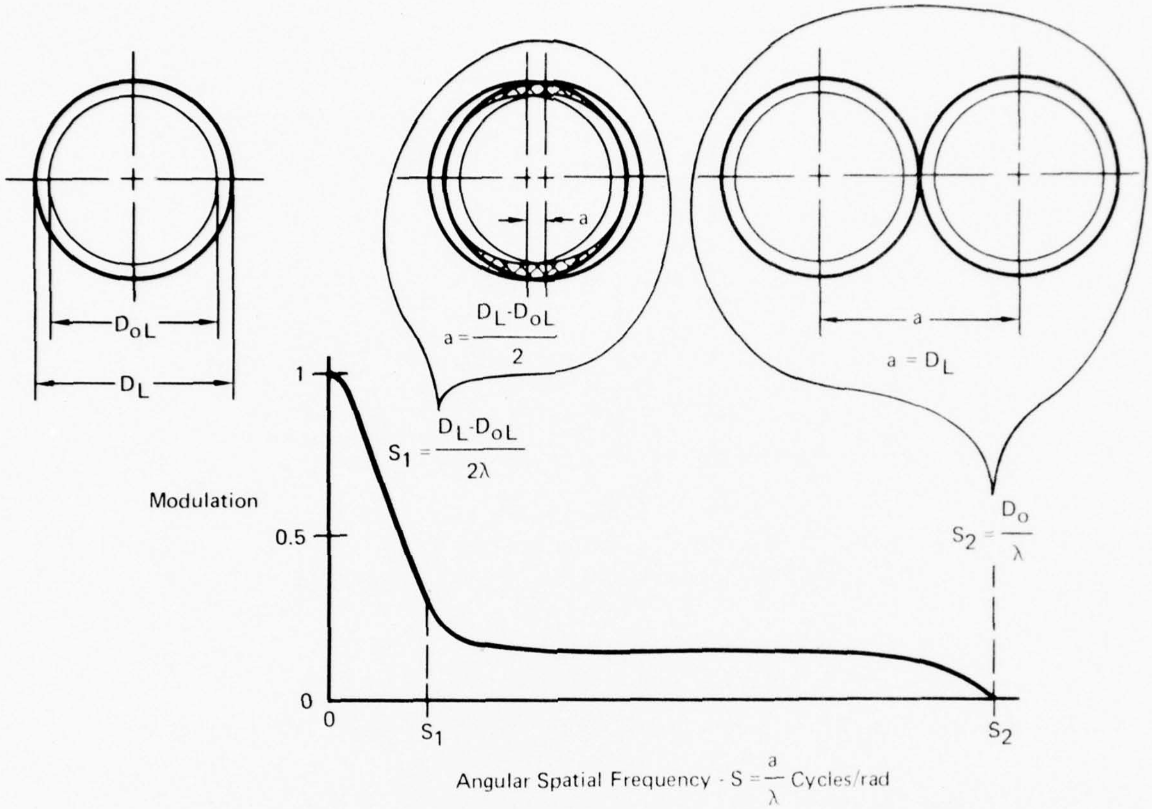

Figure 12 MTF of an Annulus

In more conventional terms the resolution is approximately the width of a half cycle.

$$\alpha = \frac{1}{2S_1} = \frac{\lambda}{f\left(\frac{1}{FNO_L} - \frac{K}{M\ FNO_S}\right)} \tag{28}$$

This function is plotted in Figure 13 for the light valve output for an obscuration ratio (K = 0.36) and F/number of 2.8 and variable magnification and the non-linear lens focal length of 2 inches and F/number of 5.6. Note that for the revised raster format, the serious MTF degradation occurs at a resolution of 0.34 milliradians or 1.2 minutes of arc. While it would be desirable to have better performance than this, it is comparable to scan line substense and no further improvement could be made. Any further increase in relay magnification would result in an increase in scan line subtense, also shown in Figure 13 for a 1023 line raster. Based on the above effort the design requirements for the relay were established, and are:

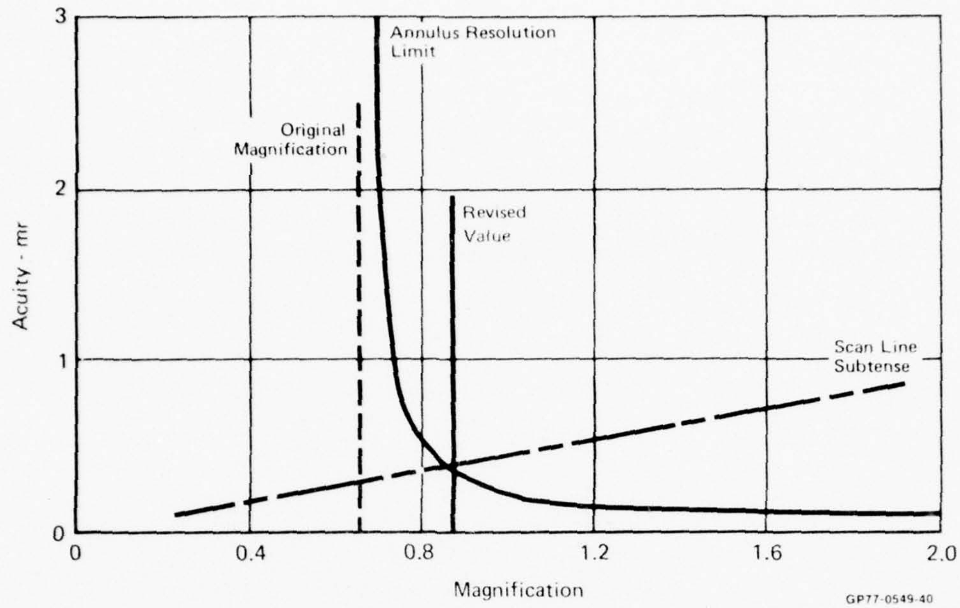

Figure 13 Effect of Magnification on System Acuity

1. A magnification of 0.87
2. Aperture shift geometry with field angle as shown in Figure 9.

The final requirement was to iterate the overall relay mechanical design including overall length, fold point locations, and diameter with the designer.

Basically, these parameters are:

Overall Length = 4 feet

Diameter = 3 inches

Critical Folds = 12 inches required between last two lenses

After considerable design effort the relay of Figure 14 evolved. On this figure an edge ray bundle is drawn to show how the desired aperture shift is achieved. Note no field lenses are utilized. This was necessary to maintain the desired aperture shift. The large size penalty normally associated with a relay design of this type is eliminated by allowing vignetting of the unused part of the light valve optical output.

The lens elements were purchased and the relay set up on an optical bench. After a small decollimation at the projector output to achieve the required magnification, performance was exactly as expected. The relay configuration using available lenses is shown in Figure 14. Figure 15 is a photograph of the relay test set-up.

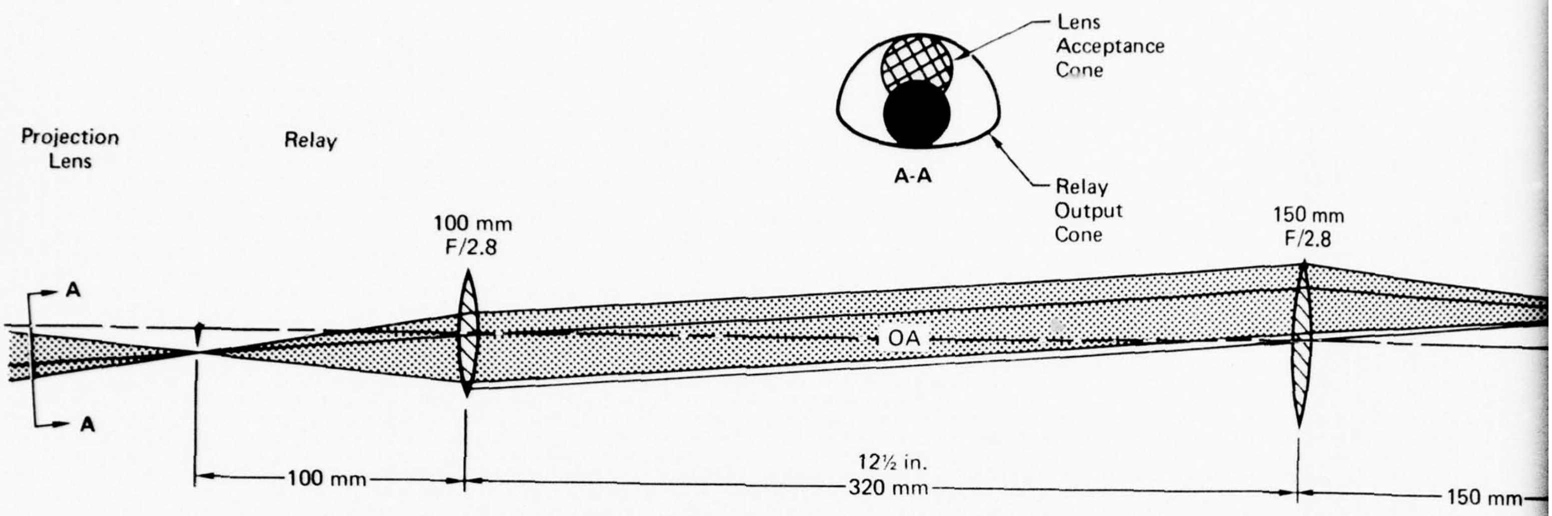

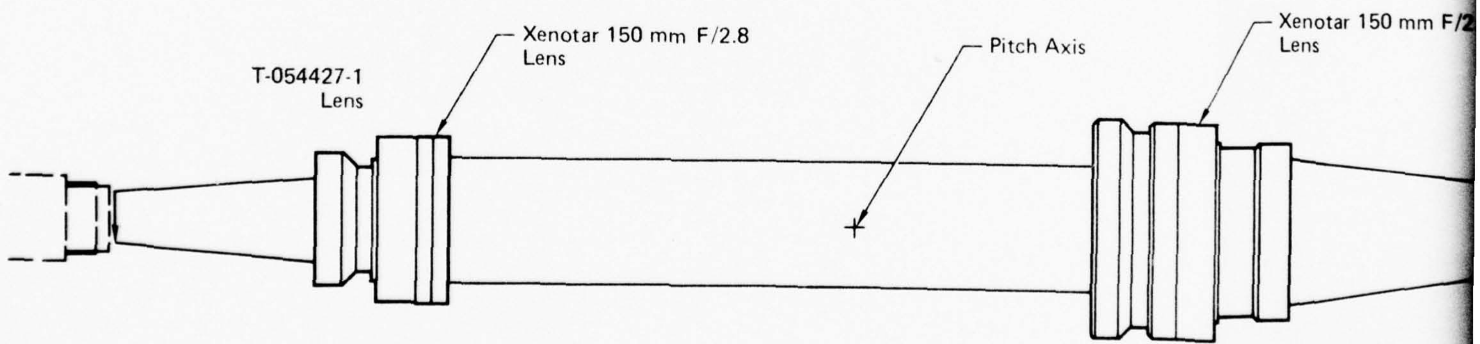

Figure 14 Projector Optical Relay

GP77-0549-53

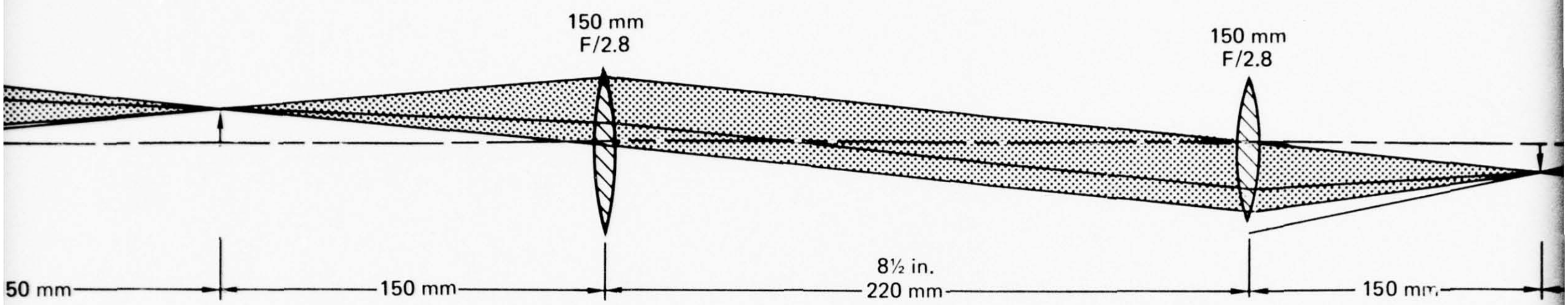
150 mm
F/2.8
150 mm
F/2.8
50 mm
150 mm
8½ in.
220 mm
150 mm

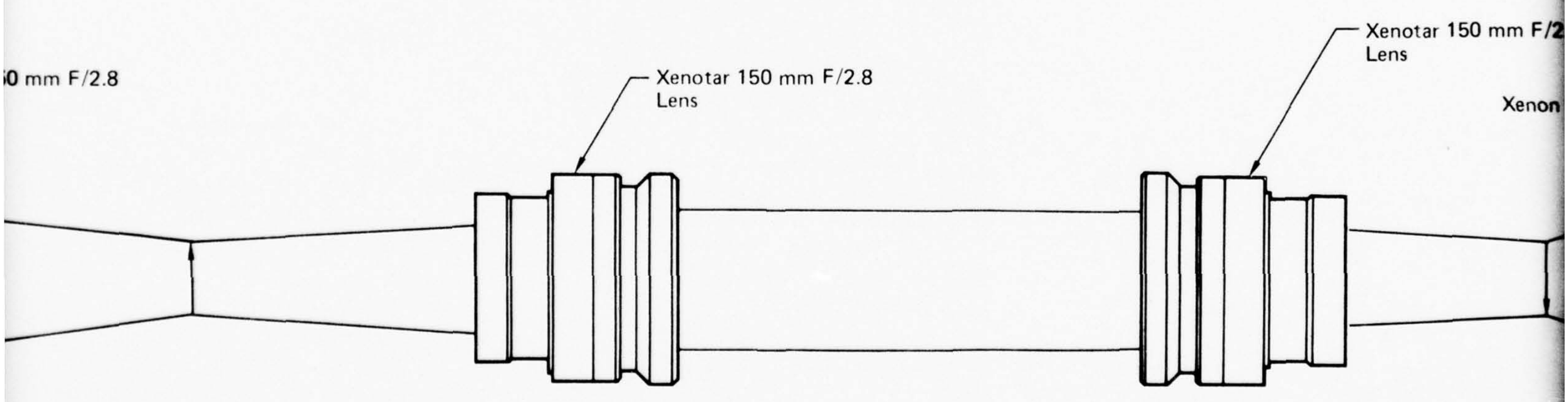
0 mm F/2.8
Xenotar 150 mm F/2.8
Lens
Xenotar 150 mm F/2
Lens
Xenon

2

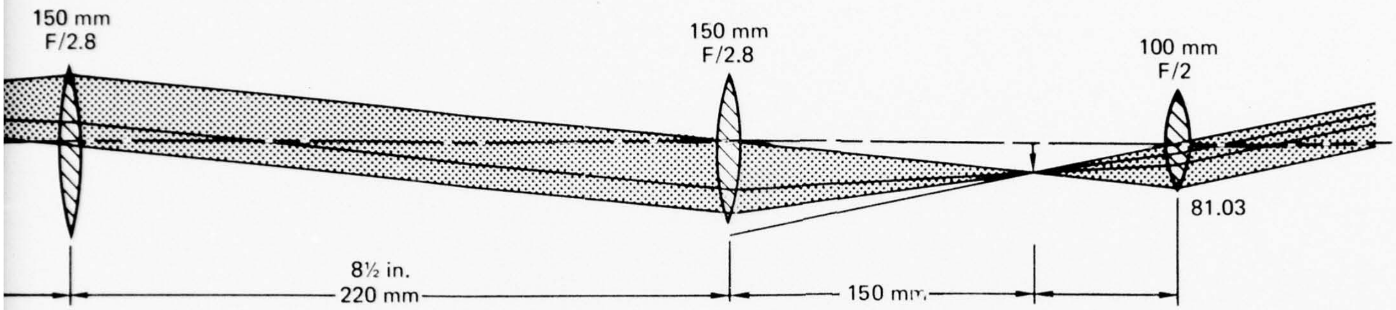
150 mm
F/2.8
150 mm
F/2.8
100 mm
F/2
81.03
8½ in.
220 mm
150 mm

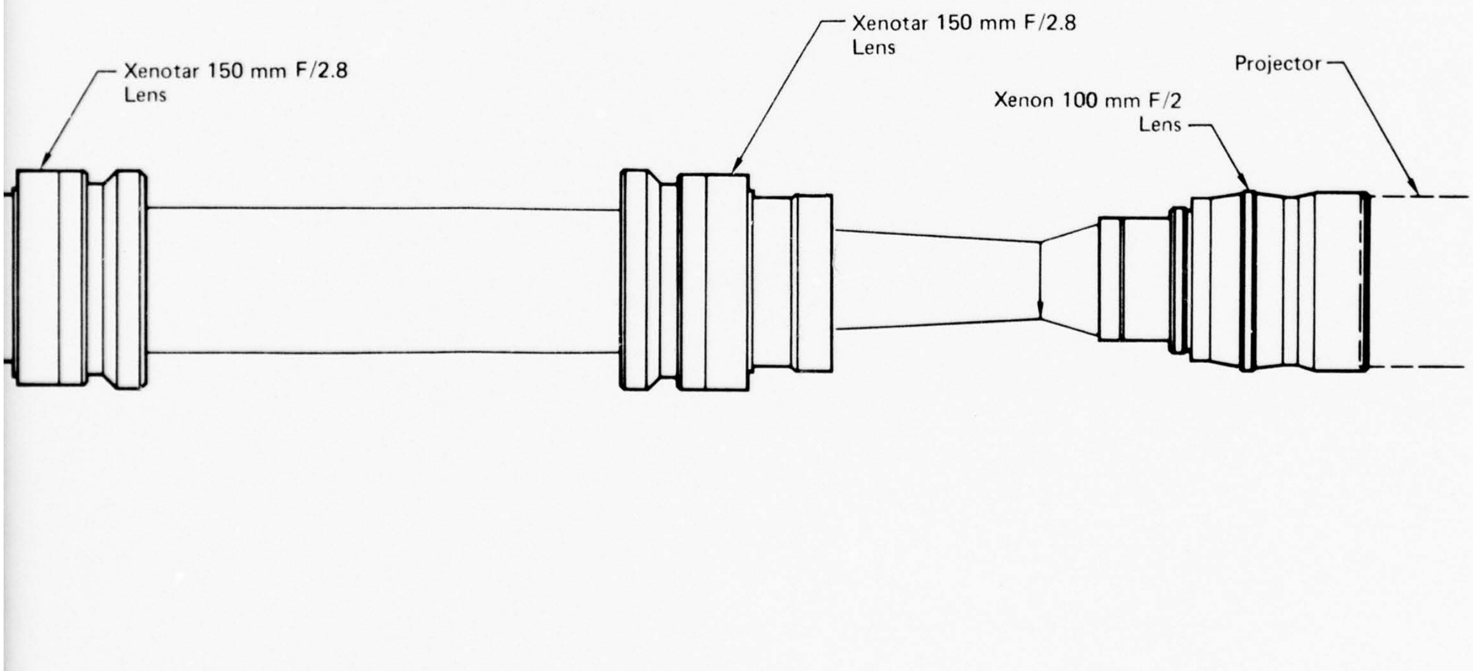
Xenotar 150 mm F/2.8
Lens
Xenotar 150 mm F/2.8
Lens
Projector
Xenon 100 mm F/2
Lens

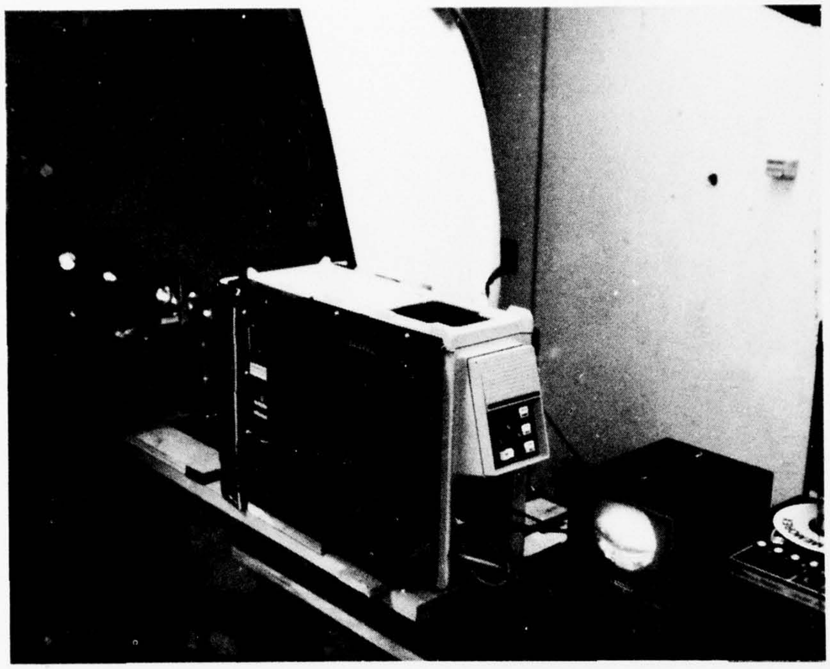

GP77-0549-78

Figure 15 Relay Test Setup

3.2.3 Focus Correction

The variable focal length nature of the projection lens creates a serious focus problem. This problem arises because the projector lens is identical to the camera lens and designed for an object located at infinity. For projection, the lens focal plane must be shifted aft by about 0.08 inch to obtain optimum on-axis focus where the lens focal length is 2 inches. At an 80° object field angle, the focal length is down to 0.04 inches. An 0.08 inch shifted image plane is obviously grossly out-of-focus for this short off-axis focal plane. To determine the magnitude of this problem, the focal plane profile for optimum focus was computed. The general case geometry of Figure 16 was used for this purpose. Here the lens equivalent optical geometry for on-axis and off-axis object angle θ is shown. For either case the general lens equation applies.

$$\frac{1}{S_1(\theta)} + \frac{1}{S_2(\theta)} = \frac{1}{f(\theta)} \tag{29}$$

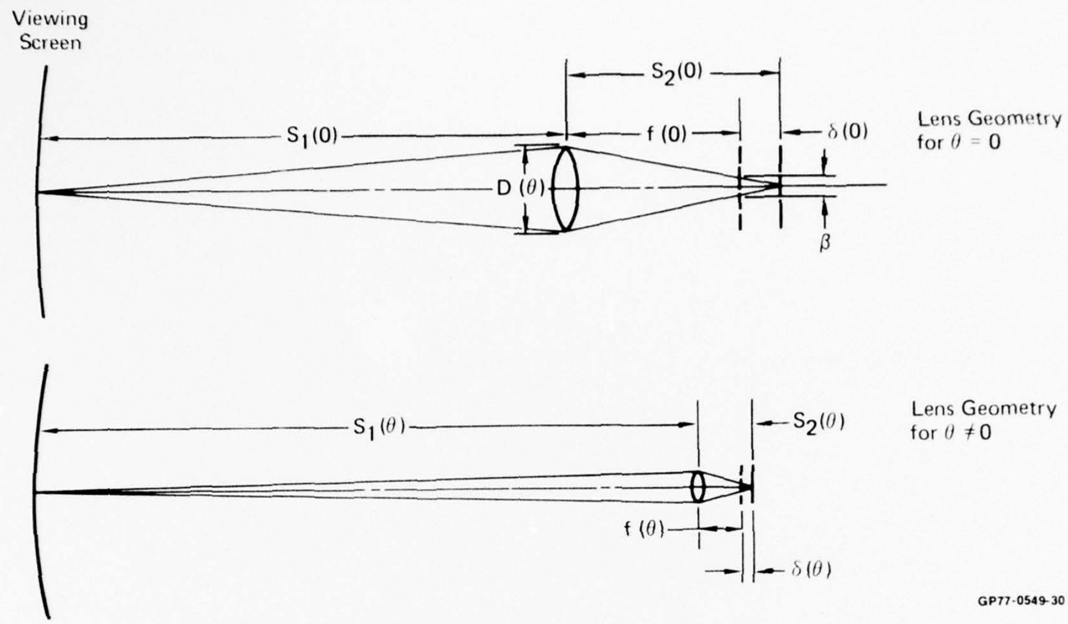

Figure 16 Projection Lens Conjugate Geometry

where $S_1(\theta)$ = Object distance

$S_2(\theta)$ = Image distance

$f(\theta)$ = Focal length

From Figure (16) and because $S_1(\theta)$ is relatively constant, the focus error is

$$\delta(\theta) = S_2(\theta) - f(\theta) \tag{30}$$

Substituting Equation (29) into (30)

$$\delta(\theta) = - \frac{f^2(\theta)}{S_1(\theta) - f(\theta)} \tag{31}$$

For a 54 inch object distanct, $(S_1(\theta))$, the error in focus for a system focused at infinity is:

$$\delta(\theta) = \frac{f^2(\theta)}{54 - f(\theta)} \tag{32}$$

This equation is plotted in Figure 17. In order to maintain optimum focus, the image plane would have to be the shape of the Figure 17 curve, i.e., 0.08 inch further back in the center relative to its edge.

Now the effect of this defocus will be related to focal plane resolution. If $\phi(\theta)$ is the required resolution, the allowable focal plane blur ($\beta(\theta)$) is

$$\beta(\theta) = f(\theta)\ \phi(\theta) \tag{33}$$

Since the focal plane spatial resolution is uniform; that is the off-axis resolution is equal to the on-axis value,

$$\beta = \text{constant} = f(\theta)\ \phi(\theta) = f(0)\ \phi(0) \tag{34}$$

If ϕ is in minutes of arc the allowable focal plane blur is

$$\beta = \frac{f(0)\ \ \phi(0)}{3440} \tag{35}$$

Relating similar triangles on Figure 16

$$\frac{D(\theta)}{S_2(\theta)} = \frac{\beta}{\delta(\theta)} \tag{36}$$

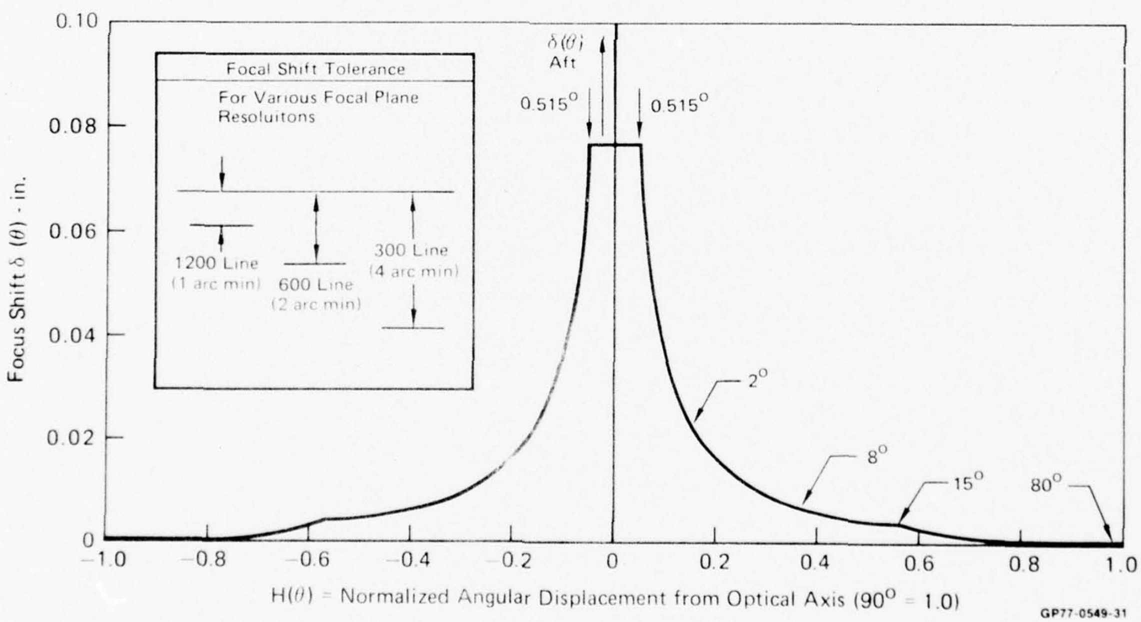

Figure 17 Image Plane Position Relative to Infinity Focus for 54 In. Conjugate Distance

Solving for $\delta(\theta)$

$$\delta(\theta) = \frac{\beta\, S_2\,(\theta)}{D\,(\theta)} \qquad (37)$$

Since the F/number is defined as

$$FNO \triangleq \frac{f(\theta)}{D(\theta)} = \text{constant} \qquad (38)$$

and

$$S_2(\theta) \cong f(\theta) \qquad (39)$$

Then

$$\delta(\theta) = \beta \text{ F/No.} \qquad (40)$$

Substituting Equation (35) and (39) into (40)

$$\delta(\theta) = \frac{\phi\,(0)}{3400} \text{ F/No. } f(0) \qquad (41)$$

For our lens the F/No. = 5.6 and f(0) = 2 inch, the allowable focal plane mislocation is

$$\delta(\theta) = 3.294 \times 10^{-3}\ \phi(0) \qquad (42)$$

This equation is plotted on Figure 17 for resolutions ($\phi(0)$) of 1, 2, and 4 arc minutes.

There are two ways of correcting this focus shift problem. The image plane can be tailored to Figure 17 with a corrector element in the lens image plane or the lens can be operated at the infinity focal plane position and a positive optical element placed at the lens output to converge the lens output to a 54 inch conjugate distance. After some experimentation with a focal plane corrector, the latter approach was selected as the only feasible method of focus correction. This is not without its problems however.

The only way of achieving a positive (converging) lens effect outside of the non-linear lens is as shown in Figure 18. It must be a deep double convex element in order to accommodate the entire field-of-view while its thickness must be held down to reduce weight and inertia of the projector pitch axis.

The following technique was used to design this element. Curvature of the surface closest to the lens was selected by fit geometry. Then the second surface radius was computed to converge the on-axis ray bundle at the 54 inch distance. Then the angular blur size as seen from the center of the dome was computed for all other field angles. These results were then compared to the inherent system acuity. The resulting lens curvature are shown on Figure 18 while blur data are shown on Figure 19.

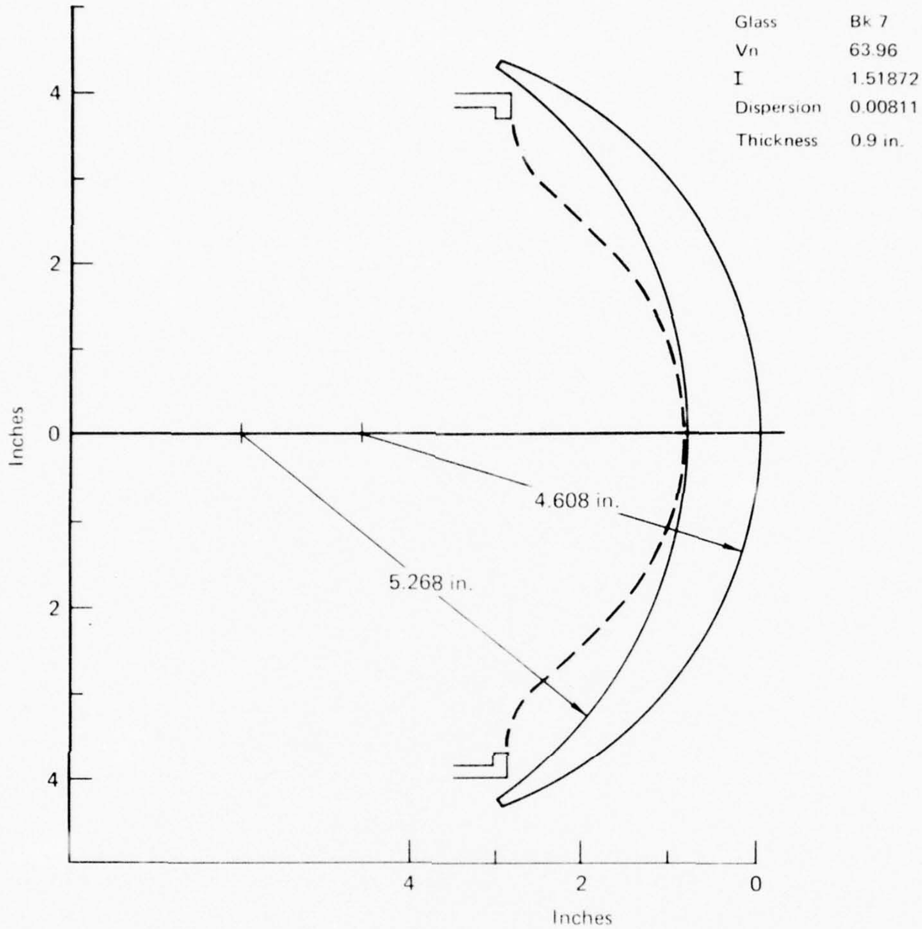

Figure 18 Focus Corrector Geometry

The blur after correction was well within the acuity tolerance for the entire 160° field.

The problem with this method of focus correction is that it generates a distortion to the non-linear lens output. Rays exiting the non-linear lens are bent towards the optical axis by an increment that increases with field angle. This is to say that while blur is acceptable, the centroid of the blur falls on the screen at the wrong location. This can and will cause false motion of points on the display as gimbal angles vary.

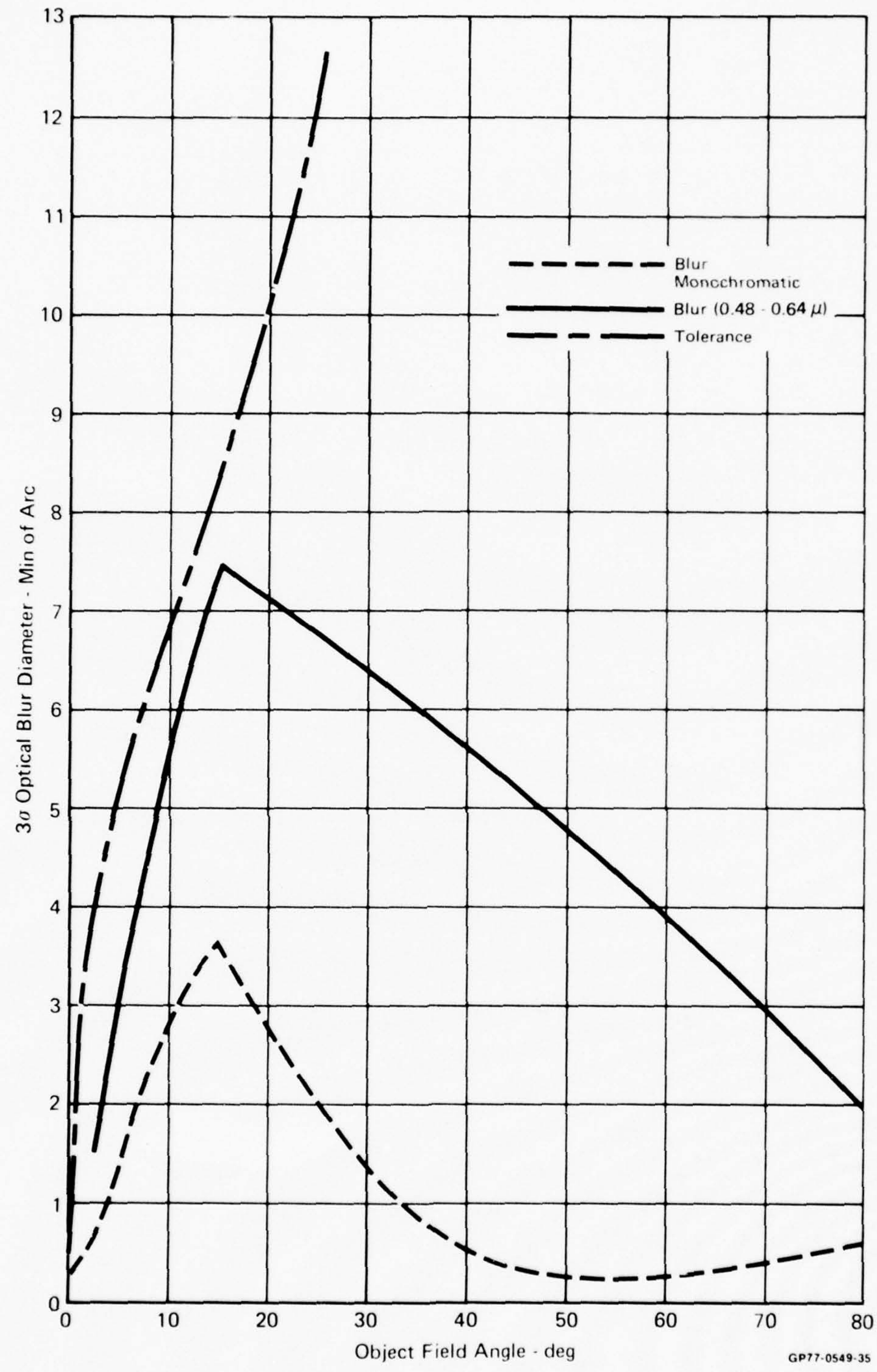

Figure 19 Corrector Angular Blur

To study importance of this effect, rays were traced from the lens to the screen at various field angles without and with the corrector lens. The angular error resulting from both cases as observed from the dome center are shown on Figure 20. With no corrector lens, an error is generated because of the nodal point shift in the non-linear lens. This shift can be seen on the chief ray trace data shown on Figure 21. The gimbal axis of the projection lens intersect very near the 45° nodal point. This make the projection correct only at 0° and 45°.

As the nodal point shifts aft or forward for the angles other than 45°, they fall on the screen at larger or smaller angles (measured from the sphere center) than they should to maintain no distortion. The worst case occurs at 80° where points are advanced by 2°, Figure 20 curve c. If the focus corrector is installed on the lens, points are directed in an opposite direction as shown by the curve e of Figure 20. Here the error increases continuously, reaching about 9° at 80° command angle. This suggests that if the size of the non-linear lens image is increased, this problem must be reduced. This was analyzed and a 2% value was found to produce minimum error over the entire field, curve d. The maximum error is about the same magnitude as it would be with no corrector. The only problem is a slight loss in field-of-view, from 160° to 140°. Since resolution is very low in this region, this is believed to be an acceptable tradeoff for a better acuity close to the optical axis. A corrector of the design shown in Figure 18 was fabricated and installation hardware designed for the projector lens.

3.2.4 Projection Surface Design

It was apparent from early experimental projections on the interior surface of the sphere that a diffuse unity gain white screen surface did not yield enough edge brigthness. This was predicted and the calculations are contained in Appendix C. As also described in the appendix, the projection/viewer geometry was optimized for a specular screen coating. The work of Reference (4) indicated that a silver screen material would increase brightness by a factor of four. Based on this, we evaluated several types of aluminum paint on the surface and we found that a screen gain of four was easily achieved. By visual observations, we concluded that sufficient brightness was being obtained out to field angles of 120°. Beyond this, performance was questionable. However, high contrast objects were easily detected out to 140°.

The aluminum paint, however, caused the imperfections in the dome joints to become very noticeable. This required expenditure of considerable effort to refill and sand the joints smooth.

3.3 HEAD TRACKING SYSTEM DESIGN

The function of the head tracker servo control system is to maintain angular alignment of projector's optical axis and the observor's nominal sightline. A head angular position sensor or a relative head/projector angular position sensor will not accomplish this beacuse of the close proximity of the viewing surface. To correctly accomplish this sensing

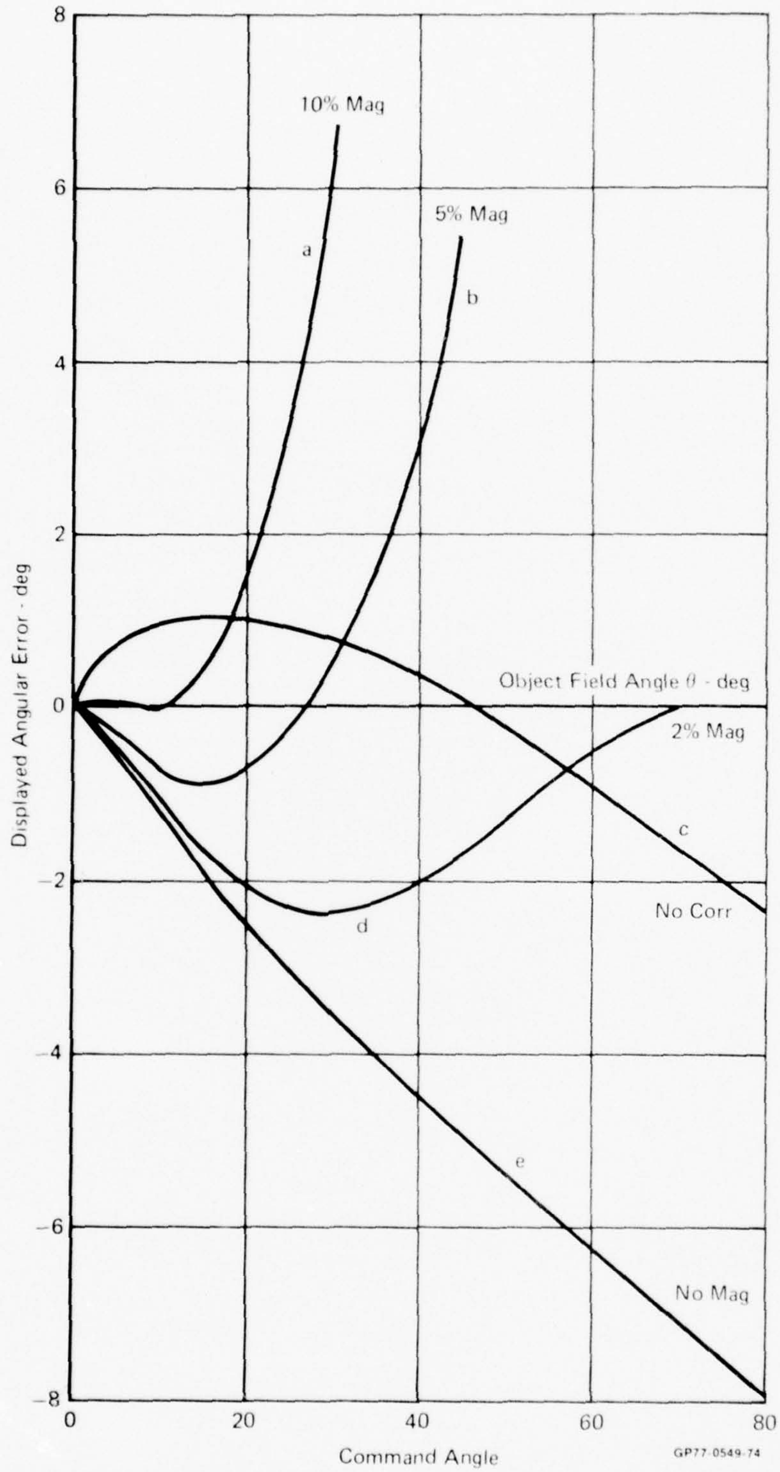

Figure 20 Display Error vs Actual Angle

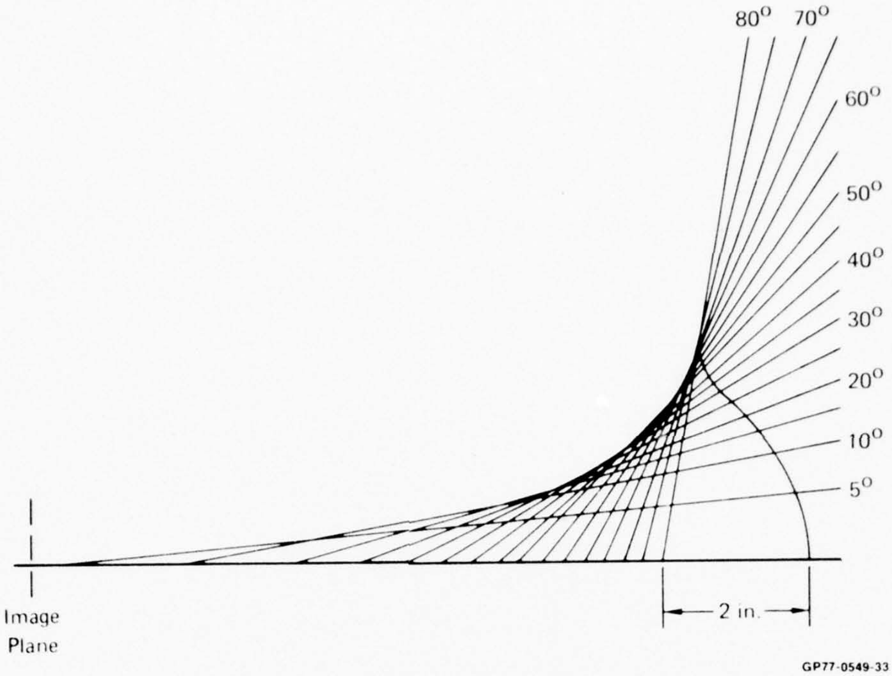

Figure 21 Nodal Point Shift of Nonlinear Lens

task, the head position must be sensed relative to the projection lens coordinates in all six dimensions. To avoid a complex sensing and computational task, an electro-optical approach was devised that inherently senses the required parameters and is shown in Figure 22.

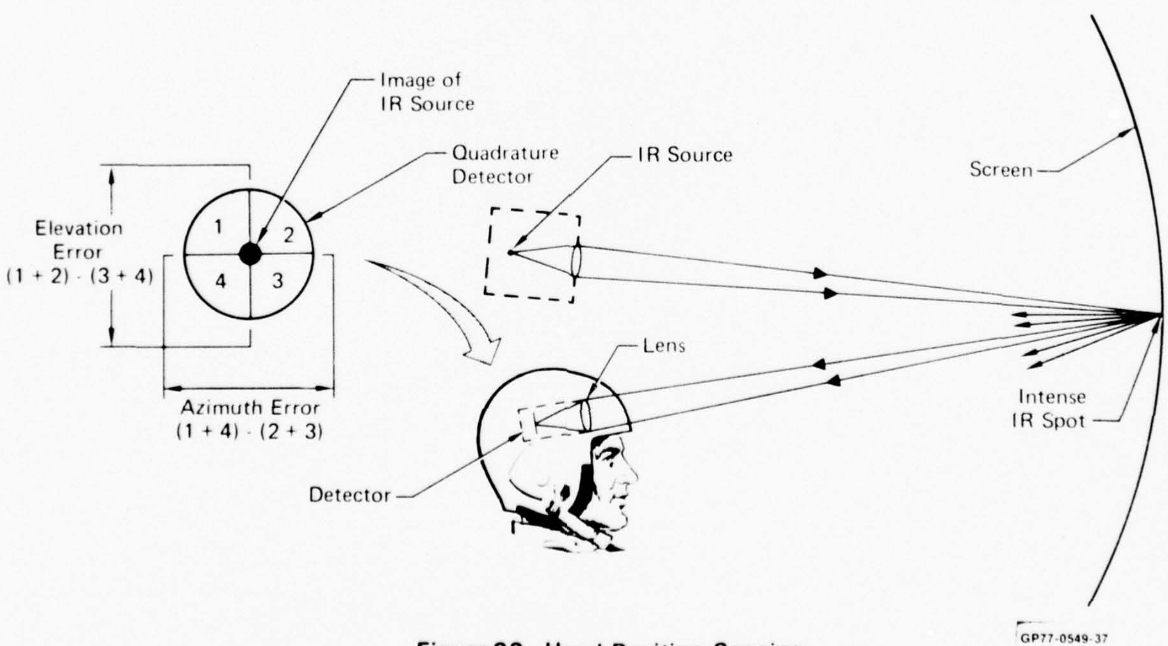

Figure 22 Head Position Sensing

For the head tracker to function properly it must have adequate sensitivity and no significant deadband. From an optical standpoint the image of the source that falls on the detector must be of sufficient size and strength to provide a useable signal/noise ratio around the null point. For this system, where uniform acuity exists over about $\pm 1°$, a threshold sensitivity of about 0.20° would seem adequate.

In the following paragraph, the sensitivity of the source will be related to other system parameters. An optical schematic and definition of terms is shown in Figure 23. The source has a radiant emittance of W_λ watts/cm^2-μ. Assuming the source has a focal length (f_1), and F/number (FNO_1), the power output of the source assembly can be computed as follows:

Assuming the source is a Lambertian emitter, its radiance is

$$N_\lambda = \frac{W_\lambda}{\pi} \text{ in } \frac{\text{watts}}{\text{steradian cm}^2\text{-}\mu} \qquad (43)$$

The power exiting the source is:

$$P_1 = N_\lambda \, \omega_1 \, A_1 \, \Delta\lambda \qquad (44)$$

where ω_1 = Solid angle subtended by the projection lens (See Figure 23)

A_1 = Source area

$\Delta\lambda$ = Source emitting bandwidth

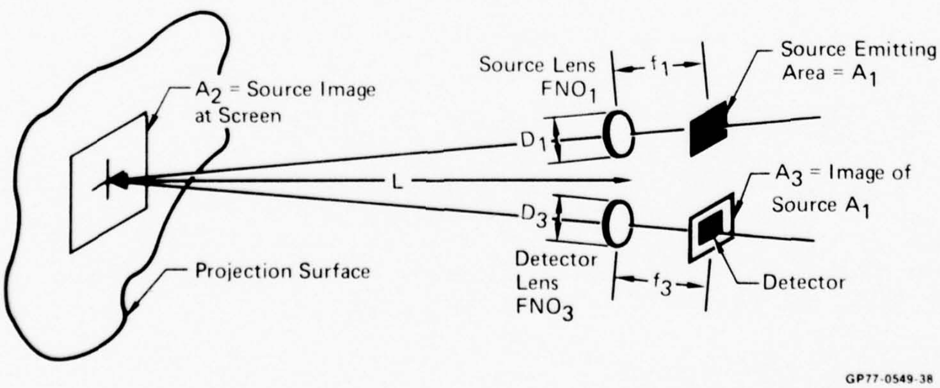

Figure 23 Head Tracking Radiometrics

The solid angle (ω_1) is

$$\omega_1 = \frac{\pi D_1^{\ 2}}{4\ f_1^{\ 2}} = \frac{\pi}{4\ FNO_1^{\ 2}} \tag{45}$$

where D_1 = Source lens diameter

f_1 = Source lens focal length

FNO_1 = Source lens F/number

It is also assumed that $\Delta\lambda$ is small enough so that N_λ remains essentially constant. If the source assembly is focused to form an image on the viewing screen a distance L from the source, the irradiance at the screen surface is

$$H = \frac{P_1}{A_2} \tag{46}$$

where A_2 = Screen area illuminated by source

From geometrical optics the source and screen areas are related by:

$$\frac{A_1}{A_2} = \left(\frac{f_1}{L}\right)^2 \tag{47}$$

and

$$A_2 = A_1 \left(\frac{L}{f_1}\right)^2 \tag{48}$$

Substituting Equation (44) through (48) into (46)

$$H = \frac{W_\lambda\ \Delta\lambda}{4\ FNO_1^{\ 2}} \left(\frac{f_1}{L}\right)^2 \tag{49}$$

Assuming a screen gain of G, the radiance of the screen is:

$$N_2 = \frac{G\ H}{\pi} = \frac{G\ W_\lambda\ \Delta\ \lambda}{4\pi\ FNO_1^{\ 2}} \left(\frac{f_1}{L}\right)^2 \tag{50}$$

The power from the screen entering the detector aperture also located a distance (L) from the screen is:

$$P_3 = N_2\ \omega_3\ A_2 \tag{51}$$

Where

$$\omega_3 = \frac{\pi D_3^2}{4L^2} \qquad (52)$$

Substituting Equations (48), (50), and (52) into (51) results in an equation defining the power incident on the detector as a function of system parameters.

$$P_3 = \frac{G W_\lambda \Delta\lambda D_3^2 A_1}{16 FNO_1^2 L^2} \qquad (53)$$

The detector selected was a UDT, Inc. PIN SC/25. Saliant characteristics for this cell are:

Spectral Response	$\pm$ 5% 350-1100 nm
Dark Current	7.5μamps Max
Position Sensitivity	0.32 amps/watt-cm
Active Area	3.5 cm^2 (.74x . 74 inches)
Minimum Spot Size	0.05 inch

For this application an output exceeding the dark current of 7.5 μamps for an angular spot displacement of 0.2° is desired. Thus the desired sensitivity to angular inputs should be:

$$S_o = \frac{\text{Dark current}}{\text{Threshold}} = \frac{7.5\ \mu\text{amp}}{0.2\ \text{deg}} = 37\ \mu\text{amp/deg} \qquad (54)$$

To define the sensitivity in terms of linear displacements, Equation (54) must be adjusted by the detector focal length, thus the desired position sensitivity is:

$$S_L = \frac{2120}{f_3} \frac{\mu\text{amps}}{\text{cm}} \qquad (55)$$

We can equate the desired position sensitivity to the cell actual position sensitivity, thus

$$S_L = \text{Actual position sensitivity x Incident Power} \qquad (56)$$

Substituting Equation (55) into (56) and solving for the incident power results in:

$$P_3 = \frac{2120}{f_3} \frac{\mu\text{amp}}{\text{cm}} \times \frac{1}{.32 \frac{\text{amp}}{\text{w-cm}}} \qquad (57)$$

$$= \frac{6.62\ (10^{-3})}{f_3} \text{ watts} \qquad (58)$$

The incident power (P_3) was defined in Equation (53). The focal length (f_3) in Equation (58) is defined in terms of F/number and lens diameter, viz:

$$f_3 = D_3 \, FNO_3 \qquad (59)$$

Substituting Equation (53) and (59) into (58) results in an equation which interrelates the detector and source parameters, viz:

$$\frac{G \, W_\lambda \, \Delta\lambda \, f_3^{\,3} \, A_1}{16 \, FNO_1^{\,2} \, FNO_3^{\,2} \, L^2} = 6.62 \, (10^{-3}) \qquad (60)$$

Of the above parameters, G and L are available from display geometry. The parameters ω_λ, $\Delta\lambda$, A_1 can be obtained from the source parameters.

A 1763 prefocused incandescent standard light bulb was chosen for mechanical reasons and has the following characteristics:

- o Temperature 4000°K
- o Source Dimensions 0.06 x 0.12 inches = 0.4645 cm^2

A Wratten No. 88A filter was selected to attenuate the visual and transmit the infrared wavelengths. This filter cuts off below 300 nm. The cell response limits the upper responsitivity to 1000 nm. This establishes the wavelength band to:

$$\Delta\lambda = 200 \text{ nm} = 0.2\mu$$

The 4000°K source has an average radiance over this wavelength band of

$$W_\lambda = 1000 \, \frac{\text{watts}}{cm^2 - \mu}$$

Using a screen gain of 4 and distance to the screen of 54 inches (137 cm) and substituting these values into Equation (60) results in

$$f_3 = 1.75 \, FNO_1^{\frac{2}{3}} \, FNO_3^{\frac{2}{3}} \qquad (61)$$

The aperture diameter of the source and receiver are related by their respective focal lengths, viz:

$$\frac{D_1}{D_3} = \frac{f_1}{f_3} \qquad (62)$$

The detector aperture (D_3) has a diameter of 0.05 cm and if the smaller dimension of the source is equal to its aperture (D_1), the focal lengths are related by:

$$\frac{f_1}{f_3} = \frac{0.1524}{0.05} = 3.05 \tag{63}$$

A 2 inch focal length lens with a 1.5 inch aperture diameter was selected for the source optics. Thus the F/number is:

$$FNO_1 = \frac{2.0}{1.5} = 1.33$$

The focal length of the detector from Equation (63) is:

$$f_3 = \frac{2}{3.05} = 0.66 \text{ inch}$$

The required detector F/number is therefore

$$FNO_3 = \sqrt{5.35 \frac{FNO_1^{\,2}}{f_3^{\,3}}} \tag{64}$$

$$FNO_3 = \sqrt{5.35 \frac{(1.33)^2}{(.66 \times 2.54)^3}} = 1.42$$

The chosen detector field-of-view can be determined by:

$$\tan \frac{\theta}{2} = \frac{\text{detector size}}{2 \times f_3} = \frac{0.74}{2 \times 0.66} \tag{65}$$

Thus the field-of-view is:

$$\theta = 58°$$

After a search of available lenses, a double convex aspheric was selected. This lens had a focal length of 0.94 inches and a diameter of 1.5 inch. Therefore its F/number is:

$$FNO_3 = \frac{.94}{1.5} = 0.63$$

While the field-of-view would be somewhat reduced with this lens i.e.,

$$\theta = 43°$$

the threshold will be improved by the ratio

$$\frac{f_3^{\;3}}{FNO_3^{\;2}} \; \frac{(FNO_3)^2}{f_3^{\;3}} = \frac{.94^3}{.63^2} \; \frac{1.42^2}{.66^3} = 14.5$$

This allows sufficient margin for more filtering if required and/or allows operation of the source at a lower power input.

The assembled sensor can be seen on Figure 24 while the source is seen on Figure 25. An additional Wratten 88A filter was found to be necessary on the detector to reduce its sensitivity to visual wavelength band. The response of the final detector system is shown on Figure 26.

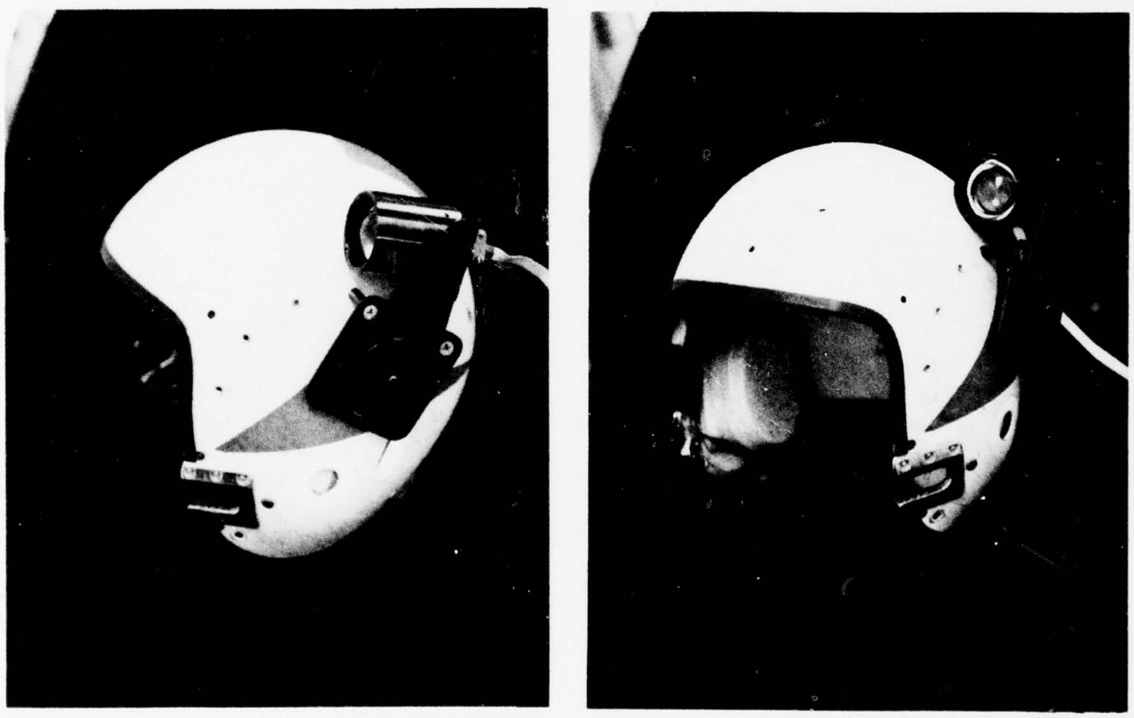

(a) (b) GP77-0549-69

Figure 24 Helmet Mounted Detector

GP77-0549-68

Figure 25 Projector Mounted Source

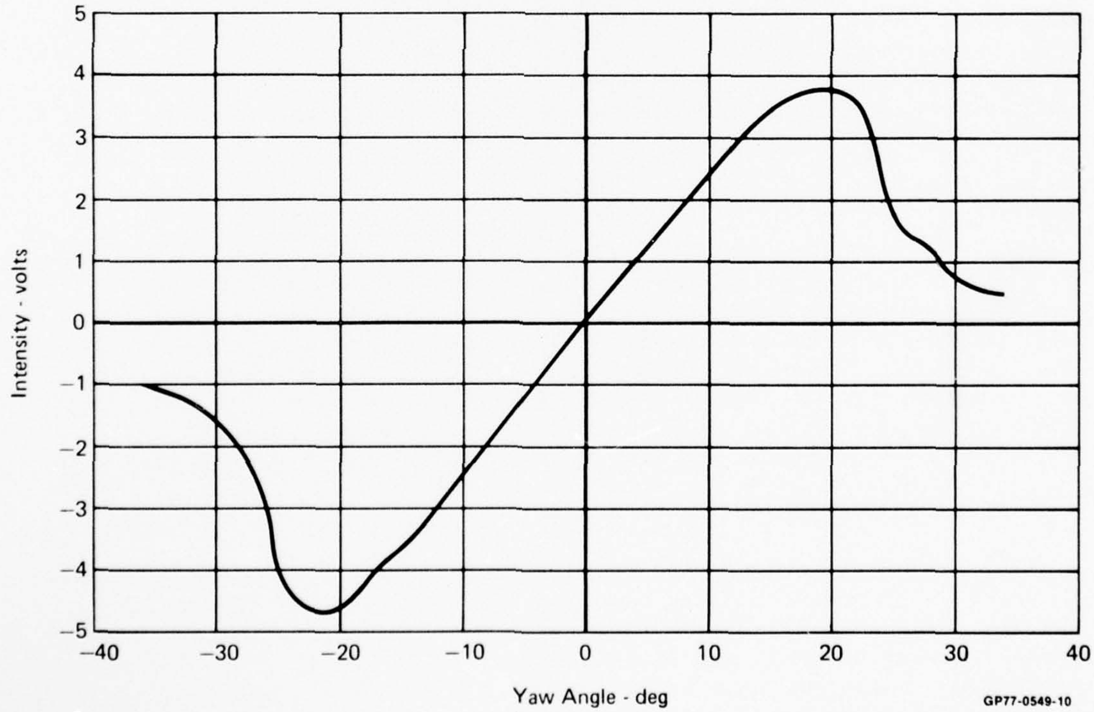

Figure 26 Response of Infrared Head Tracking Detector System

Section 4

MECHANICAL DESIGN AND FABRICATION

Detail drawings of the camera assembly and projector assembly and their components are included in this section.

4.1 CAMERA ASSEMBLY (P/N 71A050002-1001)

The camera assembly is shown in Figure 27. Camera and pitch axis assembly is supported by forks from the yaw axis assembly. Wiring for TV camera and pitch position encoder are flat cables secured to one of the forks.

PITCH AXIS (P/N 71A050002)

The pitch axis assembly is shown in Figure 28. Pitch shaft (-27) is supported on bearings in both forks. Bearings are fully retained in both forks. The pitch axis torque motor (Inland T-5135, 4 lb.-ft.) is mounted in the -49 fork, pitch position encoder (Baldwin 5X232BL) and pitch stops in the -51 fork. The pitch stops, -39 and -41 permit ± 60° rotation (from horizontal) with the yaw axis vertical as in Figure 27 or horizontal. A removeable pin is provided to lock the pitch axis in the horizontal position.

YAW AXIS (P/N 71A050003)

The yaw axis assembly is shown in Figure 29. Fork supported block is mounted on -57. Yaw shaft (-59) is supported by 2 bearings the lower of which is fully retained, the upper is free to move axially in the support housing (-65). The yaw torque motor (Inland T-5730, 7 lb.-ft.) and yaw position encoder are mounted within the support housing. Stops (not shown) limit yaw travel to ± 90°, and a removable pin locks the yaw axis at 0°.

OPTICAL ELEMENTS AND MOUNTS

The optical elements layout is shown in Figure 30. The attach points are located as shown in Figure 31. The -1 base plate is mounted on -27 pitch shaft and provides the mount for the non-linear lens (T-054427-1) the relay optics, and television camera. The optical centerline of the non-linear lens is 2 inches below the pitch axis. The axial position of all relay optics except a field lens mounted in -79 shown in Figure 30 is adjustable along the optical axis. Folding mirrors are adjustable about 2 axes. A cover (not shown) is provided and is attached to the -1 base plate.

4.2 PROJECTOR ASSEMBLY (P/N 71A050003-1001)

The projector assembly is shown in Figure 32(a) and (b) and is supported by 71A050004 support structure shown on the upper part of Figure 32(b). The yaw axis bearing is a single 25 inch I.D. "x" section bearing designed to carry moments as well as axial and radial loads. This support method was selected to preclude a long yaw axis shaft (and a pair of conrad type bearings) and permit mounting the entire assembly within the dome. The yaw torque motor

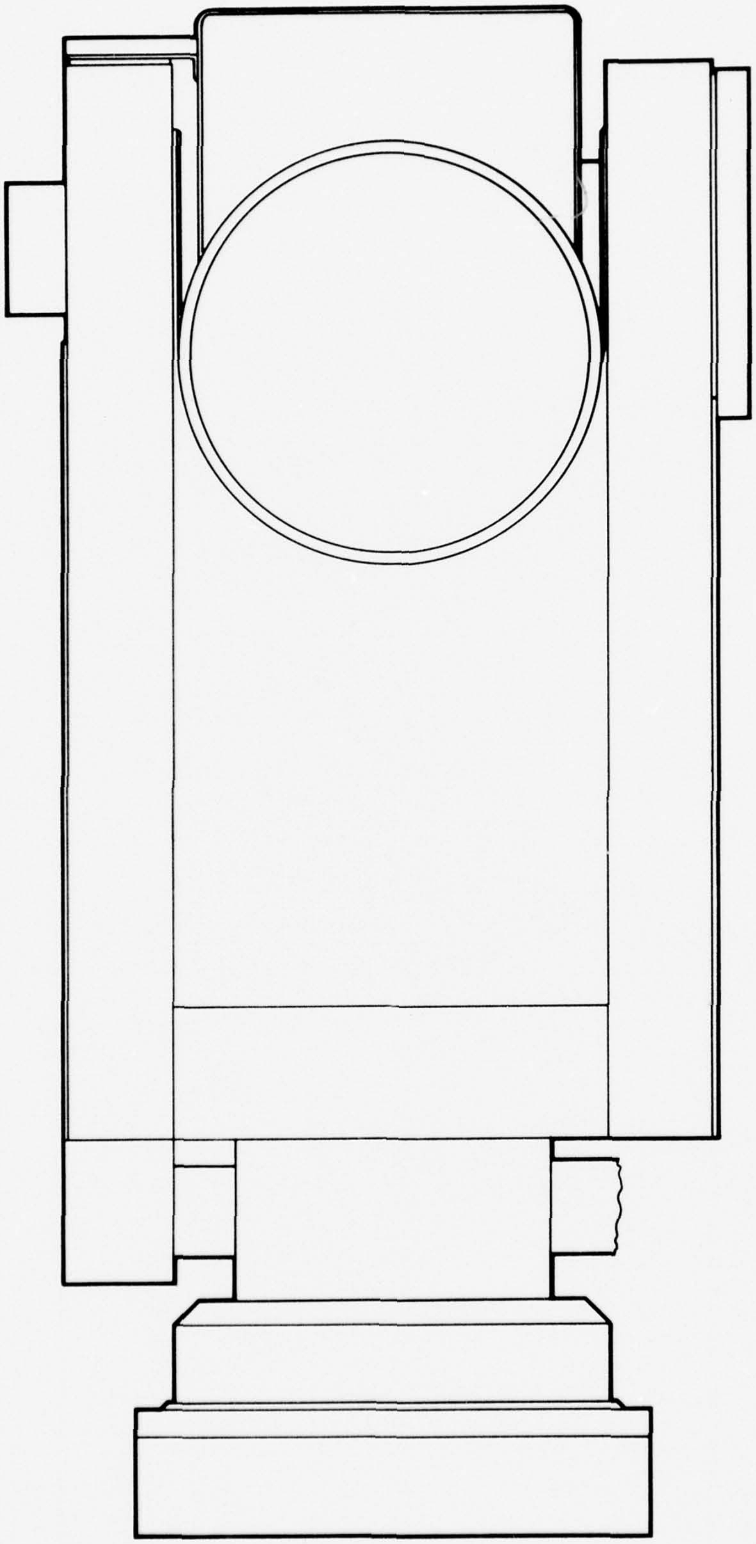

Figure 27 Camera Assembly

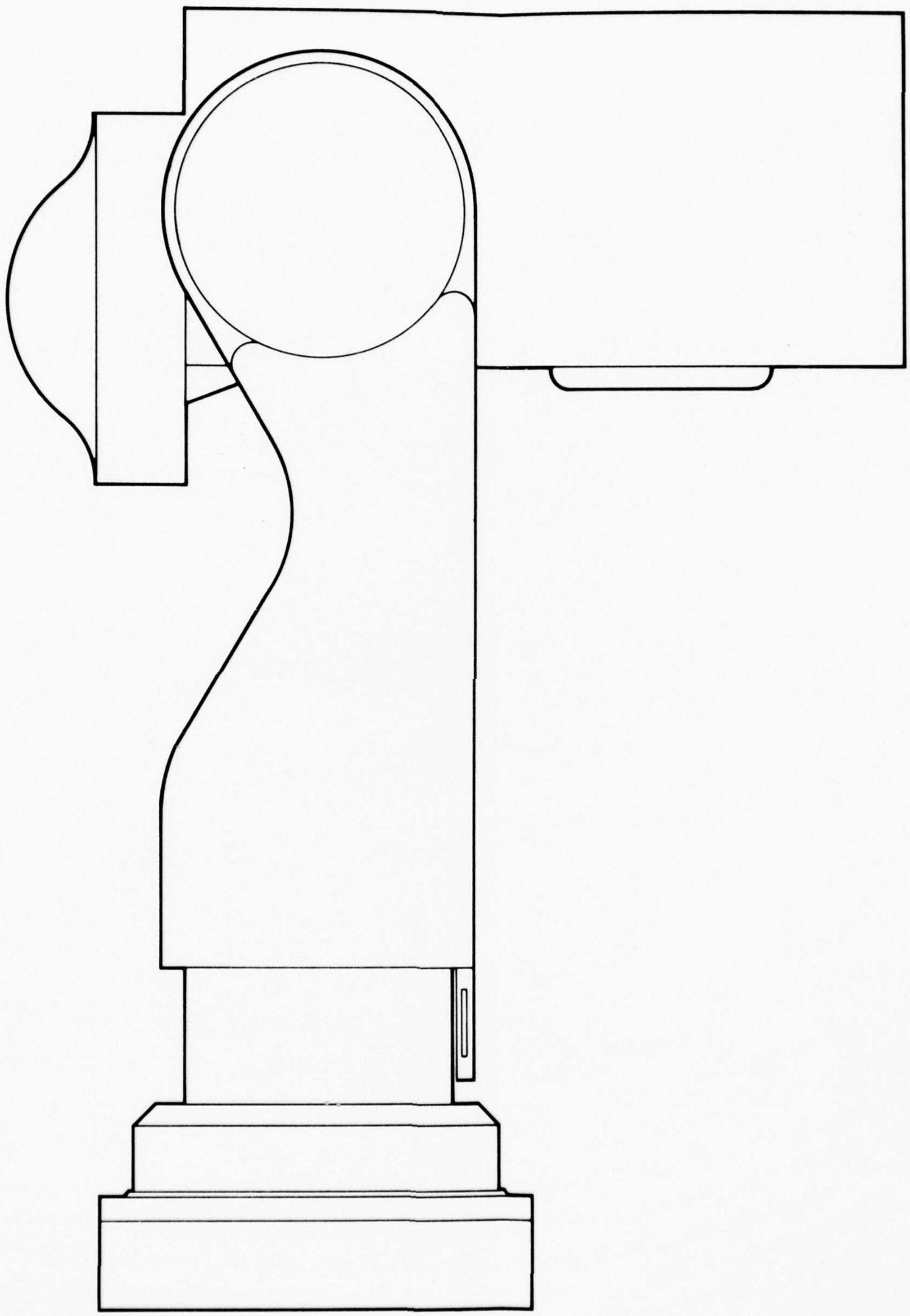

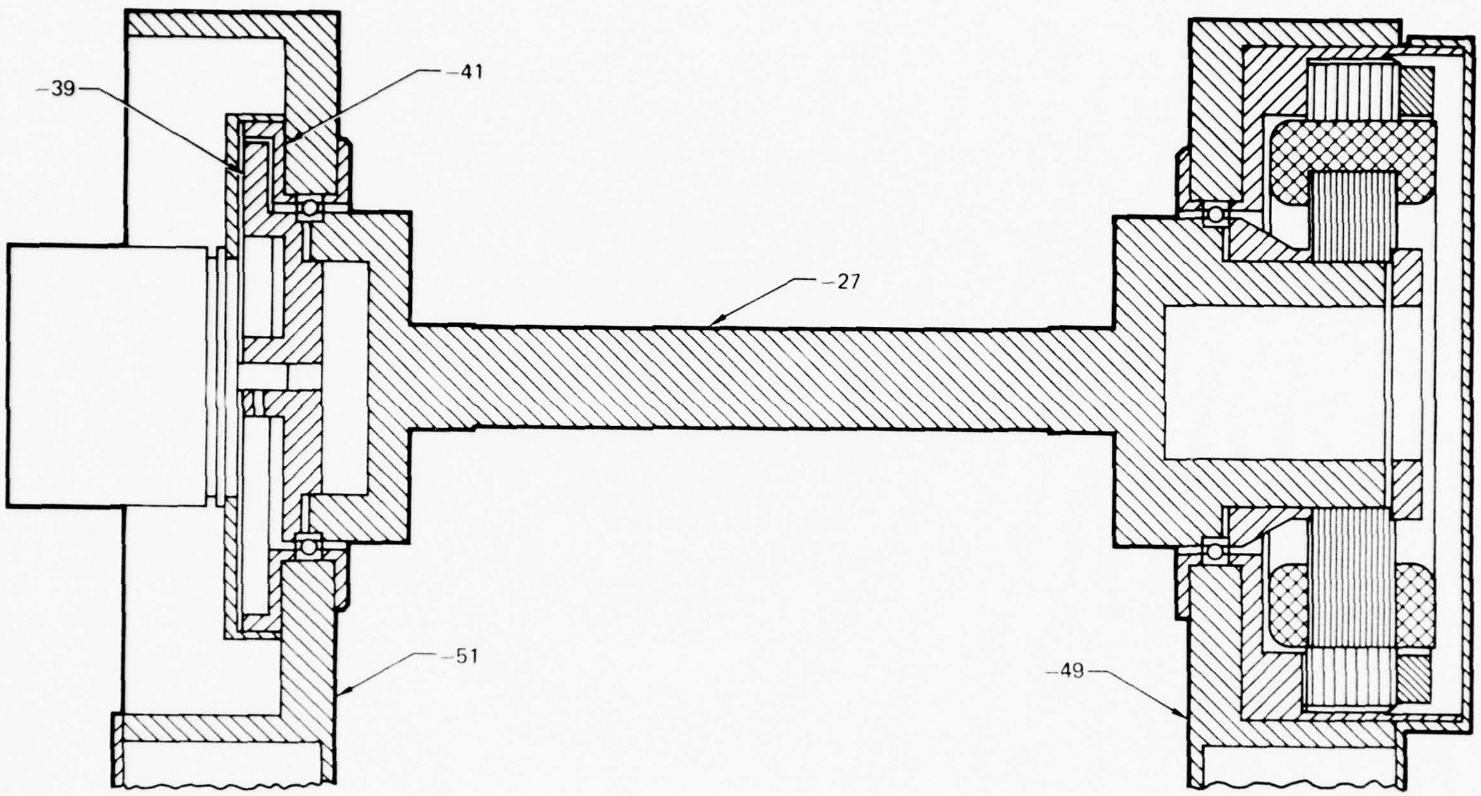

Figure 28 Pitch Axis

GP77-0549-49

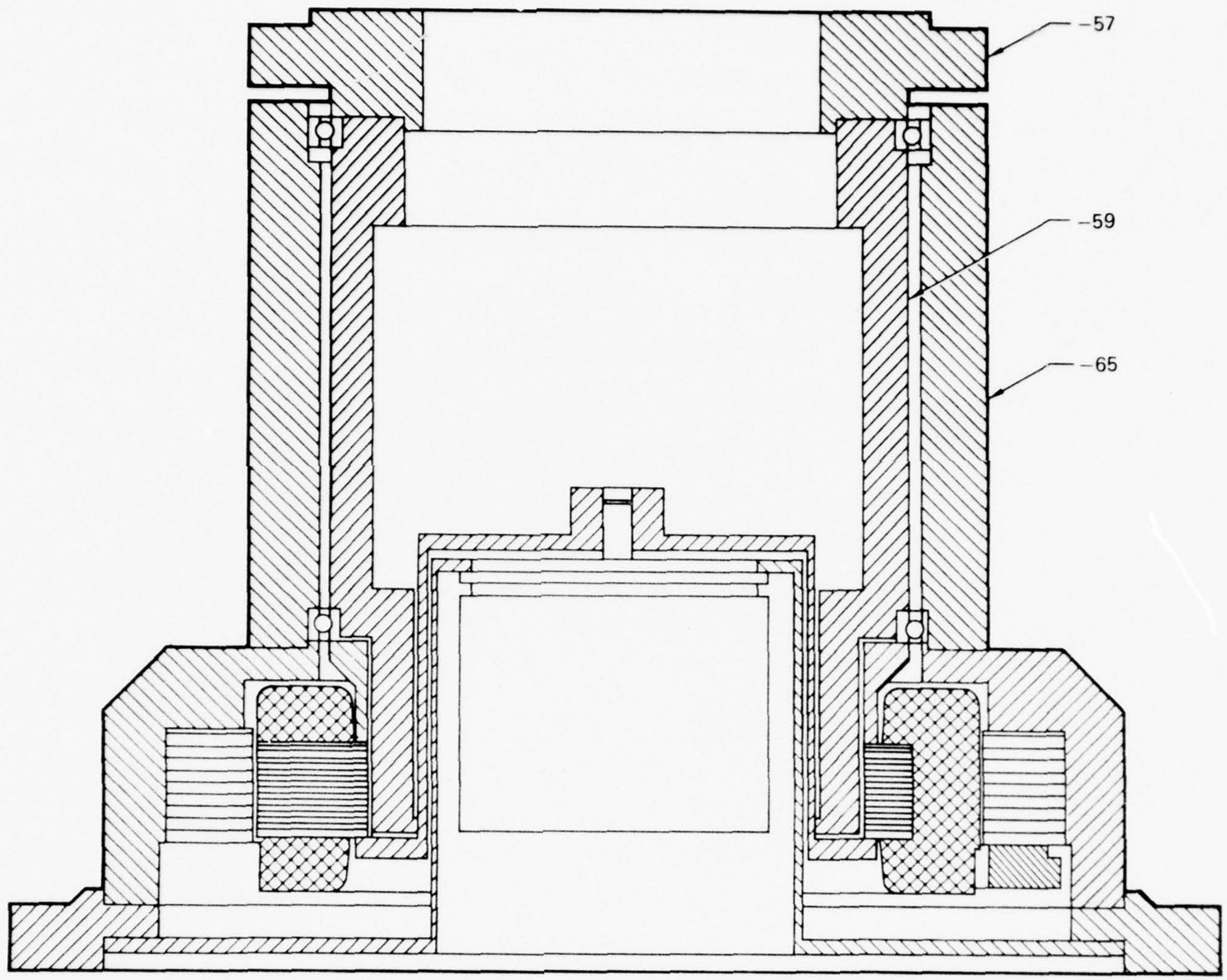

Figure 29 Yaw Axis Assembly

GP77-0549-50

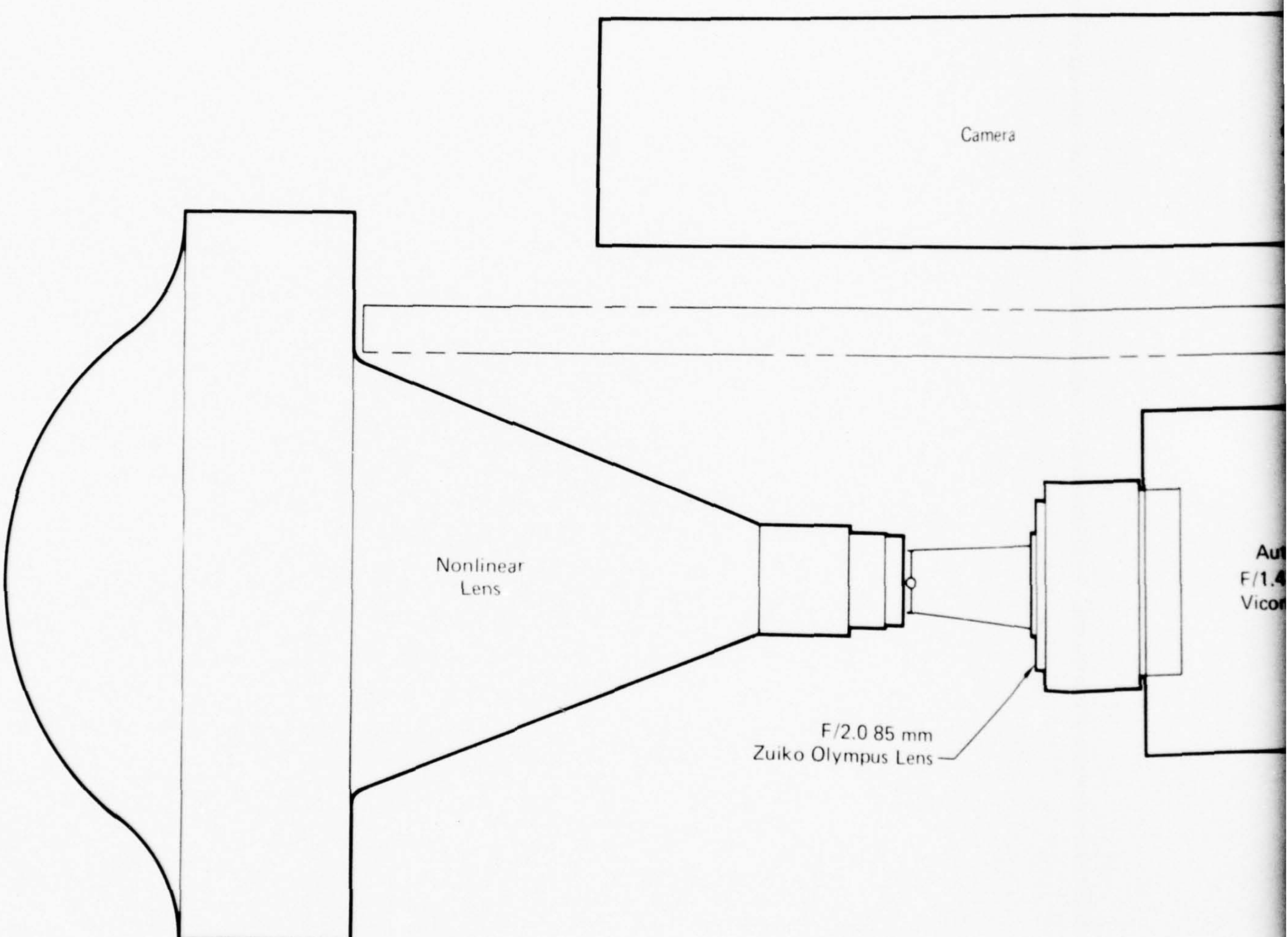

Figure 30 Camera Optical Elements

GP77-0549-51

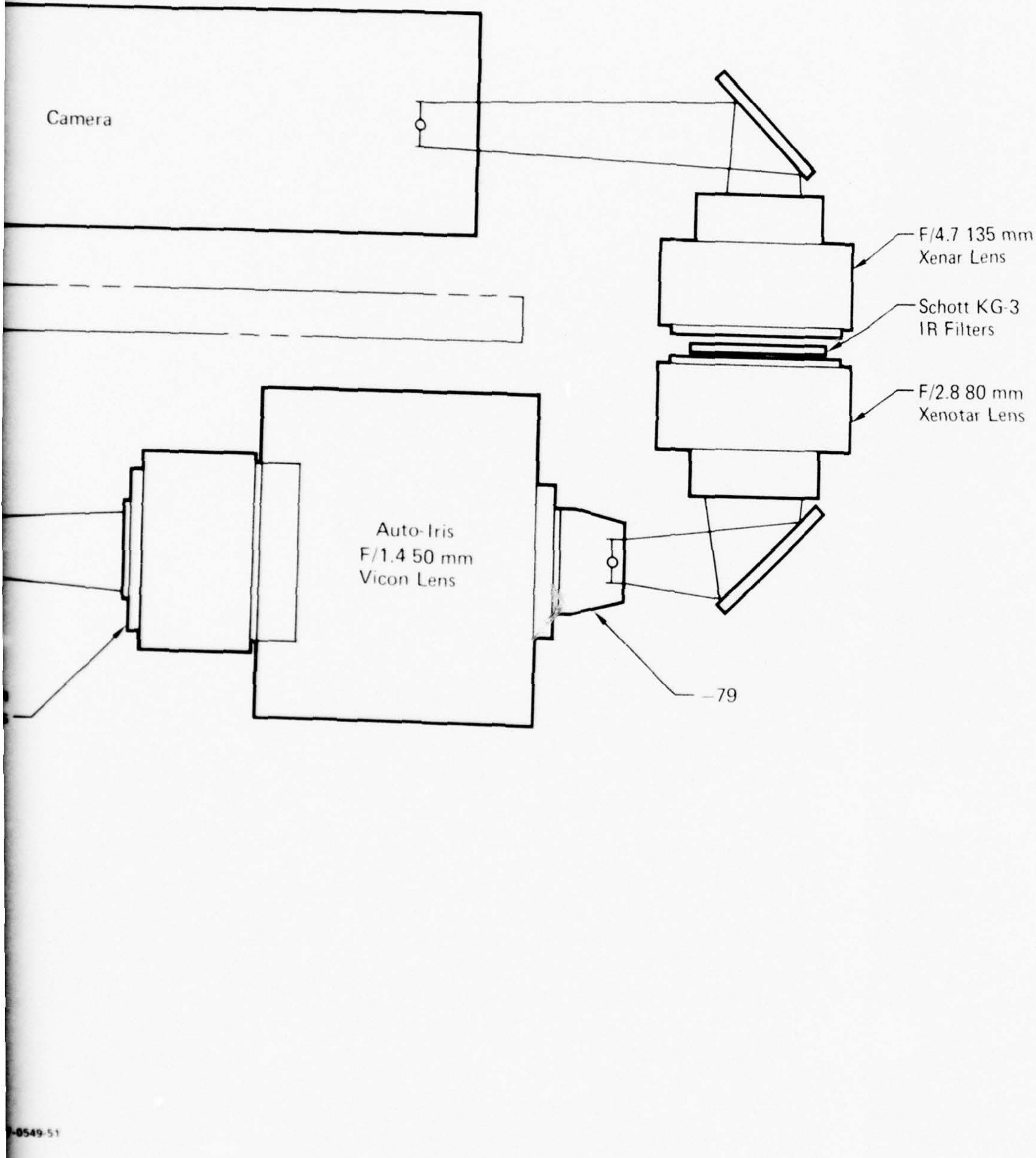
Camera
F/4.7 135 mm
Xenar Lens
Schott KG-3
IR Filters
F/2.8 80 mm
Xenotar Lens
Auto-Iris
F/1.4 50 mm
Vicon Lens
79
0549-51

2

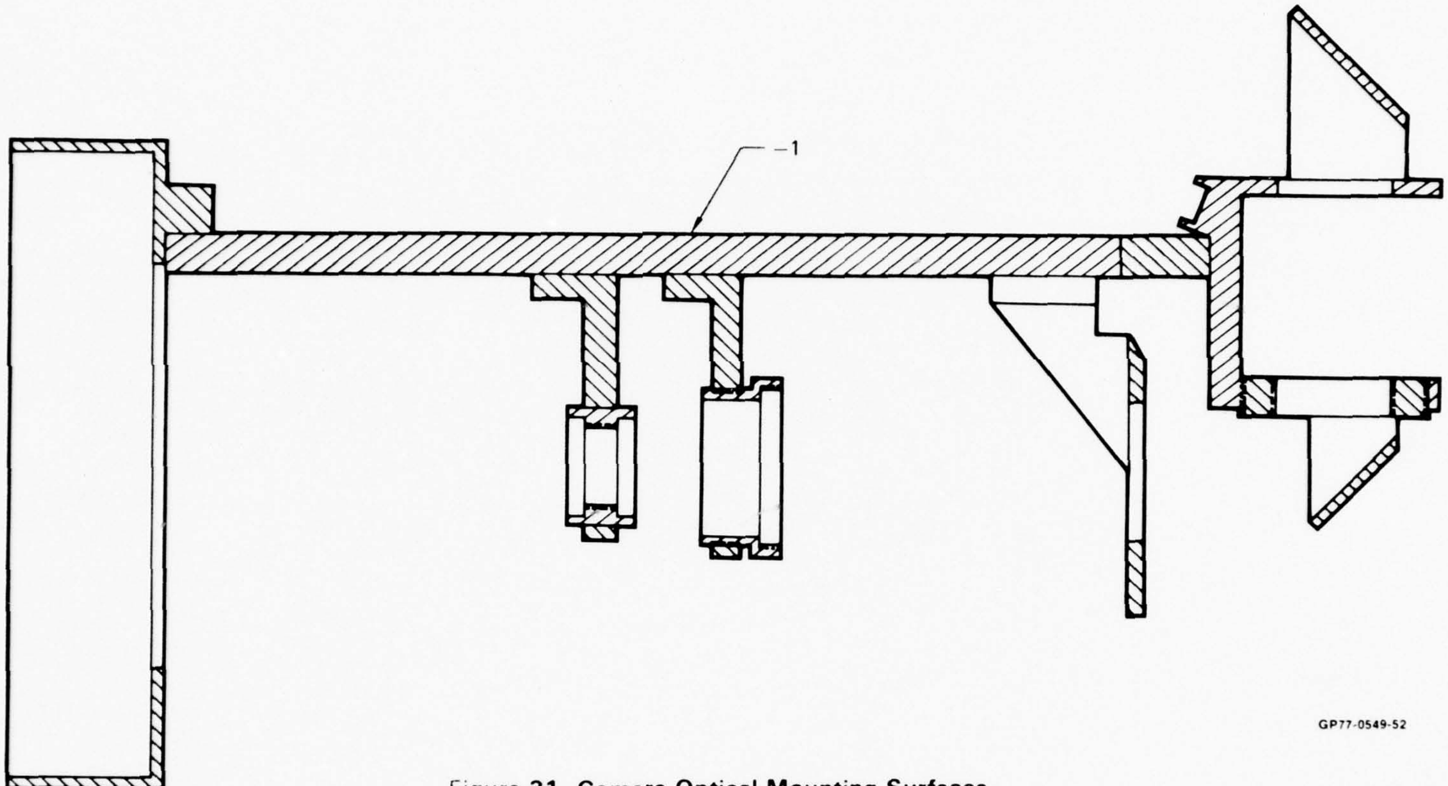

GP77-0549-52

Figure 31 Camera Optical Mounting Surfaces

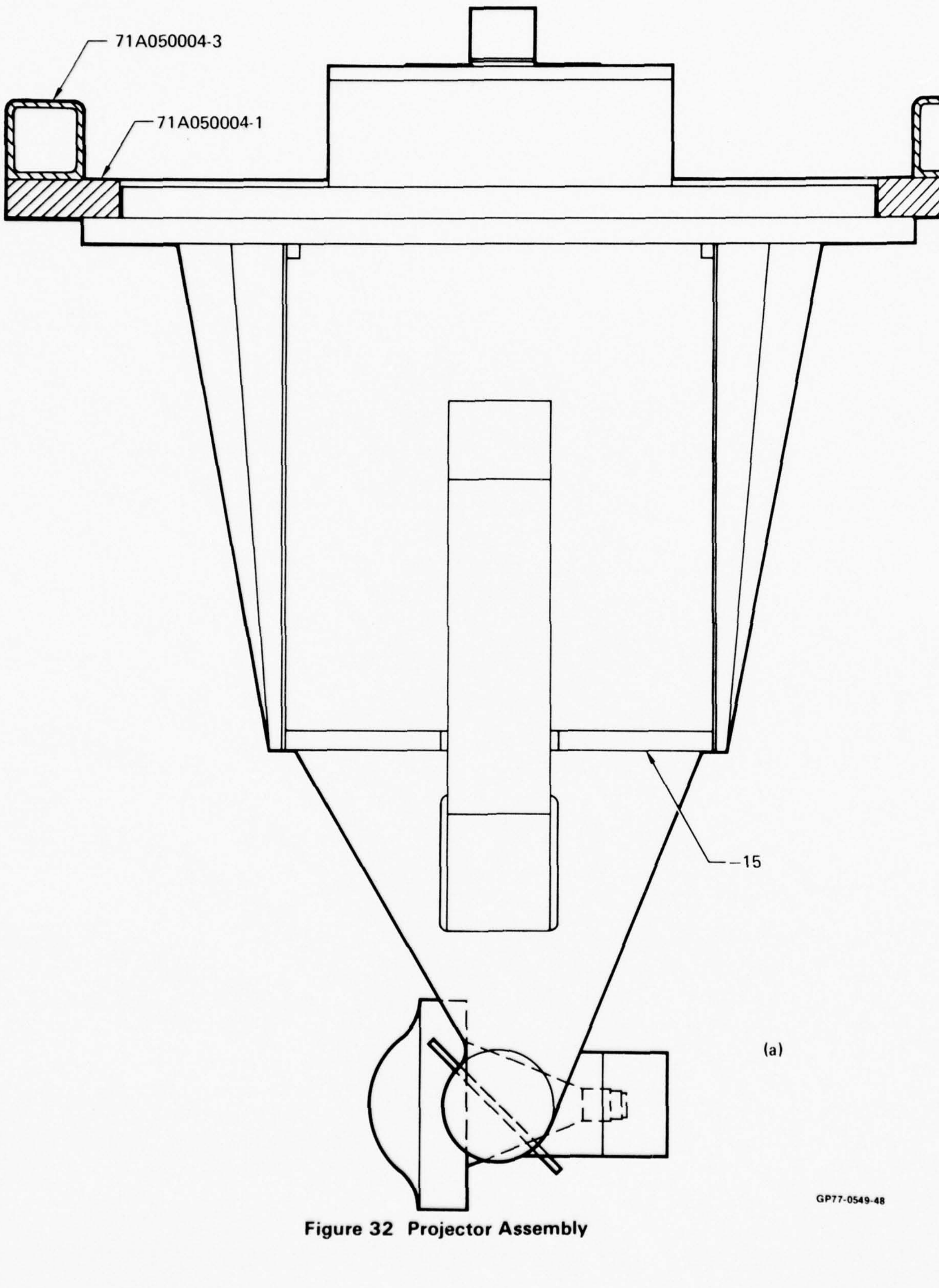

Figure 32 Projector Assembly

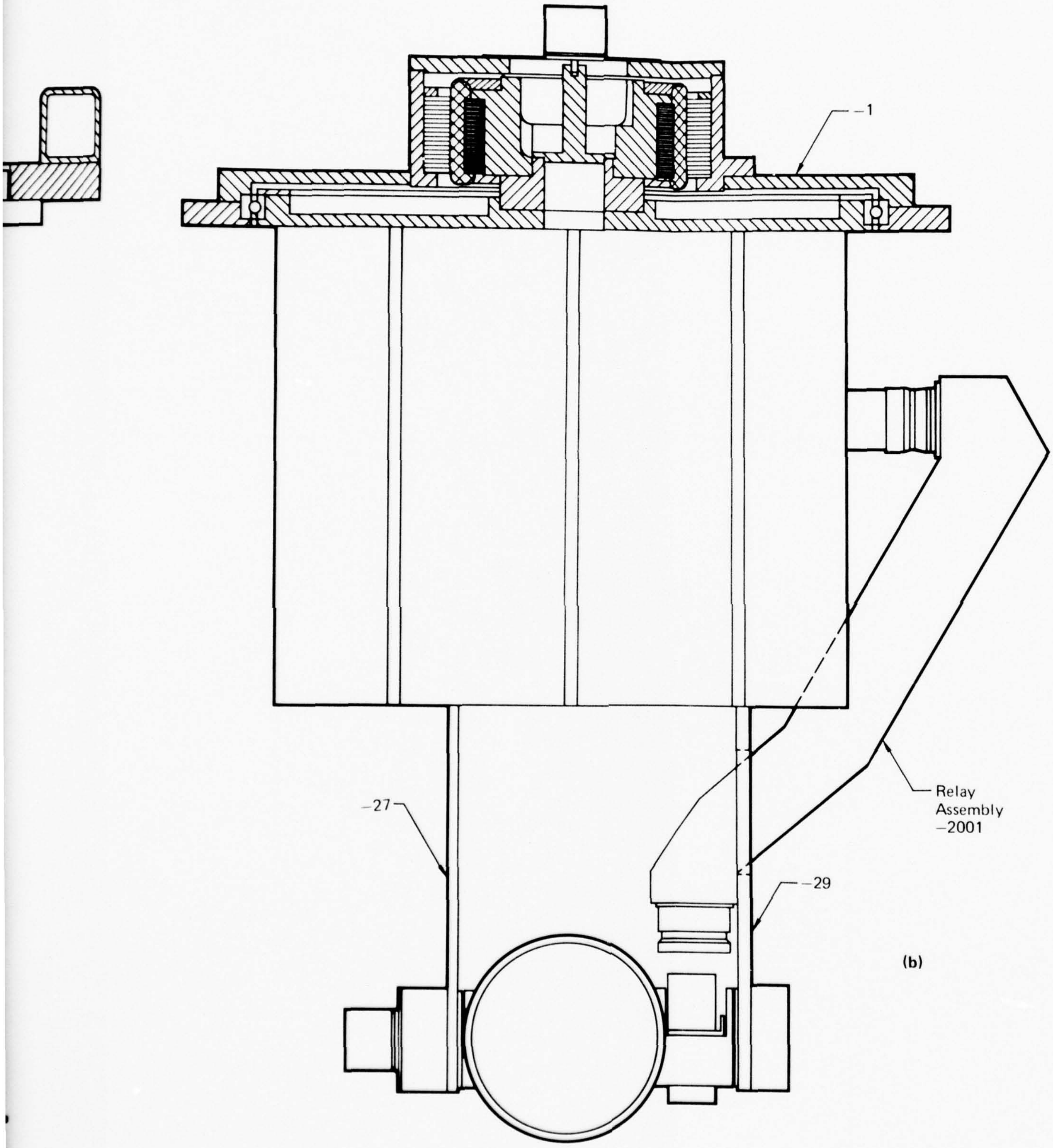

(b)

(Inland T-10035, 100 lb.-ft.) and yaw position encoder are mounted on the -1 plate above the bearing. The projector is mounted within a box structure supported by the yaw bearing. Holes in the box at appropriate locations provide access to projector controls. Bottom plate of the box supports the pitch axis forks. Yaw travel is limited by stops (not shown) on the 71A050004-1 plate to approximately $\pm 120°$. The stops are spring loaded to provide essentially uniform deceleration for 15° of rotation (of the yaw axis) before becoming "hard" stops. Limit switches short the yaw motor just before engaging either stop.

Fork arms (-27 and -29) support the pitch axis assembly. The -29 fork and bottom plate (-15) of box sturcutre support the -2001 relay assembly.

RELAY ASSEMBLY (P/N 71A050003-2001)

The relay assembly is shown on Figure 33 and supports and locates 4 of the 5 required relay lenses and 3 of the 6 required mirrors, the remaining lens and mirrors are mounted within the pitch axis assembly. All lenses in the relay assembly are adjustable along the optical axis, and all mirrors are adjustable about 2 axes.

PITCH AXIS (P/N 71A050003)

The pitch axis assembly is shown in Figure 34. The -27 fork mounts the pitch axis torque motor (Inland T-2950, 1.2 lb.-ft.) and pitch position encoder (Baldwin 5V232BL). Stops are provided to limit pitch travel to $\pm 60°$ (from horizontal). A removeable pin (in the -29 fork) locks the pitch shaft in the horizontal position. A "half angle" drive is provided for the relay mirror mounted on the -55 mirror support. The "half angle" is obtained by a differential on the -29 fork. A ring gear (PIC N3-4-5) is fixed to the differential case (-99, -47, -45), a second gear is fixed to the pitch shaft (-43, -39). The planet gears, to which is mounted the "half angle" mirror (-51, -53, -55), rotate in the same direction as the pitch shaft but at one-half the angular rate. The mirror may be "zeroed" by rotating the -47 cover with respect to the -45 housing. The -109 ring is the mount for the corrector lens (not shown).

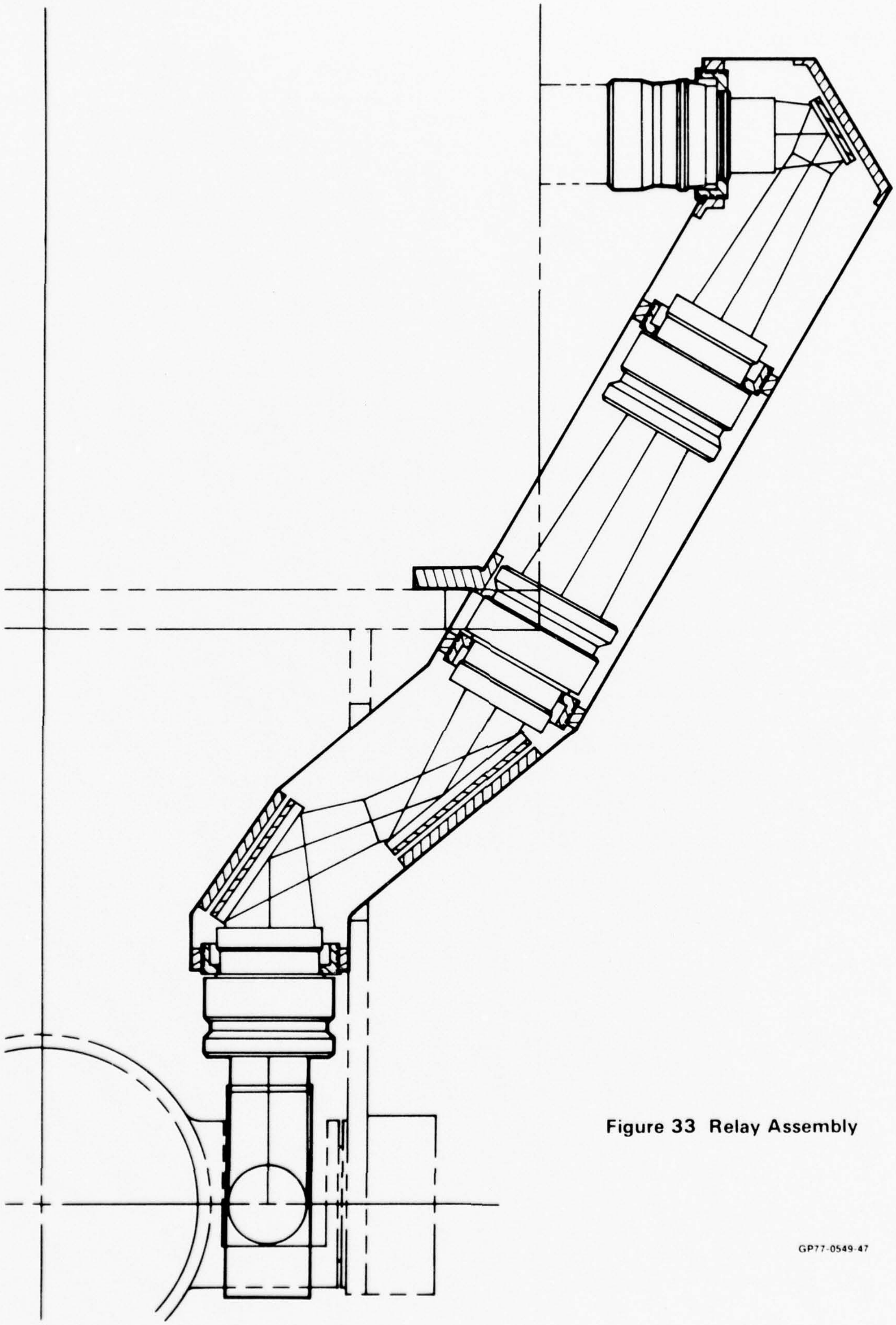

Figure 33 Relay Assembly

GP77-0549-47

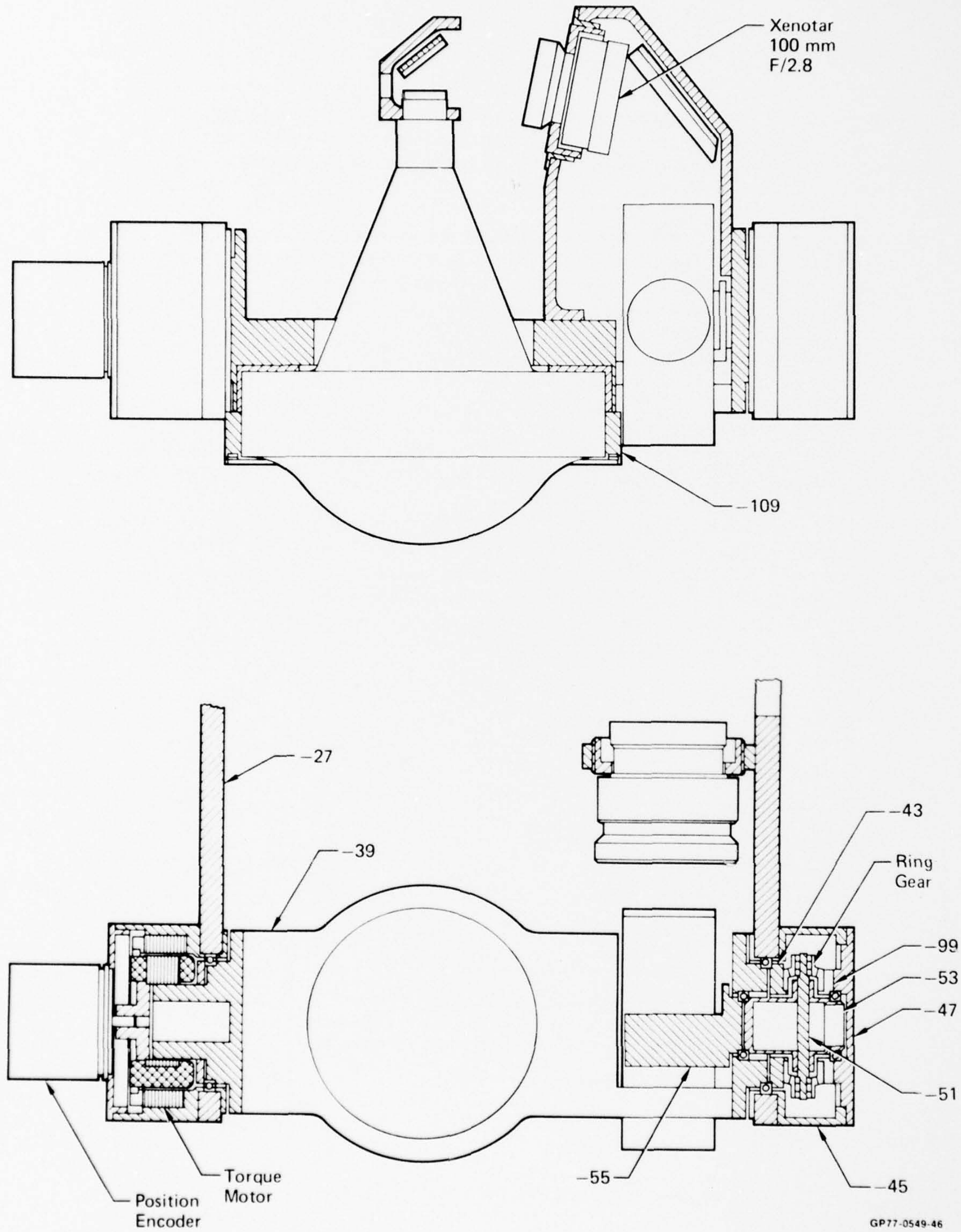

Figure 34 Projector Pitch Axis Assembly

Section 5

CONTROL SYSTEM

The function of the Control System is to command the projector to follow changes in camera angle. Camera angle changes are commanded by changes in operator head position or joy stick input. It consists of these major parts; the microprocessor, the camera electronics box, and the software.

The general design of the control system has been done digitally. The digital design of this system is in general immune from the kind of problems such as drift and error due to the manufacture of position and rate signals that beseech common analog servos. The mathematic production of rate signals from position data and digital (PCM) transmission of control signals eliminate many noise and signal related problems, although some signal errors still show up. In the case of a digital system these errors show up in varying degrees. For example, a lower order bit could be dropped and probably not be noticed by the system, but the system would surely jump if the sign bit or one of the higher bits suddenly is in error. Filters and other protective software have been programmed to help smooth out the results of such signal errors.

Figure 35 is a block diagram showing the camera and projector servos, the microprocessor which is located at the home station and the camera electronics box at the remote site. The system uses serial data to communicate between the microprocessor and the camera electronics box. Figure 36 shows a more complete block diagram of the hard wired control system. The microprocessor allows the system to be operated in three basic modes:

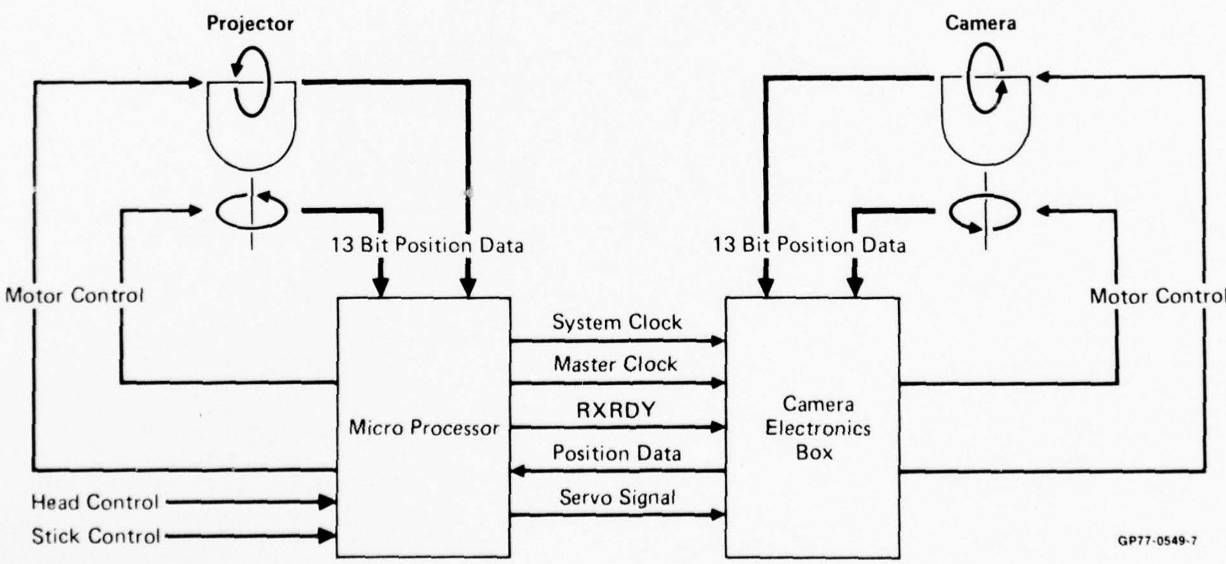

Figure 35 Servo Control Block Diagram

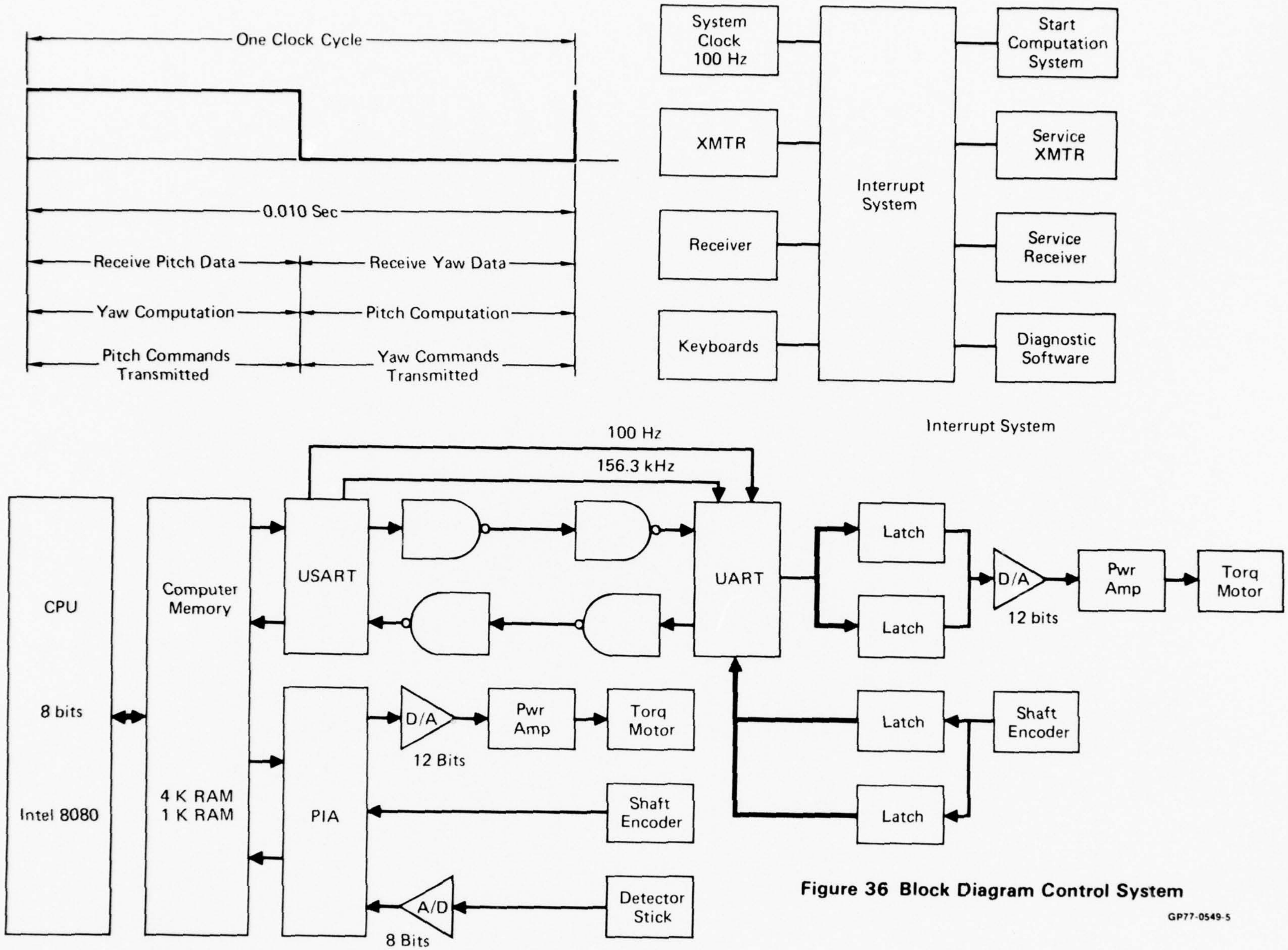

Figure 36 Block Diagram Control System

GP77-0549-5

MODE 1) Camera servo fully operational, the projector axes are pinned and the system is joy stick controlled. In this mode the high acuity spot is stationary while the "whole picture" moves about the dome.

MODE 2) The camera and projector servos are fully operational. The display picture is stabilized and the system is joy stick controlled. In this mode, the high acuity portion of the image is slewed about, using the joy stick control to the point of interest while the picture as a whole is stationary.

MODE 3) Camera and projector servos are fully operational and head controlled. This is generally the preferred mode of operation and the display is the same as in Mode 2 except that the camera and projector follow-up are controlled via a helmet mounted position detector.

These three modes allow the user to tailor the remote viewing system to his own particular needs.

This section contains a description of the control system and is divided into task oriented subsections which are: a description of the microprocessor, the camera electronics box, and software. In addition, included is a section on the head tracker and a section on the math models on which the software is based. Finally in the last section are system operation procedures.

5.1 MICROPROCESSOR HARDWARE

The basic microprocessor is the Intel 80/10 packaged in the SBC80 Modular Backplane/Card Cage with an I/O expansion board and prototype board. Diagnostic hardware, real time interrupt logic, power supplies, and some analog hardware were integrated with the Intel SBC 80 into one package resulting in a mini-computer for the Remote Viewing System.

The 80/10 Intel microprocessor board contains:

1 - 8080A Central Processor
1 - 8251 Serial I/O
1 - 8255 Parallel I/O
4 - 8708 1K-PROM-UV eraseable
1 K BYTES OF RAM

and line drivers and terminators. In addition to the hardware listed, a computer emulator and PROM programmer were available at the suppliers for scheduled use.

5.1.1 Diagnostic Hardware

The hardware consists of two hexadecimal keyboards, 5 hexadecimal LED displays, address comparators, and miscellaneous gates and logic and is shown in Figure 37. One keyboard is implemented as a function keyboard via the software and the other keyboard is implemented as a data/address keyborad via the software. The keyboards and LED Displays are front panel mounted on the computer. The rest of the hardware is mounted on the back of the front panel and on the prototype board.

Real Time Interrupt Hardware

The processor has provisions for six real time interrupts. They are designated MCLR, RXRDY, TXRDY, KB1, KB2, AND COMPARATOR on Figure 37. The basic interrupt channel is shown in Figure 38.

The computer controls the active status of the interrupt channel by inputs to the channel enable and reset gate. When the channel is active, an interrupt from an external device sets the Q output of the flip-flop. The Q output generates an interrupt pulse to the computer and sets a bit in the computer interrupt input port. The computer software interrupt handler service routines polls the interrupt input port to determine the source of the interrupt and thereby takes the desired path. During this time all other low priority interrupts are disabled. For example, if an RXRDY interrupt came in while a TXRDY interrupt was being serviced, it would not recognize the RXRDY request until the TXRDY service was completed. High priority interrupts from the keyboards are always active.

All six interrupt channels operate in the same way and are mixed together at the eight input NAND Gate. The output of this gate drives the computer interrupt line. The hardware involved in an interrupt channel is a computer output port, computer input port, and gate, and a Flip-Flop.

Operation of one interrupt channel can be described as follows. The computer has instructions which enable and disable the external interrupt line. With the interrupt line enabled, the software sets the bit that is assigned to the channel being discussed. This bit appears as input to the 7408 gate as shown in Figure 37. The line from Reset is normally high and so the input to the preset channel of the Flip-Flop is high and active. The inputs to the NAND gate are all high and the channel is ready to accept an interrupt. An interrupt from an external source causes the Flip-Flop to go low. The Flip-Flop output causes the NAND gate output to go high generating a computer interrupt and it also sets a bit assigned to this channel at a computer input port.

Software samples the input port, determines which interrupt channel has requested service, sets the active status of all interrupt channels according to the priority level of the interrupt that has just occurred and proceeds to service the interrupt. When service is complete, software resets the output port which sets the Flip-Flop and then sets the output port so that the channel is again active. It also resets the other channels and

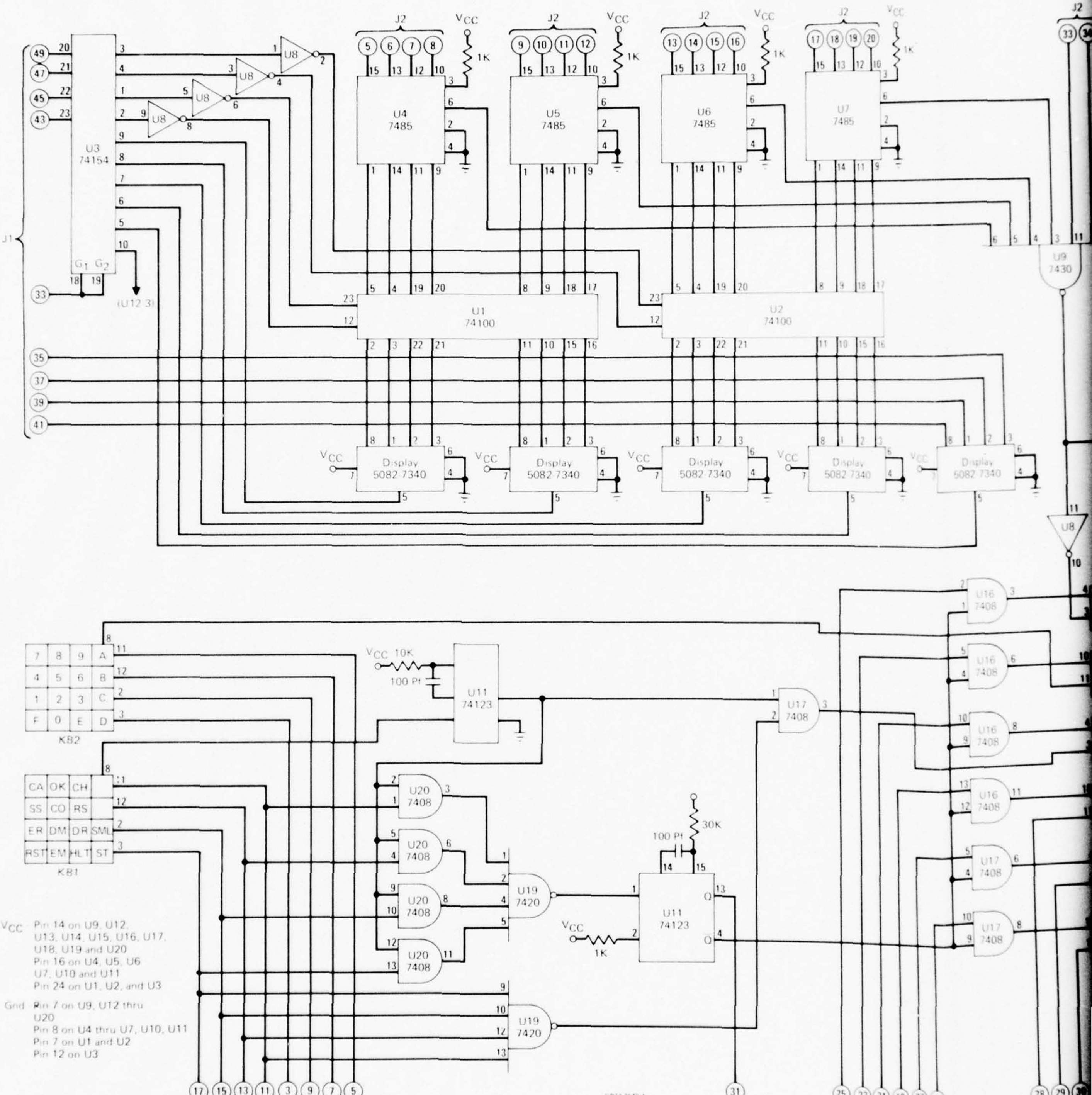
J1
J2
VCC
1K
U3
74154
G1 G2
(U12 3)
U8
U4
7485
U5
7485
U6
7485
U7
7485
U9
7430
U1
74100
U2
74100
Display
5082 7340
KB2
7 8 9 A
4 5 6 B
1 2 3 C
F 0 E D
VCC 10K
100 Pf
U11
74123
U17
7408
U16
7408
CA OK CH
SS CO RS
ER DM DR SML
RST EM HLT ST
KB1
U20
7408
U19
7420
30K
1K
VCC Pin 14 on U9, U12, U13, U14, U15, U16, U17, U18, U19 and U20
Pin 16 on U4, U5, U6 U7, U10 and U11
Pin 24 on U1, U2, and U3
Gnd Pin 7 on U9, U12 thru U20
Pin 8 on U4 thru U7, U10, U11
Pin 7 on U1 and U2
Pin 12 on U3

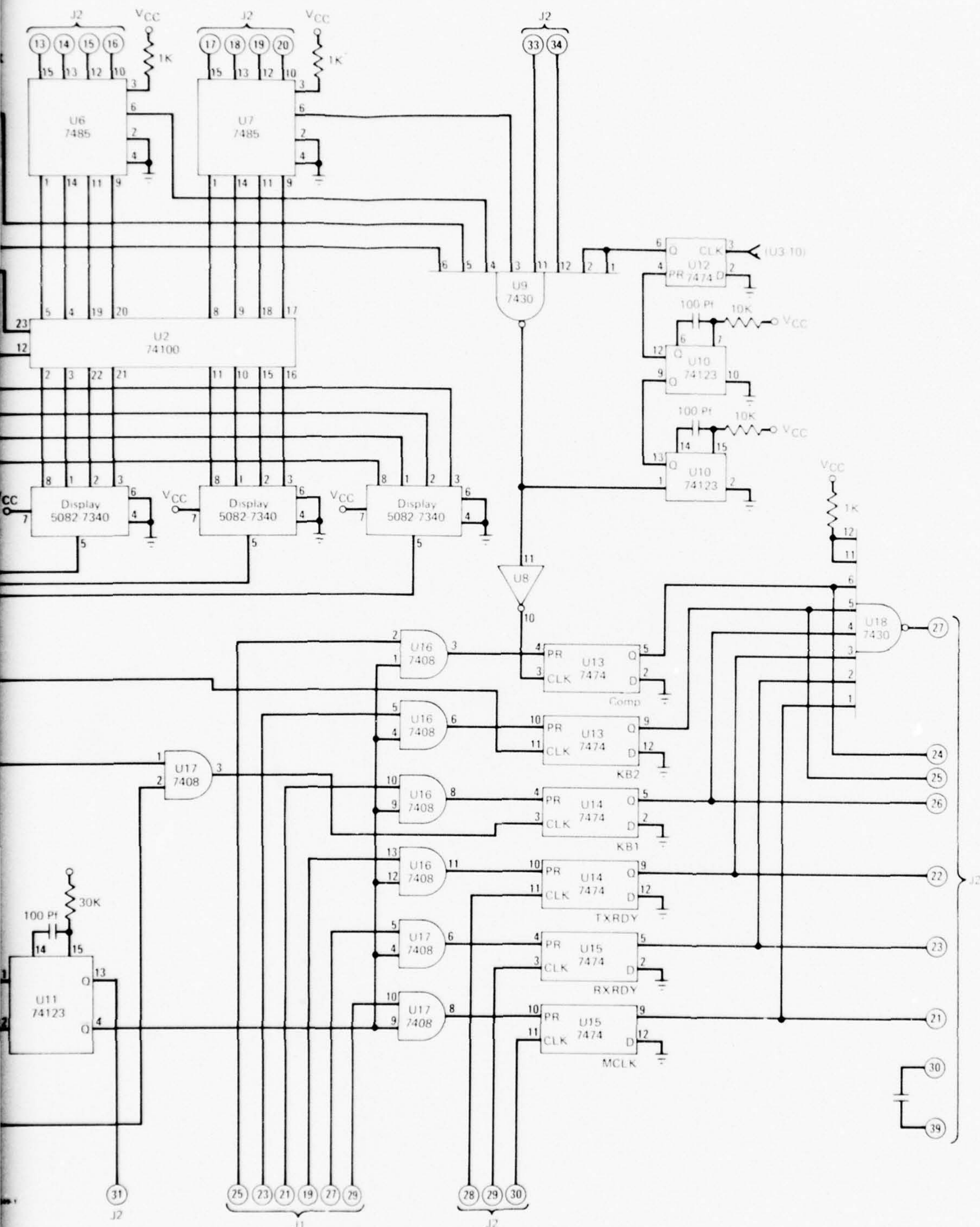
J2
VCC
1K
U6
7485
U7
7485
U9
7430
U12
7474
(U3-10)
U2
74100
100 Pf
10K
U10
74123
Display
5082-7340
U8
U13
7474
Comp
KB2
U14
7474
KB1
TXRDY
U15
7474
RXRDY
MCLK
U16
7408
U17
7408
U18
7430
U11
74123
30K
J1

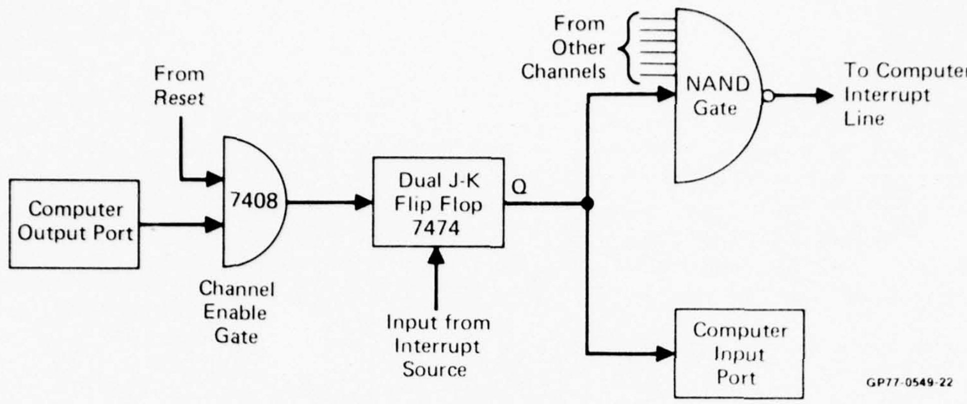

Figure 38 Interrupt Channel

makes them active. In summary, the output of the Flip-Flop is normally high, goes low when an interrupt occurs, stays low during software service, goes high when software is finished, and becomes active when the 7408 and gate output is high.

Restart

The restart function key causes U-19 on Figure 37, to change its output which in turn causes U-11 to trigger. The output of the one shot U-11 goes to the computer reset line which causes the computer to go to memory location zero. No interrupt is generated. When other keys are depressed, an interrupt is generated via U-17 as described above. In addition the keyboard output is routed via J-1, pins 17, 15, 13, 11, 3, 9, 7 and 5 to a computer parallel input port. As a consequence the software can determine which key was depressed and perform the necessary functions.

LEDS and Comparators

Circuits driving the LED displays and compare address functions involve the components U-1, U-2, U-3, U-4, U-5, U-6, U-7. J-1 pins 35, 37, 39, 41 are a computer output port on which the computer outputs the data desired to write to a specific LED. The software then outputs the code on pins 43, 45, 47, 49 of J-1 which causes U-3 to select the appropriate LED. The pins of J-2 are the address bus of the computer. When the comparators U-4, U-5, U-6, U-7 "see" the address set on the latches U-1 and U-2, a computer interrupt is generated via U-9. The one shots U-10 and U-11, reset U-12 so that the gate U-9 is disabled after the compare address has been executed. U-12 enables the gate U-9 when the software selects it via U-3. In summary, software loads the comparators with the desired address similar to the previous discussion about LED's and then software enables U-9. When the address appears at the comparators, U-9 generates an interrupt and the one shots U-10 disable the U-9 gate. Pins 34, 33 of J-2 are signals from the computer which enable U-9 only when an address is on the address bus of the computer. This is necessary since other computer data appears on the address bus and creates a timing problem solved by these inputs.

Input/Output PORTS

The system uses a total of eight input ports and five output ports. They are assigned as shown in Figure 39. The computer low order bits is shown at the right in the figure. High priority interrupts are at Input Port 1, low priority interrupts come in at Input Port 3. The A/D converters start the A/D conversion process when SYS CLK goes positive. The software checks Port E4 to verify that conversion is complete before reading the data at Ports E5 and E6.

The low order LED is selected by a 4 at port E8 and toggling bit 6 at port E-A.

5.1.2 Diagnostic Software

Intel has a computer emulator designated as ICE-80 which is used with the Intel MDS system. The in-circuit emulator interfaces to any user configured 8080 system. With the ICE-80, the designer can emulate the system 8080 in real time, single step the system program, and substitute Intellec memory and I/O for user system equivalents. It will provide address data and 8080 status information on the last 44 machine cycles emulated. It allows the user to share Intellec memory and I/O facilities and is indispensable for initial debugging. The ICE-80 was used with the RVS during Monitor Program debugging.

The RVS microprocessor has diagnostic software referred to as the Monitor Program designed primarily to facilitate operational program checkout and for enhancement of computer operation. One PROM in the processor is devoted to the Monitor Program. It is the only program input/output the computer has. Initial checkout of the processor monitor program utilized the computer emulator available on the Intel MDS System. After the Diagnostic Software checkout on the emulator was completed, it was used to troubleshoot other PROM software.

PROM #3 is devoted to the Diagnostic Software. It is stand alone software. While the computer is operational with the system software, Diagnostic Software is not used. The Monitor program is accessed when the operator depresses the Halt Key. Exit from the diagnostic software is accomplished when the Return Key is depressed.

The primary purpose of the monitor program is to implement keyboard functions which allow the operator full utilization of processor capability. Under monitor, the operator can display the contents of all memory positions, program RAM, single step the processor, and access all processor registers.

The Monitor Program contains all of the diagnostic software required to couple the two keyboards with the processor. All keyboard functions are implemented by software as opposed to hardware. Keyboard generated interrupts are routed via the interrupt handler to the monitor. Keyboard 1 is a function keyboard and Keyboard 2 is for data in hexidecimal. When a Keyboard 1 key is depressed the monitor jumps to the appropriate routine corresponding to the function represented by the key. Concurrently, the interrupt handler has

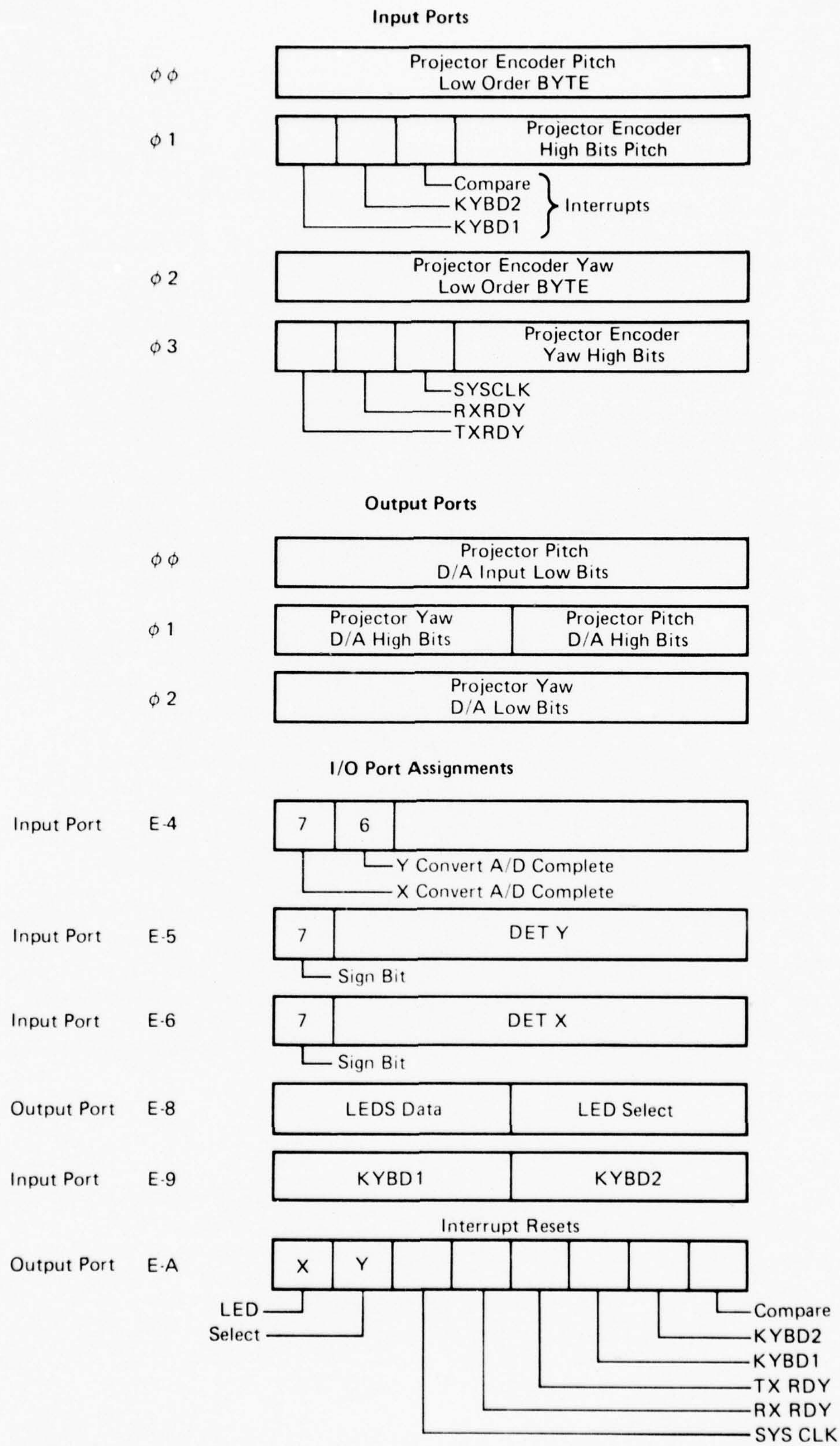

Figure 39 Computer Input and Output Ports

disabled all other interrupts so that once a keyboard interrupt has occurred they have priority. This assumes that the operator desires complete processor control. When the operator has finished his input, depressing the RST key, returns the machine to the program with all interrupts enabled.

Figure 40 is a brief explanation of keyboard functions implemented. These functions allow the operator to display contents of all memory locations, to load data into RAM, to display the contents of registers and load registers, to halt the program, to single step the program, and to stop the program at a specific program address. The SML Key used with the OK and Change Key allow the user to load or change any of the fixed multiply constants. The monitor generates fast multiply routines for each multiply constant and loads RAM with these routines. Twenty multiply constants are programmed and loaded in RAM from 3D90 to the top of RAM.

The stack pointer starts at 3CFF. The lower portion of RAM is assigned to the stack. Scratch pad RAM starts at 3D00 to 3D90. Since there are 608 locations above 3D90 and only 400 are required by the multiply routines, residual memory is available at the top of RAM.

An example of monitor will illustrate how it works. The example will illustrate how to examine a memory position (i.e., display contents of memory on the LEDS). First the operator presses the Halt button. Monitor recognizes the interrupt, halts the computer and displays on the LED's the address of the next program instruction that will be executed. Next the operator presses the display memory key. Monitor determines that the display memory function is required. It displays a 2 on the highest order LED indicating that the EM key was depressed. Then it prepares to fetch a memory location, and then halts and waits for the operator to proceed. Next the operator depresses in succession 4 keys which are the memory address entering, highest order hexidecimal number first. Monitor then moves the memory contents of that position to the LED display and waits for the next keyboard instruction. In summary, the operator presses Halt, EM, XXXX, on the numeric Keyboard and Monitor displays on the LED's the contents of memory location XXXX. If the operator wishes to see the next position he presses the continue button. This button sequences thru memory one step at a time executing the function initially loaded (i.e., deposit, or examine memory).

Keyboard Functions

The following describes the keyboard functions:

Reset	Reset causes the processor to start at location zero. The PROM program at location zero initializes the problem (see related section under software) and then the processor is programmed to Halt. This allows the operator to do necessary tasks prior to system operation. Subsequently, the operator causes the processor to proceed by depressing the Start key.
Examine Memory	Displays the contents of memory on the LED's.

Keyboard Mnemonic	Meaning	Description
HLT	Halt	Pressing this key causes an interrupt, sending program control to the diagnostic software.
RST	Reset	Hardware reset. Restores program counter to zero.
EM	Examine memory	After pressing this function key, the diagnostic software will expect four hexadecimal numbers to be input from the data keyboard, indicating the address to be examined. It will then display the contents of that memory location.
DM	Deposit memory	The DM routine expects six entries from the data keyboard. The first four of these are formed into the 16-bit address and the last two form the 8-bit data byte to be stored.
CO	Continue	Following an EXAMINE MEMORY or DEPOSIT MEMORY, the operator may automatically increment the address pointer by pressing CONTINUE. The software will then display the contents of this new location or will be ready to accept two hexadecimal digits for data entry.
ER	Examine register	After pressing ER the software expects one hexadecimal digit from the data keyboard indicating which of 8 registers is to be displayed. The routine will then display the contents of this register.
DR	Deposit register	After pressing DR the software expects three entries from the data keyboard, the first digit indicating which register is to be modified, and the last two digits formed into the 8-bit byte to be moved into the register. The registers are given the following numerical assignment: Register Number B 0 C 1 D 2 E 3 H 4 L 5 A 6 PSW 7 (Processor status word)
RS	Return	By pressing this key, the software will restore all register contents and condition bits to their values prior to entering the diagnostic software and will then return program control to the location being executed prior to entry into the diagnostics.
CA	Address compare	This function uses comparators to compare the address bus to a software stored 16-bit number. After pressing this key, the software will expect four entries from the data keyboard which are formed into the 16-bit number loaded into the comparator. A RETURN is executed automatically by the software and upon occurrence of the inserted address, program control is returned to the diagnostic software.
SS	Single step	After pressing this key, the software will automatically execute the RETURN routine and will execute the instruction prior to entering the diagnostic software. Program control is then returned to the diagnostics.
ST	Start	Causes the processor to return.
SML	Set Multiply Constant	This function expects the OK or change key to be depressed. If change is signaled it expects two hexadecimal entries. It will then generate a fast multiply routine load it in RAM and display the next multiply constant for the operator to OK or CHANGE. Twenty constant must be approved.
OK	Okay	Indicates to SML approval of constant.
CH	Change	SML expects two hexadecimal numbers to be input from the data keyboard. SML then generates multiply routine from numbers loaded and loads in RAM.

GP77-0549-72

Figure 40 Display Processor Keyboard Explanation

Halt — Causes the computer to stop and wait for a keyboard input. Halt displays the next instruction address.

Examine Register — Displays register contents on LED's.

Deposit Memory — Allows user to load any RAM position.

Deposit Register — Allows user to deposit register.

Set Multiply — User may change any multiply constant. The next constant is displayed on the LED's. Once this mode is entered all twenty multiply constants must be OK or changed.

Single Step — The computer executes one program step. The address of the next instruction is shown on the LED's.

Continue — Is used with the Examine memory, a Deposit memory function. It sequences to the next memory position implementing the same function used previously.

Restart — Is used to reenter the program from the Halt mode.

Compare Address — The computer stops at the desired address. The next instruction is displayed.

OK — Is used with SML. It leaves the constant unchanged and the next constant is displayed.

Change — Is used with SML. The user enters the desired constant on Keyboard 2.

ST — After pressing this key, the software will execute the RVS control software.

5.2 CAMERA ELECTRONICS BOX

The Camera Electronics Box (CEB) interfaces the remote camera shaft encoders and servo amplifier via the serial data transmission line to the home station microprocessor. The CEB's primary function is to send and receive data. It sends gimbal position data to the microprocessor and receives servo-motor commands from the microprocessor.

The transmitter system is split into two identical sections, one handling pitch axis data, and the other yaw axis data. The transmitter section sends the 13 bit shaft encoder word (one for each axis) up the serial line in two eight bit words to the processor. The first byte contains the eight low order bits, the second byte contains the remaining five higher order bits. The 3 excess bits (the highest bits unused) are set to zero.

The receiver system, like the transmitter is split into two identical subsystems; one for each axis, pitch and yaw. The receiver subsystem output consists of two 8 bit parallel-parallel data latches which are input to two 12 bit digital-to-analog converters.

The heart of the camera electronics box is the Universal Asynchronous Receiver/Transmitter (UART). This device is an LSI subsystem which accepts parallel binary words consisting of 5 to 8 data bits, and outputs them as serial words with one or two stop bits and a parity option. The UART is a single monolithic chip, is TTL compatible and its strobed outputs are tristate logic.

Block diagrams of the UART's Transmitting and Receiving sections are shown in Figure 41(a) and (b).

5.2.1 System Clocks and Timing

The basic computation cycle (M-clock) runs at 100 Hz. The system clocks runs at 153.6 KHz, the frequency required by the UART to establish a baud rate of 16. This is the maximum asynchronous baud rate of the Universal Synchronous Asynchronous Receiver/Transmitter (USART) and UART. The transmission of one byte takes approximately 1.2 μsec. Two bytes per half cycle of M-clock are required, thus the timing margin of the system is approximately 50%. No measurements were made of the computation cycle length but some results indicated the computer timing margin is greater than 50%. Thus, the serial transmission line determines the maximum M-clock frequency.

Increasing M-clock would allow the design of a wider bandpass system, however since many factors must be considered (i.e., motor saturation, noise levels, accuracy, load disturbances) there is not a clear cut ratio between bandpass and M-clock frequency.

The initial design proceeded with an M-clock of 100 Hz, thus the basic sample rate of the system is 10 msec, 5 msec for each axis. Synchronous transmission was considered but preliminary work indicated that it might prove difficult to operate a 400 ft. transmission line in the synchronous mode. The asynchronous mode allowed design flexibilities because the 156.3 KHz clock could be a local oscillator or it could, if feasible, be sent over the transmission line. The final design sends the system clock over the transmission line. This required careful attention to the line driver selection and impedance matching of the receiver.

5.2.2 Control Logic

The control logic routes the incoming and outgoing bytes to the transmitter and receiver sections.

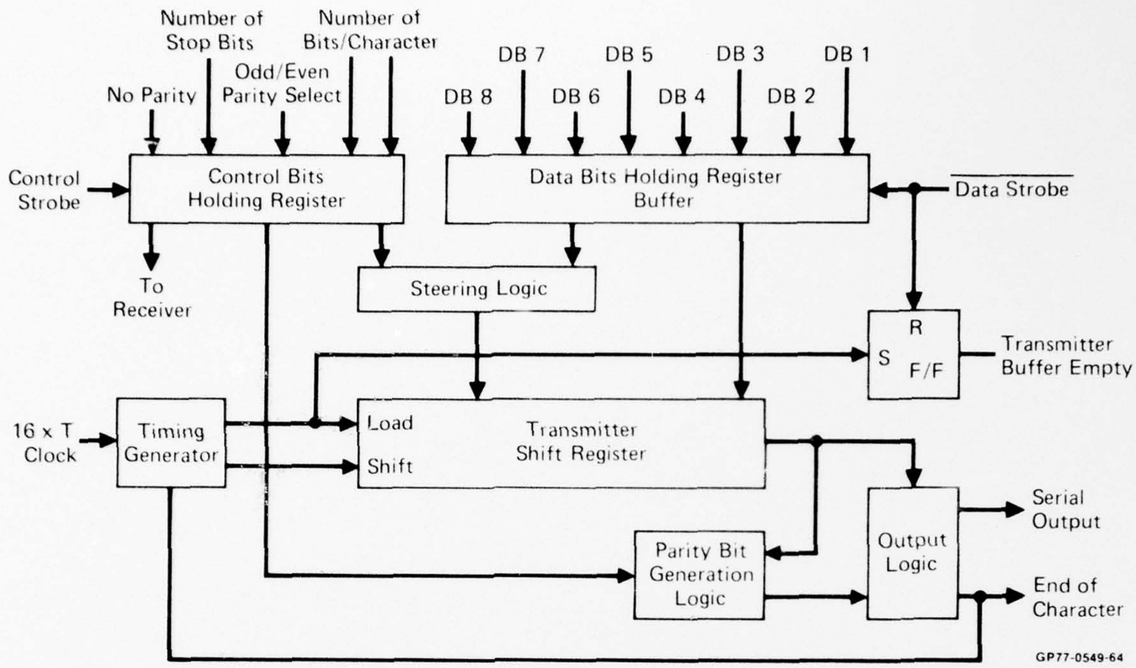

(a) Transmitter Block Diagram

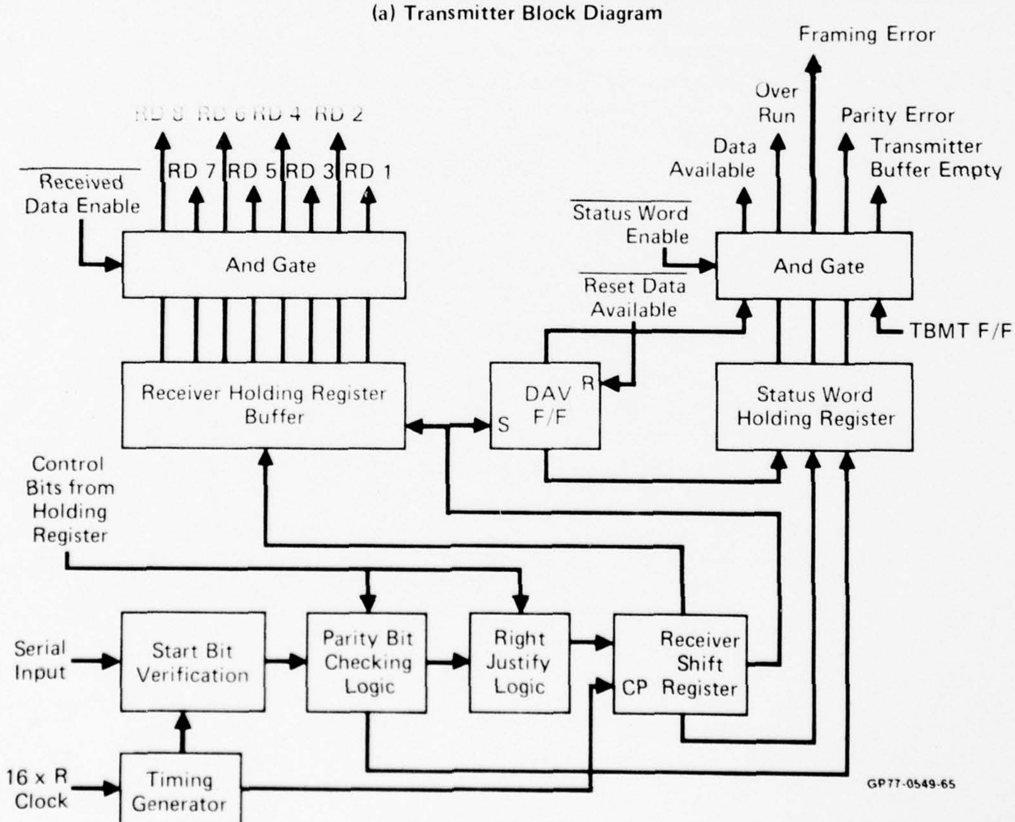

(b) Receiver Block Diagram

Figure 41 Universal Asynchronous Receiver/Transmitter

Transmitter Section

The control logic is symmetric for both axes. Figure 42 contains a block diagram of the CEB Design. The pitch axis is enabled by the positive

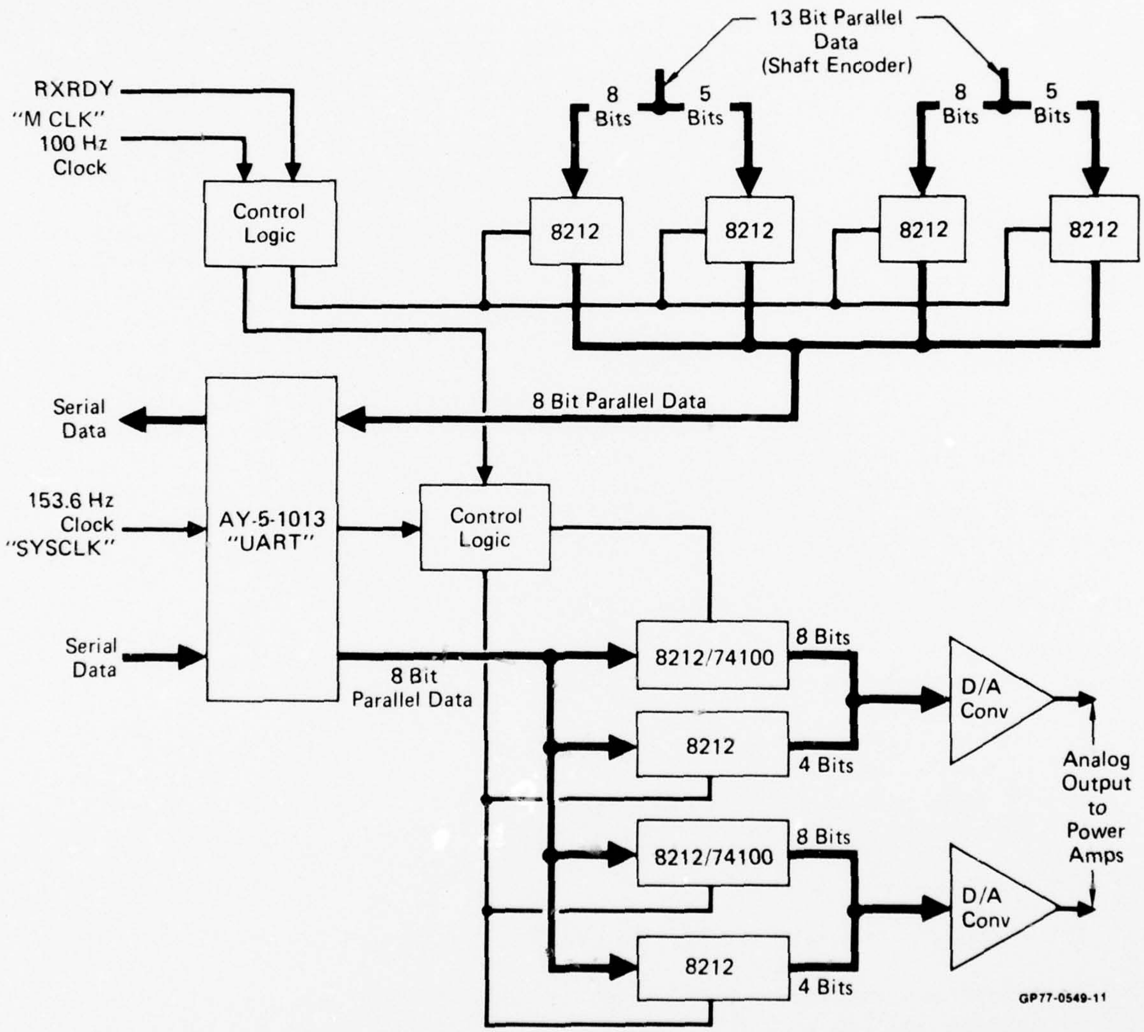

Figure 42 Camera Electronics Box Block Diagram

M-clock and the yaw axis is enabled by the negative M-clock. When M-clock goes positive the pitch axis encoder output is stored in data buffers, (the shaft encoder output continually tracks shaft position). The first buffer, (the low order bits) is strobed onto the data bus, while the other three latches are in the high impedance state. The falling edge of the data strobe (DS) pulse on the UART causes the shift register to transmit the data out on the serial output line. When the first byte of the transmission is complete, a real time interrupt is generated at the microprocessor. The microprocessor services the interrupt and generates a RXRDY pulse to the CEB. Upon receipt of the pulse, the second byte is strobed onto the data bus to the UART and the sequence is repeated. The second RXRDY pulse sent down by the microprocessor is ignored by the CEB and the box now waits for M-clock to go negative and then sends up the yaw information in the same manner. In summary, for each half cycle of the M-clock the encoders are read, stored in latches and sent to the microprocessor in two eight bit words. These bytes are received by the microprocessor and stored in memory and the microprocessor acknowledges receipt of these words to the CEB via the RXRDY pulse.

Receiver Section

The receiver section is independent of the transmitter section including UART functions, thus allowing for complete asynchronous operation. When M-clock goes positive, the microprocessor initiates transmission of the first (high order bits) pitch axis command byte. When this transmission is complete, the receiver's control logic strobes the first byte into a buffer. The microprocessor then initiates transmission of the second byte. Upon completion of the second byte transmission, the control logic loads the second byte into a buffer and then it inputs both bytes to the digital-to-analog converter for the pitch axis. The D/A (12 bits) receives a full word at one instant in time just after the receiver has loaded both bytes of information into data storage. This word remains on the D/A input until the end of the next cycle of the M-clock.

5.2.3 Camera Box Electro Mechanical Description

The camera electronics box is connected to the microprocessor via five twisted pair cables. The processor supplies the system with:

1) System clock - 153.6 KHz
2) M-clock - 100 Hz
3) RX Data - Servo-amp command signal
4) RXRDY - Microprocessor acknowledgement of receipt of Position Data

The camera box sends

1) TX Data - A Position Data down to the SBC 80 microprocessor.

The shaft encoder words are brought to the CEB from the gimbals using 2-18 wire ribbon cables and DB25 connectors, and the D/A output is sent to the power amp over two twisted pairs, through an MS3106-14S-4P connector. The power amp outputs are run in separate cables to the torque motors. Thirteen (13) bit Baldwin shaft encoders are used to determine shaft position. Figure 43(a) shows the CEB LAYOUT and Figure 43(b) shows the board layout. Component descriptions shown in the board are listed in Figure 44. Figure 45 and 46 are schematics of the transmitter and receiver sections, respectively of the CEB.

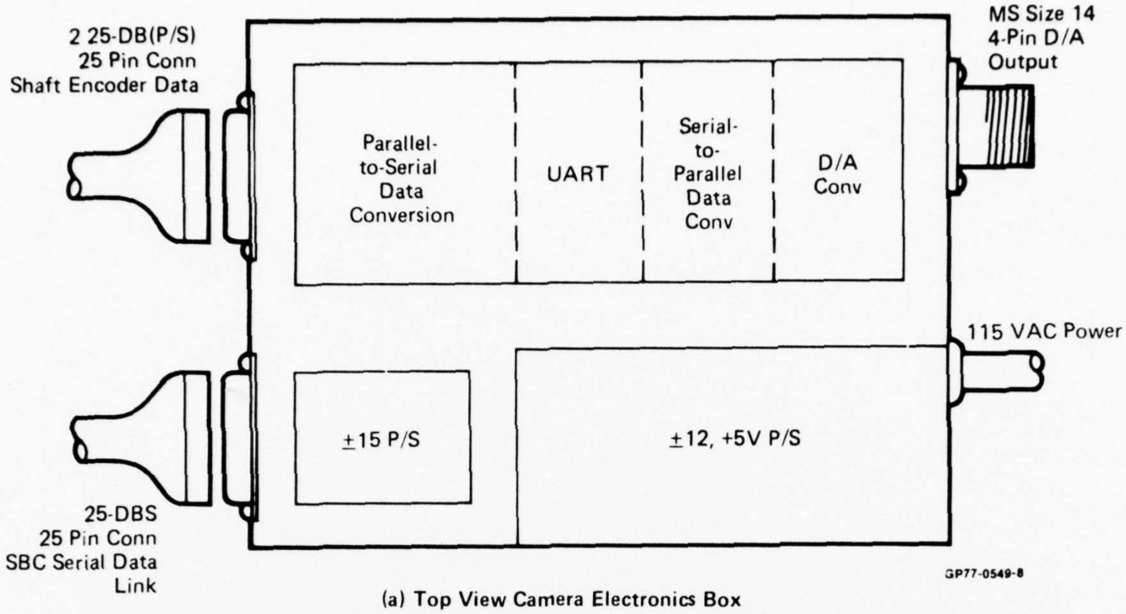

(a) Top View Camera Electronics Box

Figure 43 Camera Electronics Box

5.3 SYSTEM SOFTWARE

Each of the four PROMS are assigned a system software function for ease of PROM management. PROM #1 (memory locations 0-3FF) is devoted to the system initialization and the interrupt handler. PROM #2 (memory locations 400-7FF) contains the Yaw Axis control equation software. PROM #3 (memory locations 800-BFF) contains the diagnostic software. PROM #4 (memory location (C00-FFF) has the software for the system pitch axis. The detailed line by line listing of the software for all of the PROMS is included in Appendix D. Software flow diagrams are shown in Figure 47.

5.3.1 PROM Programming

An Intel 8080 Cross assembler is available on the PDP 11 Digital Equipment Computer. To program a PROM, a source program is created on the PDP 11 computer. It is assembled on the PDP-11 by the following commands into an 8080 binary language which is used as an input to the PROM programmer. Commands for useing the assembler are:

```
$ AS KB:, CMI
  RU INXAS
  File, LP:
```

< File since the assembler cannot handle a full PROM, a program MERGE can be used to link two programs together:

```
$ AS File 1.OBJ, 1
  AS File 2.OBJ, 2
  AS File 3, 3
  RU MERGE
```

Subsequently, the .OBJ files can be punched on paper tape with commands

```
$ AS File 3, 1
$ AS PP:, 4
  RU CHANGE
```

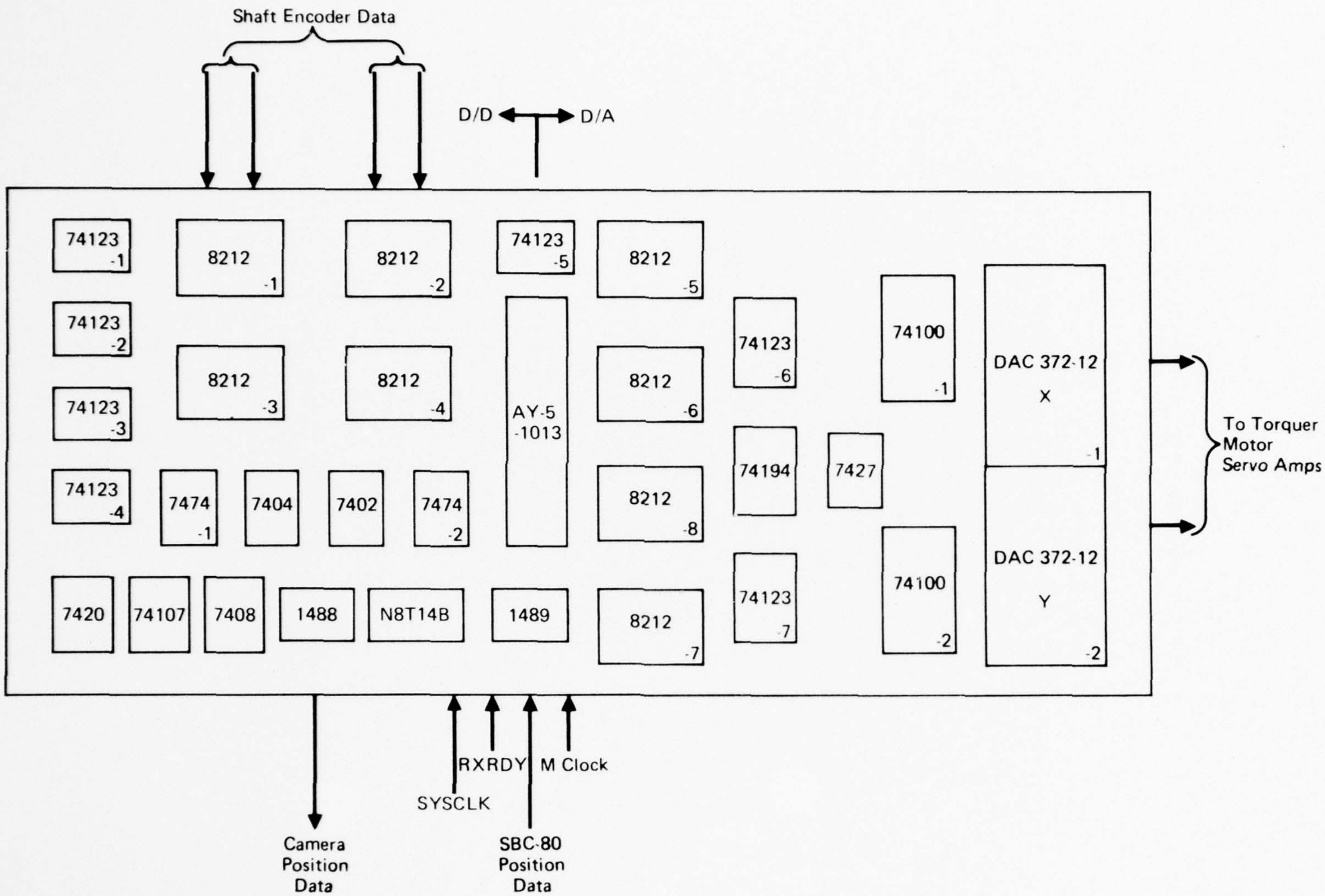

(b) SBC-80/Remote Camera Data Transfer Board

Figure 43 Camera Electonics Box

Qty	Part No.	Description
8	8212	Eight Bit Input/Output Port
7	DM74123	Dual One-Shot
2	7474	Dual D-Type Flip Flop
1	7404	Hex Inverter
1	7402	Quad 2 Input NOR
1	7420	Dual NAND
1	74107	Dual J-K Flip Flop
1	7408	Quad 2 Input AND
1	1488	Line Driver
1	1489	Line Receiver
1	74194	4 Bit Shift Register
1	7427	Triple 3 Input Positive NOR
2	74100	8 Bit Latch
2	DAC372-12	D/A Converter
1	AY5-1013	Universal Asynchronous Receiver/Transmitter
1	N8T14B	Line Receiver

GP77-0549-63

Figure 44 Camera Electronics Box Component List

The resulting paper tape can then be read into the PROM programmer.

5.3.2 PROM #1, Interrupt Handler Software

As real time interrupts are generated to the microprocessor, it is routed to memory location 38, whereas the reset button causes the computer to start at memory location zero. As a consequence, memory locations zero thru 37 are devoted to the necessary housekeeping functions required to initialize the system. The processor than encounters a program Halt. The start button causes it to advance past the Halt where it enters the active system program. The program enables all interrupts and waits in a backward forward loop located at memory positions 30 and 33 for interrupts. A listing of the program is shown in Figure D-1, Appendix D.

Interrupts

There are three system interrupts; system clock, receiver, and transmitter. The system clock generates an interrupt every 0.010 sec. Each system interrupt causes the computer to proceed thru the yaw and pitch control equations and update the system commands. Concurrently, the receiver and transmitter send data over the serial transmission line link to the remote camera. The receiver interrupt causes the computer to store the received word in memory. The transmitter interrupt causes the computer to load the transmitter with a new command word.

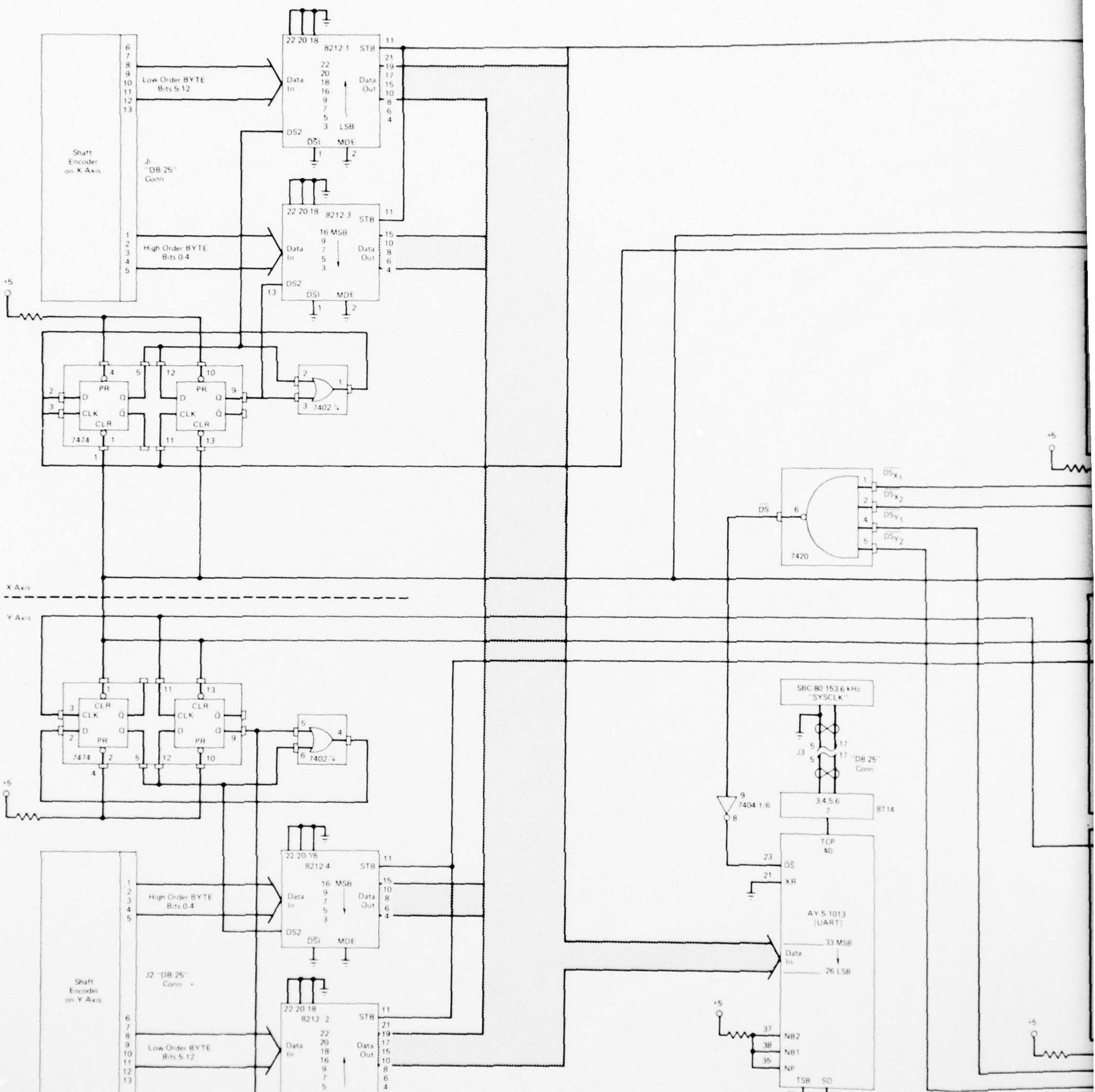

Figure 45 Camera Electronic Box Transmitter Circuit Diagram

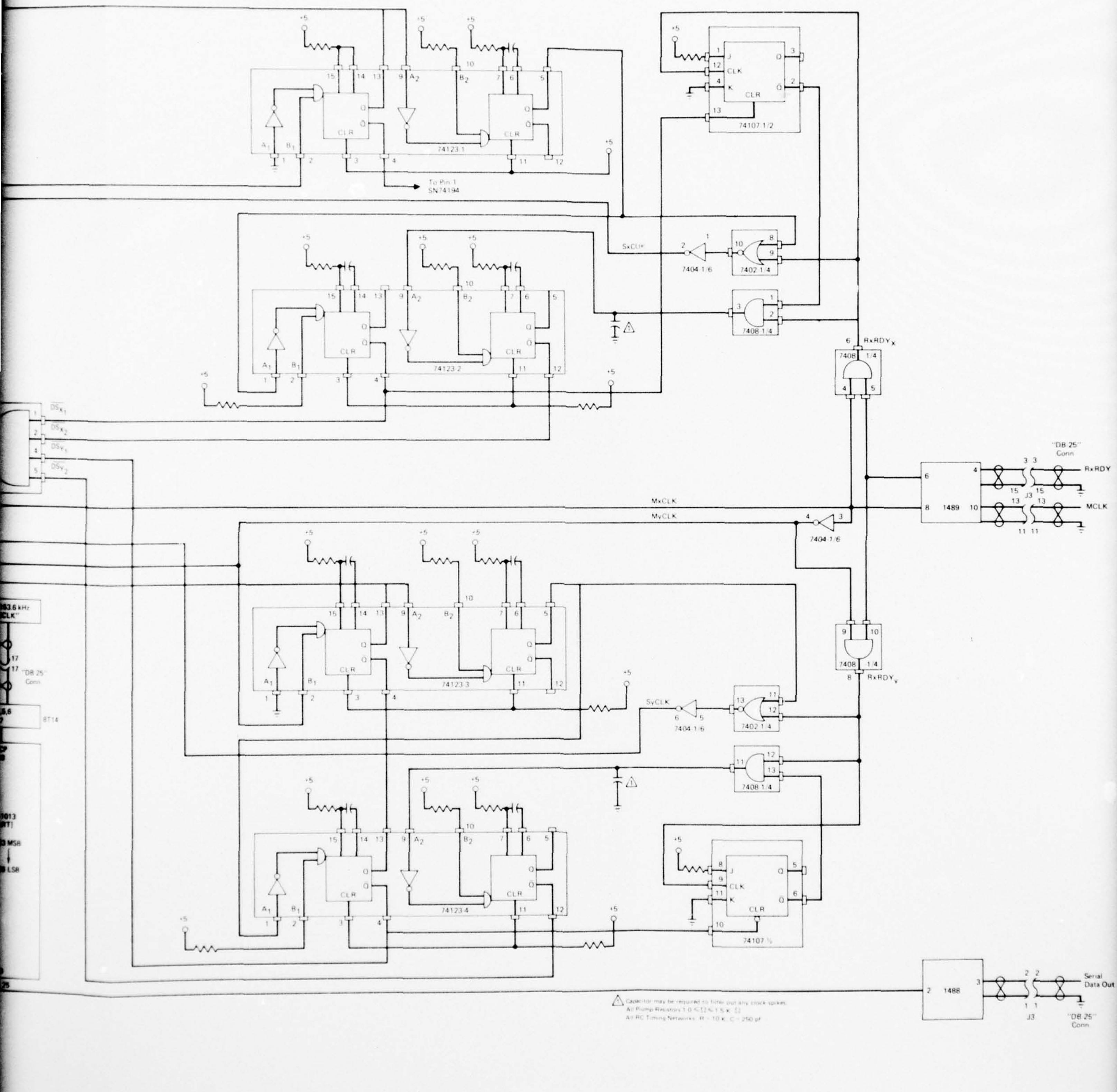
74123-1
To Pin 1
SN74194
74107 1/2
SxCLK
7404 1/6
7402 1/4
74123-2
7408 1/4
RxRDYx
MxCLK
MyCLK
"DB 25"
Conn
RxRDY
MCLK
1489
J3
74123-3
SyCLK
RxRDYy
74123-4
74107 ½
1488
Serial
Data Out
Capacitor may be required to filter out any clock spikes.
All Pump Resistors 1.0 ≤ Ω ≤ 1.5 K Ω
All RC Timing Networks: R = 10 K, C = 250 pf

2

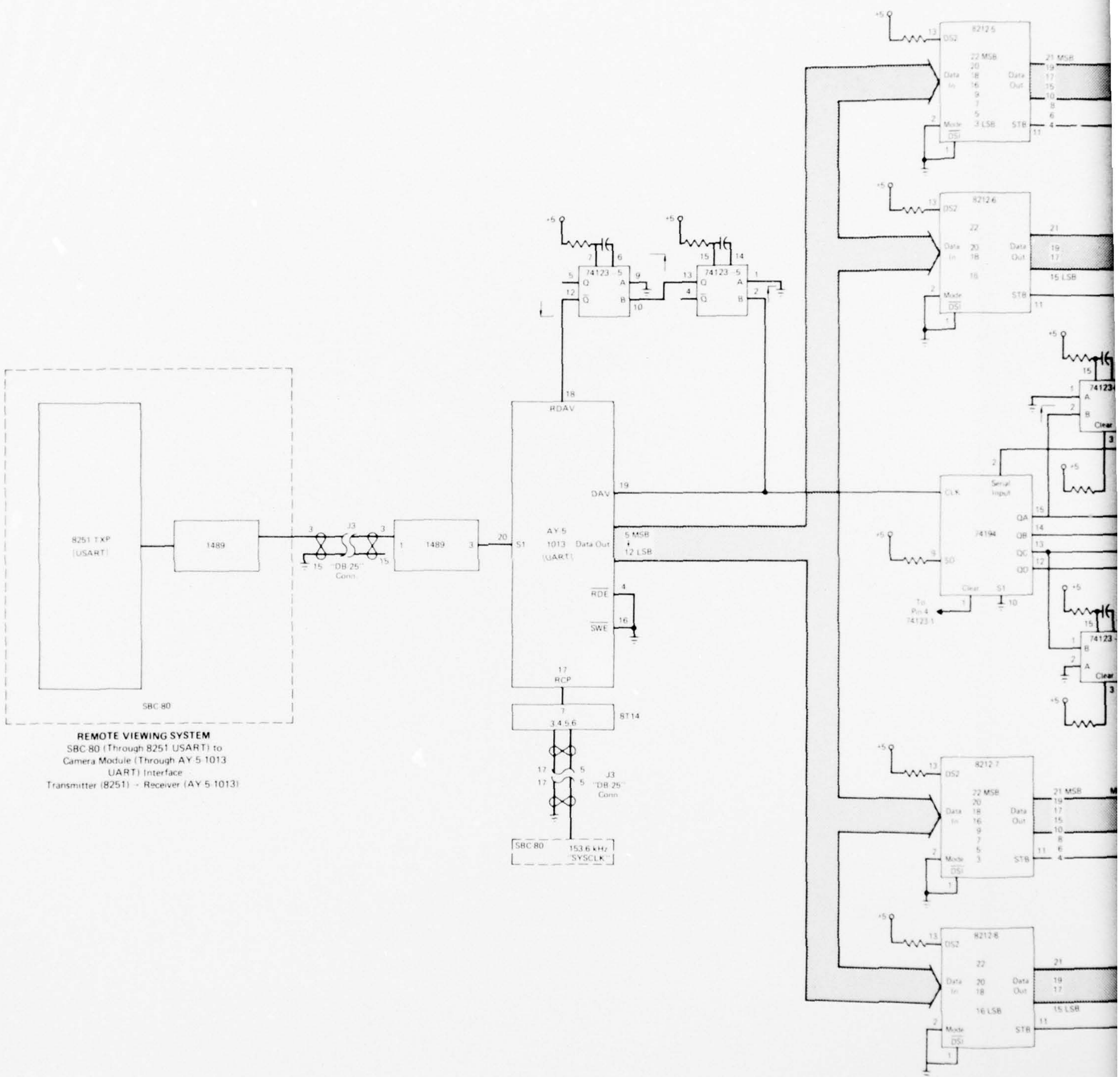

Figure 46 Camera Electronics Box Receiver Circuit Diagram

GP77-0549-3

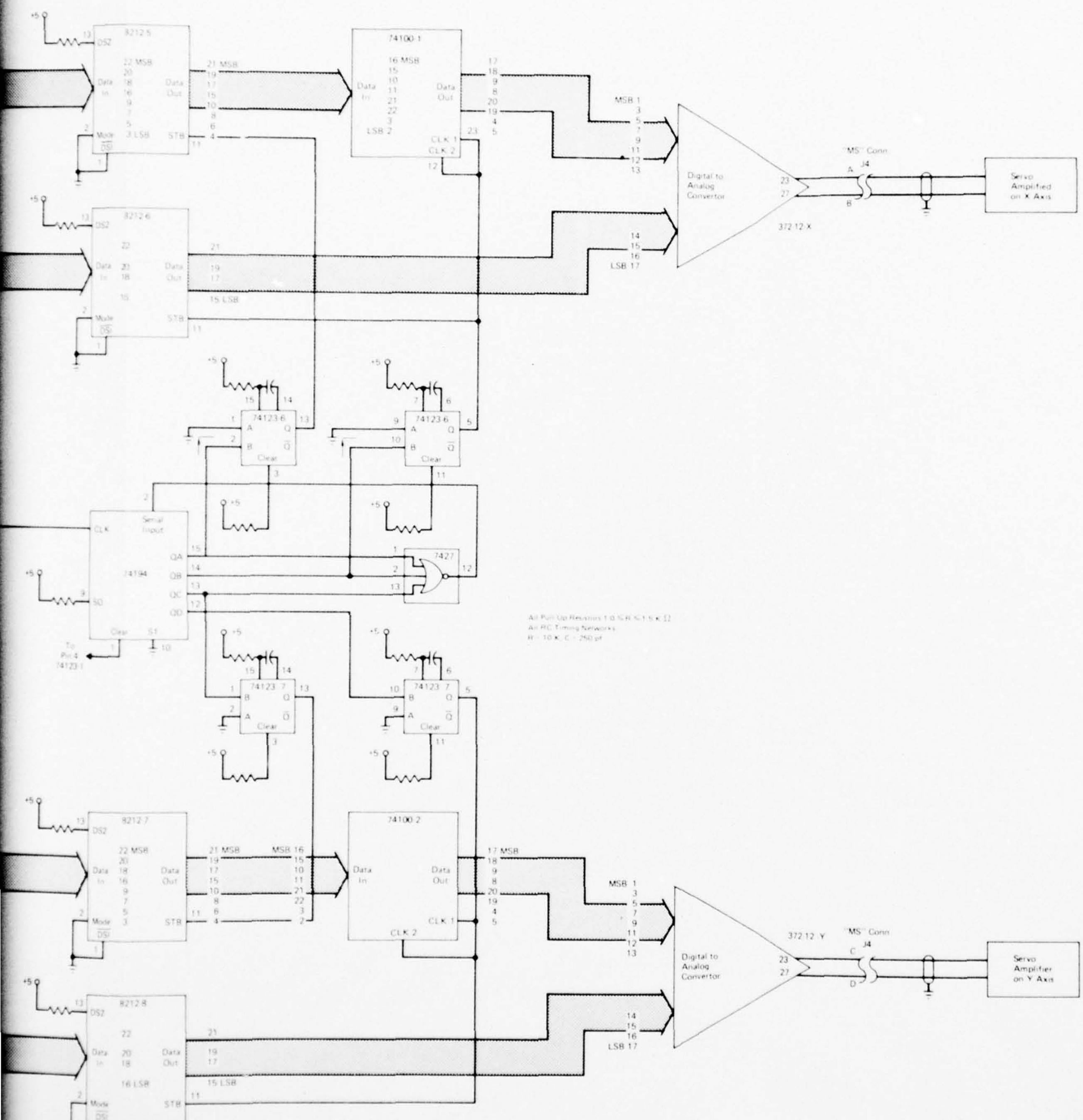
8212-5
74100-1
Data In
Data Out
Digital to Analog Convertor
"MS" Conn
J4
Servo Amplified on X Axis
372 12-X
8212-6
74123-6
Clear
Serial Input
74194
7427
74123-7
To Pin 4 74123-1
8212-7
74100-2
372 12-Y
Servo Amplifier on Y Axis
8212-8

7-0549-3

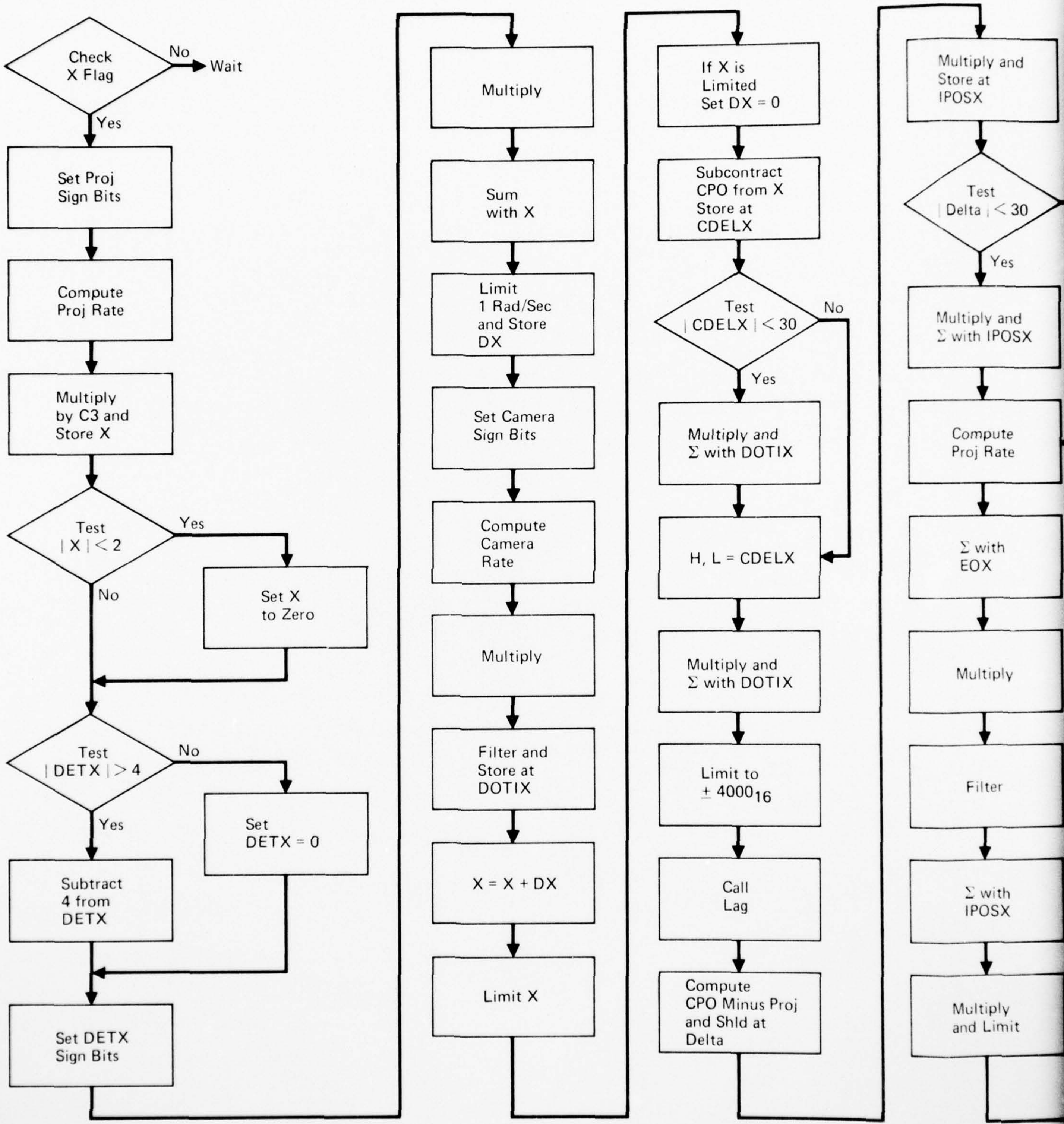

Figure 47 Software Flow Diagram

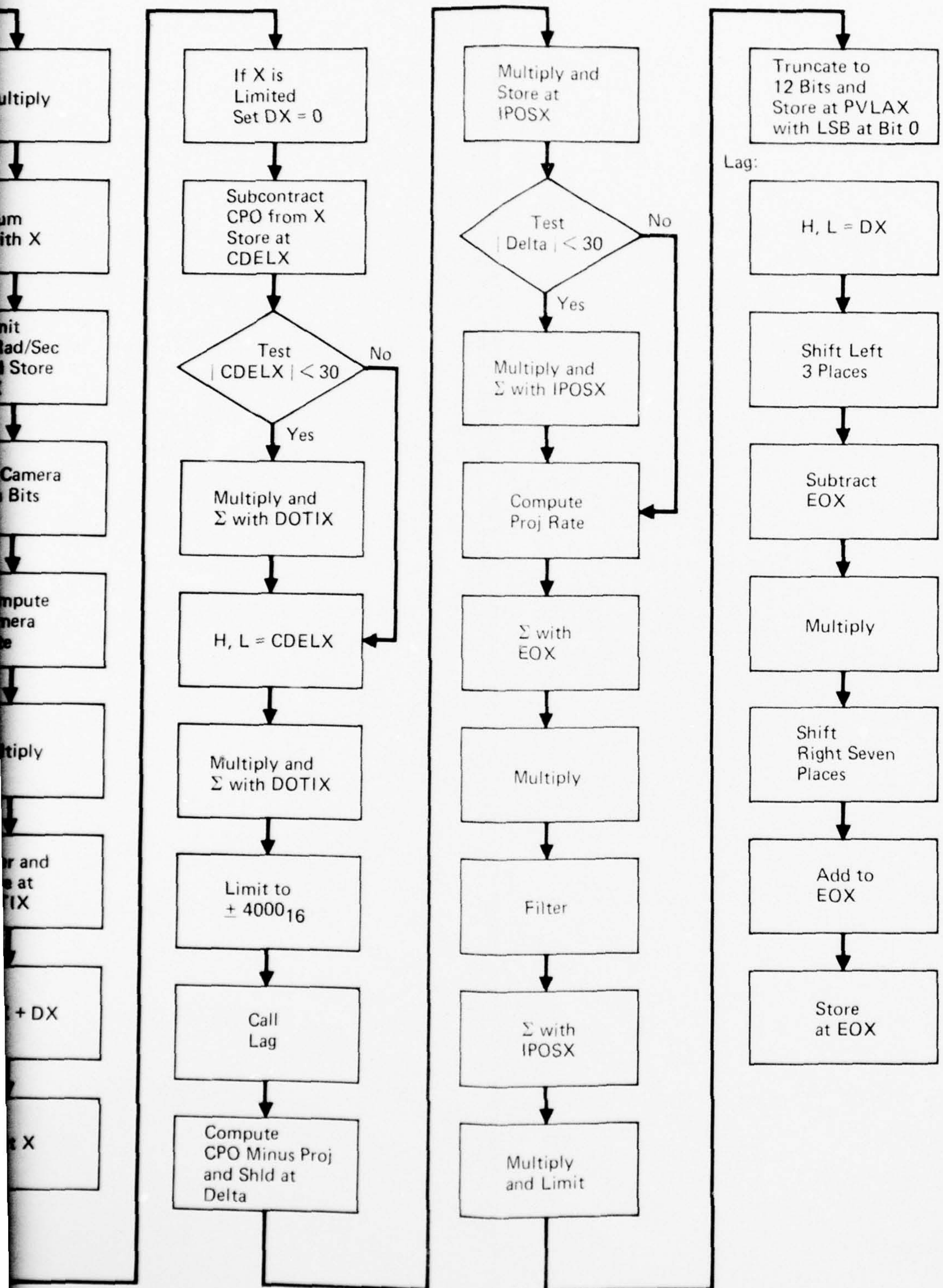

GP77-0549-29

Diagram

When an interrupt occurs, the following sequence is executed:

1) Save the status of the machine,
2) Poll the interrupt ports and determine the specific interrupt,
3) Reset all interrupts, make appropriate interrupts active determined by priority of interrupt requesting service,
4) Jump to interrupt service routine,
5) Restore status of machine and return to sequence prior to the interrupt.

System Interrupt Service Routine

This routine is the primary or key interrupt which determines the system data sample rate. The following events happen after a system interrupt:

1) Load the transmitter with a new word and load the transmitter counter used by the transmitter service routine
2) Initialize the receiver counter, Y Flag, and X Flag
3) Read the Projector Encoders
4) Output command updates to the Projector Power Amplifiers
5) Read the X and Y A/D's
6) Compute the Yaw and Pitch control equations. The output of these equations update system commands.

Receiver Interrupt Service Routines

This routine stores the word just received in memory and resets the receiver. The receiver is then ready for the next word. Initially, the service routine loads the receiver counter. Since the receiver normally reads four words per sample interval, the service routine checks the counter. If more than four words have been received an error has occurred. In this case, the data from the last cycle is loaded into the yaw axis data memory positions. If the counter is correct, the routine reads in the receiver contents and stores the data in the memory position indicated by the counter. Next the routine increments the counter and stores it in memory. When two words have been received, X Flag is loaded. This indicates that new data is ready for processing in the pitch axis control equations. If the third word has been received the routine loads the transmitter and returns to the previous program before the interrupt occurred.

5.3.3 Transmitter Service Routine

This routine loads the transmitter with words from memory each time the transmitter is ready to send a new word. The pitch data is sent out first since it is always ready at the beginning of a clock cycle. The routine loads the transmitter counter, decrements the counter and sends a word to the transmitter from memory. When the counter indicates Yaw commands (i.e. third word) the routine checks Y Flag. Y Flag indicates that the Yaw axis computation is done and that new Yaw commands are ready. If data is available the routine sends the data and returns the computer to the previous program.

5.3.4 PROM #2 Yaw Control Equations

These equations are on PROM #2 and start at location 400. Due to the complexity of the system every effort was made to keep the pitch and yaw equations alike. As a consequence PROM #4 except for changes peculiar to the pitch axis is similar in program flow to PROM #2. First the new data word is called from memory and the bits 14 thru 16 are set so that the computer treats the encoder as a double precision word with the LSB of the encoder located at the LSB of the computer. The compensation equations are calculated and placed in intermediate storage at CAMAY. CAMAY is limited to 1 rad/sec and is input to the integrator driving the camera. Next the camera servo equations are processed. These equations represent a rate command position hold servo. The camera encoder is converted to a double precision word with the LSB of the encoder corresponding to the LSB of the computer. The unfiltered first difference is computed and stored at location 3FF0. The filtered gimbal rate is limited and multiplied by the constant MYLVB. MYLVB is stored at location 3D82 as a double precision word with the decimal at the left with one sign bit. At location 4F9 the digital integrator sums in the update CAMAY and limits the integrator output at gimbal stops of $\pm 90°$. These stops are inside the mechanical stops of the gimbal. The camera encoder is subtracted from the integrator output and stored at CDEL location 3D72. Next the position feedback is limited and multiplied by the constant MYLVK. Subsequently, the rate feedback signal is summed with the position signal. This sum is multiplied by TORQY and limited. It is stored at CCMAY as a double precision word. The transmitter service routine sends CCMAY to remote station where via the hardware it is truncated to a 12 bit word as input to the D/A driving the power amp. Next LAG is called. This subroutine is a filter which provides a signal to the projector. The signal provides accurate projector to camera tracking. The camera error is tested. If it is too large, the camera input is taken as the input to the projector. The program now computes the projector servo equations which are a basic position servo with a modified rate command from LAG. The program proceeds as follows: Beginning at memory position 696 the position feedback is calculated, limited and multiplied by MULBY. This result is stored at IPOSY. At location 6C5 an integral channel is implemented for small input errors. If the error is large the integral channel is bypassed. The output is summed with the contents of IPOSY and stored at IPOSY. Next the first difference of position is calculated and stored at 3FF2 with the LSB of the result at the LSB of the computer. This unfiltered difference is summed with EOY, the LAG signal mentioned previously and the result is limited and filtered to provide a suitable rate feedback signal. It is stored at 3D64.

This result is summed with the position feedback signal. The computer word has one sign bit and the decimal to the left in the double precision word. Since the hardware requires the decimal to the right, the software truncates the word to 12 bits and shifts the result to the right so that the LSB of the word is at the LSB of the computer. This result is stored at PVLAY. Y Flag is set to indicate that new data is at PVLAY. Next the routine checks if the transmitter has already tried to send the data. This is indicated by the high order bit of Y flag. If it has the routine it initiates the transmission. If not, the routine continues to the Pitch control. The computer listing is contained in Figure D-2.

5.3.5 PROM #3 Diagnostic Software

Discussed earlier in Section 5.1.2. Computer listing is contained in Figure D-3.

5.3.6 PROM #4 Pitch Control Equations

X Flag is tested to determine if new data has been received. If not the routine waits for new data. After new data has been received, the pitch equations are processed similar to the yaw equations described above. Different multiply constants are used. A complete listing of the equations are shown in the Figure D-4. In the software equations X is used to designate the Pitch Axis and Y is used to designate the Yaw Axis of the system. The new Pitch Axis commands are stored at PVLAX as a double precision word. At the beginning of the next clock cycle the transmitter service routine sends the new words to the remote station. At the end of the Pitch Axis equations, the computer has completed all required up data processing per clock cycle and returns to loop waiting for the next interrupt. Timing margins indicate that the next interrupt will be from the receiver and transmitter routines.

5.4 MATH MODELS

The Remote Viewing System servos can be operated in three different modes. They are:

MODE 1) Stand alone servos closed around each gimbal.

MODE 2) Camera as a rate command position hold servo with rate inputs from the stick. The projector in a position servo follower to the camera.

MODE 3) Camera and Projector in closed loop with the head controller. This option includes capability to insert the stick control in lieu of the head controller without changing the control equations.

The first mode allows the camera to be used with the projector servos disabled. It simplifies system power up because the system is stable for all gain modes.

The second mode uses the stick control as input. It can be implemented by minor program changes in the microprocessor. It can be used to achieve accurate pointing and projector to camera tracking. It is ideally suited for fine pointing but is less advantageous for tracking moving targets.

The third mode is the final system configuration which provides helmet mounted control by the operator.

AD-A046 704 MCDONNELL AIRCRAFT CO ST LOUIS MO F/G 17/2
REMOTE VIEWING SYSTEM.(U)
JUN 77 R W FISHER N00014-75-C-0660
UNCLASSIFIED ONR-CR213-129-2F NL

2 OF 3
ADA
046704

5.4.1 MODE 1

Linear Transfer Function

A simplified linear model of the servo used for each gimbal is shown in Figure 48. The integral channel was implemented and used as required for fine pointing. The equivalent transfer function is:

$$H_1(s) = \frac{AKS + AM}{S^3 + ACS^2 + AKS + AM} \qquad (66)$$

where A = 1/I
K = ft #/rad
M = ft #/sec/rad
C = ft #/rad/sec
I = Gimbal Inertia

Computer studies of ramp type inputs to the servo showed that the 100 ft. lb. torque motor on the projector azimuth axis was the system limiting factor and significant saturation occurred around 1 rad/sec. The servos were designed to minimize this saturation and provide the best possible frequency response. Figure 49 shows the response of the camera to a ramp input of

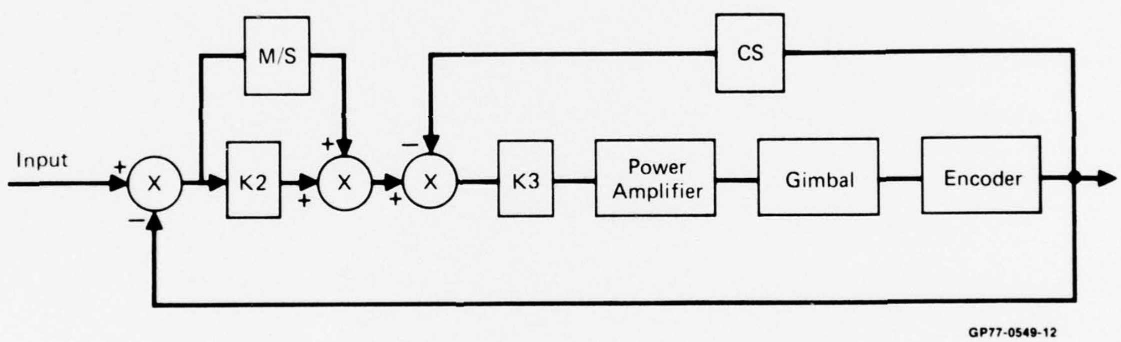

Figure 48 Mode 1 Servo Block Diagram

1 rad/sec for 0.25 sec. The camera lag is less than 0.1 sec as shown in the figure. This is consistent with an operators reaction time using stick control. Note that this lag does not cause image motion on the projector screen. The image will move because the projector remains stationary in Mode 1 operation.

Figure 49 System Response for Stick Input
Lag = 0.12 Sec

Gains

Important gains for each axis are summarized in Figure 50. Inertias shown in the table were results of measurements made when the system was first assembled. Subsequent changes in optics and mechanical design caused these inertia figures to change. Accurate information on inertias associated with the final design are unavailable. The channel gains shown in the table were used to derive the first estimate of computer gains cognizant of the effects of non-linearities. The important non-linearities in the system are saturation, threshold, and friction. These result in overall gain reduction and apparent increase in damping.

The gains of Figure 50 were required during software development. They served as a basis for software scaling and for sizing multiply routines. Subsequently, they were used during initial system checkout.

Name	Symbol	Units	Projector Azimuth	Projector Pitch	Camera Azimuth	Camera Pitch
Inertia	I	$ft\text{-}lb/sec^2$	1.58	0.052	0.28	0.113
Proportional Channel Gain	K	ft-lb/rad	632	20.8	112.5	45.2
Rate Channel Gain	C	ft-lb/rad/sec	63.2	2.08	11.25	4.52
Integral Channel Gain	M	ft-lb/rad/sec	7015	230	1249	501
Pwr amp Gain	KA	ft-lb/Computer Volt	19.2	0.493	2.28	1.4
Computer Rate Gain	G_C	–	413	530	619	406
Computer Prop Gain	G_K	–	165	212	15	10
Computer Integral Gain	G_M	–	18	23	1.7	1.1
	C	ft-lb/rad/sec	$0.1528\ G_C$	$0.0039\ G_C$	$0.018\ G_C$	$0.011\ G_C$
	K	ft-lb/rad	$3.82\ G_K$	$0.098\ G_K$	$7.27\ G_K$	$4.45\ G_K$
	M	ft-lb/sec/rad	$380\ G_M$	$9.76\ G_M$	$726\ G_M$	$445\ G_M$

Figure 50 Servo Gains

GP77-0549-14

Gains for Camera Azimuth Axis

An example of the gains involved for the camera azimuth axis are shown in Figure 51. Non-linearities not shown in the figure cause gain reduction and some phase shift. Consequently, gains were adjusted on the actual hardware to optimize gimbal performance and camera-to-projector tracking as evidenced by picture motion. The non-linearities of the system make

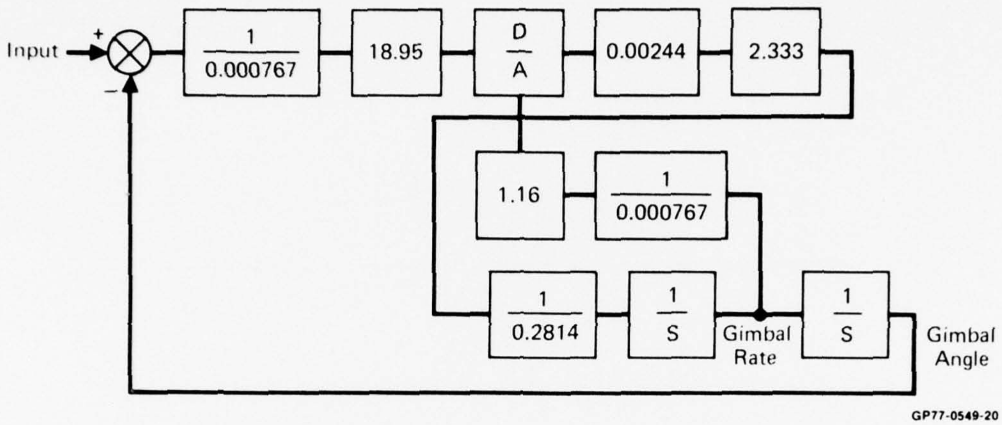

Figure 51 Camera Azimuth Axis

the frequency response of the system a function of amplitude and frequency. They tend to reduce the system bandwidth. The system was designed and optimized for ramp type inputs.

5.4.2 MODE 2

Using the projector in a servo follower mode to the camera requires careful system servo design. Any error in projector-to-camera tracking causes picture motion on the spherical screen as viewed by the observer. The servo follower inherently has dynamic lag even though integral feedback could be used to reduce steady state errors. From qualitative considerations some dynamic error is allowable because the observer cannot follow dynamic motion faster than a few hundreths of a second. Consequently, camera and projector instantaneous rates can be unequal for short time intervals providing the steady state position error remains within acceptable limits of approximately 0.01 radians.

While there are several approaches to the problem, the one used in the RVS was to feed the camera rate command signal forward to the projector. This required insertion of a lag network in series, which compensates the projector for camera velocity lag. Since the camera lag is insensitive to component changes by virtue of the feedback in the servos the circuit should remain in calibration. Adjustment of the lag can cause the projector to lead the camera or to lag the camera. Computer studies indicate the system is easier to stabilize in Mode 3 if the projector leads the camera by a slight amount. While some dynamic error still exists its magnitude and time of decay are such that no deleterious system operation is evident to the observer. A simplified linear block diagram is shown in Figure 52.

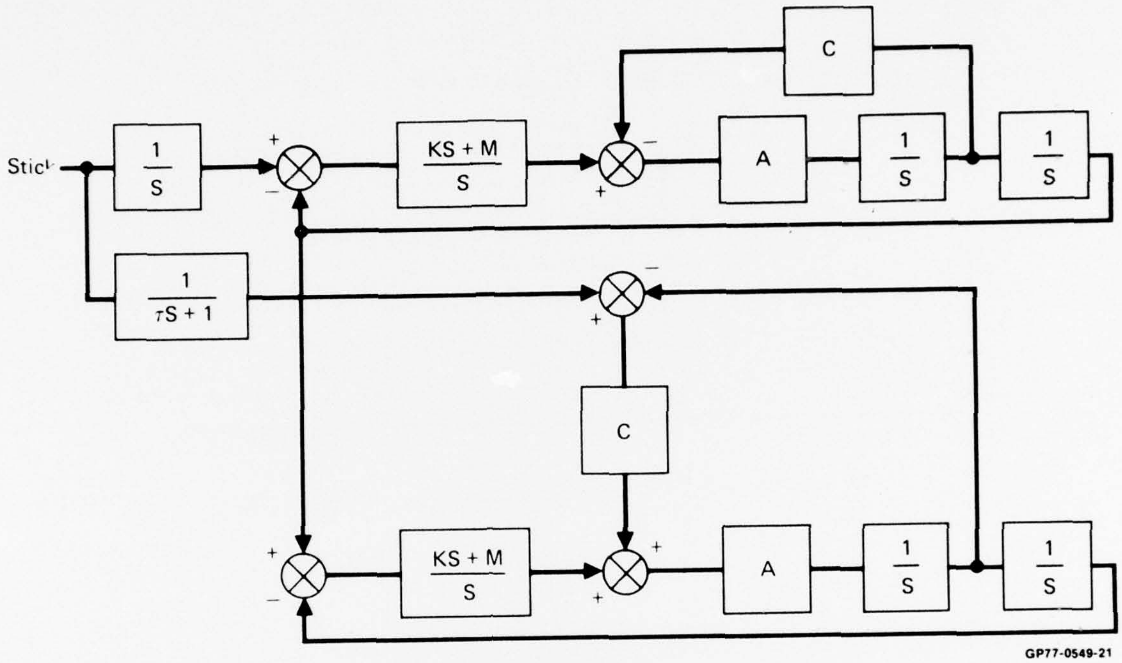

Figure 52 Mode 2 Servo Block Diagram

The output of the lag network approximates the camera velocity. If the camera velocity were being fed forward the linear projector response can be shown to be

$$H_2(s) = \frac{ACS^2 + AKS + AM}{S^3 + ASC^2 + AKS + AM} \tag{67}$$

System Response Versus Lag

Figures 49, 53, and 54 show the response of the system to maximum stick inputs of 1 rad/sec for .25 sec with values of lag in the forward loop of 0.1 and .12 sec and .14 sec. The figures show that this range of lag causes the projector to cross over the camera and change from lag to lead. The parameter was adjusted on the actual hardware to enhance projector tracking and achieve minimum picture motion.

The Figure 55 shows the system response for a stick input of max plus for 0.25 sec and then max negative for 0.25 sec. with the lag set at an optimum of 0.14 sec.

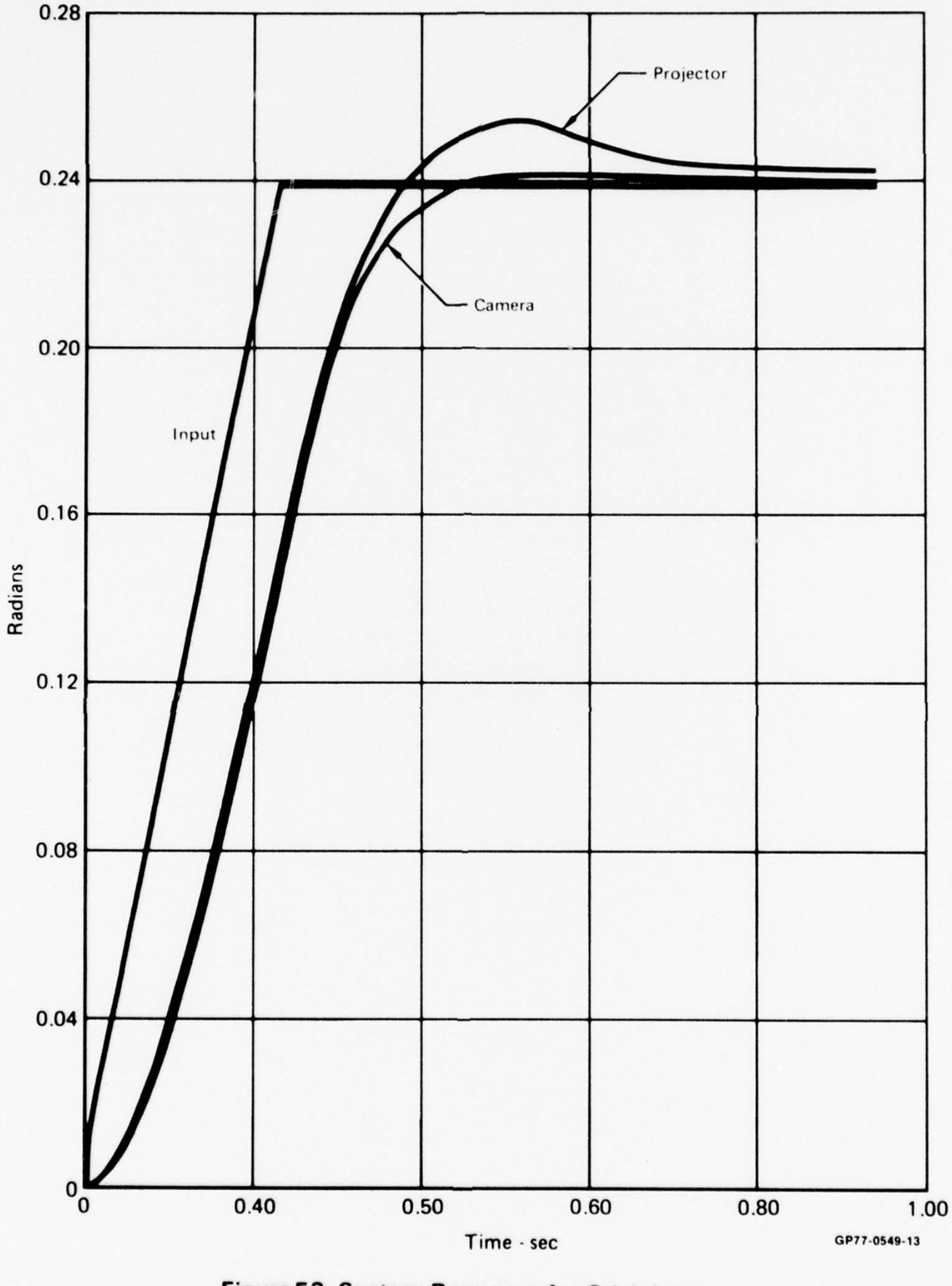

Figure 53 System Response for Stick Input
Lag = 0.10 Sec

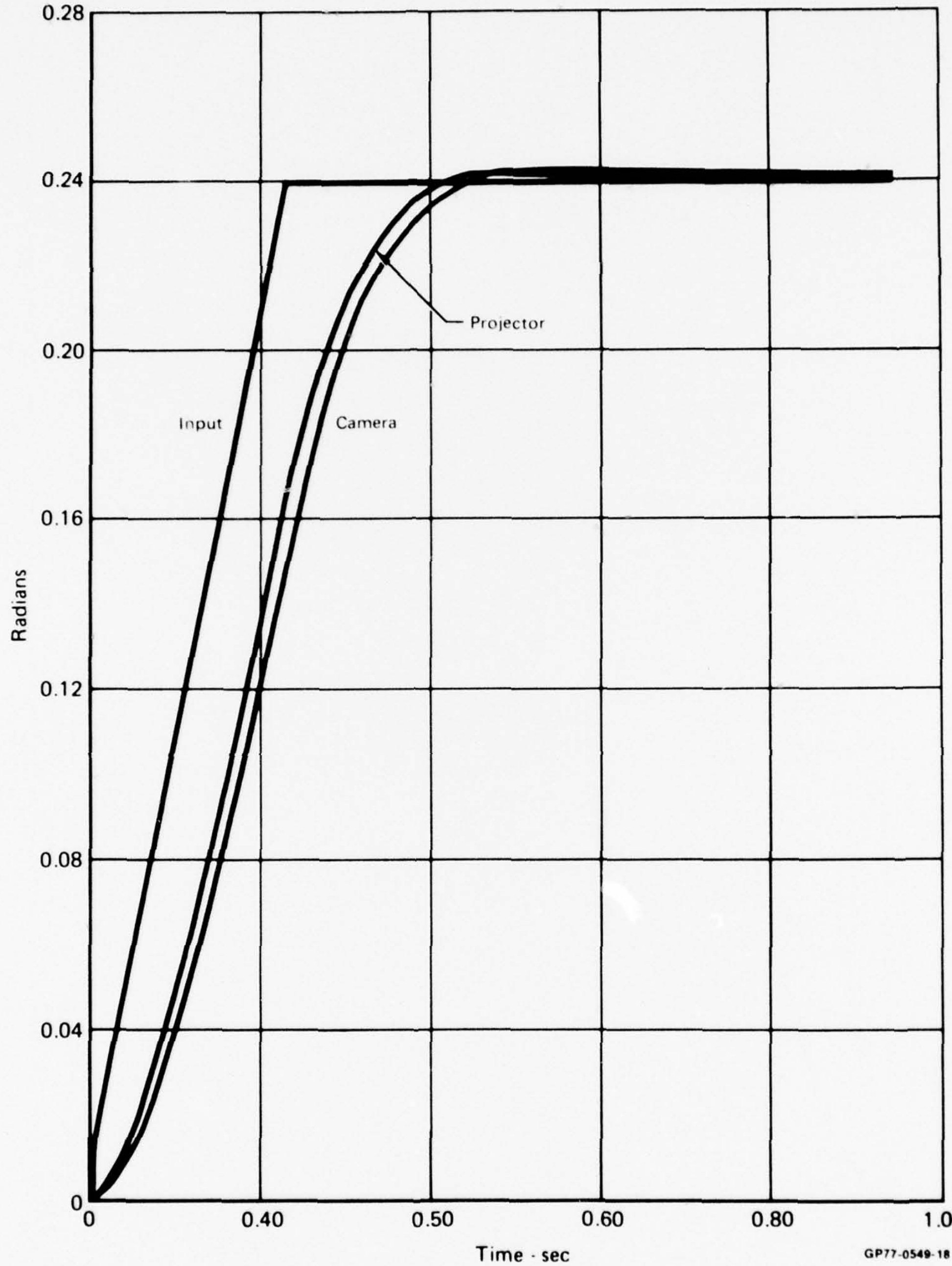

Figure 54 System Response for Stick Input
Lag = 0.14 Sec

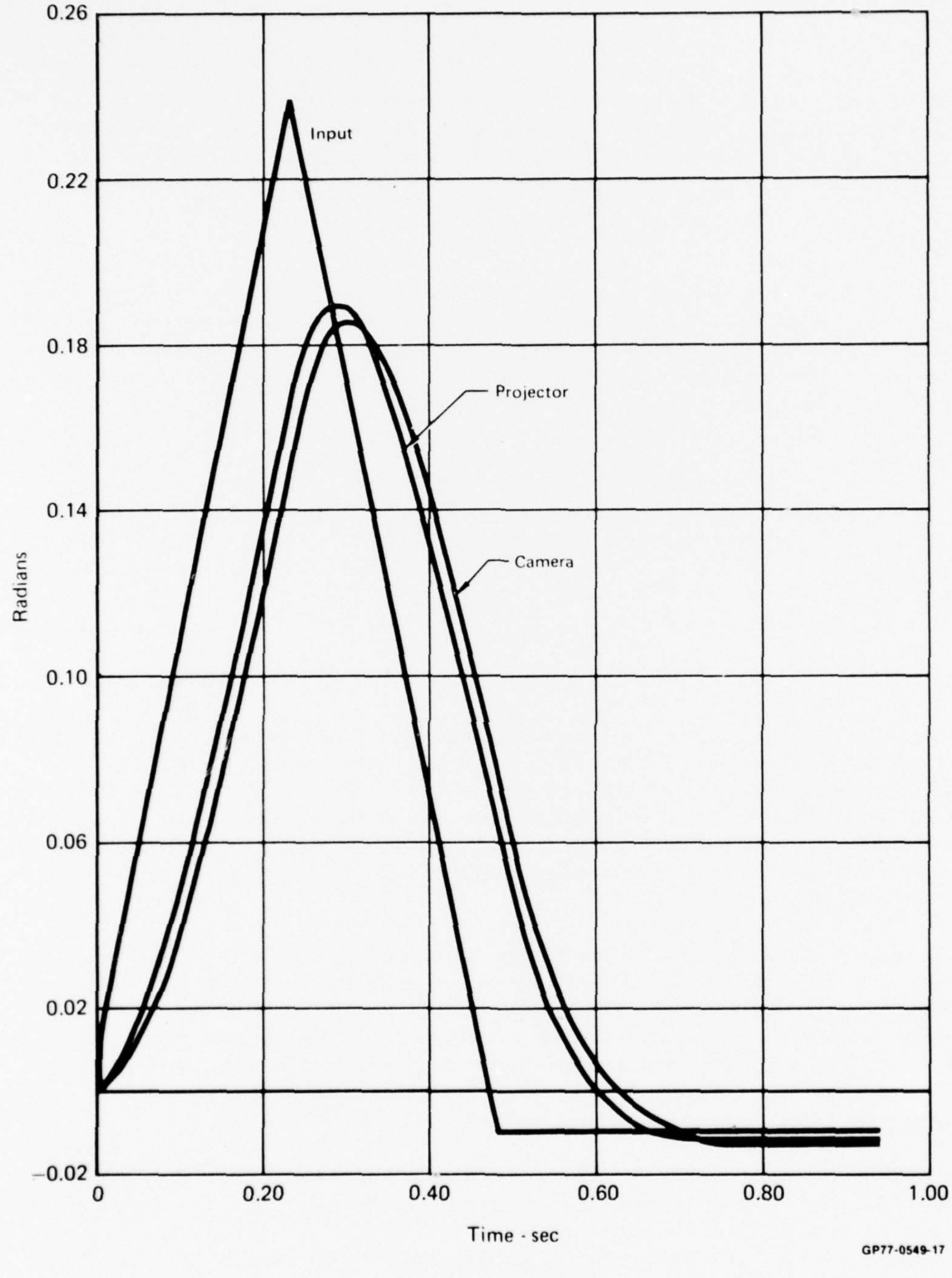

Figure 55 System Response for Stick Input
Lag = 0.14 Sec

5.4.3 MODE 3

Non-Linear Block Diagram

Figure 56 is a block diagram of the final mechanization showing the feedback loops implemented in the microprocessor. For simplicity the gimbal model is not included. The gimbals are shown as a double integration of the accelerating torque. Figures 57 and 58 show the response of the system to step inputs of the detector and for smooth Lead motion of 7 rad/sec for 0.25 sec.

Digital Model

A digital simulation of one axis of the system is shown in Figure 59. This model was used to conduct parametric studies and to determine the effects of various system non-linearities. The arithmetic and sample times of the microprocessor inherent in a sampled data system were included in the model to the extent possible. This was required to accurately predict hardware performance. Dynamic friction for the camera and the projector gimbals are included. The power amplifiers were modeled as voltage amplifiers. The torque motors for each gimbal were modeled from motor specificationa and gimbal inertias were taken from experimental results. The actual or final gains used in the microprocessor are in good agreement with those predicted by the model and in general correlation between hardware performance and that predicted by the model was very good. Quanitative information on the as built system non-linearities would further improve the simulation results.

5.5 SYSTEM OPERATION

[illegible] to system power-up, check to see that all cable connections are made. At [illegible] base, the microprocessor has two ribbon cables with DB25 connectors coming from the pitch and yaw shaft encoders, an analog output with connector (MS3106-MS-2P) which goes to two potentiometers on the input of the servo amplifiers, and the serial I/O cable (DB25) box. Also, located on the rear panel of the microprocessor are connections for the joystick control and helmet control.

The camera electronics box requires the serial cable from the microprocessor, two ribbon cables (DB25 connectors) from the shaft encoders and the analog output (MS3106-14S-4P) cable to the servo amplifiers. When all cables have been connected and the servo amplifier input gain pots turned to the off position, the microprocessor, camera electronics box, and servo amplifiers can be powered in any order. The microprocessor may now be started by pushing the "RST" button (reset) and then the "Go" button.

Next the operator turns each camera servo gain pot to maximum. He verifies that the camera is pointed straight ahead and that it is stable. Subsequently, the projector servo pots should be set to a maximum, one at a time. When the pot is maximum the camera and projector should be stationary and both pointing at the same position.

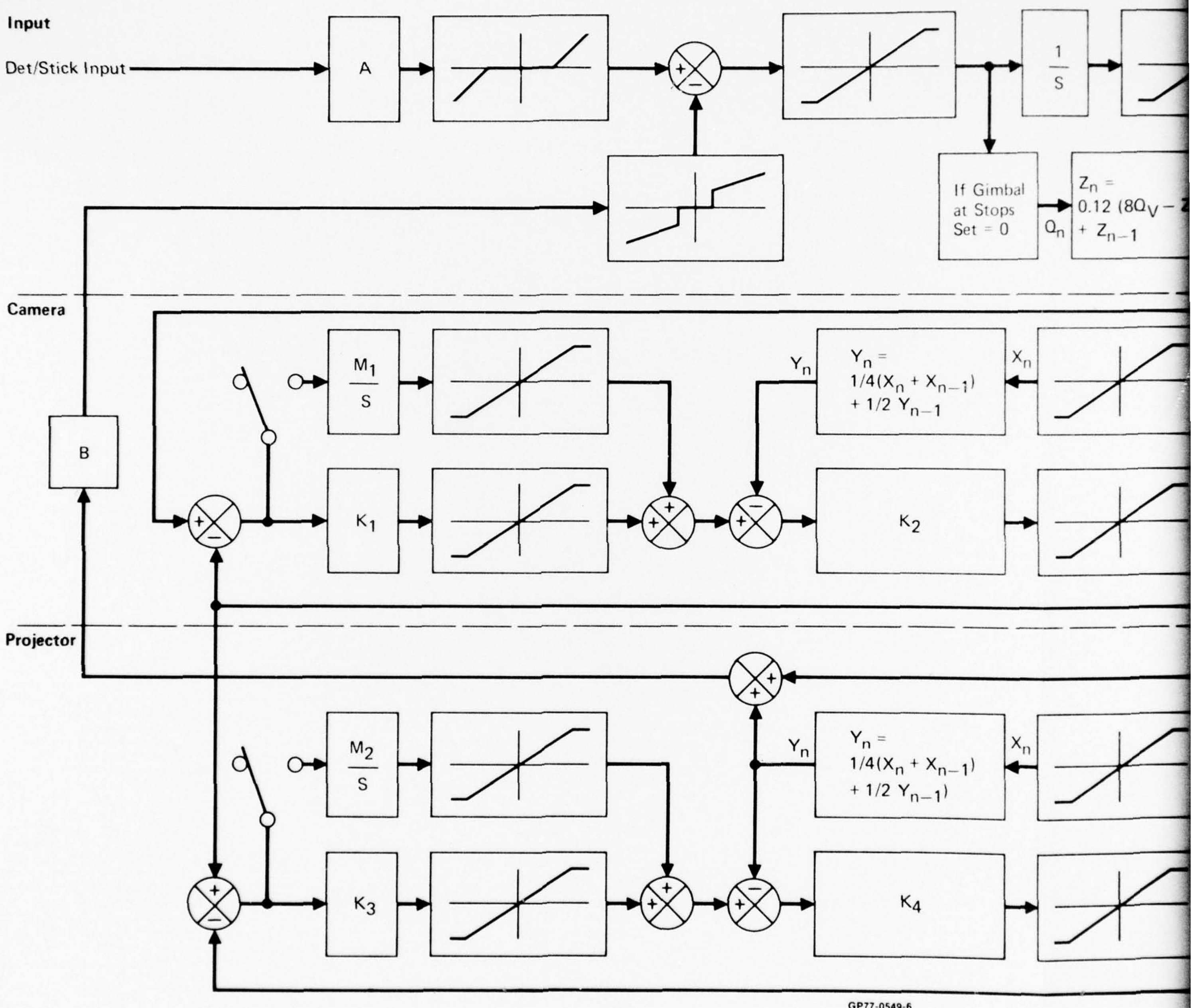

Figure 56 Pitch Servo Block Diagram

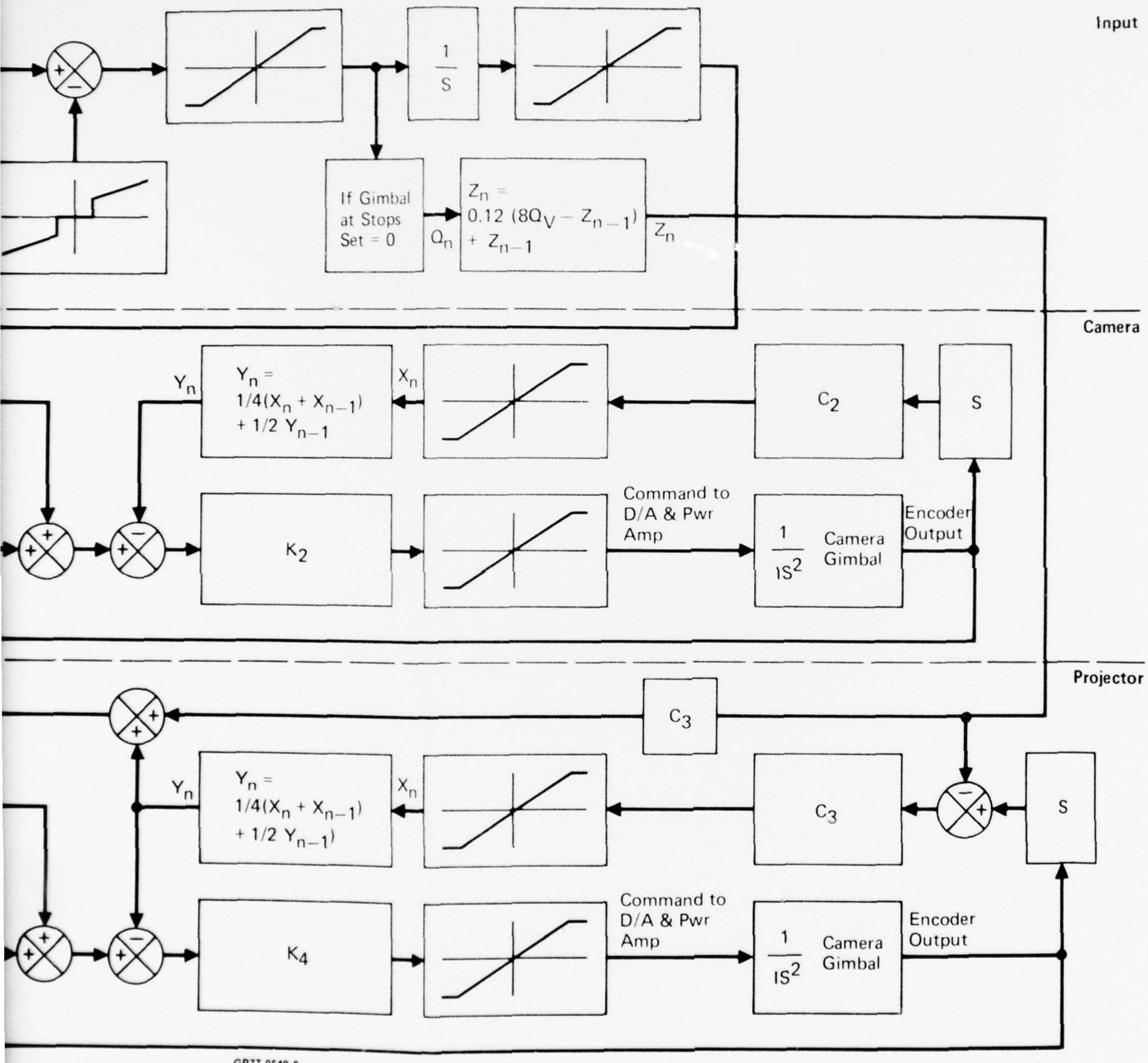

Input
1
S
If Gimbal
at Stops
Set = 0
Q_n
Z_n =
0.12 ($8Q_V - Z_{n-1}$)
+ Z_{n-1}
Z_n
Camera
Y_n
Y_n =
1/4($X_n + X_{n-1}$)
+ 1/2 Y_{n-1}
X_n
C_2
S
Command to
D/A & Pwr
Amp
K_2
1
IS^2
Camera
Gimbal
Encoder
Output
Projector
C_3
Y_n
Y_n =
1/4($X_n + X_{n-1}$)
+ 1/2 Y_{n-1})
X_n
C_3
S
Command to
D/A & Pwr
Amp
K_4
1
IS^2
Camera
Gimbal
Encoder
Output
GP77-0549-6

ram

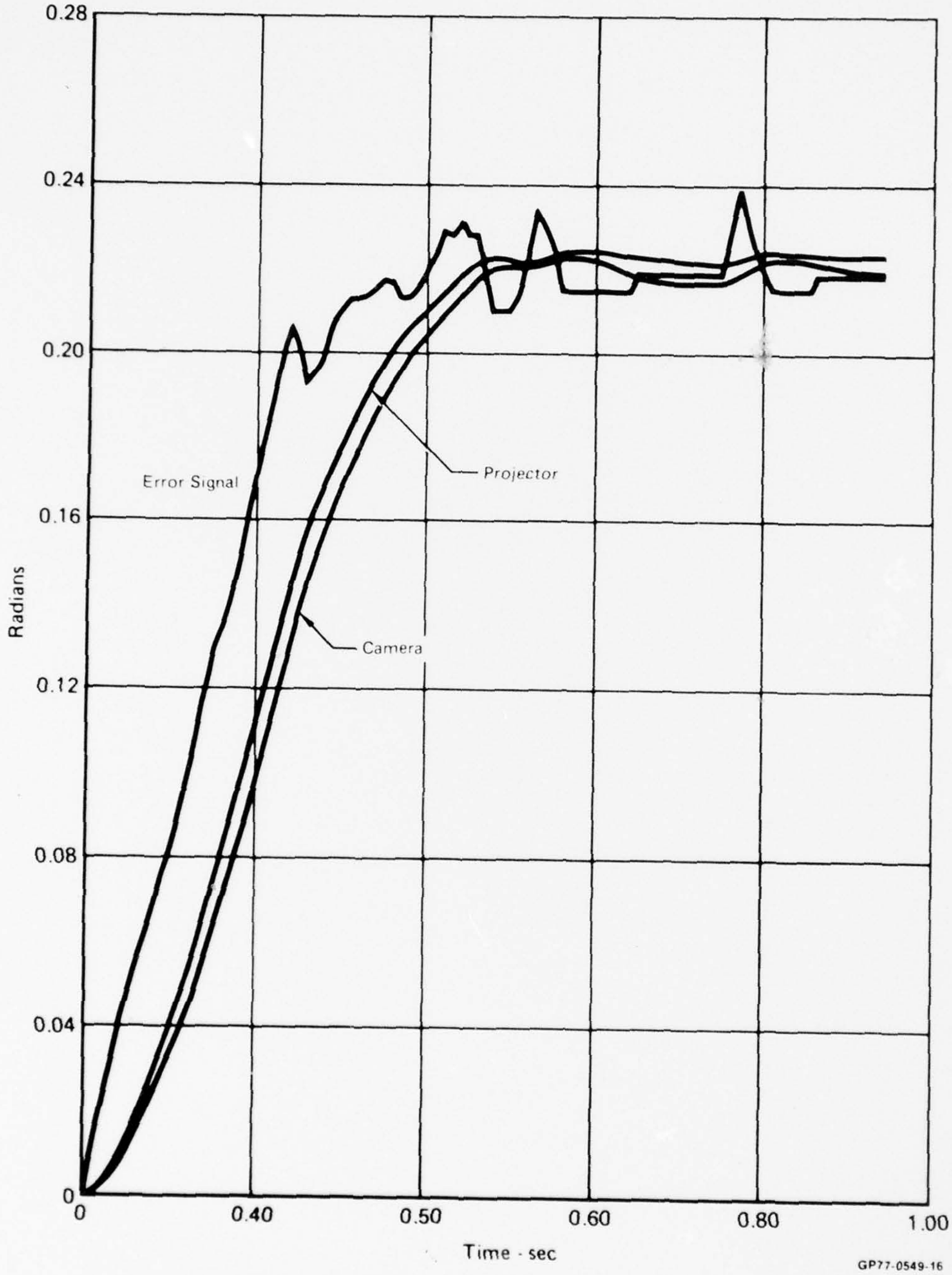

Figure 57 System Response for Ramp Input

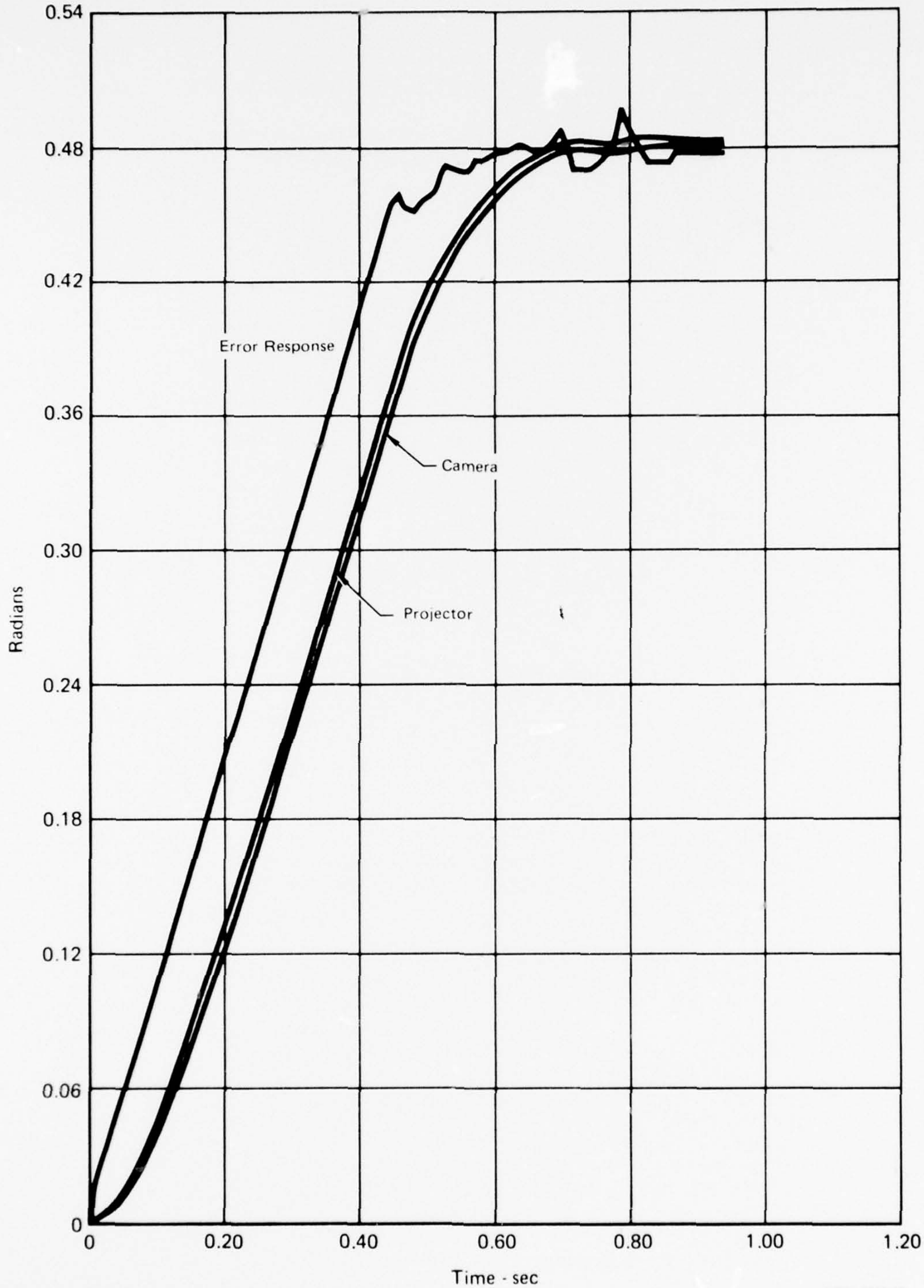

Figure 58 System Response for Step Input

```
C     PROJ CAMERA POSITION SERVOS STEP INPUT TORQ MTRS LIMITED
      INTEGER A,B,CAMR,DX,X,CER
      DIMENSION K(100),J(100),PROJ(100),V(100),M(100),JR(100),IDET(100)
      DIMENSION IV(100),IP(100),FST(100),DFST(100)
      DO 5 I=1,100
      IV(I)=0.0
      K(I)=0.0
      J(I)=0.0
      PROJ(I)=0.0
      DFST(I)=0.0
      FST(I)=0.0
      V(I)=0.0
      M(I)=0.0
      IP(I)=0.0
      JR(I)=0.0
    5 CONTINUE
      A=4
      B=-5
      EIN=0.25
      N=0
      CAMR=0
      DP=0.0
      PDOT=0.0
      DPDOT=0.0
      DT=0.010
      Z=0.00
      CR=0.0
      CRTE=0.0
      T=0.0
      RS=0.0
      DVDOT=0.0
      DV=0.0
      DO 100 I=3,100
      IDET(I)=((EIN-PROJ(I-1))*0.2)/0.000767
      KDRT=((PROJ(I-1)-PROJ(I-2))*2.0)/0.000767
      ID=IDET(I)*IDET(I)
      IF(ID.LE.16)IDET(I)=0
      CAMR=B*KDRT+A*IDET(I)
      IF(CAMR.GE.13)CAMR=13
      IF(CAMR.LE.-13)CAMR=-13
      DX=13
      N=N+1
      IF(N.GE.25)DX=0
      X=X+DX
      C=X*0.000767
      CER=X-IV(I-1)
      M(I)=CER
      DIP=M(I)*10.7*0.00244*1.333
      JR(I)=(V(I-2)-V(I-1))/0.000767
      CR=JR(I)/DT
      CRTE=CR*1.07*0.00244*1.333
      T=CRTE+DIP
```

Figure 59 System Math Model

```
      RS=T*T
      IF(T.GE.0.1)TQ=T-0.1
      IF(T.LE.0.1)TQ=T+0.1
      IF(RS.LE.0.01)TQ=0.0
      IF(RS.LE.0.01.AND.VDOT.GT.0.0)TQ=T-0.1
      IF(RS.LE.0.01.AND.VDOT.LT.0.0)TQ=T+0.1
      IF(T.GE.4.0)TQ=4.0
      IF(T.LE.-4.0)TQ=-4.0
      XLC=TQ-(VDOT*0.1824)
      DVDOT=(XLC*DT)/0.113
      VDOT=VDOT+DVDOT
      DV=VDOT*DT
      V(I)=V(I-1)+DV
      IV(I)=V(I)/0.000767
      ERR=V(I)-PROJ(I-1)
      AERR=(ERR*180.0)/3.14159
      K(I)=ERR/0.000767
      DISP=K(I)*13.0*0.00244*0.5
      J(I)=(PROJ(I-2)-PROJ(I-1))/0.000767
      DFST(I)=(DX-FST(I-1))*0.10
      FST(I)=FST(I-1)+DFST(I)
      PRT=(J(I)+FST(I))/DT
      RATE=PRT*1.30*0.00244*0.5
      DZ=K(I)*0.000152
      Z=Z+DZ
      CHK=K(I)*0.0*K(I)
      IF(CHK.GE.4900)Z=0.0
      TRQE=RATE+DISP
      TRS=TRQE*TRQE
      IF(TRQE.GE.0.1)TRE=TRQE-0.1
      IF(TRQE.LE.-0.1)TRE=TRQE+0.1
      IF(TRS.LE.0.01)TRE=0.0
      IF(TRS.LE.0.01.AND.PDOT.GT.0.0)TRE=TRQE-0.1
      IF(TRS.LE.0.01.AND.PDOT.LT.0.0)TRE=TRQE+0.1
      IF(TRQE.GE.1.2)TRE=1.2
      IF(TRQE.LE.-1.2)TRE=-1.2
      XL=TRE-(PDOT*0.02466666)
      DPDOT=(XL*DT)/0.052
      PDOT= PDOT+DPDOT
      DP= PDOT*DT
      PROJ(I)=PROJ(I-1)+DP
      IP(I)=PROJ(I)/0.000767
      WRITE(1,300) AERR,C,V(I),PROJ(I),TQ
  100  CONTINUE
  300 FORMAT (5(E11.4,1X))
      CALL EXIT
      END

ROUTINES CALLED:
EXIT

OPTIONS =/OP:2,/GO

BLOCK        LENGTH
MAIN.   3478   (015454)*
```

Figure 59 System Math Model (Concluded)

The system may be stopped at any time by turning the projector gain pots to zero. The processor may be stopped by pushing the HALT or the RESET button. The system may be restarted by repeating the sequence described above.

The mode of control may be switched between stick to head by actuating the toggle switch located on the rear panel of the microprocessor. When all gain pots are on, the system is in the stabilized mode. The projector pots can be left off for operation of system in non-stabilized display mode.

<u>Basic Monitor Functions</u>

The microprocessor has a self contained monitor program. An operator with an understanding of the servo control program, (See software section of this report) can use the monitor to troubleshoot not only software problems but also pin down the point of many electronic failures.

Using the monitor, the user can for instance examine the position data coming from the shaft encloders. To examine data, the following sequence should be used:

- o Depress halt (HLT) button
- o Depress examine memory (EM) button
- o Punch in memory address

When the address has been entered, the processor will display the 8 bit word stored at that address in a hexidecimal code. The location in memory following this address may be addressed by pushing the "CO" button. The low order bits are stored in the first location and the higher bits in the second. Camera pitch data is located at computer memory address 3D40 and 3D41. Camera yaw data is located at 3D42 and 3D43. The lower 13 bits contain the position information, highest order bits are not used and can be ignored. The lowest order bit is approximately equal to 2.6 minutes of arc.

A listing of the control program is available in the software section of this report. This listing, along with the monitor description in the same section, will allow a person familiar with the 8080 programming language to alter the system parameters and fine tune the system. The control systems gains can be adjusted directly from the monitor, but a word of caution is in order. Due to the scaling complexities and interaction of the system gains it is suggested that change not be made without a complete and thorough understanding of the software.

The quad detector mounted on the helmet has approximately a 40° full field-of-view. If the IR spot that it senses is outside its field-of-view, the microprocessor will receive no control signals and the servo will remain at rest. The observer needs to turn his head, pointing the detector toward the high acuity portion of the display. As the user does this, the system will begin to slew toward him. The sensitivity of the head controller can be adjusted by adjusting the intensity of the source. The recommended settings of the light source are 5 Vac and 5 amps.

The joy stick control has zeroing pots so that the joy stick analog output signal can be adjusted within the system's software deadband eliminating servo drift.

The microprocessor LED readouts allow the operator to determine the operational mode of the microprocessor. Upon powerup, the readout will show 43210. The same readout will occur after the RST GO sequence. The halt (HLT) button will cause a "D" to be read into the first digit and the next four show the current program counter. The restart (RS) button changes the halt display to show a 6 in the first digit and leaves the other digits unchanged. If after depressing the halt button, a "D" is not located in the first digit, the microprocessor program is not running correctly is indicated. The user should then repeat to reset sequence (RST, GO).

The torque motor on the yaw axis of the projector can exert 100 ft. lb. of torque if the power amplifier or its input should fail in a hardover mode. Hard stops and motor shorting switches have been installed on this axis to protect the light valve in the unlikely event that such a failure should occur. If the motor shorting switches are tripped, the operator must stop the system and reset the switches.

In normal operation the software limits the camera and projector axes to $\pm$ 90° in yaw and $\pm$ 45° in pitch. These software limits prevent the operator from slewing the equipment into the mechanical stops and eliminate undue rapid deceleration of the hardware.

5.6 HEAD TRACKER INTERFACE ELECTRONICS

The control signals required for the head tracking mode are generated by a dual axis position sensor. This sensor provides pitch and yaw position information from a light spot imaged on the detector surface. The source of the light imaged on the detector is a 24 watt bulb in a lens assembly focused to image the filament of the bulb on the dome surface. The detector is helmet mounted, and the light source is mounted on the projector pitch axis. Although some axes crosstalk could have been eliminated by mounting the detector on the pitch axis and the light source on the helmet, the opposite arrangement was chosen in order to keep the helmet assembly as light as possible. Both the light source and the detector are filtered with Wratten 88A filters. The detector (PIN-SC-25) manufactured by United Detector, has a position sensitivity of .32 amp/watt/cm, and a series resistance of 5KΩ. The light source is a 1763, 6 volt, 4 ampere prefocus socket bulb. The detector output signal is amplified using the circuit shown in Figure 60. This amplifier is characterized by its low input impedance and high common mode rejection. The zener diodes located on the output stage clip the signal at approximately 4.7 volts to prevent overdriving the analog to digital input of the microprocessor.

The spot imaged on the detector (the filament of the bulb)nominally has a width of 0.06 inches. The detector has a usable width of 0.74 inch. A rough calculation shows that using a 0.9 inch focal length lens the detector will have an approximate field of view of 40°. If the source imaged on the dome is outside of the field of view of the detector the microprocessor receives no signals from the detector and the system will remain at rest. As the detector is pointed toward the image on the dome surface, the projector will begin to slew toward the detector. As the projector slews toward the detector* and locks onto the detector's signal, the system's feedback loop is completed and the system will be fully head controlled.

A typical signal output vs. command angle is shown in Figure 26. The amplitude of the signal output is not only a function of the CMR amplifier, but also of the light source intensity and positioning of the detector within the return cone of the source light.

The head control system may be finetuned by adjusting the light source to provide the appropriate response in the closed loop system.

---

* In actuality, the detector directs the camera to move and the projector follows the camera.

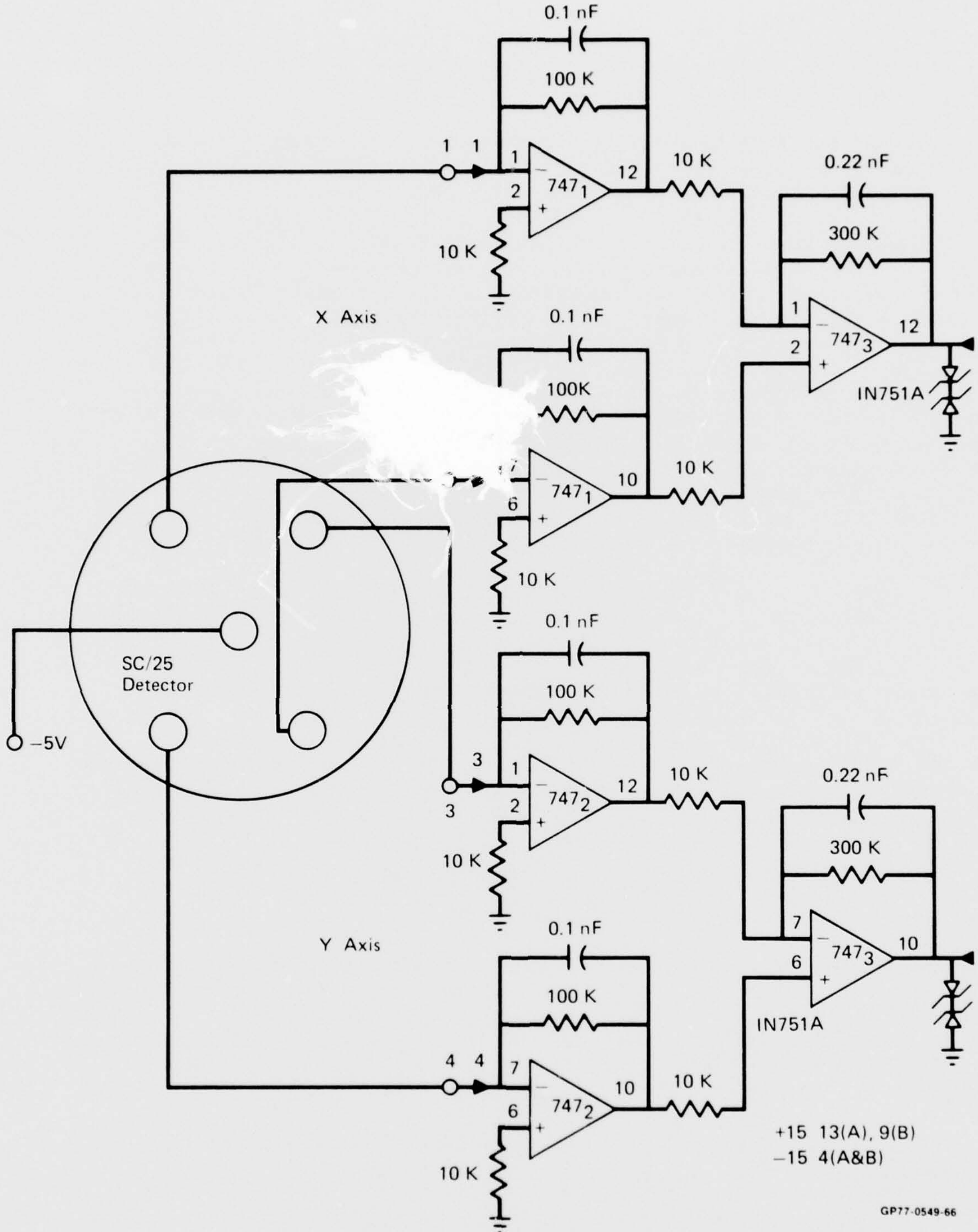

Figure 60 Head Control Detector Amplifier

Section 6

RESULTS AND CONCLUSIONS

This section details the tests that were made to document system performance as measured by system resolution and distortion and compares these data to theoretical predictions.

Resolution measurements of the total system were made using tribar targets. These measurements were made on the system as it was adjusted for the ONR demonstration. The system was set up for best overall focus, a situation which reduces on-axis resolution. The system focus problem is discussed in more detail in the focus corrector section of this report.

The lens distortion function causes no noticeable effect to radial lines while lines perpendicular to these (tangential lines) are compressed. For example, in the vertical direction, a vertical bar target which is readily resolvable has a horizontal counterpart which is not resolvable. These two target orientations were used to measure system resolution along and across the scanning line direction, (i.e. Horizontal bars used for vertical measurements).

The resolution measurements were made as a function of the angle from the optical axis (θ). These angles were computed from shaft position encoder data read from the microprocessor memory, the system geometry and lens nodal point shift data. Figure 61 shows the geometry involved to render a true θ from the encoder readings in order to determine vertical and horizontal resolution.

The target viewing distance was selected to be always greater than the lens hyperfocal distance as determined with an F11 system, and the focal length for the corresponding θ. The camera automatic iris control was disabled and set at the typical outdoor setting which was about F111. The resolution targets were illuminated using photoflood lamps, to provide proper target contrast. Now the vertical and horizontal resolution as a function of incoder reading will be determined.

The lens is located vertical distance (a) and horizontal distance (b) from the pivot point. The lens nodal point is located a horizontal distance (b-n) from the pivot point. The lens optical axes labeled Oa is pointed on azimuth angle (βa) and elevation angle (βe) with respect to the reference co-ordinate system xyz. The tibar target is located at angle θ with respect to the lens optical axis in a vertical plane.

For the vertical resolution, from the triangle with apex's labeled as 1-5-8 in Figure 61(a).

$$S_1 = \frac{L}{\cos \beta_a} \qquad (68)$$

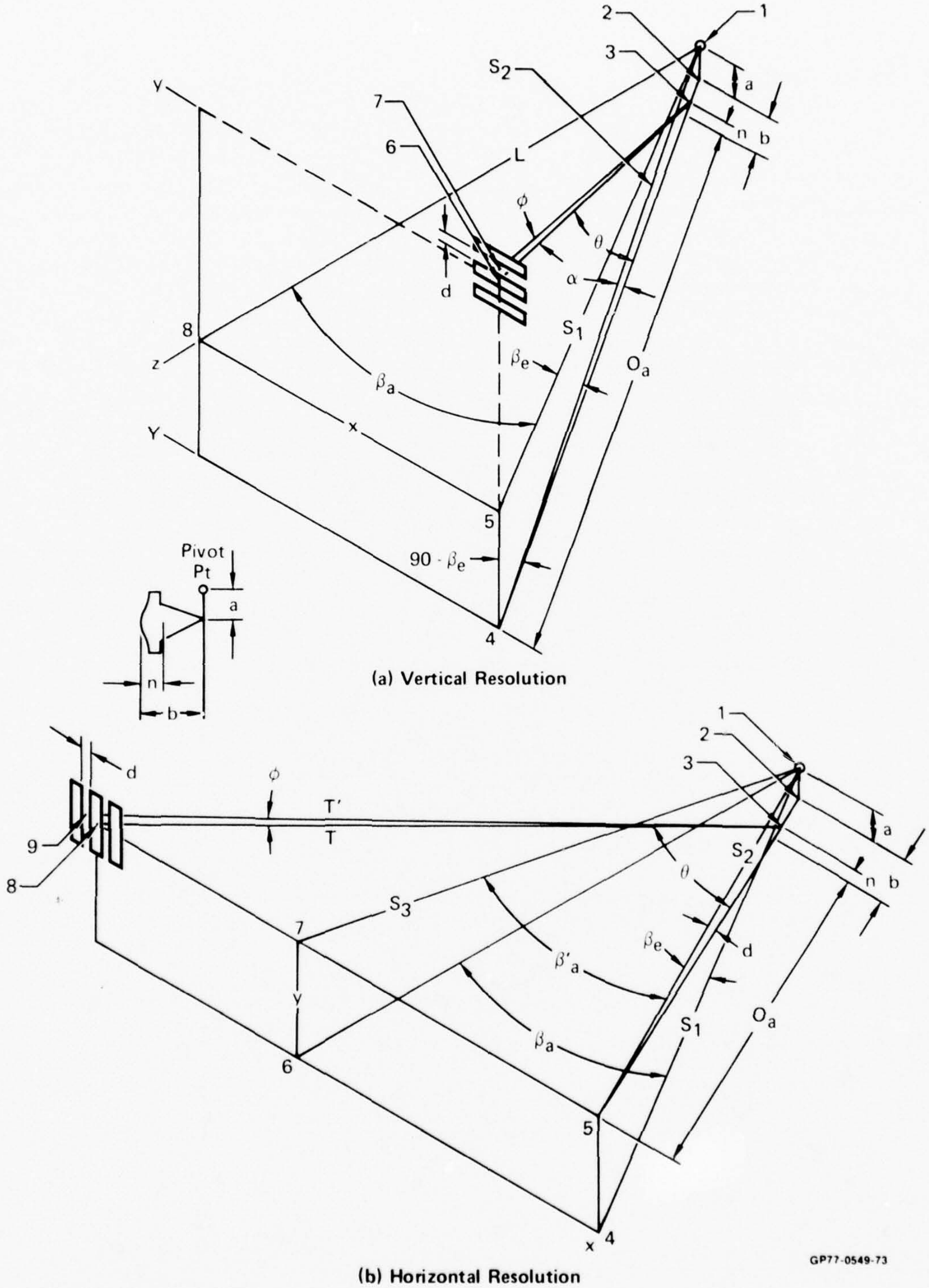

Figure 61 Geometry to Convert Shaft Encoders Readings to True Angles

From triangle 1-4-5

$$Y = S_1 \tan \beta_e \tag{69}$$

Also from triangle 1-4-5

$$S_2 = \frac{S_1}{\cos \beta_e} \tag{70}$$

From triangle 1-2-4

$$\alpha = \text{arc sin } \frac{a}{S_2} \tag{71}$$

From triangle 1-2-4, the distance 0_a is

$$0_a = S_2 \cos \alpha - b \tag{72}$$

From the oblique triangle 3-4-6, the distance T is

$$T = \sqrt{(Y + y)^2 + (0_a + n)^2 - 2(Y + y)\ (0_z + n) \cdot \cos\ (90 - \beta_e + \alpha)} \tag{73}$$

From the oblique triangle 3-4-6 the angle θ is defined as:

$$\theta = \text{arc cos} \left(\frac{-(Y + y)^2 + (0_a + n)^2 + T^2}{2\ T\ (0_a + n)} \right) \tag{74}$$

From oblique triangle 3-4-7

$$T' = \sqrt{(Y + y + d)^2 + (0_a + n)^2 - 2\ (Y + y + d) \cdot (0_a + n)\ \cos\ (90 + \alpha - \beta_e)} \tag{75}$$

Also from oblique triangle 3-4-7 the angle θ' is defined as:

$$\theta' = \text{arc cos } \frac{-(Y + y + d)^2 + (0_a + n)^2 + (T')^2}{2\ T'\ (0_a + n)} \tag{76}$$

The resolution $\emptyset$ is then

$$\emptyset = \theta' - \theta \tag{77}$$

Now the horizontal resolution case shown on Figure 61(b) where the optical axis and line to target are in the horizontal plane. From the triangle with apex labeled 1-4-6,

$$S_1 = \frac{L}{\cos \beta a} \tag{78}$$

From triangle 1-4-5

$$S_2 = \frac{S_1}{\cos \beta_e} \tag{79}$$

From triangle 1-2-5

$$\alpha = \text{arc sin } \frac{a}{S_2} \tag{80}$$

From triangle 1-4-6

$$X = L \tan \beta_a \tag{81}$$

From triangle 1-2-5

$$0_a = S_2 \cos \alpha - b \tag{82}$$

From triangle 1-6-7

$$S_3 = \sqrt{L^2 + y^2} \tag{83}$$

From triangle 1-5-7

$$\beta'_a = \text{arc tan } \frac{X}{S_3} \tag{84}$$

From oblique triangle 3-5-8

$$T = \sqrt{(X + x)^2 + (0_a + n)^2 - 2(X + x)\ (0_a + n) \cdot \cos\ (90 - \beta'_a)} \tag{85}$$

Also from oblique triangle 3-5-8

$$\theta = \text{arc cos} \left(\frac{-(X + x)^2 + (0_a + n)^2 + T^2}{2\ T\ (0_a + n)} \right) \tag{86}$$

From oblique triangle 3-5-9

$$T' = \sqrt{(X + x + d)^2 + (0_a + n)^2 - 2(X + x + d)(0_a + n) \cdot \cos(90 - \beta'_a)} \quad (87)$$

Also from triangle 3-5-9

$$\theta' = \arc\cos\left(\frac{-(X + x + d)^2 + (0_a + n)^2 + (T')^2}{2T'(0_a + n)}\right) \quad (88)$$

The horizontal resolution is:

$$\emptyset = \theta' - \theta \quad (89)$$

6.1 CAMERA PERFORMANCE

Results of the camera performance tests are shown in Figures 62 and 63. Figure 63 shows resolution in the horizontal plane while Figure 63 is the same data for the vertical plane. The expected resolution as discussed in Section 3.0 is also shown on the figures. Note that in either case the on-axis angular resolution is about 1.7 times worse than was anticipated. In order to make some meaningful comparisons the computer model of Appendix E was degraded until the measured on-axis performance was achieved. This degradation was accomplished by increasing the Guassian blur of the non-linear lens function. This required an increase from the ray trace data value of 5.5 microns (one sigma) to 50 microns. These data are shown by the solid line on the figures. Note that this data which was matched on-axis is near the actual performance for most other field angles. This indicates a uniform optical blur at the vidicon faceplate. A notable exception is the considerably worse performance in the 0.4 to 1.0 degree region caused by an incorrect aspheric element profile in the rear optical assembly of the non-linear lens. We attempted to correct for this during the contract by fabricating new elements using a new state-of-the-art pantagraph grinding technique and an air bearing spindle. Unfortunately, this was a failure. The new elements were even worse than the original hand fabricated elements. The fabricator is presently remaking these elements which will hopefully correct this problem in the near future. In this abnormal acuity region, performance drops by a factor of three. This is very distracting because performance should be best in this region to support foveal vision.

6.2 TOTAL SYSTEM PERFORMANCE

The measured performance of the overall system is shown in Figure 64 and 65 for the horizontal and vertical planes. Employing the same analytical method as in the camera case it was necessary to degrade display performance from the anticipated 15 microns (equivalent light valve spotsize) to 90 microns in order to predict horizontal on-axis performance. Then when

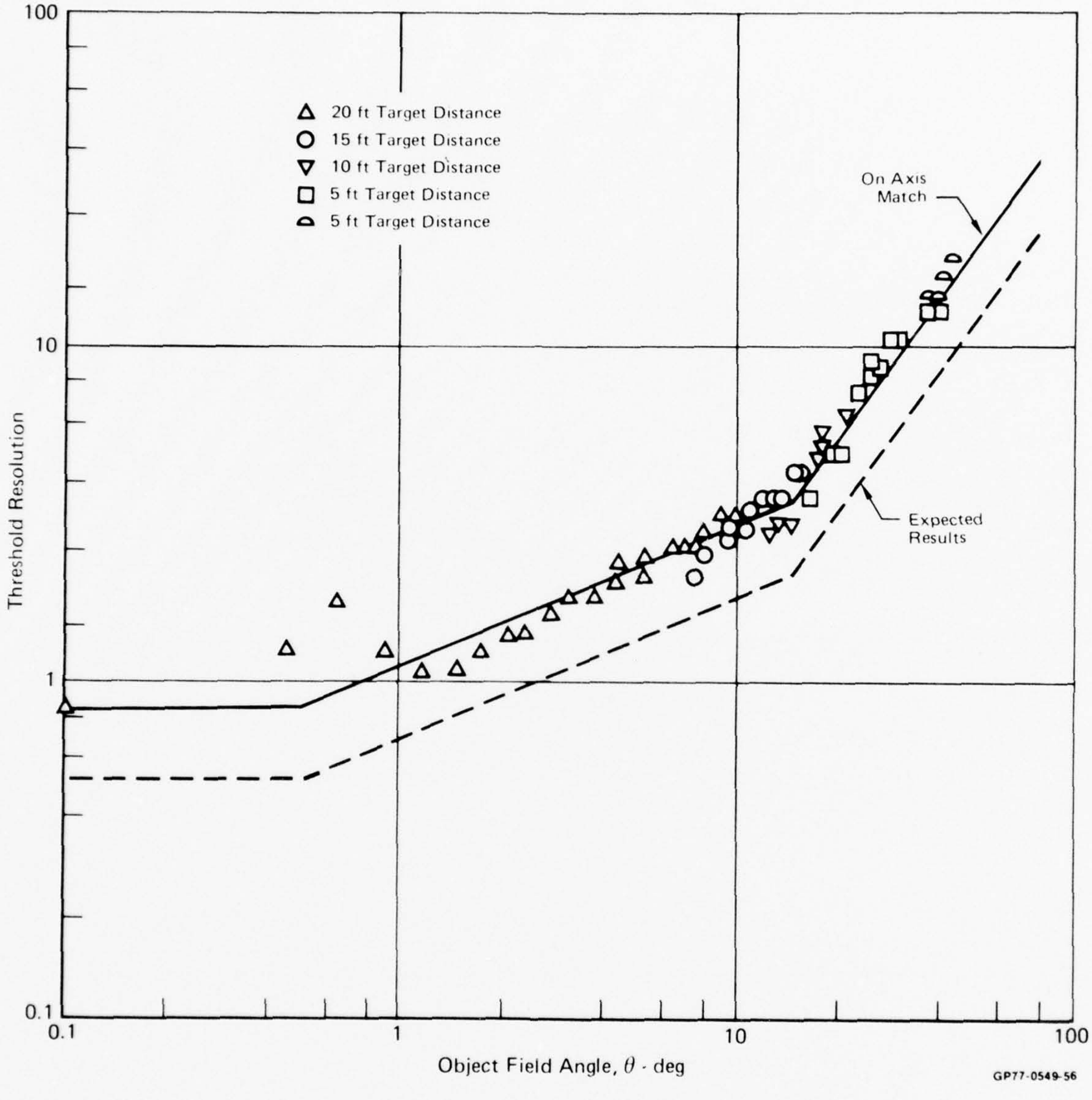

Figure 62 Threshold Resolution vs Angle from Optical Axis
Camera Only (Horizontal)

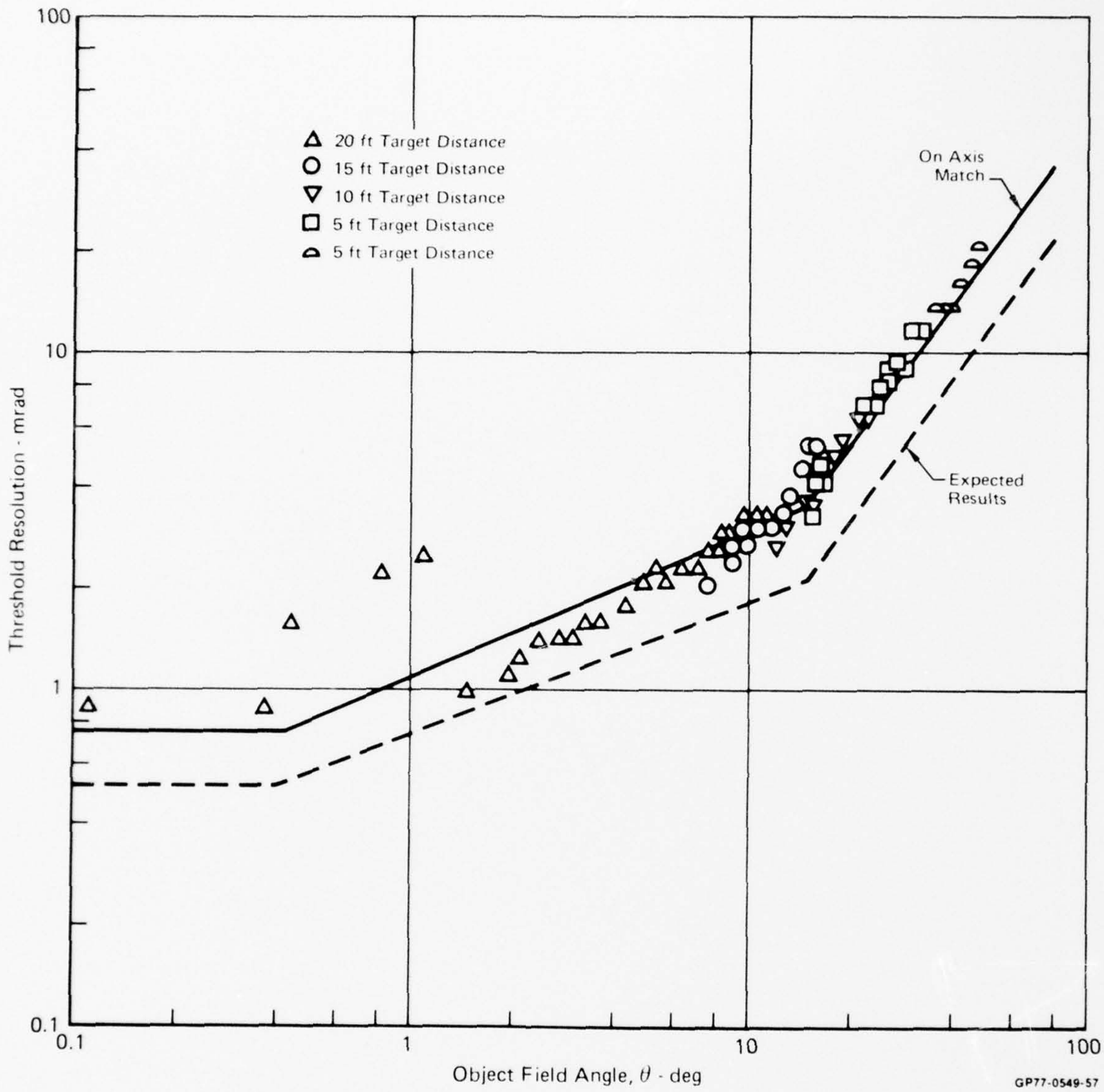

Figure 63 Threshold Resolution vs Angle from Optical Axis
Camera Only (Vertical)

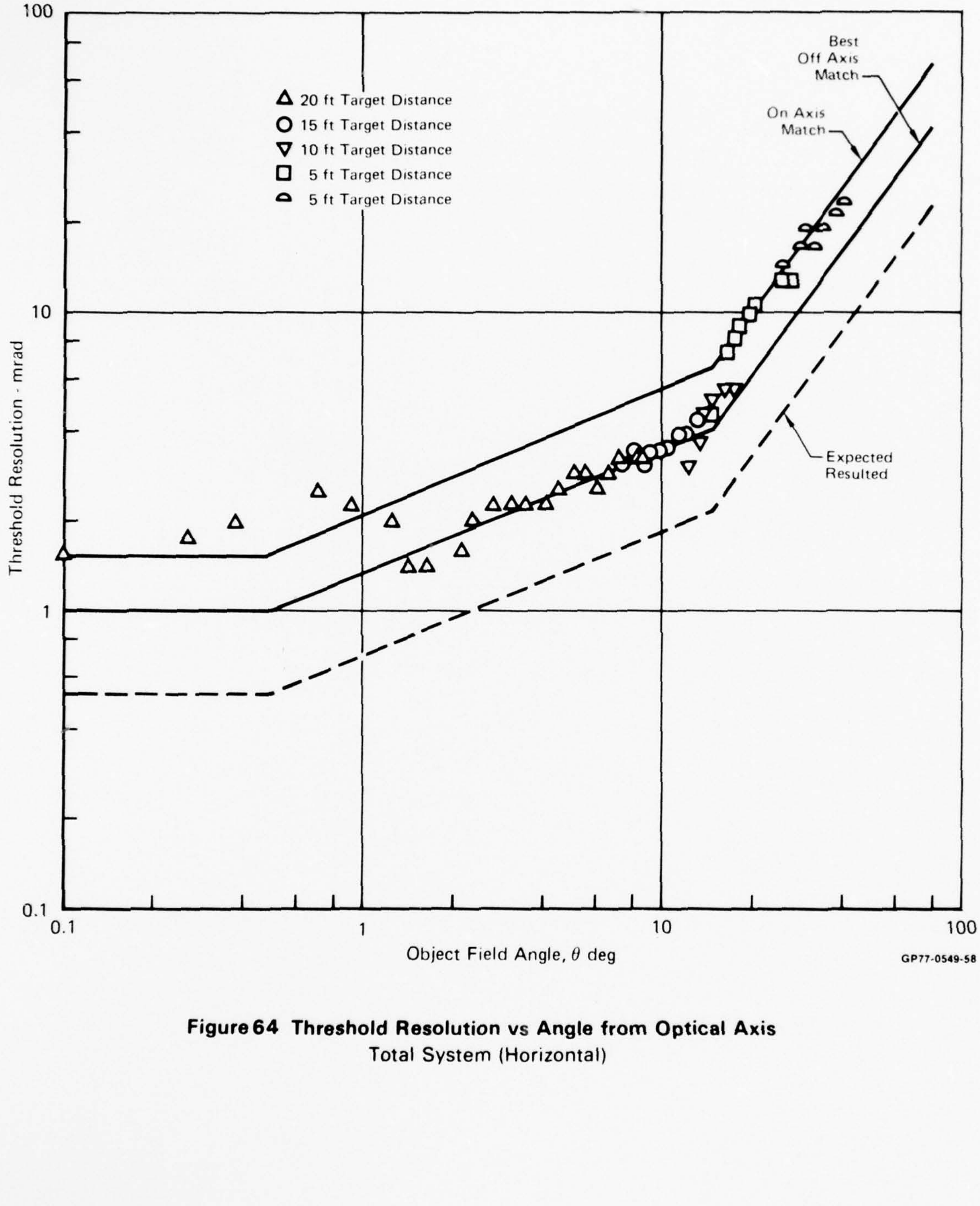

Figure 64 Threshold Resolution vs Angle from Optical Axis
Total System (Horizontal)

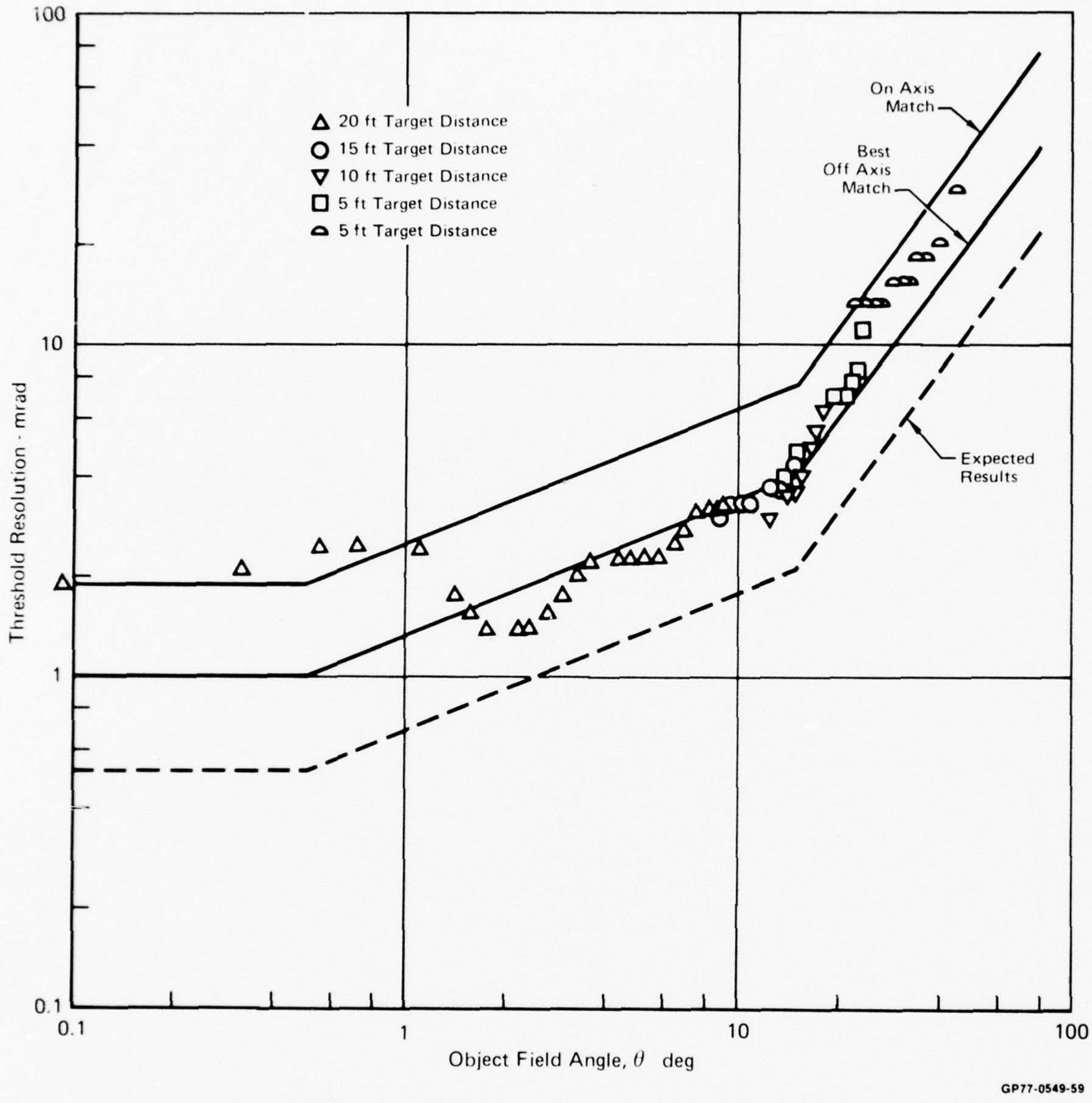

Figure 65 Threshold Resolution vs Angle from Optical Axis
Total System (Vertical)

these data were plotted on Figures 64 and 65 very poor prediction of off-axis data is obtained. This implies a nonuniform degradation at the object plane of the projection non-linear lens with much higher blur on-axis. The reason for this is the diffraction problem created by the schlierin optics which was discussed in Section 3. However it appears to be considerably worse than anticipated. To assess the remainder of the field, the display blur was reduced until a good match was obtained off-axis. (The greatest emphasis was placed on the less than 15° region because of expected magnification problems which will be discussed later). A display blur of 30 microns matched the data very well for both horizontal and vertical planes as can be seen on the figures. This is a reasonable display quality value which would produce very little additional degradation to the camera if it applied on-axis as well. The on-axis performance would only degrade from 0.85 to 1.0 milliradian if the 30 micron display quality was maintained on-axis.

The disparity in on-axis system performance between horizontal and vertical planes (1.5 to 1.9 milliradians) is undoubtedly due to schlierin alignment (horizontal at the non-linear lens focal plane) which will yield a higher diffraction cutoff spatial frequency in the horizontal direction.

The system resolution, Figures 64 and 65, show the same local region of poor performance (around 1°) that was seen on the camera only curves. The projector appears to aggrevate this region very little. The reason for this lies in the fact that the projector lens produces much better quality in this region apparently because it has a better rear lens cell.

The apparent lower system resolution at field angles larger than 20° is caused by incorrect magnification. This can be seen on Figures 66 and 67 which show measured vs. computed angular error in the projected display. Here the measured data is compared to 2%, 5% and 10% magnified images. The desired value is 2% while the horizontal magnification appears to be about 7% and the vertical about 4%.

6.2.1 Low Contrast Performance

Because of time constraints, direct measurement of low contrast performance was not possible. Therefore it is necessary to use the analytic model adjusted to yield the measured high contrast performance, to estimate performance at lower contrasts. These data are shown on Figure 68. Here the input modulation (contrast) required to resolve targets at various spatial frequencies are shown. Two curves are required for the system because of the projector problem noted above. It should be noted that the linear spatial frequency scale applies everywhere on the non-linear lens focal plane while the angular spatial frequency scale applies only on-axis. These two spatial frequency parameters are related as described in Appendix D.

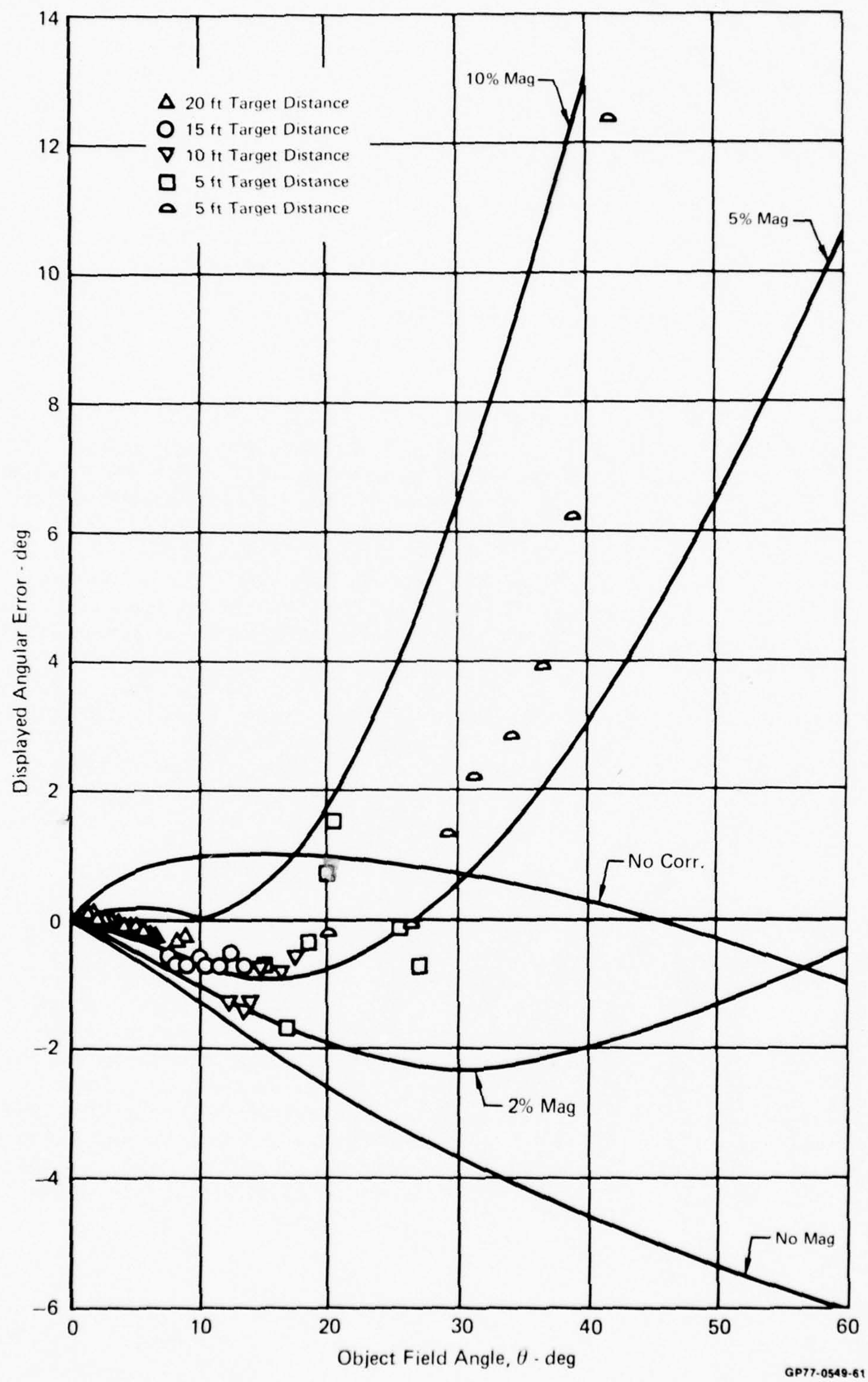

Figure 66 Horizontal Display Error vs Angle

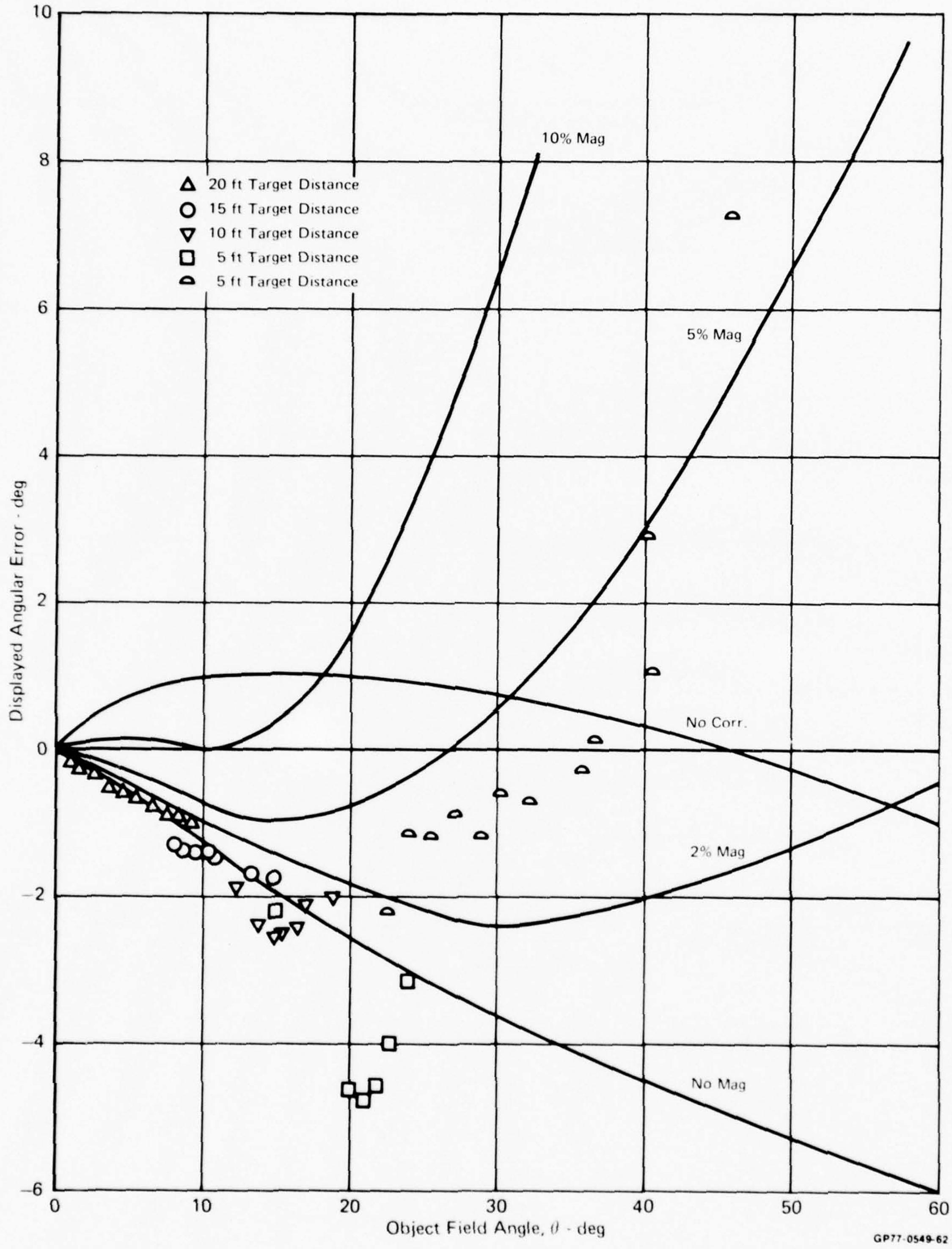

Figure 67 Vertical Display Error vs Actual Angle

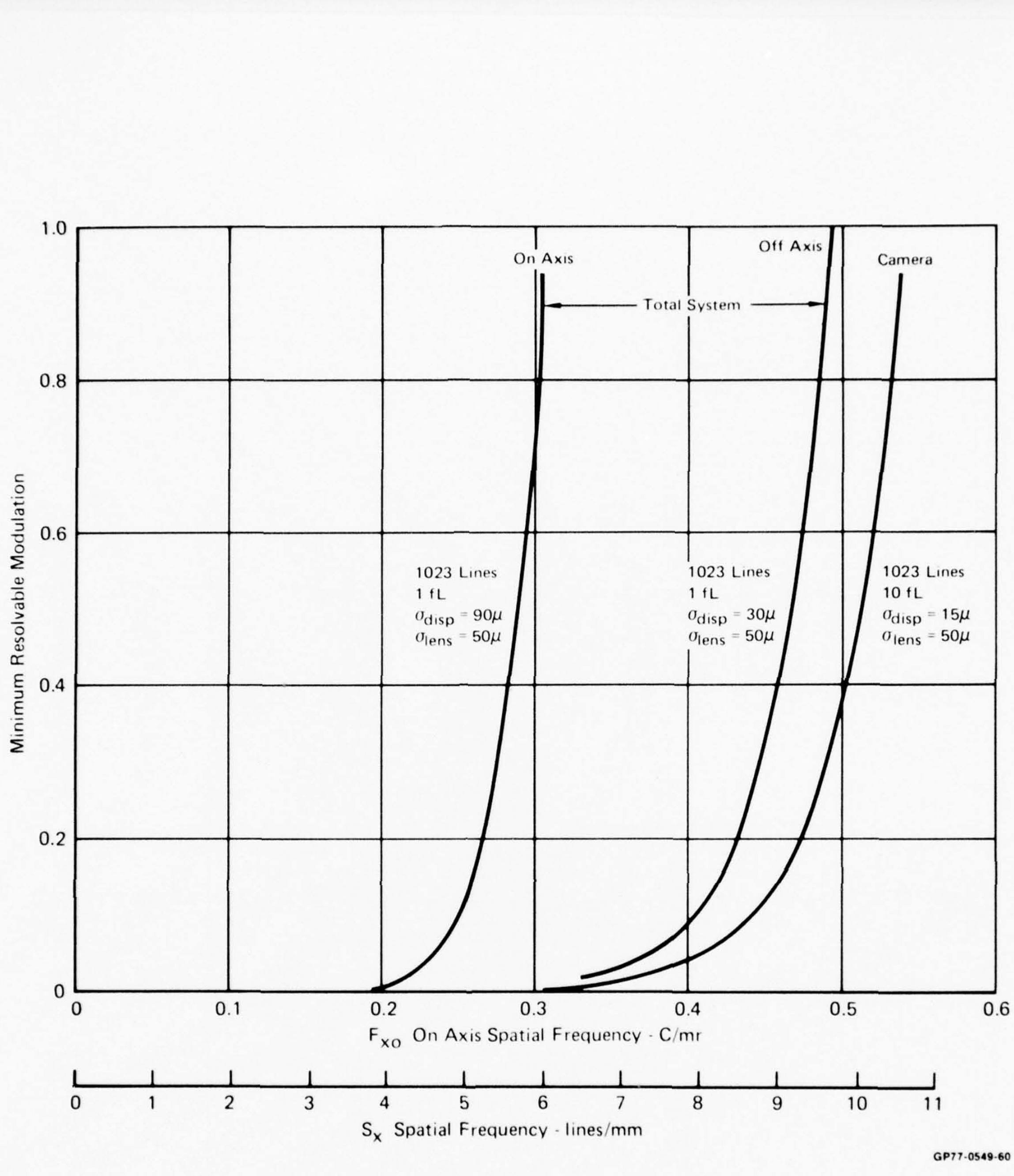

Figure 68 Minimum Resolvable Modulation Predictions

6.2.2 Demonstration Results

The system was demonstrated in the laboratory by placing the camera on the northwest corner of the roof of MCAIR Bldg. 102. A hard wire link was established to the display station which was located in the laboratory about 300 ft. away. The camera overlooked Lambert Field and Brown Road which borders the airport. A field of regard of 180° in azimuth and ± 60° in elevation was established. For comparison a 525 line conventional TV camera with a remote control zoom lens was also placed on the roof. This camera was pointed towards a sign board about 1000 ft. distant. This sensor was displayed adjacent to the RVS camera video CRT display.

To compare resolution, the RVS camera was pointed toward the same sign board and the conventional camera was zoomed until the same detail could be seen on its display as the on-axis RVS was producing. This field-of-view was about 10° x 14°. The RVS projection field-of-view was then reduced by masking to this field-of-view. The operator was then given the task of searching the field of regard of the RVS sensor using joy stick control. The usual problems with narrow fields-of-view were noted in maintaining orientation in the total field of regard and in smooth tracking of moving vehicles.

Next the mask was removed so the operator could see the entire RVS field of view and the full up head control operation established. In general all viewers liked the wide field display, especially the ease in tracking moving targets. It should be noted here that the servo control performance was excellent. No perceptible display motion occurred under any dynamic condition. This requires that the camera and projector servos track within about 0.5 milliradian under the most extreme dynamic conditions.

Most observers noted the low on-axis performance even when made aware that it was comparable to a 14° FOV conventional system. Some observers were impressed by motion and glint cueing in the peripheral very low resolution area of the display while others felt lack of sharp spatial detail in these regions would degrade these visual cues.

6.3 CONCLUSIONS AND RECOMMENDATIONS

Considering this is the first device of this type, we feel the results were very encouraging. As should be expected the only serious problems were with the new technology or state-of-the-art advancement in non-linear optics. All conventional functions within the state-of-the-art worked perfectly including the servo control, TV camera, TV projector, head tracker, etc. The value of the digital control system was demonstrated through its outstanding performance and reliability which could have been achieved only with great effort if an analog system was employed.

It appears the greatest improvement in performance could be obtained by (a) replacing the rear splines elements of the non-linear lenses and (b) solving the diffraction problem in the projector relay. The first is underway and if successful should be corrected within one to two months. The latter has no easy solution at this time. As discussed in Section 3, increased relay magnification may help but complete correction may require a different type of light valve that does not require Schlerin optics. At least two are presently under development. A KDP light valve is being developed in France while a liquid crystal light valve is under development at Hughes Aircraft in the USA. Both of these operate on a controlled polarization principle and can use conventional optics. Another possibility is to construct a new non-linear lens with a small F/number so that it can utilize more of the light valve optical ray cone.

Finally we believe the laboratory demonstration, where a scene is viewed in which most spatial detail is stationary, does not show the true potential of the system in flight control and navigation. We have seen this when projecting tape recorded video taken through the windshield of an aircraft. It appears that the somewhat low on-axis resolution is not so objectionable under these dynamic conditions. Based on these observations it may be desirable to fly the sensor in order to obtain a true performance assessment in a dynamic environment.

Section 7

REFERENCE LIST

1. RVS Display Feasibility Study, Report No. MDC A3392, 28 Feb. 1975 McDonnell Aircraft Co., St. Louis, Mo. 63166

2. Remote Viewing System Technical Proposal Report No. MDC A2486, 21 Sept. 1973, McDonnell Aircraft Co., St. Louis, Mo. 63166

3. Head Controlled Remote Viewing System Technical Proposal Report No. MDC A3020, 3 Sept. 1974, McDonnell Aircraft Co., St. Louis, Mo. 63166

4. Klaiber, R.J., Physical and Optical Properties of Projection Screens; Technical Report NAVTRADEVCEN IH-63, December 1966

Appendix A

BRIEF DESCRIPTION OF THE REMOTE VIEWING SYSTEM (RVS)

The RVS concept is based on the fact that the human visual capability can be represented by a resolution capability of about 130,000 elements, provided that these elements are sized non-linearly according to the acuity function as shown in Figure A-1. An image with this characteristic requires only about 2 MHz video bandwidth at 30 Hz frame rates. In comparison, standard techniques would require over 1,000 MHz bandwidth for this field-of-view (180°) and resolution. Even at smaller fields-of-view, the bandwidth saving is significant. A comparison of bandwidth requirements for varying fields-of-view for the conventional linear acuity function and for the RVS foveal concept is shown in Figure A-2. Approximately two orders of magnitude decrease in BW is achieved with the foveal system at FOV's greater than 20 degrees. In order to mechanize the concept described above, a method must be devised to generate an image which satisfies the optical requirements of the eye. The RVS concept contains a lens system that creates optical "distortion" by varying the spacing of the angular resolution elements to duplicate the acuity function shown in Figure A-1. This process is illustrated in Figure A-3. The lens transfer characteristic required and the technique for reconstructing the image at a remote location is also shown on this figure. System operation is as follows:

The image transmission system scans the photocathode of the vidicon or photodetectors of an imaging array, transmits this signal to the remote location, and recreates the image on a CRT or light valve tube. In the original RVS concept, the distorted image is expanded using a lens system with a transfer characteristic identical to the sensor lens and imaged on a spherical screen concentric with the nodal point of the lens.

Obviously, for the above image transmission system to perform adequately, the optical axes of both the sensor and projector must have the same alignment as the viewer's eye. The initial RVS system concept used the approach outlined in Figure A-4. The position of the projector is slaved to the camera by a high accuracy position servo, with the camera's angular position commanding the projector's position relative to fixed ground station reference coordinates. The viewer at the ground station thus has the same angular perspective as he would if he were located in the remote vehicle. The sensor and projector must also be aligned with the viewer's foveal axis. In the original concept a Honeywell oculometer was employed for this function. The oculometer measures the angle between the eye's foveal axis and the projector's optical axis. This error signal is transmitted to the remote vehicle and commands the camera to move until the angular error is reduced to zero. As the camera moves, the projector follows through the slaving loop. The control mode, presently under study, is somewhat different, however. The observer's head position instead of his eye position is utilized to point the remote camera. The operational difference resulting from this simplification is that when the viewer uses his peripheral vision, he must learn to rotate his head towards the area of interest rather than his eyes. A reticle may be required to show the observer the location of the highest acuity area of the display.

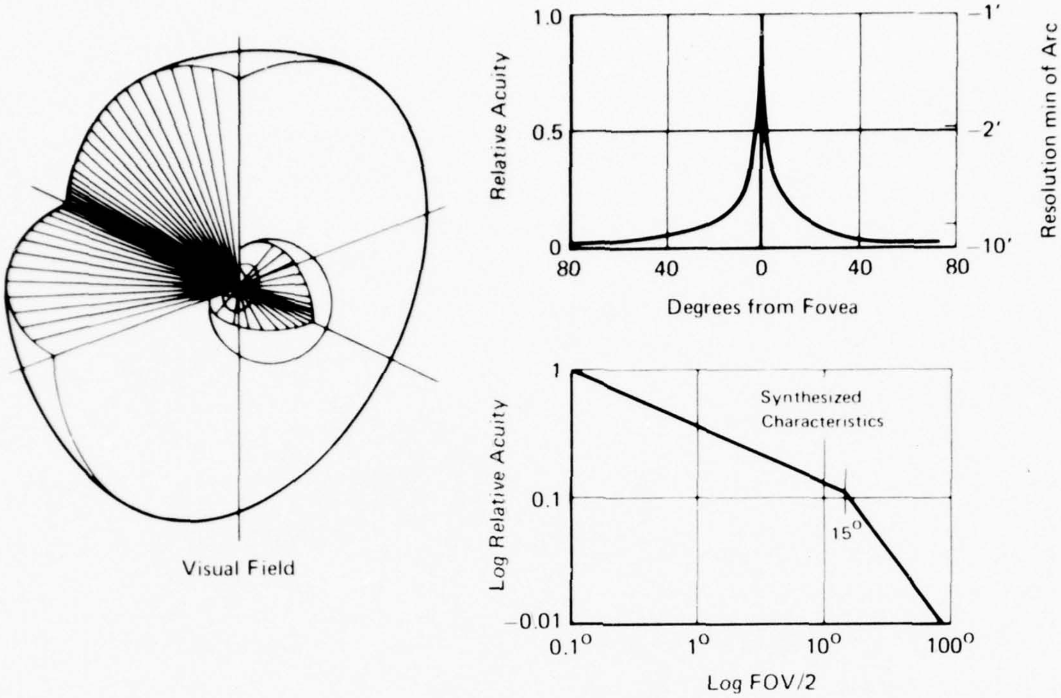

GP76-1037-112

Figure A-1. Human Eye Characteristics

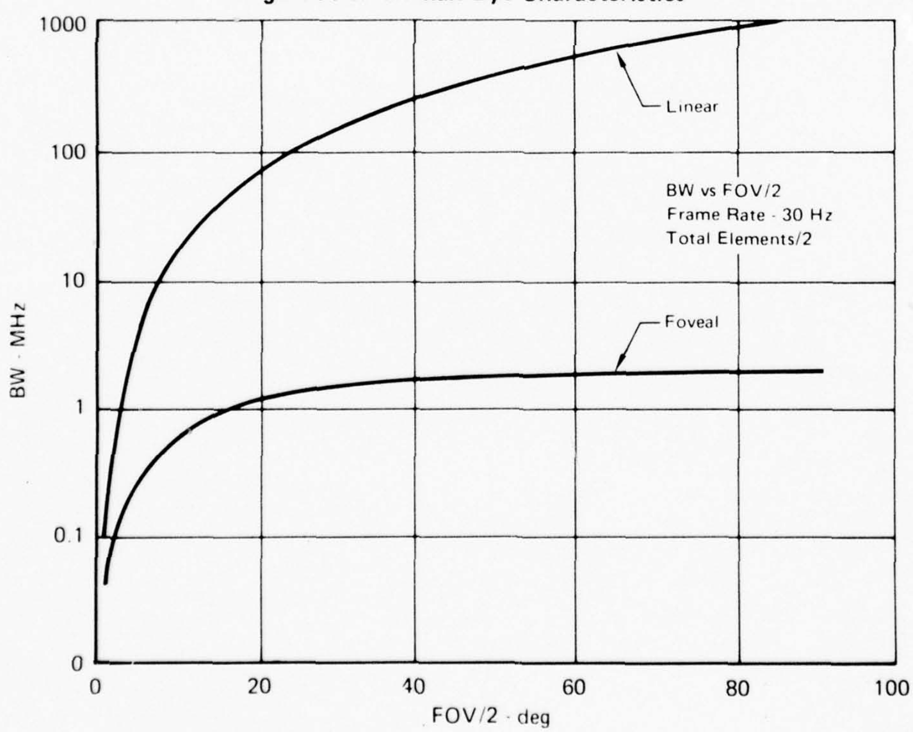

GP76-1037-113

Figure A-2. Bandwidth Requirements

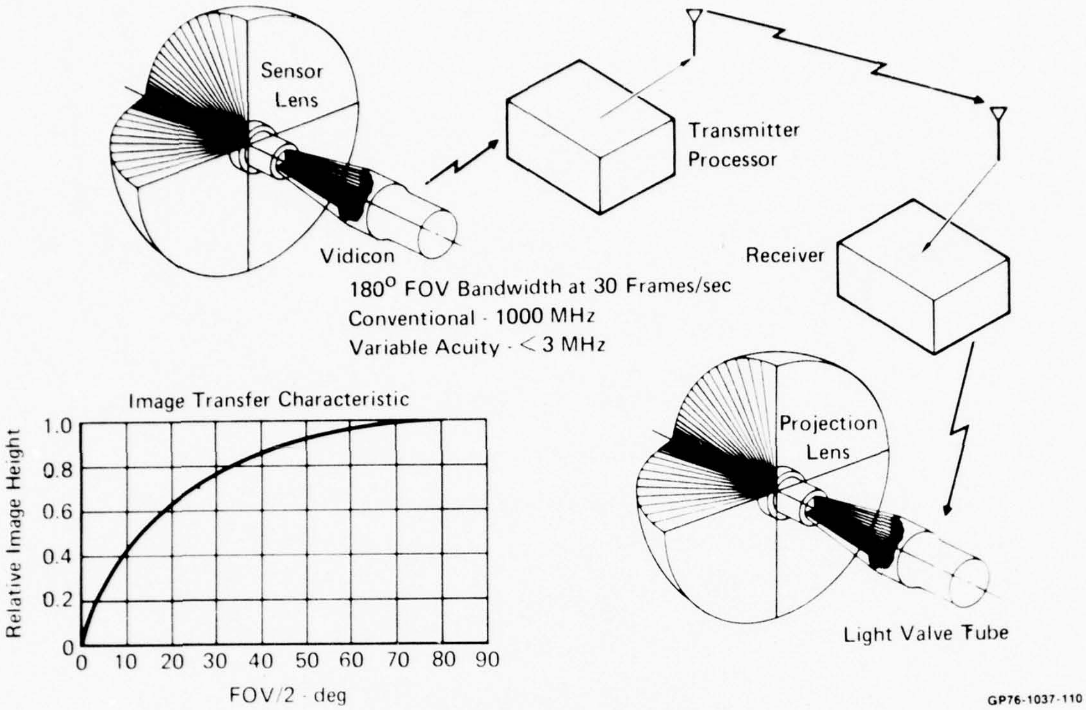

Figure A-3. Electro-Optical Schematic

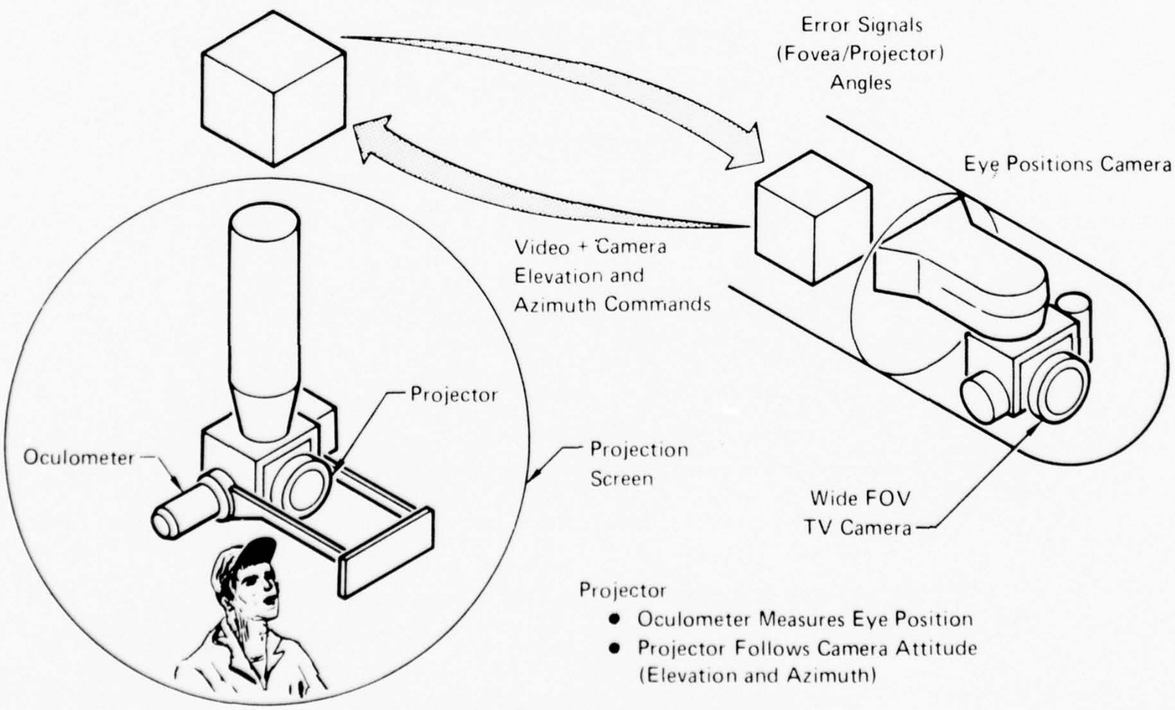

Figure A-4. Camera/Projector Interface

GP76-1037-111

Appendix B

CAMERA CONSIDERATIONS

LIGHT LEVEL CONTROL

Light level control must be accomplished by an iris in the camera optical relay. The relay is required for this purpose because no iris control is available in the non-linear lens. An iris control was not initially considered necessary because an $S_{b_2}S_3$ vidicon was contemplated which had sufficient dynamic range for good daylight performance with electronic light control. Solar damage considerations later dictated the use of a silicon vidicon which cannot be adapted to electronic light level control. The range required of the iris control is discussed below.

Assuming a GE Z7978 Epicon vidicon is utilized an average faceplate illumination of .25 ft-candles is recommended. Using conventional formulas, this relates to a scene brightness as follows:

$$E = \frac{\pi B}{4(F_{NO})2} \qquad \text{(B-1)}$$

If $E = .25$ ft-candles

$$B = \frac{.25 \times 4}{\pi}(F_{NO})^2 = .318\ (F_{NO})^2\ \frac{\text{Lumens}}{\text{Steradian-ft}^2}$$

Assuming a 1:1 relay between lens and vidicon the effective F number at the vidicon is identical to that of the non-linear lens - F/5.6. The brightness is:

$$B = 9.97\ \frac{\text{Lumens}}{\text{Steradian-ft}^2} = 31.32 \text{ ft-lambert}$$

This is the minimum brightness level capability of the camera. It is sufficient to operate anywhere in the U.S., even under heavy cloud cover.

The maximum terrain brightness anticipated is about 5000 ft-lamberts. This approximates clear weather at 70° solar elevation and .16 terrain reflectance. The F number required to attenuate this brightness to .25 ft-candles at the vidicon faceplate is (per Equation (B-1))

$$\frac{5000}{\pi} = \frac{.25 \times 4}{\pi} (F_{NO})^2 \qquad \text{(B-2)}$$

$$(F_{NO})^2 = 5000$$

$$F_{NO} = 70.7$$

This small aperture would cause serious diffraction in the image quality. For this reason, a filter is considered. Because of sensitivity of the silicon vidicon to IR radiation a Schott KG3 filter is recommended. This filter provides about 20% transmission in the visual spectrum. This reduces the maximum F number requirements to about F/16, which is easily obtainable in the optical relay between camera and lens.

In summary, the camera optical relay must have sufficient aperture to couple all the energy in the F/5.6 non-linear lens image ray bundle to the vidicon. The iris control in the relay must have the capability of reducing this F/5.6 ray bundle at the vidicon to F/16. This variable iris should be servo controlled to maintain the required vidicon faceplate illumination under varying terrain illumination and reflectance characteristics.

The average video level from the vidicon can be used as the drive signal. This is possible because the foveal region occupies most of the vidicon photocathode area. Therefore an average video level will optimize brightness in this area as desired.

SOLAR DAMAGE CONSIDERATIONS

Utilizing the sun brightness value of:

$$B_S = 2.09 \times 10^8 \frac{\text{Lumen}}{\text{Steradian ft}^2} \quad \text{[From Reference (B-1)]}$$

At F/5.6 the vidicon faceplate illumination would be [from Equation (B-1)]

$$E = \frac{\pi}{4} \frac{2.09 \times 10^8}{(5.6)^2} = .523 \times 10^7 \text{ foot candles}$$

This gives a 2x safety factor over the 10^7 foot candle maximum rating of the vidicon proposed for the RVS camera. Operationally the safety margin is considerably better than this because any time the sun is visible to the RVS the automatic light level control will certainly have the camera stopped down to F/8 or greater. The margin is at least 4x when this is considered. The IR filter discussed in the previous paragraph also increases the safety margin.

Appendix C

PROJECTOR STUDIES

INTRODUCTION

The projection brightness problem is illustrated in Figure C-1. Here uniform size area elements are shown in the projector object plane at three different distances from the optical axis. If the object plane is of uniform brightness (which is the case for the RVS intermediate image or projector object) the screen illumination decreases as object area elements displace from the optical axis. Each area in the object plane contains the same light flux, which is spread over a greater area on the projection screen. In the actual case, area elements are projected 1000 times larger in the extreme peripheral region (90°) than in the foveal region (0°) of the display. This, of course, is completely unacceptable to the viewer.

Two alternatives are possible for solving the above problem.

(a) A variable density filter to properly attenuate the foveal area of projection so that it matches the peripheral field in screen brightness. This is, of course, feasible only if image brightness is sufficient to generate acceptable brightness in the peripheral field of the displayed image.

(b) Employ a direct or virtual image viewing system. This is much more efficient and inherently results in uniform display brightness if the exit pupil is large enough to support the entire eye aperture (or the interocular spacing if binocular viewing is to be achieved).

Selection of the best display approach requires a thorough analysis of the two above approaches.

In the past year, MCAIR IRAD on the RVS has been 95% devoted to trade-offs of display concepts. The results of these studies, analyses, and tests are outlined below.

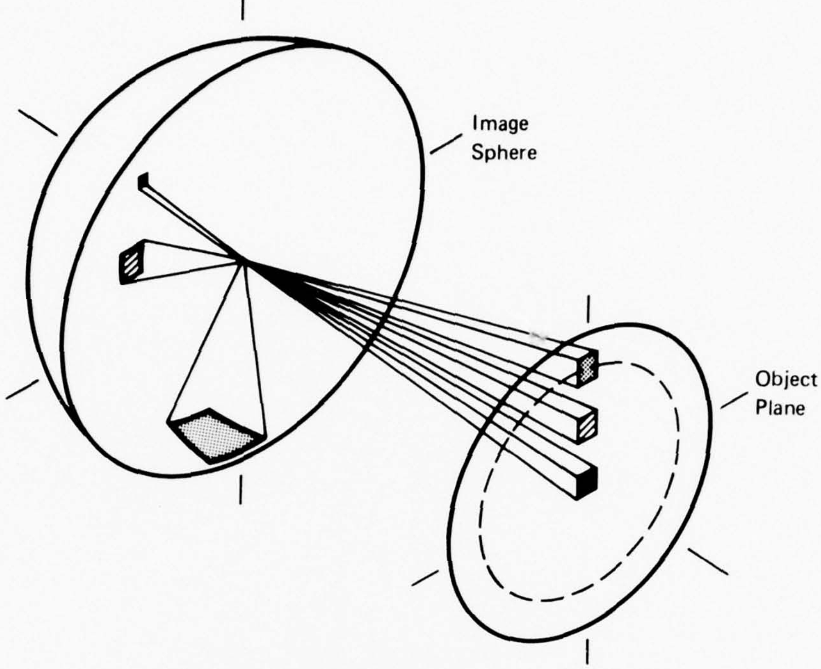

FIGURE C-1
GENERAL PROJECTION GEOMETRY

PROJECTION SCREEN APPROACH

The geometry of the projection screen approach is shown in Figure C-2. An element of area dA with brightness B is projected through a lens of aperture D and focal length f to a viewing screen located at distance L. The image of dA on the viewing screen appears as dA_s. This area re-radiates over solid angle ω_s. The apparent screen brightness $B_s(\theta)$, as seen by the observer also at distance L, but offset by distance ℓ, is calculated as follows.

The light flux through aperture D from image area dA is:

$$F = B \times \omega \times dA \quad \text{(C-1)}$$

where

ω is the solid angle of light collection by the projector lens.

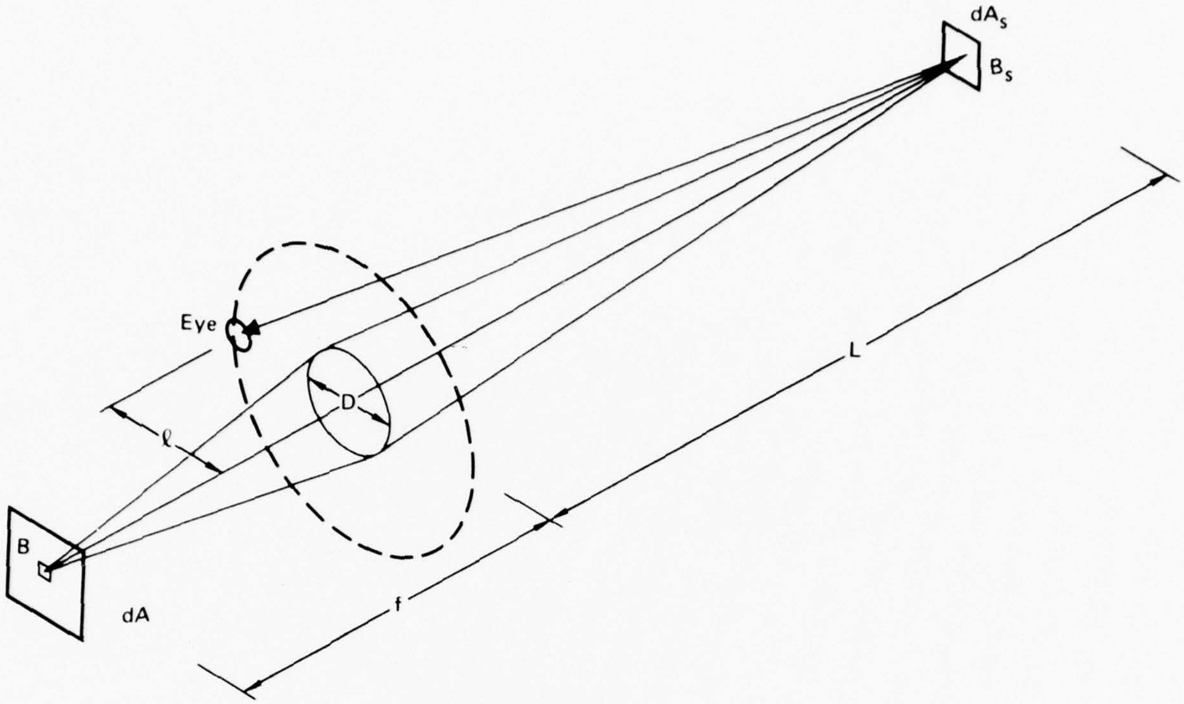

FIGURE C-2
DISPLAY BRIGHTNESS GEOMETRY

Accordingly:

$$\omega = \frac{\pi[D(\theta)]^2}{4[f(\theta)]^2} = \frac{\pi}{4\left(F_{NO}\right)^2} \qquad \text{(C-2)}$$

Development of ω in terms of F_{NO} instead of lens aperture and focal length is preferred because both theory and experiment show that the latter vary with field angle (θ) on the non-linear lens while F_{NO} does not.

Combining these two equations yields:

$$F = \frac{B\pi dA}{4\left(F_{NO}\right)^2} \qquad \text{(C-3)}$$

This is the total flux that illuminates dA_s at the screen.

Screen illumination (E) is:

$$E = \frac{F}{dA_s} = \frac{B\pi}{4\left(F_{NO}\right)^2} \frac{dA}{dA_s(\theta)} \qquad \text{(C-4)}$$

The screen brightness is therefore

$$B_s(\theta) = \frac{E}{\omega} = \frac{B\pi}{4\left(F_{NO}\right)^2 \omega} \frac{dA}{dA_s(\theta)} \qquad \text{(C-5)}$$

Note that B_s will have the same units as B if A and A_s have identical units.

For the on-axis case, zero subscript is used:

$$\frac{dA}{dA_s(0)} = \frac{[f(0)]^2}{L^2} = \frac{\left(F_{NO}\right)^2 [D(0)]^2}{L^2} \qquad \text{(C-6)}$$

Therefore:

$$B_{s_o} = \frac{B\pi D(0)^2}{4\omega L^2} \qquad \text{(C-7)}$$

For the developed lens, D(0) = .356". Accordingly:

$$\frac{B_s(0)}{B} = \frac{.0995}{\omega L^2} \qquad \text{(C-8)}$$

If L = 60":

$$\frac{B_s(0)}{B} = \frac{2.76 \times 10^{-5}}{\omega} \qquad \text{(C-9)}$$

<u>WORST CASE</u>

If the screen is perfectly diffuse

$\omega = \pi$ steradians

<u>BEST CASE</u>

If the screen has optimum characteristics

$$\omega \cong \frac{\pi \ell^2}{L^2}$$

WORST CASE

$$\frac{B_s(0)}{B} = 8.78 \times 10^{-6}$$

For $B_s(0)$ = 1 ft-lambert

B = 114,000 ft-lambert

If the screen is perfectly diffuse

BEST CASE

If ℓ = 10" (About the minimum projector/eye separation)

$$\omega = \pi \frac{10^2}{60} = .0873 \text{ steradians}$$

If the screen has optimum characteristics

$$\frac{B_s(0)}{B} = 3.161 \times 10^{-4}$$

For $B_s(0)$ = 1 ft-lambert

B = 3160 ft-lambert

The above calculations show an object brightness in the 3000 to 100,000 ft-lambert range is required for acceptable display brightness in the foveal region of the projected display. For reasons shown on Figure C-1, it is not the foveal region, but the peripheral region that puts the greatest requirement on B.

In calculating peripheral display brightness it is most convenient to normalize Equation (C-5) by the on-axis brightness. The result is a fall-off ratio of brightness anticipated in the projected display.

$$\frac{B_s(\theta)}{B_s(0)} = \frac{dA_s(0)}{dA_s(\theta)} \qquad \text{(C-10)}$$

Equation (C-10) assumes a constant F_{NO} for the lens and ω for the screen. The former has been verified experimentally while the latter will be assured by spherical screen geometry and uniform coating.

The display brightness at any angle, θ, can be computed by determining the axial brightness using Equation (C-7) or (C-9) and multiplying by the ratio of Equation (C-10). The area ratios of Equation (C-10) are available from lens design data and have been verified experimentally. These data are plotted on Figure C-3. Note that at 90°, brightness is down by 10^{-3}. It is obvious from this that the 3000 to 100,000 ft-lambert range required for on-axis brightness must be increased to 3,000,000 to

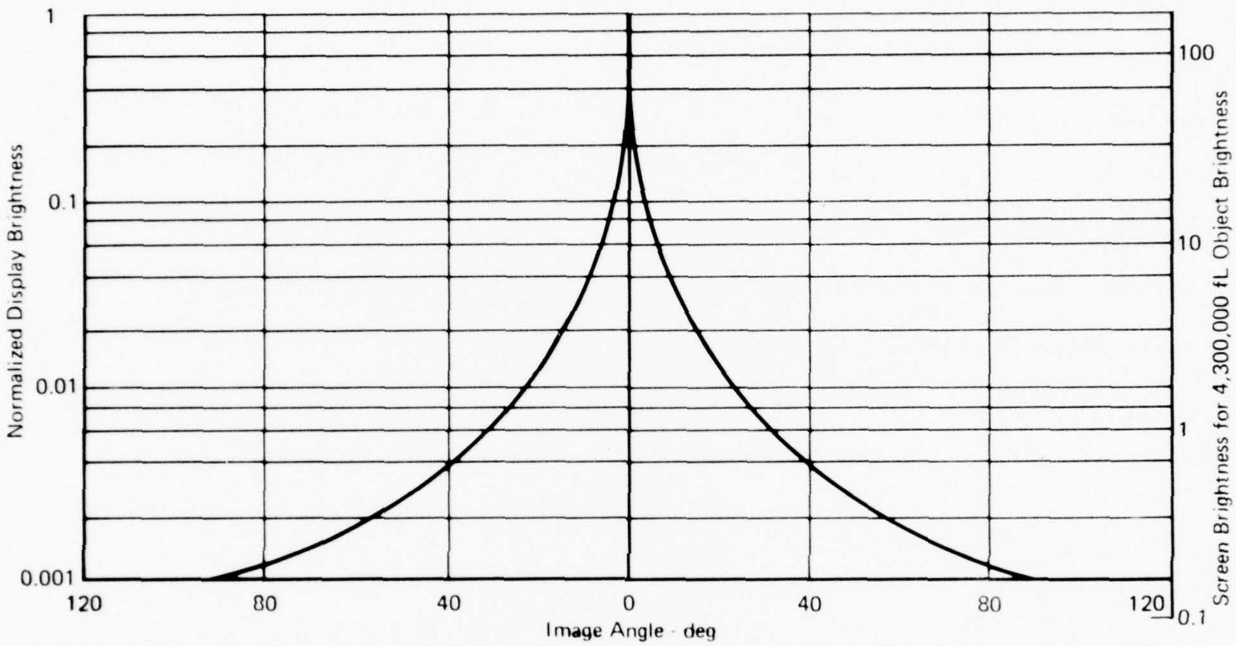

FIGURE C-3
NORMALIZED DISPLAY BRIGHTNESS

GP73-0782-47

100,000,000 ft-lambert to support peripheral vision. This exceedingly high requirement for object brightness initially led us to discard this approach and proceed to direct view display approaches. Difficulty in achieving sufficient exit pupil size and field of view (to be discussed later) with those approaches directed effort back to screen viewing techniques.

Since Equation (C-10) is constant (a function of the original concept) the clue to increasing display brightness must be found in the equation for axial brightness (Equation (C-7)).

Possible parameters are:

1. Screen Characteristics (ω)

2. Projection Lens Aperture (D)

3. Screen/Projector Distance (L)

4. Object Brightness (B)

Screen Solid Angle - In the previous example a minimum value of ω was computed to determine a lower limit of object brightness for the display projector. Since this minimum may not be practical it was studied in more detail. The first observation was that projector/viewer geometry could be improved for a specular coating. This is illustrated in Figure C-4. The eye and lens are equally displaced on each side of the sphere center. This aligns the centroid of the reflected light towards the eye position - making a large ω unnecessary.

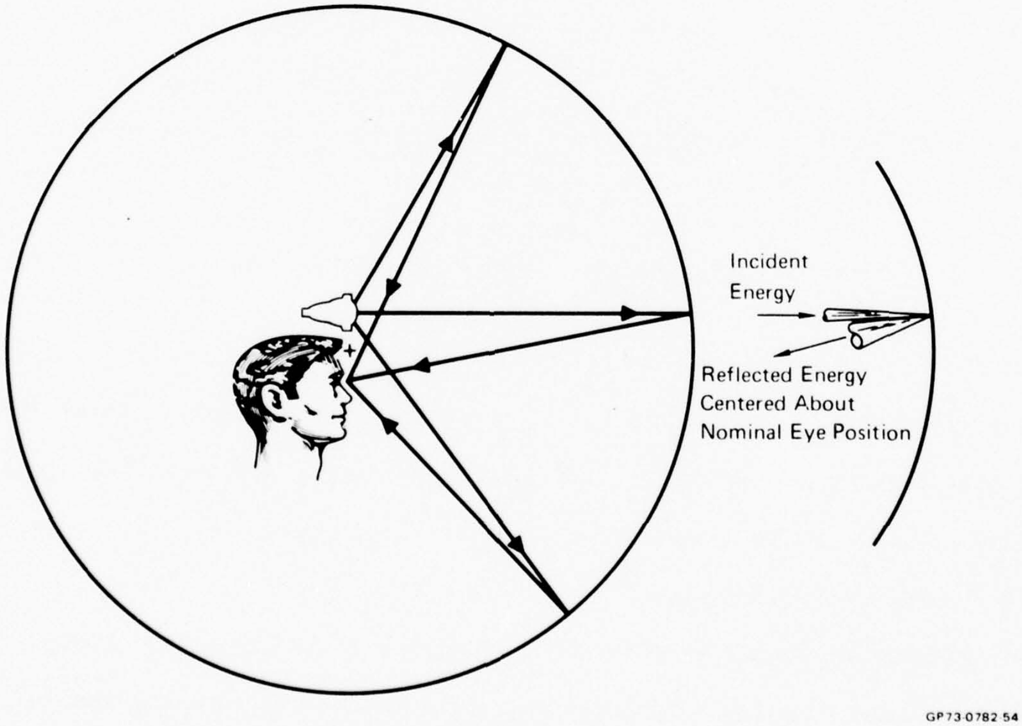

FIGURE C-4
OPTIMUM GEOMETRY FOR SPECULAR SCREEN COATINGS

In reviewing available screen materials from Reference (C-1) Stewart Filmscreen Silvergrain appears good for our application. This screen has a gain of four. While higher gain screens exist, they tend to be retroreflective rather than specular.

Calculating object brightness requirements using this ω yields:

$B = 25 \times 10^6$ ft-lambert for a 1 ft-lambert screen brightness and full hemispheric projection

The Stewart screen coating discussed above develops a considerably larger dispersion than is required by our concept - i.e., about $\frac{\pi}{4}$ steradians, which is equivalent to 30" dispersion at the head location if L = 60 inches. Using the geometry of Figure C-4 the dispersion required could be as small as half the interocular distance plus anticipated head motion. Allowing a 2 inch head motion, about 3 inches would be sufficient. Allowing an additional 2 inches for surface irregularities (about 2°) the solid angle would be

$$\omega = \frac{\pi\, 5^2}{60^2} = .0218 \text{ steradians}$$

From Equation (B-9)

$$\frac{B_{s(0)}}{B} = \frac{2.76 \times 10^{-5}}{.0218} = .00126$$

at 90° this requires

$$\frac{B_{90}}{} = \frac{B_{s_0}}{1000} = 1.26 \times 10^{-6} B$$

For B_{90} = 1 ft-lambert

$$B = \frac{1}{1.26 \times 10^{-6}} = 794{,}000 \text{ ft-lambert}$$

This is a substantial reduction below the 25×10^6 required using the Stewart coating.

The natural question at this point is if this type of screen could be fabricated. Theoretically it could be - as shown in Figure C-5. This figure shows the

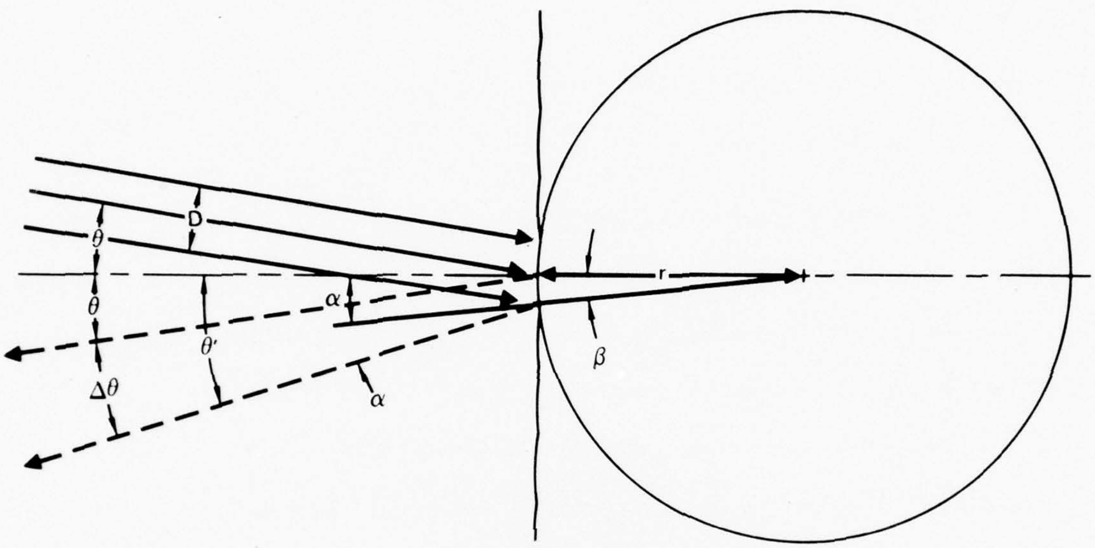

FIGURE C-5
OPTIMUM SCREEN COATING

general construction that would receive the minimum beam dimension D and expand it into a diverging cone having a radius ℓ at distances L (D<<1).

From simple geometry it can be seen that

$$\cos \theta = \frac{D}{2h} \qquad B = (\alpha - \theta)$$

$$h = \frac{D}{2 \cos \theta} \qquad \alpha = \theta + B$$

$$\sin B = \frac{h}{r}$$

$$\theta' = \alpha + B = \theta + 2B$$

$$\Delta\theta = \theta' - \theta$$

$$\Delta\theta = 2 \text{ arc sin } \frac{h}{r}$$

$$\Delta\theta = 2 \text{ arc sin } \frac{D}{2r \cos \theta}$$

$$\sin (\frac{\theta}{2}) = \frac{D}{2r \cos \theta}$$

$$r = \frac{D}{2 \cos \theta \sin (\frac{\Delta\theta}{2})}$$

The $\Delta\theta$ required to make 5" dispersion at 60" is

$$\theta = \text{arc tan } \frac{5}{60} = 4.76°$$

For our lens the minimum D = .00356"

θ is obtained from the projector lens/eye geometry which also is (by coincidence)

$$\theta = 4.76°$$

Therefore,

$$r = \frac{.00356}{2 \cos 4.76 \sin \frac{4.76}{2}} = .043 \text{ inch}$$

Spacing of sphere centers would be $2h \cong D$

The optimum screen would therefore use specular reflective sections of .043 inch radius spheres - spaces at .0035" centers.

The above calculations show how the projector object brightness requirements could be reduced over 30 times through an optimized screen coating. Construction of such a coating might be expensive however.

Exit Aperture - Brightness requirements reduce by the square of the lens aperture D. Therefore, a new lens design would appear to be of significant value. For instance, if $F_{NO} = 1$ could be achieved, object brightness could be reduced by $(5.6)^2$ or about 30 times. Unfortunately the size of the projection lens would grow at least by 5.6 times. This means the present 9" diameter would increase to about 50". Besides being very expensive, a lens this size would force expansion of screen geometry. If everything was scaled by 5.6, the advantage of the large aperture would be exactly negated by the increase in projection distance L. Barring a completely different lens design, it appears that questionable advantage can be gained by scaling lens geometry.

If through a new projector lens design, aperture could be made to increase with image angle θ, some compensation in B_s could be achieved while reducing B requirements. The limit of this would probably be $F_{NO} = 1$ in the peripheral field. Applying Equation (C-7), the object brightness requirements would now be:

B = 800,000 ft-lambert (Stewart Screen Coating)

This level of improvement may be achievable through the expense and effort of a completely new non-linear lens design for projection only.

Considering the degree of technical advancement that was required to design a lens with correct distortion, such a redesign for projection appears to be a high risk.

Projection Distance L - Reducing the projection distance, L, is as effective as increasing D is reducing object brightness requirements. However, shown in Figure C-4, parallax angles of both projector/screen and viewer/screen are increased. Also, binocular viewing becomes impaired as L is reduced.

Quite arbitrarily at this time, a parallax of 5° is considered the maximum acceptable. Laboratory tests in projecting transparencies show that this value is acceptable in maintaining focus of the projected image. Since at the time of this writing a full hemispherical projection has not been achieved, it is impossible to determine if 5° is acceptable to the viewer.

It will be shown later that parallax can be eliminated and L reduced through hybrid projection techniques. They require considerable development, however, involving some technical risks.

Maintaining the 5° parallax angle with the existing non-linear lens requires about 60" projection distance. This is considered the minimum acceptable (L) at this time.

Object Brightness - At this point in the analysis it appears that between $.8 \times 10^6$ to 25×10^6 ft-lambert object brightness is required. Standard CRT's are in the 1000-3000 ft-lambert categories and are obviously unusable. Projection CRT's are better but still fall considerably short of the brightness requirements (10,000 - 20,000 ft-lambert) and add a x-ray radiation hazard that would probably make them unacceptable in the RVS application.

Eidophor light valve approaches eliminate the x-ray problem, but are quite large and have a mechanical pointing limit. Their high output, however, makes them a promising candidate. For this reason an available G.E. light valve was studied. The PJ 700 light valve has a monochrome output of 750 lumens and requires approximately F/3 relay optics. This indicates the geometry shown on Figure C-6. Since the non-linear lens requires only F/5.6 solid angle input and an image reduction is required to relay the light valve to the lens, the image brightness is equal to the light valve object brightness. This brightness can be computed as follows:

$$B = \frac{\text{Flux}}{\text{Area x Solid Angle}} = \frac{750 \text{ lumens}}{6.3 \times 10^{-3} \times .0872}$$

$$B = 1,365,000 \frac{\text{lumens}}{\text{Ft}^2 \text{ steradian}} = 4,290,000 \text{ ft-lambert}$$

This value lies between requirements of the two screen coatings discussed above. For the Stewart coating, this value is about six times below that desired, or would deliver only .17 ft-lambert at 90° projection.

The scale to the right of Figure C-3 shows actual screen brightness that would be achieved versus field angle for the Stewart screen coating. This figure shows the desired 1 ft-lambert could be achieved out to 32° view angle. At 80°, the

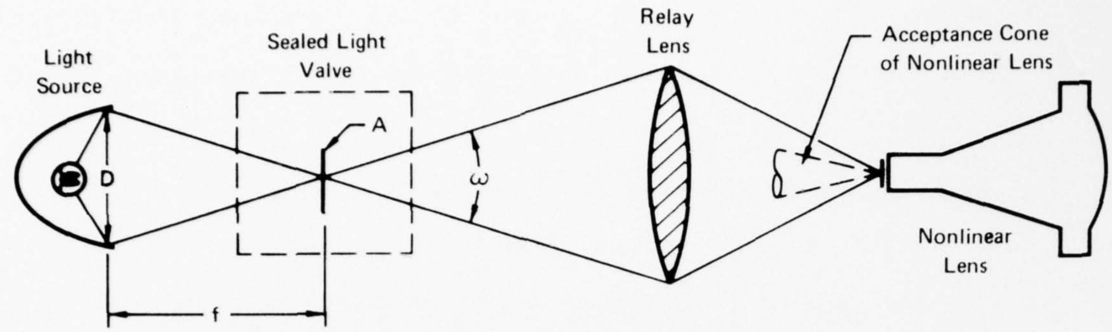

FIGURE C-6
LIGHT VALVE GEOMETRY

assured max field from the existing non-linear lens, the brightness is about .2 ft-lambert.

While Eidophor light valves exist with outputs as high as 4000 lumens, which is sufficient to achieve the desired display brightness, problems such as price, bulkiness, and reliability lead to the off-the-shelf G.E. system being a better choice for a near-term demonstration model. The .2 ft-lambert minimum screen brightness, we believe, is sufficient for these purposes. In the more distant future, single-crystal ferroelectric light valves can be expected to replace the Eidophor type [Reference (C-2)]. In addition to furnishing more light, these devices have a storage capability which will eliminate flicker in the peripheral field of the projected display - (an inherent problem in wide field displays). Therefore, we believe the light valve projection technique, using the existing non-linear lens and existing screen coatings, is a very feasible approach. If performance proves to be marginal, a specialized screen coating can correct the deficiency and assure a display brightness of over 5 ft-lambert.

Appendix D

PROM 1, PROM 2, PROM 3, AND PROM 4 COMPUTER PROGRAM LISTINGS

Figure D-1 is a listing of the PROM No. 1 Computer Program. Figure D-2 is PROM No. 2, Figure D-3 is PROM No. 3, and Figure D-4 is PROM No. 4.

```
INTEL 6. J CROSS ASSEMBLER                    14:32:39   09-MA. .7   PAGE  1

                  ;************
                  ;
                  ;
                  ;
                  ;       SYSTEM EQUATES
                  ;
                  ;
                  ;*************************
                  ;
                  ;
                  ;
    0000          SETML   EQU     *HA14
    0000          FIRST   EQU     *H3FE0
    0000          OUTPT   EQU     *H981
    0000          OSTAT   EQU     *H3D8A
    0000          YAW     EQU     *H0400
    0000          PITCH   EQU     *H0C00
    0000          CAMAX   EQU     *H3D00
    0000          CAMBX   EQU     *H3D01
    0000          CAMAY   EQU     *H3D02
    0000          CAMBY   EQU     *H3D03
    0000          CCMAX   EQU     *H3D04
    0000          CCMBX   EQU     *H3D05
    0000          CCMAY   EQU     *H3D06
    0000          CCMBY   EQU     *H3D07
    0000          CPOAX   EQU     *H3D08
    0000          CPOBX   EQU     *H3D09
    0000          CPOAY   EQU     *H3D0A
    0000          CPOBY   EQU     *H3D0B
    0000          CPLAX   EQU     *H3D0C
    0000          CPLBX   EQU     *H3D0D
    0000          CPLAY   EQU     *H3D0E
    0000          CPLBY   EQU     *H3D0F
    0000          DETX    EQU     *H3D10
    0000          DETY    EQU     *H3D11
    0000          IPRJX   EQU     *H3D1A
    0000          IPRJY   EQU     *H3D1C
    0000          IPOSX   EQU     *H3D1E
    0000          IPOSY   EQU     *H3D20
    0000          MULCX   EQU     *H3D90
    0000          MULDX   EQU     MULCX+20
    0000          MXLVB   EQU     MULDX+20
    0000          MXLVK   EQU     MXLVB+20
    0000          MULAX   EQU     MXLVK+20
    0000          MULBX   EQU     MULAX+20
    0000          MULCY   EQU     MULBX+20
    0000          MULDY   EQU     MULCY+20
    0000          MYLVB   EQU     MULDY+20
    0000          MYLVK   EQU     MYLVB+20
    0000          MULAY   EQU     MYLVK+20
```

Figure D-1 Prom No. 1 Service Interrupt Handler Software

```
0000            MULBY   EQU     MULAY+20
0000            NCPOX   EQU     *H3D22
0000            NCPOY   EQU     *H3D24
0000            PRJAX   EQU     *H3D26
0000            PRJBX   EQU     *H3D27
0000            PRJAY   EQU     *H3D28
0000            PRJBY   EQU     *H3D29
0000            PRLAX   EQU     *H3D2A
0000            PRLBX   EQU     *H3D2B
0000            PRLAY   EQU     *H3D2C
0000            PRLBY   EQU     *H3D2D
0000            PVLAX   EQU     *H3D2E
0000            PVLBX   EQU     *H3D2F
0000            PVLAY   EQU     *H3D30
0000            PVLBY   EQU     *H3D31
0000            RSTRT   EQU     *H3D40
0000            RINT    EQU     *H3D34
0000            TSTRT   EQU     *H3D47
0000            TINT    EQU     *H3D38
0000            X       EQU     *H3D3A
0000            XY      EQU     *H3D3C
0000            XFLAG   EQU     *H3D3E
0000            YFLAG   EQU     *H3D3F
0000            USCMD   EQU     *H00ED
0000            USDAO   EQU     *H00EC
0000            USDAI   EQU     *H00EE
0000            PRTA1   EQU     *H0000
0000            PRTB1   EQU     *H0001
0000            PRTC1   EQU     *H0002
0000            PRTA2   EQU     *H0003
0000            PRTB2   EQU     *H00E5
0000            PRTC2   EQU     *H0000
0000            PRTD1   EQU     *H0001
0000            PRTD2   EQU     *H0002
0000            PRTD3   EQU     *H00E6
0000            PIOI1   EQU     *H00E7
0000            PIOI2   EQU     *H00EB
0000            MDW1    EQU     *H009B
0000            MDW2    EQU     *H0082
0000            N1      EQU     *H0001
0000            N2      EQU     *H0003
0000            PRSET   EQU     *HEA
0000            KYBD1   EQU     *H800
0000            KYBD2   EQU     *H9AB
0000            COMPAR  EQU     *H816
0000                    ORG     0
0000 F3                 DI
0001 31FF3C             LXI     SP,*H3CFF
0004 CD8101             CALL    INIT
0007 3EC0               MVI     A,*HC0
```

Figure D-1 Prom No. 1 Service Interupt Handler Software (Continued)

```
0009 328A3D          STA     OSTAT
000C 2F              CMA
000D D3EA            OUT     PRSET
000F 3EC7            MVI     A,#HC7
0011 2F              CMA
0012 D3EA            OUT     PRSET
0014 CDC301          CALL    SETUP
0017 FB              EI
0018 0604            MVI     B,#H04
001A 78      LEDS:   MOV     A,B
001B CD8109          CALL    OUTPT
001E 3E11            MVI     A,#H11
0020 80              ADD     B
0021 47              MOV     B,A
0022 FE59            CPI     #H59
0024 C21A00          JNZ     LEDS
0027 CDA401          CALL    ZERO
002A 76              HLT
002B 3EFF            MVI     A,#HFF
002D 2F              CMA
002E D3EA            OUT     PRSET
0030 C33300  BKWRD:  JMP     FRWRD
0033 C33000  FRWRD:  JMP     BKWRD
0036                 DS      #H38-$
0038 C5      SRV:    PUSH    B          ;S
0039 D5              PUSH    D          ; A
003A E5              PUSH    H          ;   V   REG
003B F5              PUSH    PSW        ;     E     ISTERS
003C DB01            IN      N1         ;INPUT LAST 3 BITS OF PROJ X
003E F61F            ORI     #H1F
0040 FE1F            CPI     #H1F
0042 CA5D00          JZ      PTY
0045 47              MOV     B,A
0046 3EC0            MVI     A,#HC0
0048 2F              CMA
0049 D3EA            OUT     PRSET
004B 3EC7            MVI     A,#HC7
004D 2F              CMA
004E D3EA            OUT     PRSET
0050 78              MOV     A,B
0051 217B00          LXI     H,JTAB
0054 07      LOOP:   RLC
0055 DA7300          JC      ST
0058 23              INX     H
0059 23              INX     H
005A C35400          JMP     LOOP
005D DB03    PTY:    IN      N2
005F F61F            ORI     #H1F
0061 47              MOV     B,A
0062 3EC0            MVI     A,#HC0
```

Figure D-1 Prom No. 1 Service Interupt Handler Software (Continued)

```
0064 2F               CMA
0065 D3EA             OUT     PRSET
0067 3EFF             MVI     A,#HFF
0069 2F               CMA
006A D3EA             OUT     PRSET
006C 78               MOV     A,B
006D 218300           LXI     H,JTAB+8
0070 C35400           JMP     LOOP
0073 FB      ST:      EI
0074 EB               XCHG
0075 1A               LDAX    D
0076 6F               MOV     L,A
0077 13               INX     D
0078 1A               LDAX    D
0079 67               MOV     H,A
007A E9               PCHL
007B 8B00    JTAB:    DW      KB1     ;J       T
007D 9100             DW      KB2     ; U       A
007F 9700             DW      COMPR   ;  M       B
0081 AC00             DW      DBRF
0083 9D00             DW      RXRDY   ;    P       L
0085 A300             DW      TXRDY   ;             E
0087 A900             DW      SYSCLK  ;              S
0089 AC00             DW      DBRF
008B CD0008  KB1:     CALL    KYBD1   ;SERVICE
008E C3AC00           JMP     DBRF    ;
0091 CDAB09  KB2:     CALL    KYBD2   ;         ROUTINES
0094 C3AC00           JMP     DBRF    ;
0097 CD1608  COMPR:   CALL    COMPAR  ;                 FOR
009A C3AC00           JMP     DBRF    ;
009D CD5001  RXRDY:   CALL    RX      ;                       INTER
00A0 C3AC00           JMP     DBRF    ;
00A3 CD2D01  TXRDY:   CALL    TX      ;                            RUPTS
00A6 C3AC00           JMP     DBRF    ;
00A9 CDB100  SYSCLK:  CALL    SYS     ;
00AC F1      DBRF:    POP     PSW     ;REST
00AD E1               POP     H       ;    ORE
00AE D1               POP     D       ;         REGIS
00AF C1               POP     B       ;              TERS
00B0 C9               RET
00B1 21473D  SYS:     LXI     H,TSTRT
00B4 7E               MOV     A,M
00B5 D3EC             OUT     USDAO
00B7 2B               DCX     H
00B8 22383D           SHLD    TINT
00BB 21403D           LXI     H,RSTRT
00BE 22343D           SHLD    RINT
00C1 213F3D           LXI     H,YFLAG
00C4 3E00             MVI     A,#H00
00C6 77               MOV     M,A
```

Figure D-1 Prom No. 1 Service Interupt Handler Software (Continued)

```
00C7 213E3D           LXI     H,XFLAG
00CA 77               MOV     M,A
00CB DB00             IN      PRTA1
00CD 2F               CMA
00CE 32263D           STA     PRJAX
00D1 DB01             IN      PRTB1
00D3 2F               CMA
00D4 E61F             ANI     #H1F
00D6 32273D           STA     PRJBX
00D9 DB02             IN      PRTC1
00DB 2F               CMA
00DC 32283D           STA     PRJAY
00DF DB03             IN      PRTA2
00E1 2F               CMA
00E2 E61F             ANI     #H1F
00E4 32293D           STA     PRJBY
00E7 3A2E3D           LDA     PVLAX
00EA 2F               CMA
00EB D300             OUT     PRTC2
00ED 3A2F3D           LDA     PVLBX
00F0 E60F             ANI     #H0F
00F2 322F3D           STA     PVLBX
00F5 3A313D           LDA     PVLBY
00F8 E6F0             ANI     #HF0
00FA 57               MOV     D,A
00FB 3A2F3D           LDA     PVLBX
00FE B2               ORA     D
00FF 2F               CMA
0100 D301             OUT     PRTD1
0102 3A303D           LDA     PVLAY
0105 2F               CMA
0106 D302             OUT     PRTD2
0108 DBE4     PORT:   IN      #HE4
010A 07               RLC
010B DA1101           JC      SCND
010E D20801           JNC     PORT
0111 DBE4     SCND:   IN      #HE4
0113 07               RLC
0114 07               RLC
0115 D21101           JNC     SCND
0118 DBE6             IN      PRTD3
011A C680             ADI     #H80
011C 32103D           STA     DETX
011F DBE5             IN      PRTB2
0121 C680             ADI     #H80
0123 32113D           STA     DETY
0126 CD0004           CALL    YAW
0129 CD000C           CALL    PITCH
012C C9               RET
012D 2A383D   TX:     LHLD    TINT
```

Figure D-1 Prom No. 1 Service Interupt Handler Software (Continued)

```
0130 7D              MOV   A,L
0131 FE45            CPI   #H45
0133 CA4101          JZ    YF
0136 DA4001          JC    ET
0139 7E      CONT:   MOV   A,M
013A 2B              DCX   H
013B 22383D          SHLD  TINT
013E D3EC            OUT   USDAO
0140 C9      ET:     RET
0141 213F3D  YF:     LXI   H,YFLAG
0144 7E              MOV   A,M
0145 C680            ADI   #H80
0147 77              MOV   M,A
0148 1F              RAR
0149 2A383D          LHLD  TINT
014C DA3901          JC    CONT
014F C9              RET
0150 2A343D  RX:     LHLD  RINT
0153 7D              MOV   A,L
0154 FE44            CPI   #H44
0156 CA7A01          JZ    CM
0159 DBEC            IN    USDAO
015B 77              MOV   M,A
015C 23              INX   H
015D 22343D          SHLD  RINT
0160 7D              MOV   A,L
0161 FE42            CPI   #H42
0163 CA7301          JZ    BM
0166 FE43            CPI   #H43
0168 CA6C01          JZ    AM
016B C9              RET
016C 2A383D  AM:     LHLD  TINT
016F 7E              MOV   A,M
0170 D3EC            OUT   USDAO
0172 C9              RET
0173 213E3D  BM:     LXI   H,XFLAG
0176 3E01            MVI   A,#H01
0178 77              MOV   M,A
0179 C9              RET
017A 2A0E3D  CM:     LHLD  CPLAY
017D 220A3D          SHLD  CPOAY
0180 C9              RET
0181 3E9B    INIT:   MVI   A,MDW1
0183 D3E7            OUT   PIOI1
0185 3E82    INIT1:  MVI   A,MDW2
0187 D3EB            OUT   PIOI2
0189 AF      UCLEAR: XRA   A
018A D3ED            OUT   USCMD
018C D3ED            OUT   USCMD
018E D3ED            OUT   USCMD
```

Figure D-1 Prom No. 1 Service Interupt Handler Software (Continued)

```
0190 3E40            MVI     A,#H40
0192 D3ED            OUT     USCMD
0194 3E6E            MVI     A,#H6E
0196 D3ED            OUT     USCMD
0198 3E37            MVI     A,#H37
019A D3ED            OUT     USCMD
019C DBEE            IN      USDAI
019E DBEE            IN      USDAI
01A0 AF              XRA     A
01A1 D3EC            OUT     USDAO
01A3 C9              RET
01A4 210000 ZERO:    LXI     H,#H0000
01A7 223A3D          SHLD    #H3D3A
01AA 223C3D          SHLD    #H3D3C
01AD 22603D          SHLD    #H3D60
01B0 22703D          SHLD    #H3D70
01B3 22743D          SHLD    #H3D74
01B6 22783D          SHLD    #H3D78
01B9 22EE3F          SHLD    #H3FEE
01BC 22EA3F          SHLD    #H3FEA
01BF 22EC3F          SHLD    #H3FEC
01C2 C9              RET
01C3 AF     SETUP:   XRA     A
01C4 32E03F          STA     FIRST   ;FIRST=0, THEN FIRST=FF
01C7 CD140A          CALL    SETML
01CA 3EFF            MVI     A,#HFF
01CC 32E03F          STA     FIRST
01CF C9              RET
01D0                 END
```

Figure D-1 Prom No. 1 Service Interupt Handler Software (Continued)

INTEL 8086 CROSS ASSEMBLER SYMBOL TABLE

```
PVLBX= 3D2F    PVLAY= 3D30    PVLBY= 3D31    RSTRT= 3D40
RINT  = 3D34   TSTRT= 3D47    TINT  = 3D38   X     = 3D3A
XY    = 3D3C   XFLAG= 3D3E    YFLAG= 3D3F    USCMD= 00ED
USDA0= 00EC    USDAI= 00EE    PRTA1= 0000    PRTB1= 0001
PRTC1= 0002    PRTA2= 0003    PRTB2= 00E5    PRTC2= 0000
PRTD1= 0001    PRTD2= 0002    PRTD3= 00E6    PRSET= 00EA
COMPA= 0816    LEDS   001A    BKWRD  0030    FRWRD  0033
SRV    0038    LOOP   0054    PTY    005D    ST     0073
JTAB   007B    COMPR  0097    RXRDY  009D    TXRDY  00A3
SYSCL  00A9    SYS    00B1    PORT   0108    SCND   0111
TX     012D    CONT   0139    ET     0140    YF     0141
RX     0150    N1    = 0001   KB1    008B    KB2    0091
N2    = 0003   BM     0173    CM     017A    A     = 0007
INIT   0181    INIT1  0185    B     = 0000   UCLEA  0189
ZERO   01A4    C     = 0001   SETUP  01C3    D     = 0002
E     = 0003   KYBD1= 0800    KYBD2= 09AB    PIOI1= 00E7
MDW1  = 009B   MDW2  = 0082   PIOI2= 00EB    DBRF   00AC
AM     016C    H     = 0004   CAMAX= 3D00    CAMBX= 3D01
CAMAY= 3D02    CAMBY= 3D03    CCMAX= 3D04    CCMBX= 3D05
CCMAY= 3D06    CCMBY= 3D07    PITCH= 0C00    CPOAX= 3D08
CPLAX= 3D0C    L     = 0005   CPOBX= 3D09    CPOAY= 3D0A
M     = 0006   SETML= 0A14    CPOBY= 3D0B    FIRST= 3FE0
CPLBX= 3D0D    CPLAY= 3D0E    OSTAT= 3D8A    CPLBY= 3D0F
DETX  = 3D10   YAW   = 0400   DETY  = 3D11   IPRJX= 3D1A
SP    = 0006   IPRJY= 3D1C    IPOSX= 3D1E    OUTPT= 0981
IPOSY= 3D20    MULCX= 3D90    PSW   = 0006   MULDX= 3DA4
MXLVB= 3DB8    MXLVK= 3DCC    MULAX= 3DE0    MULBX= 3DF4
MULCY= 3E08    MULDY= 3E1C    MYLVB= 3E30    MYLVK= 3E44
MULAY= 3E58    MULBY= 3E6C    NCPOX= 3D22    NCPOY= 3D24
PRJAX= 3D26    PRJBX= 3D27    PRJAY= 3D28    PRJBY= 3D29
PRLAX= 3D2A    PRLBX= 3D2B    PRLAY= 3D2C    PRLBY= 3D2D
PVLAX= 3D2E

ERRORS DETECTED:  0
```

Figure D-1 Prom No. 1 Service Interupt Handler Software (Concluded)

```
INTEL 8080 CROSS ASSEMBLER                        14:35:20   09-MA[illegible] 77   PAGE  1

                  ;************
                  ;
                  ;
                  ;
                  ;       SYSTEM EQUATES
                  ;
                  ;
                  ;**************************
                  ;
                  ;
                  ;
      0000        CAMAX   EQU     *H3D00
      0000        CAMBX   EQU     *H3D01
      0000        CAMAY   EQU     *H3D02
      0000        CAMBY   EQU     *H3D03
      0000        CCMAX   EQU     *H3D46
      0000        CCMAY   EQU     *H3D44
      0000        CPOAX   EQU     *H3D40
      0000        CPOBX   EQU     *H3D41
      0000        CPOAY   EQU     *H3D42
      0000        CPOBY   EQU     *H3D43
      0000        CPLAX   EQU     *H3D0C
      0000        CPLBX   EQU     *H3D0D
      0000        CPLAY   EQU     *H3D0E
      0000        CPLBY   EQU     *H3D0F
      0000        DETX    EQU     *H3D10
      0000        DETY    EQU     *H3D11
      0000        DDOTX   EQU     *H3D12
      0000        DDOTY   EQU     *H3D14
      0000        DOTIX   EQU     *H3D16
      0000        DOTIY   EQU     *H3D18
      0000        IPRJX   EQU     *H3D1A
      0000        IPRJY   EQU     *H3D1C
      0000        IPOSX   EQU     *H3D1E
      0000        IPOSY   EQU     *H3D20
      0000        MULCX   EQU     *H3D90
      0000        MULDX   EQU     MULCX+20
      0000        MXLVB   EQU     MULDX+20
      0000        MXLVK   EQU     MXLVB+20
      0000        MULAX   EQU     MXLVK+20
      0000        MULBX   EQU     MULAX+20
      0000        MULCY   EQU     MULBX+20
      0000        MULDY   EQU     MULCY+20
      0000        MYLVB   EQU     MULDY+20
      0000        MYLVK   EQU     MYLVB+20
      0000        MULAY   EQU     MYLVK+20
      0000        MULBY   EQU     MULAY+20
      0000        MICH    EQU     MULBY+20
      0000        MICHY   EQU     MICH+20
      0000        CMIY    EQU     MICHY+20
```

Figure D-2 Prom No. 2 Yaw Control Software

```
0000          CMIX    EQU    CMIY+20
0000          TORQY   EQU    CMIX+20
0000          TORQX   EQU    TORQY+20
0000          PTQX    EQU    TORQX+20
0000          NCPOX   EQU    *H3D22
0000          NCPOY   EQU    *H3D24
0000          PRJAX   EQU    *H3D26
0000          PRJBX   EQU    *H3D27
0000          PRJAY   EQU    *H3D28
0000          PRJBY   EQU    *H3D29
0000          PRLAX   EQU    *H3D2A
0000          PRLBX   EQU    *H3D2B
0000          PRLAY   EQU    *H3D2C
0000          PRLBY   EQU    *H3D2D
0000          PVLAX   EQU    *H3D2E
0000          PVLBX   EQU    *H3D2F
0000          PVLAY   EQU    *H3D30
0000          PVLBY   EQU    *H3D31
0000          RINT    EQU    *H3D34
0000          TINT    EQU    *H3D38
0000          X       EQU    *H3D3A
0000          XY      EQU    *H3D3C
0000          XFLAG   EQU    *H3D3E
0000          YFLAG   EQU    *H3D3F
0000          DELY    EQU    *H3D68
0000          ICHY    EQU    *H3D70
0000          CDEL    EQU    *H3D72
0000          CIY     EQU    *H3D74
0000          USDAO   EQU    *H00EC
0000          PRTA1   EQU    *H0000
0000          PRTB1   EQU    *H0001
0000          PRTC1   EQU    *H0002
0000          PRTA2   EQU    *H0003
0000          PRTB2   EQU    *H00E5
0000          PRTC2   EQU    *H0000
0000          PRTD1   EQU    *H0001
0000          PRTD2   EQU    *H0002
0000          PRTD3   EQU    *H00E6
              ;
              ;    SYSTEM COMPENSATION NETWORK
              ;
              ;
0400                  ORG    *H400
0400 2A2C3D   YAW:    LHLD   PRLAY
0403 EB               XCHG
0404 3A293D           LDA    PRJBY
0407 E610             ANI    *H10
0409 FE10             CPI    *H10
040B C21604           JNZ    RA
040E 3A293D           LDA    PRJBY
```

Figure D-2 Prom No. 2 Yaw Control Software (Continued)

```
0411 C6E0           ADI   #HE0
0413 32293D         STA   PRJBY
0416 2A283D  RA:    LHLD  PRJAY
0419 CD4305         CALL  MINUS
041C 19             DAD   D
041D CD4305         CALL  MINUS
0420 EB             XCHG
0421 CD083E         CALL  MULCY
0424 22143D         SHLD  DDOTY
0427 DBEC           IN    USDAO
0429 3A113D         LDA   DETY
042C FE04           CPI   #H04
042E F24004         JP    PAA
0431 FEFC           CPI   #HFC
0433 FA3B04         JM    MAN
0436 3E00           MVI   A,#H00
0438 C34204         JMP   ING
043B C604    MAN:   ADI   #H04
043D C34204         JMP   ING
0440 C6FC    PAA:   ADI   #HFC
0442 5F      ING:   MOV   E,A
0443 FE00           CPI   #H00
0445 3E00           MVI   A,#H00
0447 F24B04         JP    ZP
044A 2F             CMA
044B 57      ZP:    MOV   D,A
044C CD1C3E         CALL  MULDY
044F EB             XCHG
0450 2A143D         LHLD  DDOTY
0453 19             DAD   D
0454 EB             XCHG
0455 7A             MOV   A,D
0456 07             RLC
0457 DA6404         JC    FIVE
045A 21CCFF         LXI   H,#HFFCC
045D 19             DAD   D
045E DA7204         JC    PL
0461 C36B04         JMP   TWO
0464 213400  FIVE:  LXI   H,#H0034
0467 19             DAD   D
0468 D27B04         JNC   ML
046B EB      TWO:   XCHG
046C 22023D         SHLD  CAMAY
046F C38404         JMP   EXT
0472 213400  PL:    LXI   H,#H34
0475 22023D         SHLD  CAMAY
0478 C38404         JMP   EXT
047B 21CCFF  ML:    LXI   H,#HFFCC
047E 22023D         SHLD  CAMAY
0481 C38404         JMP   EXT
```

Figure D-2 Prom No. 2 Yaw Control Software (Continued)

```
                 ;
                 ;           CAMERA SERVO
                 ;
0484 3A433D EXT:     LDA     CPOBY
0487 E61F            ANI     #H1F
0489 32433D          STA     CPOBY
048C E610            ANI     #H10
048E FE10            CPI     #H10
0490 C29B04          JNZ     WP
0493 3A433D          LDA     CPOBY
0496 C6E0            ADI     #HE0
0498 32433D          STA     CPOBY
049B 2A423D WP:      LHLD    CPOAY
049E CD4305          CALL    MINUS
04A1 22243D          SHLD    NCPOY
04A4 EB              XCHG
04A5 2A0E3D          LHLD    CPLAY
04A8 19              DAD     D
04A9 22F03F          SHLD    #H3FF0
04AC 29              DAD     H
04AD 29              DAD     H
04AE EB              XCHG
04AF 2A423D          LHLD    CPOAY
04B2 220E3D          SHLD    CPLAY
04B5 7A              MOV     A,D
04B6 07              RLC
04B7 D2C404          JNC     OGDR
04BA 211101          LXI     H,#H111
04BD 19              DAD     D
04BE D2D404          JNC     DECR
04C1 C3DA04          JMP     MUL
04C4 21EFFE OGDR:    LXI     H,#HFEEF
04C7 19              DAD     D
04C8 DACE04          JC      LMAR
04CB C3DA04          JMP     MUL
04CE 210040 LMAR:    LXI     H,#H4000
04D1 C3DD04          JMP     FLTR
04D4 2100C0 DECR:    LXI     H,#HC000
04D7 C3DD04          JMP     FLTR
04DA CD303E MUL:     CALL    MYLVB
04DD CD4B05 FLTR:    CALL    SHIFT
04E0 CD4B05          CALL    SHIFT
04E3 EB              XCHG
04E4 2A803D          LHLD    #H3D80
04E7 19              DAD     D
04E8 EB              XCHG
04E9 22803D          SHLD    #H3D80
04EC 2A823D          LHLD    #H3D82
04EF CD4B05          CALL    SHIFT
04F2 19              DAD     D
```

Figure D-2 Prom No. 2 Yaw Control Software (Continued)

```
04F3 22823D          SHLD    #H3D82
04F6 22183D          SHLD    DOTIY
04F9 2A023D          LHLD    CAMAY
04FC EB              XCHG
04FD 2A3C3D          LHLD    XY
0500 19              DAD     D
0501 EB              XCHG
0502 7A              MOV     A,D
0503 07              RLC
0504 DA1205          JC      PAP
0507 21D0E2          LXI     H,#HE2D0
050A 19              DAD     D
050B DA1D05          JC      ONE
050E EB              XCHG
050F C33205          JMP     THRE
0512 21041E PAP:     LXI     H,#H1E04
0515 19              DAD     D
0516 D22905          JNC     FOUR
0519 EB              XCHG
051A C33205          JMP     THRE
051D 210000 ONE:     LXI     H,0
0520 22023D          SHLD    CAMAY
0523 21301D          LXI     H,#H1D30
0526 C33205          JMP     THRE
0529 210000 FOUR:    LXI     H,0
052C 22023D          SHLD    CAMAY
052F 21FCE1          LXI     H,#HE1FC
0532 223C3D THRE:    SHLD    XY
0535 EB              XCHG
0536 2A243D          LHLD    NCPOY
0539 29              DAD     H
053A 29              DAD     H
053B 19              DAD     D
053C 22723D          SHLD    CDEL
053F EB              XCHG
0540 C30006          JMP     #H600
0543 7C     MINUS:   MOV     A,H
0544 2F              CMA
0545 67              MOV     H,A
0546 7D              MOV     A,L
0547 2F              CMA
0548 6F              MOV     L,A
0549 23              INX     H
054A C9              RET
054B 7C     SHIFT:   MOV     A,H
054C 07              RLC
054D 7C              MOV     A,H
054E 1F              RAR
054F 67              MOV     H,A
0550 7D              MOV     A,L
```

Figure D-2 Prom No. 2 Yaw Control Software (Continued)

```
251  0551 1F        RAR
252  0552 6F        MOV    L,A
253  0553 C9        RET
254  0554           END
```

Figure D-2 Prom No. 2 Yaw Control Software (Continued)

```
                ;************
                ;
                ;
                ;
                ;       SYSTEM EQUATES
                ;
                ;
                ;****************************
                ;
                ;
                ;
0000            LAGX    EQU     *H3F0C
0000            LAGY    EQU     *H3F20
0000            CDEL    EQU     *H3D72
0000            EOY     EQU     *H3FEC
0000            CAMAX   EQU     *H3D00
0000            CAMBX   EQU     *H3D01
0000            CAMAY   EQU     *H3D02
0000            CAMBY   EQU     *H3D03
0000            CCMAX   EQU     *H3D46
0000            CCMAY   EQU     *H3D44
0000            CPOAX   EQU     *H3D40
0000            CPOBX   EQU     *H3D41
0000            CPOAY   EQU     *H3D42
0000            CPOBY   EQU     *H3D43
0000            CPLAX   EQU     *H3D0C
0000            CPLBX   EQU     *H3D0D
0000            CPLAY   EQU     *H3D0E
0000            CPLBY   EQU     *H3D0F
0000            DETX    EQU     *H3D10
0000            DETY    EQU     *H3D11
0000            DDOTX   EQU     *H3D12
0000            DDOTY   EQU     *H3D14
0000            DOTIX   EQU     *H3D16
0000            DOTIY   EQU     *H3D18
0000            IPRJX   EQU     *H3D1A
0000            IPRJY   EQU     *H3D1C
0000            IPOSX   EQU     *H3D1E
0000            IPOSY   EQU     *H3D20
0000            MULCX   EQU     *H3D90
0000            MULDX   EQU     MULCX+20
0000            MXLVB   EQU     MULDX+20
0000            MXLVK   EQU     MXLVB+20
0000            MULAX   EQU     MXLVK+20
0000            MULBX   EQU     MULAX+20
0000            MULCY   EQU     MULBX+20
0000            MULDY   EQU     MULCY+20
0000            MYLVB   EQU     MULDY+20
0000            MYLVK   EQU     MYLVB+20
0000            MULAY   EQU     MYLVK+20
```

Figure D-2 Prom No. 2 Yaw Control Software (Continued)

```
0000            MULBY   EQU     MULAY+20
0000            MICH    EQU     MULBY+20
0000            MICHY   EQU     MICH+20
0000            CMIY    EQU     MICHY+20
0000            CMIX    EQU     CMIY+20
0000            TORQY   EQU     CMIX+20
0000            TORQX   EQU     TORQY+20
0000            PTQX    EQU     TORQX+20
0000            NCPOX   EQU     #H3D22
0000            NCPOY   EQU     #H3D24
0000            PRJAX   EQU     #H3D26
0000            PRJBX   EQU     #H3D27
0000            PRJAY   EQU     #H3D28
0000            PRJBY   EQU     #H3D29
0000            PRLAX   EQU     #H3D2A
0000            PRLBX   EQU     #H3D2B
0000            PRLAY   EQU     #H3D2C
0000            PRLBY   EQU     #H3D2D
0000            PVLAX   EQU     #H3D2E
0000            PVLBX   EQU     #H3D2F
0000            PVLAY   EQU     #H3D30
0000            PVLBY   EQU     #H3D31
0000            RINT    EQU     #H3D34
0000            TINT    EQU     #H3D38
0000            X       EQU     #H3D3A
0000            XY      EQU     #H3D3C
0000            XFLAG   EQU     #H3D3E
0000            YFLAG   EQU     #H3D3F
0000            DELY    EQU     #H3D68
0000            ICHY    EQU     #H3D70
0000            USDAO   EQU     #H00EC
0000            PRTA1   EQU     #H0000
0000            PRTB1   EQU     #H0001
0000            PRTC1   EQU     #H0002
0000            PRTA2   EQU     #H0003
0000            PRTB2   EQU     #H00E5
0000            PRTC2   EQU     #H0000
0000            PRTD1   EQU     #H0001
0000            PRTD2   EQU     #H0002
0000            PRTD3   EQU     #H00E6
0600                    ORG     #H600
0600 7A                 MOV     A,D
0601 07                 RLC
0602 DA1506             JC      YMI
0605 2100F0             LXI     H,#HF000
0608 19                 DAD     D
0609 DA0F06             JC      YLM
060C C32506             JMP     KV
060F 210040 YLM:        LXI     H,#H4000
0612 C32806             JMP     YE
```

Figure D-2 Prom No. 2 Yaw Control Software (Continued)

```
0615 210010 YMI:   LXI    H,#H1000
0618 19            DAD    D
0619 D21F06        JNC    YDE
061C C32506        JMP    KV
061F 2100C0 YDE:   LXI    H,#HC000
0622 C32806        JMP    YE
0625 CD443E KV:    CALL   MYLVK
0628 EB     YE:    XCHG
0629 2A183D        LHLD   DOTIY
062C 19            DAD    D
062D EB            XCHG
062E 7A            MOV    A,D
062F 07            RLC
0630 DA4306        JC     KAD
0633 21BCFB        LXI    H,#HFBBC
0636 19            DAD    D
0637 DA3D06        JC     OH
063A C35306        JMP    GOSH
063D 210040 OH:    LXI    H,#H4000
0640 C35606        JMP    OSH
0643 214404 KAD:   LXI    H,#H444
0646 19            DAD    D
0647 D24D06        JNC    WOW
064A C35306        JMP    GOSH
064D 2100C0 WOW:   LXI    H,#HC000
0650 C35606        JMP    OSH
0653 CDD03E GOSH:  CALL   TORQY
0656 22443D OSH:   SHLD   CCMAY
                   ;
                   ;PROJECTOR SERVO
                   ;
                   ;
0659 CDAC07        CALL   LAG
065C 2A723D        LHLD   CDEL
065F EB            XCHG
0660 7A            MOV    A,D
0661 07            RLC
0662 D26F06        JNC    YYY
0665 210004        LXI    H,#H400
0668 19            DAD    D
0669 D27906        JNC    LARGE
066C C38806        JMP    GO
066F 2100FC YYY:   LXI    H,#HFC00
0672 19            DAD    D
0673 DA7906        JC     LARGE
0676 C38806        JMP    GO
0679 2A3C3D LARGE: LHLD   XY
067C CDA407        CALL   MINUS
067F CD9B07        CALL   SHIFT
0682 CD9B07        CALL   SHIFT
```

Figure D-2 Prom No. 2 Yaw Control Software (Continued)

```
0685 22243D             SHLD    NCPOY
0688 2A283D  GO:        LHLD    PRJAY
068B CDA407             CALL    MINUS
068E 221C3D             SHLD    IPRJY
0691 EB                 XCHG
0692 2A243D             LHLD    NCPOY
0695 19                 DAD     D
0696 22683D             SHLD    DELY
0699 EB                 XCHG
069A 7A                 MOV     A,D
069B 07                 RLC
069C D2B506             JNC     OGD
069F 216600             LXI     H,#H0066
06A2 19                 DAD     D
06A3 D2AF06             JNC     DEC
06A6 C3BC06             JMP     BY
06A9 210040  LMA:       LXI     H,#H4000
06AC C3BF06             JMP     IP
06AF 2100C0  DEC:       LXI     H,#HC000
06B2 C3BF06             JMP     IP
06B5 219AFF  OGD:       LXI     H,#HFF9A
06B8 19                 DAD     D
06B9 DAA906             JC      LMA
06BC CD6C3E  BY:        CALL    MULBY
06BF 22203D  IP:        SHLD    IPOSY
06C2 2A683D             LHLD    DELY
06C5 EB                 XCHG
06C6 7A                 MOV     A,D
06C7 07                 RLC
06C8 D2D506             JNC     CLA
06CB 213000             LXI     H,#H30
06CE 19                 DAD     D
06CF D21307             JNC     OUT
06D2 C3DC06             JMP     GAIN
06D5 21D0FF  CLA:       LXI     H,#HFFD0
06D8 19                 DAD     D
06D9 DA1307             JC      OUT
06DC CD943E  GAIN:      CALL    MICHY
06DF EB                 XCHG
06E0 2A703D             LHLD    ICHY
06E3 19                 DAD     D
06E4 22703D             SHLD    ICHY
06E7 EB                 XCHG
06E8 7A                 MOV     A,D
06E9 07                 RLC
06EA DAF706             JC      PA
06ED 2100C0             LXI     H,#HC000
06F0 19                 DAD     D
06F1 DA0107             JC      PB
06F4 C30C07             JMP     PC
```

Figure D-2 Prom No. 2 Yaw Control Software (Continued)

```
06F7 210040 PA:    LXI    H,#H4000
06FA 19            DAD    D
06FB D20807        JNC    PD
06FE C30C07        JMP    PC
0701 210040 PB:    LXI    H,#H4000
0704 EB            XCHG
0705 C30C07        JMP    PC
0708 2100C0 PD:    LXI    H,#HC000
070B EB            XCHG
070C 2A203D PC:    LHLD   IPOSY
070F 19            DAD    D
0710 22203D        SHLD   IPOSY
0713 2A2C3D OUT:   LHLD   PRLAY
0716 EB            XCHG
0717 2A283D        LHLD   PRJAY
071A 222C3D        SHLD   PRLAY
071D 2A1C3D        LHLD   IPRJY
0720 19            DAD    D
0721 22F23F        SHLD   #H3FF2
0724 29            DAD    H
0725 29            DAD    H
0726 29            DAD    H
0727 29            DAD    H
0728 29            DAD    H
0729 EB            XCHG
072A 2AEC3F        LHLD   EOY
072D CDA407        CALL MINUS
0730 19            DAD    D
0731 29            DAD    H
0732 EB            XCHG
0733 7A            MOV    A,D
0734 07            RLC
0735 D24207        JNC    OGDR
0738 210004        LXI    H,#H400
073B 19            DAD    D
073C D25207        JNC    DECR
073F C35807        JMP    BXR
0742 2100FC OGDR:  LXI    H,#HFC00
0745 19            DAD    D
0746 DA4C07        JC     LMAR
0749 C35807        JMP    BXR
074C 210040 LMAR:  LXI    H,#H4000
074F C35B07        JMP    IPR
0752 2100C0 DECR:  LXI    H,#HC000
0755 C35B07        JMP    IPR
0758 CD583E BXR:   CALL   MULAY
075B CD9B07 IPR:   CALL   SHIFT
075E CD9B07        CALL   SHIFT
0761 EB            XCHG
0762 2A623D        LHLD   #H3D62
```

Figure D-2 Prom No. 2 Yaw Control Software (Continued)

```
0765 19              DAD    D
0766 EB              XCHG
0767 22623D          SHLD   *H3D62
076A 2A643D          LHLD   *H3D64
076D CD9B07          CALL   SHIFT
0770 19              DAD    D
0771 22643D          SHLD   *H3D64
0774 EB              XCHG
0775 2A203D          LHLD   IPOSY
0778 19              DAD    D
0779 22303D          SHLD   PVLAY
077C 29              DAD    H
077D 29              DAD    H
077E 29              DAD    H
077F 29              DAD    H
0780 7C              MOV    A,H
0781 32303D          STA    PVLAY
0784 213F3D          LXI    H,YFLAG
0787 7E              MOV    A,M
0788 C601            ADI    *H01
078A 77              MOV    M,A
078B 07              RLC
078C DA9007          JC     ALT
078F C9              RET
0790 2A383D ALT:     LHLD   TINT
0793 7E              MOV    A,M
0794 2B              DCX    H
0795 22383D          SHLD   TINT
0798 D3EC            OUT    USDAO
079A C9              RET
079B 7C     SHIFT:   MOV    A,H
079C 07              RLC
079D 7C              MOV    A,H
079E 1F              RAR
079F 67              MOV    H,A
07A0 7D              MOV    A,L
07A1 1F              RAR
07A2 6F              MOV    L,A
07A3 C9              RET
07A4 7C     MINUS:   MOV    A,H
07A5 2F              CMA
07A6 67              MOV    H,A
07A7 7D              MOV    A,L
07A8 2F              CMA
07A9 6F              MOV    L,A
07AA 23              INX    H
07AB C9              RET
07AC 2A023D LAG:     LHLD   CAMAY
07AF 29              DAD    H
07B0 29              DAD    H
```

Figure D-2 Prom No. 2 Yaw Control Software (Continued)

```
07B1 29          DAD    H
07B2 EB          XCHG
07B3 2AEC3F      LHLD   EOY
07B6 CDA407      CALL   MINUS
07B9 19          DAD    D
07BA EB          XCHG
07BB CDA83E      CALL   CMIY
07BE CD9B07      CALL   SHIFT
07C1 CD9B07      CALL   SHIFT
07C4 CD9B07      CALL   SHIFT
07C7 CD9B07      CALL   SHIFT
07CA CD9B07      CALL   SHIFT
07CD CD9B07      CALL   SHIFT
07D0 CD9B07      CALL   SHIFT
07D3 EB          XCHG
07D4 2AEC3F      LHLD   EOY
07D7 19          DAD    D
07D8 22EC3F      SHLD   EOY
07DB C9          RET
07DC             END
```

Figure D-2 Prom No. 2 Yaw Control Software (Concluded)

```
0800                    ORG     #H800
0800           KBIN2    EQU     #HE9      ;KEYBOARD INPUT PORT
0800           PRSET    EQU     #HEA      ;INTERRUPT FLIP-FLOP PRESET OUTPUT PO
0800           LEDCM    EQU     #HE8      ;LED AND COMPARATOR OUTPUT PORT
0800           SETML   EQU      #HA14
0800           OK       EQU       #HA64
0800           CHANG    EQU       #HA52
0800           READA    EQU     #H3D80    ;3D80 THRU 3D83 IS ADDRESS INFORMATIO
0800           READD    EQU     READA+4   ;3D84 THRU 3D85 IS DATA INFORMATION
0800           READF    EQU     READD+2   ;3D86 IS FUNCTION INFORMATION
0800           FSTAT    EQU     READF+1   ;3D87 IS FUNCTION STATUS
0800           PSAVE    EQU     FSTAT+1   ;PSAVE IS THE RETURN LOCATION IN INTE
0800           OSTAT    EQU     PSAVE+2   ;CODE FOR EXPECTED KEYBOARD INPUT
               ;KBRD1 IS THE FUNCTION KEYBOARD SERVICE ROUTINE
0800 DBE9      KBRD1:   IN      KBIN2     ;INPUT FUNCTION INFORMATION
0802 E6F0               ANI     #HF0      ;WE'RE ONLY INTERESTED IN HIGH ORDER
0804 47                 MOV     B,A       ;SAVE FOR LATER
0805 32863D             STA     READF     ;STORE INFORMATION READ
0808 FEB0               CPI     #HB0      ;IS THIS A MAJOR OR MINOR FUNCTION
080A DA1F08             JC      FUNCT     ;MINOR FUNCTION-JUMP TO FUNCT
               ;    OSTAT=C0 MEANS MAJOR FUNCTION IS EXPECTED
               ;    OSTAT=20 MEANS MINOR MONITOR FUNCTION IS EXPECTED
               ;    OSTAT=10 MEANS MINOR SETML FUNCTION (CHANG OR OK) IS EXPE
               ;    OSTAT=8 MEANS NUMBER IS EXPECTED
               ;          LDA   OSTAT
               ;          CPI   #HC0
               ;          JNZ   ERROR
080D 78                 MOV     A,B
0802 FED0               CPI     #HD0      ;FIND PARTICULAR MAJOR FUNCTION
0810 DA140A             JC      SETML     ;JUMP TO SETML IF ACC=C0
0813 CAB309             JZ      START     ;JUMP TO START IF ACC=D0
               ;COMPR IS THE ENTRY POINT WHEN A COMPARE INTERRUPT OCCURS
0816 3E20      COMPR:   MVI     A,#H20    ;MONITOR OR COMPARE INTERRUPT HAS OCC
0818 328A3D             STA     OSTAT     ;GET READY FOR MONITOR MINOR FUNCTION
081B 78                 MOV     A,B
081C C32E08             JMP     MONITR
081F FE80      FUNCT:   CPI     #H80      ;CHECK FOR MONITOR MINOR OR SETML MIN
0821 DA2D08             JC      DIAG      ;IF LESS THAN 80 IT'S A MONITOR MINOR
               :          LDA   OSTAT     ;CHECK FOR SETML MINOR FUNCTION
               :          ANI   #H10
               :          JZ    ERROR
0824 78                 MOV     A,B       ;IS IT AN OK OR A CHANG
0825 FE90               CPI     #H90
0827 DA640A             JC      OK        ;IF ACC=80,OK
082A C3520A             JMP     CHANG
               ;DIAG IS THE ROUTINE FOR MONITOR MINOR FUNCTIONS
               ;DIAG:     LDA   OSTAT     ;CHECK TO SEE THAT THE
               ;          ANI   #H20      ; FUNCTION SELECTED
               ;          JZ    ERROR     ; WAS EXPECTED
082D C9        DIAG:    RET
```

Figure D-3 Prom No. 3 Monitor Program

```
082E 3E70   MONITR:  MVI   A,#H70     ;GET READY
0830 32873D          STA   FSTAT      ;  FOR SINGLE STEP
0833 3ED8            MVI   A,#HD8     ;DISPLAY "D" ON HIGHEST
0835 CD8109          CALL  OUTPT      ;  ORDER LED
0838 E1              POP   H          ;STORE THE OLD PROGRAM COUNTER AT LOC
0839 22883D          SHLD  PSAVE      ;  PSAVE(LOCATION IN INTERRUPT HANDLE
083C 210800          LXI   H,8        ;POINT TO THE LOCATION CPU WAS EXECUT
083F 39              DAD   SP         ;  WHEN INTERRUPT OCCURRED
0840 EB              XCHG             ;DISPLAY ADDRESS
0841 1A              LDAX  D          ;  OF INSTRUCTION
0842 CDD108          CALL  SPLIT      ;   TO BE EXECUTED
0845 13              INX   D          ;    AFTER RETURN
0846 1A              LDAX  D          ;     TO ORIGINAL
0847 CDD308          CALL  SECND      ;      PROGRAM
084A 3E20   NEXT:    MVI   A,#H20     ;PREPARE FOR MONITOR MINOR FUNCTION
084C 328A3D          STA   OSTAT
084F 76              HLT              ;WAIT FOR KEYBOARD INTERRUPT
0850 3A863D          LDA   READF      ;LOAD FUNCTION
0853 CD1B09 ARND:    CALL  JUMP       ;JUMP TO APPROPRIATE
0856 E9              PCHL             ;  ROUTINE
0857 6708   EM:      DW    EXAMM      ;J
0859 7708   ER:      DW    EXAMR      ; U
085B 8608   DM:      DW    DEPM       ;  M
085D 9508   DR:      DW    DEPR       ;T  P
085F A408   SS:      DW    SSTEP      ; A
0861 AC08   CO:      DW    CONT       ;  B
0863 BD08   RS:      DW    RESET      ;   L
0865 CB08   CA:      DW    COMPA      ;    E
                     ;EXAMM IS THE MEMORY EXAMINATION ROUTINE
0867 CD0309 EXAMM:   CALL  E1         ;READ FOUR HEX DIGITS FROM KEYBOARD
086A CD5809          CALL  CONCAT     ;CONCATENATE INTO 16-BIT ADDRESS
086D CD7509          CALL  ZERO       ;ZERO OUT LOW ORDER FOUR DISPLAYS
0870 1A              LDAX  D          ;DISPLAY CONTENTS
0871 CDD108          CALL  SPLIT      ;  OF THAT ADDRESS
0874 C34A08          JMP   NEXT
                     ;EXAMR EXAMINES THE CONTENTS OF A PARTICULAR REGISTER
0877 1601   EXAMR:   MVI   D,1        ;
0879 CD0509          CALL  E2         ;READ ONE HEXADECIMAL DIGIT
087C CD3709          CALL  MEMORY     ;FIND LOCATION IN STACK
087F 7E              MOV   A,M        ;DISPLAY CONTENTS OF
0880 CDD108          CALL  SPLIT      ;  THAT REGISTER
0883 C34A08          JMP   NEXT
                     ;DEPM DEPOSITS DATA INTO A SPECIFIED RAM LOCATION
0886 CD0309 DEPM:    CALL  E1         ;READ FOUR HEX DIGITS FROM KEYBOARD
0889 CD5809          CALL  CONCAT     ;CONCATENATE INTO 16-BIT ADDRESS
088C CD7509          CALL  ZERO       ;ZERO OUT LOW ORDER FOUR DISPLAYS
088F CD4309          CALL  TWO        ;READ IN TWO MORE DIGITS, CONCATENATE
0892 C34A08          JMP   NEXT
                     ;DEPR DEPOSITS DATA INTO A SPECIFIED REGISTER
0895 1601   DEPR:    MVI   D,1
```

Figure D-3 Prom No. 3 Monitor Program (Continued)

```
0897 CD0509          CALL  E2          ;READ IN ONE DIGIT
089A CD3709          CALL  MEMORY      ;FIND LOCATION OF REGISTER IN STACK
089D EB              XCHG
089E CD4309          CALL  TWO         ;READ IN TWO MORE DIGITS, CONCATENATE
08A1 C34A08          JMP   NEXT
             ;SSTEP CAUSES ONE INSTRUCTION OF THE SOURCE PROGRAM TO BE
             ; EXECUTED FOLLOWED BY A RETURN TO THE DIAGNOSTIC
             ; ROUTINE
08A4 3E09    SSTEP:   MVI   A,9         ;SET THE CMPR FLIP-FLOP
08A6 CD8109           CALL OUTPT
08A9 C3BD08          JMP   RESET
             ;CONT AUTOMATICALLY INCREMENTS THE TABLE POINTER FOR THE
             ; DEPM AND EXAMM FUNCTIONS
08AC 3A873D  CONT:    LDA   FSTAT       ;EXAMM OR DEPM?
08AF CD1B09          CALL  JUMP        ;GET READY TO JUMP TO 3RD
08B2 3E06            MVI   A,6         ;  INSTRUCTION OF DEPM OR
08B4 85              ADD   L           ;  EXAMM. ADDRESS IN RAM IS
08B5 6F               MOV L,A          ;  INCREMENTED BY ONE
08B6 3E00             MVI   A,0        ;ADD
08B8 17               RAL              ; CARRY
08B9 84               ADD   H          ;  OUT OF
08BA 67               MOV H,A          ;   L TO H
08BB 13               INX   D          ;INFORMATION AT READA THRU
08BC E9              PCHL              ;  READA+3 IS UNCHANGED.
             ;RESET RESTORES THE REGISTERS AND INTERRUPT STATUS AND
             ; OLD PROGRAM COUNTER
08BD 3EC0    RESET:   MVI   A,#HC0      :GET READY TO
08BF 328A3D           STA   OSTAT       ; SAY GOODBYE
08C2 3EFF             MVI   A,#HFF      ;ENABLE
08C4 2F               CMA               ; ALL INTERRUPT
08C5 D3EA             OUT   PRSET       ;  FLIP-FLOPS
08C7 2A883D           LHLD PSAVE        ;GET THE INTERRUPT HANDLER ADDRESS
08CA E9               PCHL              ;RETURN
             ;COMPA LOADS THE COMPARE ADDRESS BUFFERS AND THEN RETURNS
             ; TO THE SOURCE PROGRAM
08CB CD0709  COMPA:   CALL  E1          ;READ IN FOUR HEX DIGITS
08CE C3A408           JMP   SSTEP       ;  AND LOAD COMPARE ADDRESS
             ;SPLIT DECODES A 16-BIT NUMBER SO THAT IT CAN BE DISPLAYED
             ; ON THE FRONT PANEL
08D1 0E04    SPLIT:   MVI   C,4         ;REGISTER C POINTS TO LED DISPLAY
08D3 6F      SECND:   MOV   L,A         ;SPLIT ACCUMULATOR INTO TWO HEX
08D4 29               DAD   H           ;  DIGITS,CONTAINED IN LOW ORDER
08D5 29               DAD   H           ;  FOUR BITS OF H AND L REGISTERS.
08D6 29               DAD   H
08D7 29               DAD   H
08D8 7D               MOV   A,L
08D9 CDEF08           CALL  LOW
08DC 0C               INR   C
08DD 44               MOV   B,H
08DE CDE808           CALL  DATA
```

Figure D-3 Prom No. 3 Monitor Program (Continued)

```
08E1 0C                 INR   C
08E2 C9                 RET
               ;STORE STORES THE DATA READ IN
08E3 E60F      STORE:   ANI   #HF       ;LOOK AT LOW ORDER FOUR
08E5 77                 MOV   M,A       ;  BITS  READ IN. MOVE INTO READA
08E6 23                 INX   H         ;  INCREMENT READA TABLE POINTER.
08E7 47                  MOV  B,A
08E8 78        DATA:    MOV   A,B       ;MOV DATA TO
08E9 E60F               ANI   #HF       ;  HIGH ORDER
08EB 07                 RLC             ;    FOUR BITS
08EC 07                 RLC
08ED 07                 RLC
08EE 07                 RLC
08EF B1        LOW:     ORA   C         ;OUTPUT DATA
08F0 CD8109              CALL OUTPT     ;  TO APPROPRIATE
08F3 47                 MOV   B,A       ;    DISPLAY
08F4 3A873D             LDA   FSTAT     ;IS THIS PERHAPS A COMPARE
08F7 FE70               CPI   #H70      ;  ADDRESS OR SINGLE STEP?
08F9 C0                 RNZ
08FA 78                 MOV   A,B       ;IF AC OR SS LOAD
08FB D604               SUI   4         ;  COMPARE ADDRESS BUFFERS
08FD EEF0                XRI  #HF0      ;COMPLEMENT THE HIGH ORDER FOUR BITS
08FF CD8109              CALL OUTPT
0902 C9                 RET
               ;E1,E2,SHARE AND REPEAT ARE ENTRY POINTS TO A ROUTINE THAT
               ;  CONTROLS THE READING AND STORING OF DATA.
0903 1604      E1:      MVI   D,4       ;D CONTAINS # OF DIGITS OT BE READ.
0905 0E07      E2:      MVI   C,7       ;C CONTAINS DISPLAY POINTER
0907 21803D    SHARE:   LXI   H,READA
090A 3E08      REPEAT:   MVI  A,8
090C 328A3D              STA  OSTAT
090F CD7109              CALL READ
0912 CDE308             CALL  STORE     ;STORE AND
0915 0D                 DCR   C         ;  DISPLAY DIGIT
0916 15                 DCR   D         ;    READ
0917 C8                 RZ
0918 C30A09             JMP   REPEAT
               ;JUMP DETERMINES THE ADDRESS OF THE DIAGNOSTIC ROUTINE
               ;  TO BE USED
091B FE50      JUMP:    CPI   #H50      ;STORE THE FUNCTION READ AT FSTAT
091D CA2A09             JZ    AROUND    ;  AND DISPLAY ON HIGH ORDER
0920 32873D             STA   FSTAT     ;  DISPLAY (IF OTHER THAN CONT).
0923 F5                 PUSH  PSW
0924 F608               ORI   8
0926 CD8109              CALL OUTPT
0929 F1                 POP   PSW
092A 0F        AROUND:  RRC             ;COMPUTE
092B 0F                 RRC             ;  JUMP
092C 0F                 RRC             ;    TABLE
092D 215708             LXI   H,EM      ;      POSITION
```

Figure D-3 Prom No. 3 Monitor Program (Continued)

```
0930 85                ADD   L
0931 6F                MOV   L,A
0932 7E                MOV   A,M
0933 23                INX   H
0934 66                MOV   H,M
0935 6F                MOV   L,A
0936 C9                RET
               ;MEMORY DETERMINES WHERE IN THE STACK A PARTICULAR
               ;  REGISTER IS STORED
0937 3A803D MEMORY:    LDA   READA    ;STEP BACK 11 LOCATIONS THRU
093A 210900             LXI  H,9      ;  STACK.  H AND L POINT
093D 2F                CMA            ;  TO B REGISTER
093E 3C                INR   A        ;NOW STEP FORWARD NUMBER
093F 85                ADD   L        ;  OF LOCATIONS CORRESPONDING
0940 6F                MOV   L,A      ;  TO REGISTER NUMBER.
0941 39                DAD   SP
0942 C9                RET
               ;TWO READS IN TWO DIGITS FROM THE KEYBOARD AND FORMS
               ;  THESE INTO AN 8-BIT BYTE
0943 D5     TWO:       PUSH  D        ;STORE ADDRESS OF LOCATION
0944 1602              MVI   D,2      ;  TO BE MODIFIED
0946 0E05              MVI   C,5
0948 21843D            LXI   H,READD  ;READ IN
094B CD0A09            CALL  REPEAT   ;  TWO DIGITS
094E E1                POP   H
094F 01843D            LXI   B,READD  ;CONCATENATE
0952 CD5B09            CALL  ENT      ;  AND
0955 72                MOV   M,D      ;    STORE
0956 EB                XCHG           ;D AND E ARE AGAIN THE
0957 C9                RET            ;  ADDRESS POINTER
               ;CONCAT TAKES FOUR 4-BIT NUMBERS (STORED IN THE LOW ORDER
               ;  FOUR BITS OF FOUR MEMORY LOCATIONS) AND CONCATENATES THEM
               ;  INTO A 16-BIT NUMBER
0958 01803D CONCAT:    LXI   B,READA  ;LOAD ACCUMULATOR WITH
095B 0A     ENT:       LDAX  B        ;  HIGH ORDER HEX DIGIT
095C 07                RLC            ;  OF READA TABLE
095D 07                RLC
095E 07                RLC
095F 07                RLC
0960 57                MOV   D,A
0961 03                INX   B
0962 0A                LDAX  B        ;CONCATENATE TWO HIGHEST ORDER
0963 B2                ORA   D        ;  DIGITS BY OR-ING A WITH D.
0964 57                MOV   D,A      ;STORE RESULT IN D.
0965 03                INX   B        ;SAME THING WITH NEXT
0966 0A                LDAX  B        ;  TWO DIGITS AND
0967 07                RLC            ;  STORE IN E REGISTER.
0968 07                RLC
0969 07                RLC
096A 07                RLC
```

Figure D-3 Prom No. 3 Monitor Program (Continued)

```
0968 5F                 MOV   E,A
096C 03                 INX   B
096D 0A                 LDAX  B
096E B3                 ORA   E
096F 5F                 MOV   E,A
0970 C9                 RET
                ;READ READS IN THE DATA LINES OF THE KEYBOARD AND STORES
                ;  THIS SEQUENCE IN REGISTER A.
0971 76         READ:   HLT               ;WAIT FOR KEYBOARD INTERRUPT
0972 DBE9               IN    KB1N2
0974 C9                 RET
                ;ZERO WRITES ZEROES ON THE DISPLAYS
0975 3E04       ZERO:   MVI   A,4         ;OUTPUT ZEROES TO
0977 CD8109     LOOP:   CALL  OUTPT       ;  FOUR LOWEST ORDER DISPLAYS
097A 3C                 INR   A
097B FE08               CPI   8
097D C27709             JNZ   LOOP
0980 C9                 RET
0981 F5         OUTPT:  PUSH  PSW         ;SAVE THE ACCUMULATOR
0982 2F                 CMA               ;OUTPT THE NUMBER TO THE
0983 D3E8               OUT   LEDCM       ;  LED AND COMPARATOR OUTPUT PORT
0985 3E47               MVI   A,#H47      ;TOGGLE
0987 2F                 CMA               ; THE
0988 D3EA               OUT   PRSET       ;  74154
098A 3EC7               MVI   A,#HC7      ;   ENABLE
098C 2F                 CMA               ;    PIN
098D D3EA               OUT   PRSET
098F F1                 POP   PSW         ;RESTORE THE ACCUMULATOR
0990 C9                 RET
0991 3EB8       ERROR:  MVI   A,#HB8      ;OUTPUT ERROR MESSAGE
0993 CD8109             CALL  OUTPT
0996 3E07               MVI   A,7
0998 CD8109             CALL  OUTPT
099B 3E06               MVI   A,6
099D CD8109             CALL  OUTPT
09A0 3EB5               MVI   A,#HB5
09A2 CD8109             CALL  OUTPT
09A5 3EB4               MVI   A,#HB4
09A7 CD8109             CALL  OUTPT
09AA C9                 RET
09AB 3A8A3D     KBRD2:  LDA   OSTAT       ;NUMERIC KEYBOARD SERVICE RETURN
09AE FE08               CPI   8
09B0 C29109             JNZ   ERROR
09B3 C9         START:  RET
09B4                    END
```

Figure D-3 Prom No. 3 Monitor Program (Continued)

```
INTEL 8[illegible] CROSS ASSEMBLER                    14:46:02   09-MA[illegible]7   PAGE  1

0A00                      ORG     #HA00
0A00          FIRST    EQU     #H3FE0
0A00          FSTAT    EQU     #H3D87
0A00          ZERO       EQU     #H975
0A00          SPLIT      EQU     #H8D1
0A00          TWO        EQU      #H943
0A00          OSTAT      EQU     #H3D8A
0A00          TEMP       EQU     OSTAT+1
0A00          COUNT      EQU     TEMP+1
0A00          CNSNT      EQU     COUNT+1  ;3D8D HAS MULTIPLY CONSTANT READ FROM
0A00          MPNTR      EQU     CNSNT+1  ;3D8E THRU 3D8F HAS MULTIPLY ROUTINE
0A00          MULCX      EQU     MPNTR+2  ;3D90 HAS STARTING LOCATION OF 1ST MU
              ;CTAB IS THE MULTIPLY CONSTANT TABLE
0A00 08       CTAB:      DB      8
0A01 01               DB         1
0A02 3C               DB         #H3C
0A03 01               DB         1
0A04 04               DB         4
0A05 01               DB         1
0A06 06               DB         6
0A07 01               DB         1
0A08 3C               DB         #H3C
0A09 04               DB         4
0A0A 1A               DB         #H1A
0A0B A0               DB         #HA0
0A0C 00               DB         0
0A0D 00               DB         #H0
0A0E 0D               DB         #HD
0A0F 00               DB         0
0A10 09               DB         9
0A11 0A               DB         #HA
0A12 D0               DB         #HD0
0A13 0D               DB         #HD
              ;SETML CREATES FAST MEMORY ROUTINES IN RAM
0A14 3E10     SETML:     MVI     A,#H10    ;GET READY FOR SETML MINOR FUNCTION
0A16 328A3D              STA     OSTAT
0A19 3E00             MVI        A,0      ;CERTAIN SUBROUTINES USED BY THIS
0A1B 32873D           STA        FSTAT    ;SECTION REQUIRE A VALUE FOR FSTAT
0A1E CD7509              CALL    ZERO      ;ZERO OUT DISPLAY
0A21 21903D              LXI     H,MULCX
0A24 228E3D              SHLD    MPNTR     ;INITIALIZE MULTIPLY ROUTINE POINTER
0A27 11000A              LXI     D,CTAB    ;INITIALIZE TABLE POINTER
0A2A 3E14                MVI     A,20      ;INITIALIZE LOOP COUNT
0A2C 328C3D INSPT:       STA     COUNT
0A2F 1A                  LDAX    D         ;LOAD THE ACCUMULATOR WITH TABLE ENTR
0A30 328D3D              STA     CNSNT     ;STORE TABLE ENTRY
0A33 CDD108              CALL    SPLIT     ;DISPLAY TABLE ENTRY
0A36 3AE03F           LDA        FIRST    ;CHECK FOR FIRST TIME THRU
0A39 17               RAL                 ;MSB DECIDES
0A3A DA430A           JC         HALT     ;IF C=1, FIRST TIME THRU
```

Figure D-3 Prom No. 3 Monitor Program (Continued)

```
0A3D CD640A          CALL   OK       ;OTHERWISE, SET UP MULTIPLIES
0A40 C3440A          JMP    NEXT     ;  INTERACTION FROM KEYBOARD
0A43 76      HALT:   HLT             ;WAIT FOR A KEYBOARD INTERRUPT
0A44 13      NEXT:   INX    D        ;PREPARE FOR NEXT TABLE ENTRY
0A45 3A8C3D          LDA    COUNT
0A48 3D              DCR    A        ;DECREMENT LOOP COUNTER
0A49 C22C0A          JNZ    INSPT
0A4C 3EC0            MVI    A,#HC0   ;PREPARE FOR NEXT MAJOR FUNCTION
0A4E 328A3D          STA    OSTAT
0A51 C9              RET
             ;CHANG READS TWO HEX NUMBERS FROM THE NUMERIC KEYBOARD AND USE
             ;NUMBER RATHER THAN THE ONE IN CTAB TO GENERATE A MULTIPLY ROU
0A52 118B3D  CHANG:  LXI    D,TEMP
0A55 CD4309          CALL   TWO      ;READ KEYBOARD
0A58 3E10            MVI    A,#H10   ;PREPARE FOR NEXT SETML MINOR FUNCTIO
0A5A 328A3D          STA    OSTAT
0A5D 3A8B3D          LDA    TEMP     ;THIS THE NEW MULTIPLY CONSTANT
0A60 CD700A          CALL   MULT     ;SET UP THE MULTIPLY ROUTINE
0A63 C9              RET
             ;OK TAKES THE NUMBER FROM THE TABLE AND GENERATES THE
             ;CORRESPONDING MULTIPLY ROUTINE
0A64 3E10    OK:     MVI    A,#H10   ;PREPARE FOR NEXT SETML MINOR FUNCTIO
0A66 328A3D          STA    OSTAT
0A69 3A8D3D          LDA    CNSNT    ;LOAD THE TABLE ENTRY INTO THE ACCUMU
0A6C CD700A          CALL   MULT     ;SET UP MULTIPLY ROUTINE
0A6F C9              RET
             ;MULT WRITES A ROUTINE IN RAM TO MULTIPLY VARIABLE BY SOME CON
             ;THE CONSTANT IS IN THE ACCUMULATOR. THE ROUTINE CORRESPONDING
             ;TO THE CONSTANT 5 IS GIVEN BELOW:
             ;
             ;                                  LXI H,0
             ;                                  DAD D
             ;                                  DAD H
             ;                                  DAD H
             ;                                  DAD D
             ;                                  RET
0A70 2A8E3D  MULT:   LHLD   MPNTR    ;GET THE STARTING LOCATION FOR THE MU
0A73 3621            MVI    M,#H21   ;WRITE AN 'LXI H,0' INTO MEMORY
0A75 23              INX    H
0A76 3600            MVI    M,0
0A78 23              INX    H
0A79 3600            MVI    M,0
0A7B 23              INX    H
0A7C 0608            MVI    B,8      ;B IS THE LOOP COUNTER
0A7E 07      LPCY:   RLC             ;IGNORE LEADING ZEROES
0A7F DA890A          JC     OWT      ;JUMP OUT WHEN FIRST ONE IS FOUND
0A82 05              DCR    B
0A83 C27E0A          JNZ    LPCY
0A86 C3990A          JMP    ZCNT     ;NO ONES, NUMBER IS ZERO
0A89 0F      OWT:    RRC
```

Figure D-3 Prom No. 3 Monitor Program (Continued)

```
INTEL 8080 CROSS ASSEMBLER                     14:46:31   09-MAY-77   PAGE 3

0A8A 07      TOP:     RLC              ;CHECK FOR ZERO OR ONE
0A8B D2910A           JNC    GO2       ;IF ZERO, JUST WRITE A 'DAD H'
0A8E 3619    GO1:     MVI    M,#H19    ;OTHERWISE WRITE A 'DAD D'
0A90 23               INX    H         ;  AND THEN A 'DAD H'
0A91 3629    GO2:     MVI    M,#H29
0A93 23               INX    H
0A94 05               DCR    B         ;CONTINUE FOR ALL REMAINING BITS
0A95 C28A0A           JNZ    TOP
0A98 2B               DCX    H         ;WRITE OVER LAST 'DAD H'
0A99 36C9    ZCNT:    MVI    M,#HC9    ;  WITH A 'RET'
0A9B 2A8E3D           LHLD   MPNTR     ;ADD 20 TO THE OLD STARTING
0A9E 011400           LXI    B,#H14    ;  LOCATION TO GET THE NEW
0AA1 09               DAD    B         ;STARTING LOCATION
0AA2 228E3D           SHLD   MPNTR
0AA5 C9               RET
0000
```

```
INTEL 8080 CROSS ASSEMBLER SYMBOL TABLE

A      = 0007     B      = 0000     GO1      0A8E     GO2      0A91
C      = 0001     D      = 0002     E      = 0003     CTAB     0A00
CHANG    0A52     H      = 0004     HALT     0A43     L      = 0005
M      = 0006     FSTAT= 3D87       TEMP   = 3D8B     FIRST= 3FE0
COUNT= 3D8C       CNSNT= 3D8D       SPLIT= 08D1       OSTAT= 3D8A
MULCX= 3D90       ZERO   = 0975     MPNTR= 3D8E       SETML    0A14
SP     = 0006     INSPT    0A2C     NEXT     0A44     OK       0A64
MULT     0A70     LPCY     0A7E     PSW    = 0006     TWO    = 0943
ONT      0A89     TOP      0A8A     ZCNT     0A99

ERRORS DETECTED:  0
```

Figure D-3 Prom No. 3 Monitor Program (Concluded)

INTEL 8080 CROSS ASSEMBLER   14:47:34   09-MAY-77   PAGE 1

```
                ;***********
                ;
                ;
                ;
                ;       SYSTEM EQUATES
                ;
                ;
                ;************************
                ;
                ;
                ;
0000            CAMAX   EQU     #H3D00
0000            CAMBX   EQU     #H3D01
0000            CAMAY   EQU     #H3D02
0000            CAMBY   EQU     #H3D03
0000            CCMAX   EQU     #H3D46
0000            CCMAY   EQU     #H3D44
0000            CPOAX   EQU     #H3D40
0000            CPOBX   EQU     #H3D41
0000            CPOAY   EQU     #H3D42
0000            CPOBY   EQU     #H3D43
0000            CPLAX   EQU     #H3D0C
0000            CPLBX   EQU     #H3D0D
0000            CPLAY   EQU     #H3D0E
0000            CPLBY   EQU     #H3D0F
0000            DETX    EQU     #H3D10
0000            DETY    EQU     #H3D11
0000            DDOTX   EQU     #H3D12
0000            DDOTY   EQU     #H3D14
0000            DOTIX   EQU     #H3D16
0000            DOTIY   EQU     #H3D18
0000            IPRJX   EQU     #H3D1A
0000            IPRJY   EQU     #H3D1C
0000            IPOSX   EQU     #H3D1E
0000            IPOSY   EQU     #H3D20
0000            MULCX   EQU     #H3D90
0000            MULDX   EQU     MULCX+20
0000            MXLVB   EQU     MULDX+20
0000            MXLVK   EQU     MXLVB+20
0000            MULAX   EQU     MXLVK+20
0000            MULBX   EQU     MULAX+20
0000            MULCY   EQU     MULBX+20
0000            MULDY   EQU     MULCY+20
0000            MYLVB   EQU     MULDY+20
0000            MYLVK   EQU     MYLVB+20
0000            MULAY   EQU     MYLVK+20
0000            MULBY   EQU     MULAY+20
0000            MICH    EQU     MULBY+20
0000            MICHY   EQU     MICH+20
0000            CMIY    EQU     MICHY+20
```

Figure D-4 Prom No. 4 Pitch Control Software

```
0000            CMIX    EQU     CMIY+20
0000            NCPOX   EQU     #H3D22
0000            NCPOY   EQU     #H3D24
0000            PRJAX   EQU     #H3D26
0000            PRJBX   EQU     #H3D27
0000            PRJAY   EQU     #H3D28
0000            PRJBY   EQU     #H3D29
0000            PRLAX   EQU     #H3D2A
0000            PRLBX   EQU     #H3D2B
0000            PRLAY   EQU     #H3D2C
0000            PRLBY   EQU     #H3D2D
0000            PVLAX   EQU     #H3D2E
0000            PVLBX   EQU     #H3D2F
0000            PVLAY   EQU     #H3D30
0000            PVLBY   EQU     #H3D31
0000            RINT    EQU     #H3D34
0000            TINT    EQU     #H3D38
0000            X       EQU     #H3D3A
0000            XY      EQU     #H3D3C
0000            XFLAG   EQU     #H3D3E
0000            YFLAG   EQU     #H3D3F
0000            CDELX   EQU     #H3D76
0000            CIX     EQU     #H3D78
0000            USDAO   EQU     #H00EC
0000            PRTA1   EQU     #H0000
0000            PRTB1   EQU     #H0001
0000            PRTC1   EQU     #H0002
0000            PRTA2   EQU     #H0003
0000            PRTB2   EQU     #H00E5
0000            PRTC2   EQU     #H0000
0000            PRTD1   EQU     #H0001
0000            PRTD2   EQU     #H0002
0000            PRTD3   EQU     #H00E6
0C00                    ORG     #HC00
                ;
                ;   SYSTEM COMPENSATION NETWORK
                ;
                ;
0C00 213E3D PITCH:      LXI     H,XFLAG
0C03 7E                 MOV     A,M
0C04 1F                 RAR
0C05 D2000C             JNC     PITCH
0C08 2A2A3D             LHLD    PRLAX
0C0B EB                 XCHG
0C0C 3A273D             LDA     PRJBX
0C0F E610               ANI     #H10
0C11 FE10               CPI     #H10
0C13 C21E0C             JNZ     RA
0C16 3A273D             LDA     PRJBX
0C19 C6E0               ADI     #HE0
```

Figure D-4 Prom No. 4 Pitch Control Software (Continued)

```
INTEL 8080 CROSS ASSEMBLER                    14:48:03   09-MAY-77   PAGE  3

0C1B 32273D           STA     PRJBX
0C1E 2A263D RA:       LHLD    PRJAX
0C21 CDD20D           CALL    MINUS
0C24 19               DAD     D
0C25 EB               XCHG
                ;*******SPECIAL LEAD NETWORK
                ;
                ;   *****************************************
0C26 2A523D           LHLD    #H3D52
0C29 EB               XCHG
0C2A 2AEA3F           LHLD    #H3FEA
0C2D CDDA0D           CALL    SHIFT
0C30 CDD20D           CALL    MINUS
0C33 19               DAD     D
0C34 CDDA0D           CALL    SHIFT
0C37 CDDA0D           CALL    SHIFT
                ;     CALL    MULCX
0C3A 22123D           SHLD    DDOTX
0C3D EB               XCHG
0C3E 7A               MOV     A,D
0C3F 07               RLC
0C40 DA530C           JC      FEE
0C43 21FEFF           LXI     H,#HFFFE
0C46 19               DAD     D
0C47 DA600C           JC      DET
0C4A 210000           LXI     H,0
0C4D 22123D           SHLD    DDOTX
0C50 C3600C           JMP     DET
0C53 210200 FEE:      LXI     H,2
0C56 19               DAD     D
0C57 D2600C           JNC     DET
0C5A 210000           LXI     H,0
0C5D 22123D           SHLD    DDOTX
0C60 3A103D DET:      LDA     DETX
0C63 FE04             CPI     #H04
0C65 F2770C           JP      PDL
0C68 FEFC             CPI     #HFC
0C6A FA720C           JM      MDL
0C6D 3E00             MVI     A,#H00
0C6F C3790C           JMP     ING
0C72 C604   MDL:      ADI     #H04
0C74 C3790C           JMP     ING
0C77 C6FC   PDL:      ADI     #HFC
0C79 5F     ING:      MOV     E,A
0C7A FE00             CPI     #H00
0C7C 3E00             MVI     A,#H00
0C7E F2820C           JP      ZAP
0C81 2F               CMA
0C82 57     ZAP:      MOV     D,A
0C83 CDA43D           CALL    MULDX
```

Figure D-4 Prom No. 4 Pitch Control Software (Continued)

```
0C86 EB                   XCHG
0C87 2A123D               LHLD    DDOTX
0C8A 19                   DAD     D
0C8B EB                   XCHG
0C8C 7A                   MOV     A,D
0C8D 07                   RLC
0C8E DA9B0C               JC      FIVE
0C91 21CCFF               LXI     H,#HFFCC
0C94 19                   DAD     D
0C95 DAA90C               JC      PLMT
0C98 C3A20C               JMP     TWO
0C9B 213400  FIVE:        LXI     H,#H0034
0C9E 19                   DAD     D
0C9F D2B20C               JNC     MLMT
0CA2 EB      TWO:         XCHG
0CA3 22003D               SHLD    CAMAX
0CA6 C3BB0C               JMP     EXIT
0CA9 213400  PLMT:        LXI     H,#H34
0CAC 22003D               SHLD    CAMAX
0CAF C3BB0C               JMP     EXIT
0CB2 21CCFF  MLMT:        LXI     H,#HFFCC
0CB5 22003D               SHLD    CAMAX
0CB8 C3BB0C               JMP     EXIT
             ;
             ;            CAMERA SERVO
             ;
0CBB 3A413D  EXIT:        LDA     CPOBX
0CBE E61F                 ANI     #H1F
0CC0 32413D               STA     CPOBX
0CC3 E610                 ANI     #H10
0CC5 FE10                 CPI     #H10
0CC7 C2D20C               JNZ     WP
0CCA 3A413D               LDA     CPOBX
0CCD C6E0                 ADI     #HE0
0CCF 32413D               STA     CPOBX
0CD2 3A403D  WP:          LDA     CPOAX
0CD5 2F                   CMA
0CD6 6F                   MOV     L,A
0CD7 3A413D               LDA     CPOBX
0CDA 2F                   CMA
0CDB 67                   MOV     H,A
0CDC 23                   INX     H
0CDD 22223D               SHLD    NCPOX
0CE0 EB                   XCHG
0CE1 2A0C3D               LHLD    CPLAX
0CE4 19                   DAD     D
0CE5 22F43F               SHLD    #H3FF4
0CE8 29                   DAD     H
0CE9 29                   DAD     H
0CEA EB                   XCHG
```

Figure D-4 Prom No. 4 Pitch Control Software (Continued)

```
0CEB 2A403D          LHLD    CPOAX
0CEE 220C3D          SHLD    CPLAX
0CF1 7A              MOV     A,D
0CF2 07              RLC
0CF3 D2000D          JNC     OGDR
0CF6 211101          LXI     H,#H111
0CF9 19              DAD     D
0CFA D2100D          JNC     DECR
0CFD C3160D          JMP     MUL
0D00 21EFFE OGDR:    LXI     H,#HFEEF
0D03 19              DAD     D
0D04 DA0A0D          JC      LMAR
0D07 C3160D          JMP     MUL
0D0A 210040 LMAR:    LXI     H,#H4000
0D0D C3190D          JMP     FLTR
0D10 2100C0 DECR:    LXI     H,#HC000
0D13 C3190D          JMP     FLTR
0D16 CDB83D MUL:     CALL    MXLVB
0D19 CDDA0D FLTR:    CALL    SHIFT
0D1C CDDA0D          CALL    SHIFT
0D1F EB              XCHG
0D20 2A843D          LHLD    #H3D84
0D23 19              DAD     D
0D24 EB              XCHG
0D25 22843D          SHLD    #H3D84
0D28 2A863D          LHLD    #H3D86
0D2B CDDA0D          CALL    SHIFT
0D2E 19              DAD     D
0D2F 22863D          SHLD    #H3D86
0D32 22163D          SHLD    DOTIX
0D35 2A003D          LHLD    CAMAX
0D38 EB              XCHG
0D39 2A3A3D          LHLD    X
0D3C 19              DAD     D
0D3D EB              XCHG
0D3E 7A              MOV     A,D
0D3F 07              RLC
0D40 DA4E0D          JC      PAP
0D43 2100F2          LXI     H,#HF200
0D46 19              DAD     D
0D47 DA590D          JC      ONE
0D4A EB              XCHG
0D4B C36E0D          JMP     THRE
0D4E 21100B PAP:     LXI     H,#H0B10
0D51 19              DAD     D
0D52 D2650D          JNC     FOUR
0D55 EB              XCHG
0D56 C36E0D          JMP     THRE
0D59 210000 ONE:     LXI     H,#H0
0D5C 22003D          SHLD    CAMAX
```

165 165

Figure D-4 Prom No. 4 Pitch Control Software (Continued)

```
0D5F 21000E        LXI    H,#H0E00
0D62 C36E0D        JMP    THRE
0D65 210000 FOUR:  LXI    H,0
0D68 22003D        SHLD   CAMAX
0D6B 21F0F4        LXI    H,#HF4F0
0D6E 223A3D THRE:  SHLD   X
0D71 EB            XCHG
0D72 2A223D        LHLD   NCPOX
0D75 29            DAD    H
0D76 29            DAD    H
0D77 19            DAD    D
0D78 29            DAD    H
0D79 29            DAD    H
0D7A 22763D        SHLD   CDELX
0D7D EB            XCHG
0D7E 7A            MOV    A,D
0D7F 07            RLC
0D80 D28D0D        JNC    CLA
0D83 213000        LXI    H,#H30
0D86 19            DAD    D
0D87 D2CB0D        JNC    OUT
0D8A C3940D        JMP    GAIN
0D8D 21D0FF CLA:   LXI    H,#HFFD0
0D90 19            DAD    D
0D91 DACB0D        JC     OUT
0D94 CDBC3E GAIN:  CALL   CMIX
0D97 EB            XCHG
0D98 2A783D        LHLD   CIX
0D9B 19            DAD    D
0D9C 22783D        SHLD   CIX
0D9F EB            XCHG
0DA0 7A            MOV    A,D
0DA1 07            RLC
0DA2 DAAF0D        JC     PA
0DA5 2100C0        LXI    H,#HC000
0DA8 19            DAD    D
0DA9 DAB90D        JC     PB
0DAC C3C40D        JMP    PC
0DAF 210040 PA:    LXI    H,#H4000
0DB2 19            DAD    D
0DB3 D2C00D        JNC    PD
0DB6 C3C40D        JMP    PC
0DB9 210040 PB:    LXI    H,#H4000
0DBC EB            XCHG
0DBD C3C40D        JMP    PC
0DC0 2100C0 PD:    LXI    H,#HC000
0DC3 EB            XCHG
0DC4 2A163D PC:    LHLD   DOTIX
0DC7 19            DAD    D
0DC8 22163D        SHLD   DOTIX
```

Figure D-4 Prom No. 4 Pitch Control Software (Continued)

```
INTEL 8080 CROSS ASSEMBLER                    14:48:32   09-MAY-77   PAGE  7

0DCB 2A763D OUT:      LHLD      CDELX
0DCE EB               XCHG
0DCF C3E60D           JMP    *HDE6
0DD2 7C     MINUS:    MOV       A,H
0DD3 2F               CMA
0DD4 67               MOV       H,A
0DD5 7D               MOV       A,L
0DD6 2F               CMA
0DD7 6F               MOV       L,A
0DD8 23               INX       H
0DD9 C9               RET
0DDA 7C     SHIFT:    MOV       A,H
0DDB 07               RLC
0DDC 7C               MOV       A,H
0DDD 1F               RAR
0DDE 67               MOV       H,A
0DDF 7D               MOV       A,L
0DE0 1F               RAR
0DE1 6F               MOV       L,A
0DE2 C9               RET
0DE3                  END
```

Figure D-4 Prom No. 4 Pitch Control Software (Continued)

```
INTEL 8080 CROSS ASSEMBLER                    14:49:39   09-MAY-77   PAGE  1

                    ;***********
                    ;
                    ;
                    ;
                    ;       SYSTEM EQUATES
                    ;
                    ;
                    ;*************************
                    ;
                    ;
                    ;
 0000               CAMAX   EQU     *H3D00
 0000               EOX     EQU     *H3FEA
 0000               CAMBX   EQU     *H3D01
 0000               CAMAY   EQU     *H3D02
 0000               CAMBY   EQU     *H3D03
 0000               CCMAX   EQU     *H3D46
 0000               CCMAY   EQU     *H3D44
 0000               CPOAX   EQU     *H3D40
 0000               CPOBX   EQU     *H3D41
 0000               CPOAY   EQU     *H3D42
 0000               CPOBY   EQU     *H3D43
 0000               CPLAX   EQU     *H3D0C
 0000               CPLBX   EQU     *H3D0D
 0000               CPLAY   EQU     *H3D0E
 0000               CPLBY   EQU     *H3D0F
 0000               DETX    EQU     *H3D10
 0000               DETY    EQU     *H3D11
 0000               DDOTX   EQU     *H3D12
 0000               DDOTY   EQU     *H3D14
 0000               DOTIX   EQU     *H3D16
 0000               DOTIY   EQU     *H3D18
 0000               IPRJX   EQU     *H3D1A
 0000               IPRJY   EQU     *H3D1C
 0000               IPOSX   EQU     *H3D1E
 0000               IPOSY   EQU     *H3D20
 0000               MULCX   EQU     *H3D90
 0000               MULDX   EQU     MULCX+20
 0000               MXLVB   EQU     MULDX+20
 0000               MXLVK   EQU     MXLVB+20
 0000               MULAX   EQU     MXLVK+20
 0000               MULBX   EQU     MULAX+20
 0000               MULCY   EQU     MULBX+20
 0000               MULDY   EQU     MULCY+20
 0000               MYLVB   EQU     MULDY+20
 0000               MYLVK   EQU     MYLVB+20
 0000               MULAY   EQU     MYLVK+20
 0000               MULBY   EQU     MULAY+20
 0000               MICH    EQU     MULBY+20
 0000               MICHY   EQU     MICH+20
```

Figure D-4 Prom No. 4 Pitch Control Software (Continued)

```
0000            CMIY    EQU   MICHY+20
0000            CMIX    EQU   CMIY+20
0000            TORQY   EQU   CMIX+20
0000            TORQX   EQU   TORQY+20
0000            PTQX    EQU   TORQX+20
0000            NCPOX   EQU   *H3D22
0000            NCPOY   EQU   *H3D24
0000            PRJAX   EQU   *H3D26
0000            PRJBX   EQU   *H3D27
0000            PRJAY   EQU   *H3D28
0000            PRJBY   EQU   *H3D29
0000            PRLAX   EQU   *H3D2A
0000            PRLBX   EQU   *H3D2B
0000            PRLAY   EQU   *H3D2C
0000            PRLBY   EQU   *H3D2D
0000            PVLAX   EQU   *H3D2E
0000            PVLBX   EQU   *H3D2F
0000            PVLAY   EQU   *H3D30
0000            PVLBY   EQU   *H3D31
0000            RINT    EQU   *H3D34
0000            TINT    EQU   *H3D38
0000            X       EQU   *H3D3A
0000            XY      EQU   *H3D3C
0000            XFLAG   EQU   *H3D3E
0000            YFLAG   EQU   *H3D3F
0000            DELTA   EQU   *H3D58
0000            ICHAN   EQU   *H3D60
0000            USDAO   EQU   *H00EC
0000            PRTA1   EQU   *H0000
0000            PRTB1   EQU   *H0001
0000            PRTC1   EQU   *H0002
0000            PRTA2   EQU   *H0003
0000            PRTB2   EQU   *H00E5
0000            PRTC2   EQU   *H0000
0000            PRTD1   EQU   *H0001
0000            PRTD2   EQU   *H0002
0000            PRTD3   EQU   *H00E6
0DE6                    ORG   *HDE6
0DE6 7A                 MOV   A,D
0DE7 07                 RLC
0DE8 DAF50D             JC    MIB
0DEB 2100C0             LXI   H,*HC000
0DEE 19                 DAD   D
0DEF DAFF0D             JC    ALM
0DF2 C30B0E             JMP   XVK
0DF5 210040     MIB:    LXI   H,*H4000
0DF8 19                 DAD   D
0DF9 D2050E             JNC   CDE
0DFC C30D0E             JMP   XVK
0DFF 210040     ALM:    LXI   H,*H4000
```

Figure D-4 Prom No. 4 Pitch Control Software (Continued)

```
0E02 C30E0E          JMP     ETR
0E05 2100C0 CDE:     LXI     H,#HC000
0E08 C30E0E          JMP     ETR
0E0B CDCC3D XVK:     CALL    MXLVK
0E0E EB     ETR:     XCHG
0E0F 2A163D          LHLD    DOTIX
0E12 19              DAD     D
0E13 EB              XCHG
0E14 7A              MOV     A,D
0E15 07              RLC
0E16 DA290E          JC      KAD
0E19 219AF9          LXI     H,#HF99A
0E1C 19              DAD     D
0E1D DA230E          JC      OH
0E20 C3390E          JMP     GOSH
0E23 210040 OH:      LXI     H,#H4000
0E26 C33C0E          JMP     OSH
0E29 216606 KAD:     LXI     H,#H666
0E2C 19              DAD     D
0E2D D2330E          JNC     WOW
0E30 C3390E          JMP     GOSH
0E33 2100C0 WOW:     LXI     H,#HC000
0E36 C33C0E          JMP     OSH
0E39 CDE43E GOSH:    CALL    TORQX
0E3C 22463D OSH:     SHLD    CCMAX
                     ;
                     ;PROJECTOR SERVO
                     ;
                     ;
0E3F CDCE0F          CALL    LAG
0E42 2A2C3D          LHLD    PRJAX
0E45 CD840F          CALL    MINUS
0E48 221A3D          SHLD    IPRJX
0E4B EB              XCHG
0E4C 2A403D          LHLD    CPOAX
0E4F 19              DAD     D
0E50 22583D          SHLD    DELTA
0E53 EB              XCHG
0E54 7A              MOV     A,D
0E55 07              RLC
0E56 D2630E          JNC     OGD
0E59 210040          LXI     H,#H4000
0E5C 19              DAD     D
0E5D D2730E          JNC     DEC
0E60 C3790E          JMP     BX
0E63 2100C0 OGD:     LXI     H,#HC000
0E66 19              DAD     D
0E67 DA6D0E          JC      LMA
0E6A C3790E          JMP     BX
0E6D 210040 LMA:     LXI     H,#H4000
```

Figure D-4 Prom No. 4 Pitch Control Software (Continued)

INTEL 8080 CROSS ASSEMBLER 14:50:16 09-MAY-77 PAGE 4

```
0E70 C37C0E          JMP     IP
0E73 2100C0 DEC:     LXI     H,#HC000
0E76 C37C0E          JMP     IP
0E79 CDF43D BX:      CALL    MULBX
0E7C 221E3D IP:      SHLD    IPOSX
0E7F 2A583D          LHLD    DELTA
0E82 EB              XCHG
0E83 7A              MOV     A,D
0E84 07              RLC
0E85 D2920E          JNC     CLA
0E88 213000          LXI     H,#H30
0E8B 19              DAD     D
0E8C D2D00E          JNC     OUT
0E8F C3990E          JMP     GAIN
0E92 21D0FF CLA:     LXI     H,#HFFD0
0E95 19              DAD     D
0E96 DAD00E          JC      OUT
0E99 CD803E GAIN:    CALL    MICH
0E9C EB              XCHG
0E9D 2A603D          LHLD    ICHAN
0EA0 19              DAD     D
0EA1 22603D          SHLD    ICHAN
0EA4 EB              XCHG
0EA5 7A              MOV     A,D
0EA6 07              RLC
0EA7 DAB40E          JC      PA
0EAA 2100C0          LXI     H,#HC000
0EAD 19              DAD     D
0EAE DABE0E          JC      PB
0EB1 C3C90E          JMP     PC
0EB4 210040 PA:      LXI     H,#H4000
0EB7 19              DAD     D
0EB8 D2C50E          JNC     PD
0EBB C3C90E          JMP     PC
0EBE 210040 PB:      LXI     H,#H4000
0EC1 EB              XCHG
0EC2 C3C90E          JMP     PC
0EC5 2100C0 PD:      LXI     H,#HC000
0EC8 EB              XCHG
0EC9 2A1E3D PC:      LHLD    IPOSX
0ECC 19              DAD     D
0ECD 221E3D          SHLD    IPOSX
0ED0 2A2A3D OUT:     LHLD    PRLAX
0ED3 EB              XCHG
0ED4 2A263D          LHLD    PRJAX
0ED7 222A3D          SHLD    PRLAX
0EDA 2A1A3D          LHLD    IPRJX
0EDD 19              DAD     D
0EDE 22F63F          SHLD    #H3FF6
0EE1 29              DAD     H
```

Figure D-4 Prom No. 4 Pitch Control Software (Continued)

AD-A046 704 MCDONNELL AIRCRAFT CO ST LOUIS MO F/G 17/2
REMOTE VIEWING SYSTEM.(U)
JUN 77 R W FISHER N00014-75-C-0660
UNCLASSIFIED ONR-CR213-129-2F NL

3 OF 3
ADA
046704

END
DATE
FILMED
12-77
DDC

```
0EE2 29              DAD     H
0EE3 29              DAD     H
0EE4 29              DAD     H
0EE5 29              DAD     H
0EE6 EB              XCHG
0EE7 2AEA3F          LHLD    EOX
0EEA 19              DAD     D
0EEB CD7B0F          CALL    SHIFT
0EEE CD7B0F          CALL    SHIFT
0EF1 CD7B0F          CALL    SHIFT
0EF4 EB              XCHG
0EF5 7A              MOV     A,D
0EF6 07              RLC
0EF7 D2040F          JNC     OGDR
0EFA 215515          LXI     H,#H1555
0EFD 19              DAD     D
0EFE D2140F          JNC     DECR
0F01 C31A0F          JMP     BXR
0F04 21ABEA OGDR:    LXI     H,#HEAAB
0F07 19              DAD     D
0F08 DA0E0F          JC      LMAR
0F0B C31A0F          JMP     BXR
0F0E 210040 LMAR:    LXI     H,#H4000
0F11 C31D0F          JMP     IPR
0F14 2100C0 DECR:    LXI     H,#HC000
0F17 C31D0F          JMP     IPR
0F1A CDE03D BXR:     CALL    MULAX
0F1D CD7B0F IPR:     CALL    SHIFT
0F20 CD7B0F          CALL    SHIFT
0F23 EB              XCHG
0F24 2A503D          LHLD    #H3D50
0F27 19              DAD     D
0F28 EB              XCHG
0F29 22503D          SHLD    #H3D50
0F2C 2A523D          LHLD    #H3D52
0F2F CD7B0F          CALL    SHIFT
0F32 19              DAD     D
0F33 22523D          SHLD    #H3D52
0F36 EB              XCHG
0F37 2A1E3D          LHLD    IPOSX
0F3A 19              DAD     D
0F3B EB              XCHG
0F3C 7A              MOV     A,D
0F3D 07              RLC
0F3E D24B0F          JNC     VOGD
0F41 214E00          LXI     H,#H4E
0F44 19              DAD     D
0F45 D25B0F          JNC     VDEC
0F48 C3610F          JMP     VBX
0F4B 21B2FF VOGD:    LXI     H,#HFFB2
```

Figure D-4 Prom No. 4 Pitch Control Software (Continued)

```
0F4E 19                DAD    D
0F4F DA550F            JC     VLMA
0F52 C3610F            JMP    VBX
0F55 210040  VLMA:     LXI    H,#H4000
0F58 C3640F            JMP    VIP
0F5B 2100C0  VDEC:     LXI    H,#HC000
0F5E C3640F            JMP    VIP
0F61 CDF83E  VBX:      CALL   PTQX
0F64 7C      VIP:      MOV    A,H
0F65 0F                RRC
0F66 0F                RRC
0F67 0F                RRC
0F68 0F                RRC
0F69 322F3D            STA    PVLBX
0F6C E6F0              ANI    #HF0
0F6E 67                MOV    H,A
0F6F 7D                MOV    A,L
0F70 0F                RRC
0F71 0F                RRC
0F72 0F                RRC
0F73 0F                RRC
0F74 E60F              ANI    #H0F
0F76 B4                ORA    H
0F77 322E3D            STA    PVLAX
0F7A C9                RET
0F7B 7C      SHIFT:    MOV    A,H
0F7C 07                RLC
0F7D 7C                MOV    A,H
0F7E 1F                RAR
0F7F 67                MOV    H,A
0F80 7D                MOV    A,L
0F81 1F                RAR
0F82 6F                MOV    L,A
0F83 C9                RET
0F84 7C      MINUS:    MOV    A,H
0F85 2F                CMA
0F86 67                MOV    H,A
0F87 7D                MOV    A,L
0F88 2F                CMA
0F89 6F                MOV    L,A
0F8A 23                INX    H
0F8B C9                RET
0F8C 21523D            LXI    H,#H3D52
0F8F 34                INR    M
0F90 7E                MOV    A,M
0F91 FE64              CPI    #H64
0F93 FAB00F            JM     ALED
0F96 FEC8              CPI    #HC8
0F98 FA9E0F            JM     BLED
0F9B 3E00              MVI    A,#H00
```

Figure D-4 Prom No. 4 Pitch Control Software (Continued)

```
0F9D 77                MOV     M,A
0F9E 0654     BLED:    MVI     B,#H54
0FA0 78       SLED:    MOV     A,B
0FA1 CDC00F            CALL    OUTPT
0FA4 3E11              MVI     A,#H11
0FA6 80                ADD     B
0FA7 47                MOV     B,A
0FA8 FEA9              CPI     #HA9
0FAA C2A00F            JNZ     SLED
0FAD C3BF0F            JMP     BOX
0FB0 06A4     ALED:    MVI     B,#HA4
0FB2 78       PLED:    MOV     A,B
0FB3 CDC00F            CALL    OUTPT
0FB6 3E11              MVI     A,#H11
0FB8 80                ADD     B
0FB9 47                MOV     B,A
0FBA FEF9              CPI     #HF9
0FBC C2B20F            JNZ     PLED
0FBF C9       BOX:     RET
0FC0 2F       OUTPT:   CMA
0FC1 D3E8              OUT     #HE8
0FC3 3E3F              MVI     A,#H3F
0FC5 2F                CMA
0FC6 D3EA              OUT     #HEA
0FC8 3EFF              MVI     A,#HFF
0FCA 2F                CMA
0FCB D3EA              OUT     #HEA
0FCD C9                RET
0FCE 2A003D   LAG:     LHLD    CAMAX
0FD1 29                DAD     H
0FD2 29                DAD     H
0FD3 29                DAD     H
0FD4 EB                XCHG
0FD5 2AEA3F            LHLD    EOX
0FD8 CD840F            CALL    MINUS
0FDB 19                DAD     D
0FDC EB                XCHG
0FDD CD0C3F            CALL    #H3F0C
0FE0 CD7B0F            CALL    SHIFT
0FE3 CD7B0F            CALL    SHIFT
0FE6 CD7B0F            CALL    SHIFT
0FE9 CD7B0F            CALL    SHIFT
0FEC CD7B0F            CALL    SHIFT
0FEF CD7B0F            CALL    SHIFT
0FF2 CD7B0F            CALL    SHIFT
0FF5 EB                XCHG
0FF6 2AEA3F            LHLD    EOX
0FF9 19                DAD     D
0FFA 22EA3F            SHLD    EOX
0FFD C9                RET
```

Figure D-4 Prom No. 4 Pitch Control Software (Continued)

```
351  0FFE              END
```

Figure D-4 Prom No. 4 Pitch Control Software (Continued)

INTEL 8080 CROSS ASSEMBLER SYMBOL TABLE

PRLAX= 3D2A	PRLBX= 3D2B	PRLAY= 3D2C	PRLBY= 3D2D
PVLAX= 3D2E	PVLBX= 3D2F	PVLAY= 3D30	PVLBY= 3D31
RINT = 3D34	TINT = 3D38	X = 3D3A	XY = 3D3C
YFLAG= 3D3F	DELTA= 3D58	USDAO= 00EC	PRTA1= 0000
PRTB1= 0001	PRTC1= 0002	PRTA2= 0003	PRTB2= 00E5
PRTC2= 0000	PRTD1= 0001	PRTD2= 0002	PRTD3= 00E6
MIB 0DF5	ALM 0DFF	XVK 0E0B	ETR 0E0E
OH 0E23	WOW 0E33	GOSH 0E39	OSH 0E3C
OGD 0E63	LMA 0E6D	BX 0E79	IP 0E7C
PA 0EB4	PB 0EBE	PD 0EC5	PC 0EC9
OUT 0ED0	OGDR 0F04	LMAR 0F0E	BXR 0F1A
IPR 0F1D	VOGD 0F4B	VLMA 0F55	VDEC 0F5B
VBX 0F61	VIP 0F64	SHIFT 0F7B	A = 0007
MINUS 0F84	SLED 0FA0	B = 0000	PLED 0FB2
BOX 0FBF	C = 0001	OUTPT 0FC0	D = 0002
CDE 0E05	DEC 0E73	E = 0003	KAD 0E29
CLA 0E92	BLED 0F9E	ALED 0FB0	LAG 0FCE
ICHAN= 3D60	GAIN 0E99	DECR 0F14	H = 0004
CAMAX= 3D00	CAMBX= 3D01	CAMAY= 3D02	CAMBY= 3D03
CCMAX= 3D46	CCMAY= 3D44	MICH = 3E80	XFLAG= 3D3E
CPOAX= 3D40	CPLAX= 3D0C	CPLBX= 3D0D	L = 0005
CPOBX= 3D41	CPOAY= 3D42	M = 0006	CPOBY= 3D43
CPLAY= 3D0E	EOX = 3FEA	CPLBY= 3D0F	DETX = 3D10
DETY = 3D11	DDOTX= 3D12	DDOTY= 3D14	DOTIX= 3D16
DOTIY= 3D18	IPRJX= 3D1A	SP = 0006	IPRJY= 3D1C
IPOSX= 3D1E	IPOSY= 3D20	MULCX= 3D90	MULDX= 3DA4
PSW = 0006	MXLVB= 3DB8	MXLVK= 3DCC	MULAX= 3DE0
MULBX= 3DF4	MULCY= 3E08	MULDY= 3E1C	MYLVB= 3E30
MYLVK= 3E44	MULAY= 3E58	MULBY= 3E6C	MICHY= 3E94
CMIY = 3EA8	CMIX = 3EBC	TORQY= 3ED0	TORQX= 3EE4
PTQX = 3EF8	NCPOX= 3D22	NCPOY= 3D24	PRJAX= 3D26
PRJBX= 3D27	PRJAY= 3D28	PRJBY= 3D29	

ERRORS DETECTED: 0

Figure D-4 Prom No. 4 Pitch Control Software (Concluded)

Appendix E

APPLICATION OF THE NIGHT VISION LABORATORY (NVL) THERMAL VIEWING SYSTEM STATIC PERFORMANCE MODEL TO THE RVS

It was suggested that the NVL Thermal Viewing System Static Performance Model, Reference (E-1) be used to evaluate the performance of the Remote Viewing System (RVS). However, repeated attempts to convert the RCS parameters directly to the NVL model have led to the following problem. The radial distortion function of the foveal lens does not lend itself to an MTF analysis as a function of object field angular spatial frequency as called for in the NVL model. All parameters can be converted successfully except for the scan velocity term because a linear raster scan on the lens image plane will create a variable angular velocity and variable direction scan in the object field. This is depicted in Figure E-1. Extreme complexity results when attempts are made to convert spatial into temporal frequency. This is illustrated by the rotation of the f_x bar pattern in the lens image plane shown in Figure E-1. Given enough time, an analysis could be made in a manner compatible with the NVL model. However, the analysis is much simpler if performed, not in object field angular frequency (cycles/milliradian) but in spatial frequency terms (cycles/millimeter). For our purpose of optimizing the RVS lens, it is simpler to work in terms of spatial frequency on the foveal lens focal plane.

This simplicity arises because seven of the nine MTF's are independent of object field angle at this foveal lens focal plane location, and the scan velocity is undirectional and uniform at this location, thereby making easy conversion from spatial to temporal parameters. The only non-linear conversions necessary are simple geometrical ones which translate from focal plane to object field and display space. The advantages of working in the spatial frequency terms will become clear as the analysis is developed. In the following development, the NVL model approach will be used precisely but will be applied in the foveal lens focal plane as a function of linear spatial frequency (cy/mm). Parameters will be covered in the same order as they are in the NVL Report Reference E-1, which describes the model in detail.

E.1 MTF's

Optical MTF The optical MTF's consist of a diffraction MTF and a Gaussian MTF.

(a) Diffraction In angular terms, the diffraction MTF is referenced as Equations (9) and (10) of the NVL report:

$$H_{opt}(f_x, \theta) = \frac{2}{\pi}\left[\cos^{-1} A - A(1 - A^2)^{1/2}\right] \qquad \text{(E-1)}$$

where $$A = \lambda F_{\#} f_x / L(\theta) \qquad \text{(E-2)}$$

where $L(\theta)$ is the equivalent focal length which changes over a 50/1 range as object field angle θ changes. The angle θ is the absolute angle between the point of interest and the lens optical axis. At the foveal lens image plane

$$S_x = \frac{f_\mu}{L(\theta)} \qquad \text{(E-3)}$$

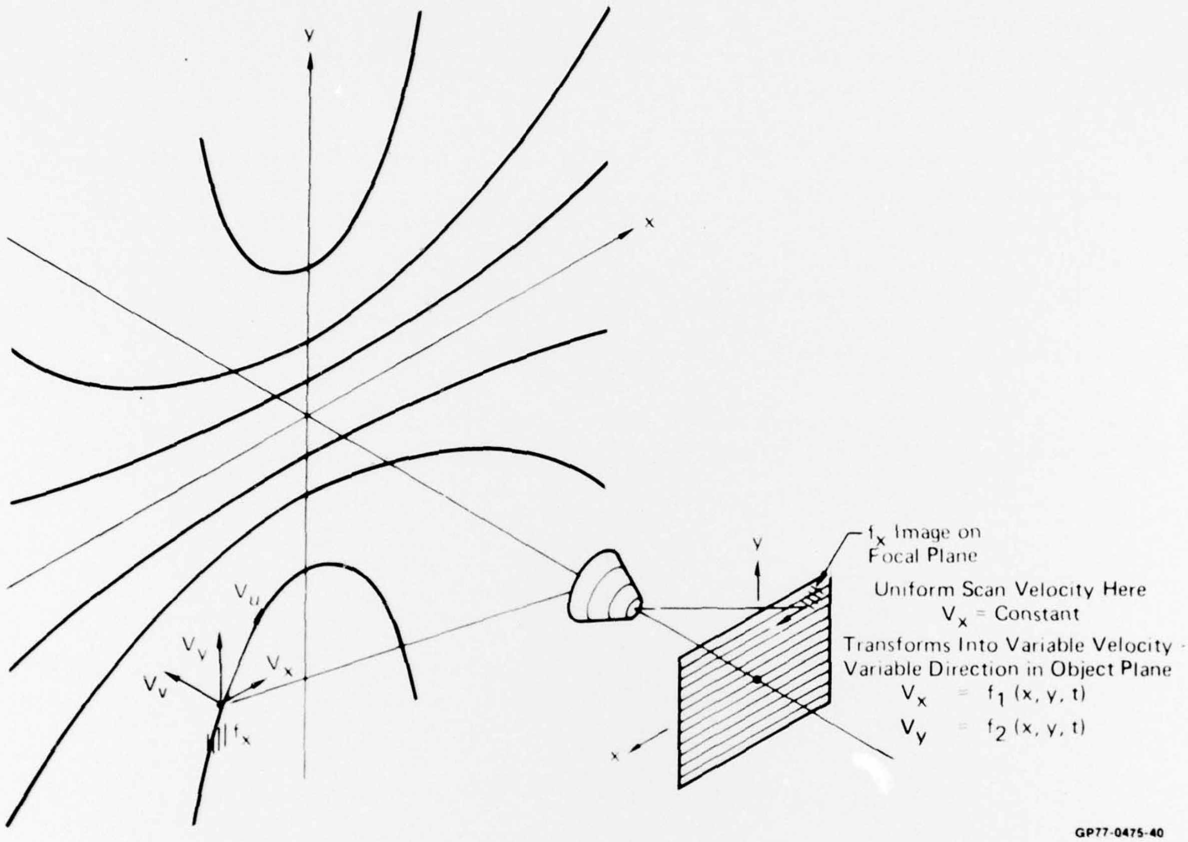

FIGURE E-1
SCAN DISTORTION INTRODUCED BY FOVEAL LENS

where S_x is the image plane spatial frequency and f_μ is its object field angular equivalent measured along the scan line projection in the object field (μ direction on Figure E-1). Solving for f_μ in Equation(E-3) and substituting this for f_x in Equation (E-2).

$$A = \lambda F_{\#} S_x \qquad \text{(E-4)}$$

Since the F/number of our lens is constant, the diffraction MTF is no longer a function of object field angle. Thus we may write $H_{opt}(S_x)$ which indicates that the MTF is a function of the independent variable S_x only. Note, however, that conversion to object field angular spatial frequency is very simple because focal length is constant over small angular increments and may be determined from

$$f_\mu = S_x L(\theta) \tag{E-5}$$

where μ is along the scan line projection in the object field

likewise

$$f_w = S_y L(\theta) \tag{E-6}$$

where w is normal to the scan direction in the object field

(b) Blur - A similar simplicity exists here. The MTF equation with the angular term b of Equation (11) of Reference(E-1) replaced with its equivalent is:

$$H_{blur}(f_x,\theta) = \exp\left[-\frac{2\pi^2\sigma^2}{L(\theta)^2} f_x^{\,2}\right] \tag{E-7}$$

The foveal lens inherently has a constant spatial blur over its entire focal plane, so that the sigma (σ) of Equation(E-7) is a constant. Substituting Equation(E-5) into (E-7) we see the blur MTF simplifies to

$$H_{blur}(S_x) = \exp\left[-2\pi^2\sigma^2 S_x^{\,2}\right] \tag{E-8}$$

Thus this MTF like the diffraction MTF, is no longer a function of object field angle because the focal length variable has been removed.

Detection MTF - The spatial filter MTF of the detector is defined as:

$$H_{Det}(f_x,\theta) = \frac{\sin(\pi f_x \Delta x)}{\pi f_x \Delta x} \triangleq \mathrm{Sinc}(f_x \Delta x) \tag{E-9}$$

It is also complex in our system because the angular projection of the detector into the object field ($\Delta\theta$) in this equation varies with absolute object field angle (θ). Since the detector height is still uniform at the lens focal plane, shown in Figure(E-2) as Δh, Equation(D-9) can be restated as:

$$H_{Det}(S_x) = \frac{\sin(\pi S_x \Delta h_x)}{\pi S_x \Delta h_x} \tag{E-10}$$

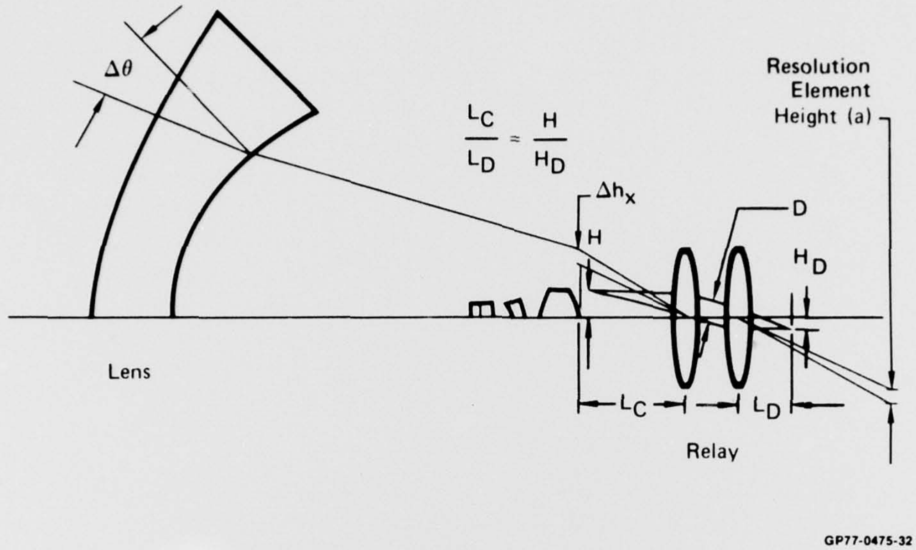

FIGURE E-2
OPTICAL RELAY PARAMETERS

Again the MTF becomes independent of object field angle. Note from Figure(E-2)that the detector height (Δh_x) is a function of detector size(a), detector system focal length (L_D), and relay focal length (L_C), viz:

$$\Delta h_x \simeq a_x \frac{L_C}{L_D} \qquad \text{(E-11)}$$

If the detector characteristics are known, the focal lengths are a function of detector size (Δh) projected unto the image plane as shown in Figure(E-2). Detector size Δh can be computed directly from either the on-axis resolution required, the number of scan lines required across the vertical FOV, or bandwidth/response restrictions and frame rate requirements. The focal lengths, L_C and L_D, are then selected to make the detector dimension appear as the required Δh at the foveal lens focal plane. The detector MTF becomes:

$$H_{Det}(S_x) = \text{Sinc}\ \frac{S_x\ a_x\ L_C}{L_D} \qquad \text{(E-15)}$$

Again this MTF is independent of object field angle.

Detector Electronics MTF - It is in the MTF, the detector electrical response, that we get into real trouble trying to work in object field angular space. For a conventional linear optical system, a linear detector scan velocity converts into a scaled but linear angular scan in the object field. This is not true in our system as was shown in Figure E-1. A linear scan in the x direction on the image plane results in angular velocities in both θ_x and θ_y directions in the angular object field. Both of these angular components are nonlinear functions of both x and y position on the image plane. Thus, converting from spatial frequency to temporal frequency becomes very complex. All of this can be avoided by working in linear spatial plane terms. If the scanner has an angular scan velocity β, then the linear motion of the instantaneous FOV on the foveal lens image is

$$V_x = \beta L_C \quad \text{(E-16)}$$

The conversion to temporal frequency (f) is therefore

$$f = V_x S_x \quad \text{(E-17)}$$

This is a constant conversion and not a function of time. Therefore, all electronic MTF's of the NVL model are valid. These are

$$H'_{Det}(f)$$

$$H_{Elect}(f)$$

$$H_B(f)$$

Display - The RVS display is the inverse of the foveal lens, which results in a conventional linear raster generated on the CRT. The CRT has a constant spot size and the expansion optics has a constant blur at the object focal plane. Again this MTF, if derived in the linear spatial plane, will not be a function of object angle. If the optical blur and CRT spot size are combined and assumed to have a Gaussian MTF, a composite sigma (σ_d) results and the MTF is:

$$H_{Disp}(S_x) = \exp\left[-2\pi^2 (r\sigma_d)^2 S_x{}^2\right] \quad \text{(E-18)}$$

where r is the physical ratio of format sizes; viz

$$r = \frac{H_{LENS\ IMAGE}}{H_{DISPLAY\ CRT}} \quad \text{(E-19)}$$

By contrast, if this were accomplished in the object angular plane, the MTF would be much more complex, viz

$$H_{Disp}(f_x,\theta,M) = \exp\left[-\frac{2\pi^2(r\sigma_d)^2 f_x^{\,2}}{L(\theta)^2 M^2}\right] \tag{E-20}$$

where M is any system angular magnification from object field to the viewer. Again the simplicity is obvious.

Stabilization and Eyeball - The remaining two MTF's are the only two that are not simplified by working in linear spatial rather than angular terms. First, stabilization tends to be angular input to the system. Using the MTF from the NVL report:

$$H_{Los}(f_x) = \exp\,(-Pf_x^{\,2}) \tag{E-21}$$

Converting to the foveal lens image plane results in

$$H_{Los}(S_x,\theta) - \exp\left[-PS_x^{\,2}L(\theta)^2\right] \tag{E-22}$$

Similarly, the eye views the display in angular terms. The NVL MTF is

$$H_{Eye}(f_x) = \exp\left[-\frac{\Gamma f_x}{M}\right] \tag{E-23}$$

Equation(E-23) must be converted to the foveal lens image plane

$$H_{Eye}(S_x,\theta) = \exp\left[-\frac{\Gamma S_x L(\theta)}{M}\right] \tag{E-24}$$

In conclusion, seven MTF's have been simplified at the expense of two that have been made slightly more complex by the conversion to linear spatial frequency.

E.2 NOISE EQUIVALENT MODULATION (NEM)

For visual spectrum applications noise equivalent modulation must replace NEΔT in the NVL model. In the visual model, the primary noise source is the detector which is a silicon vidicon. Its NEM was extracted from data of Reference (E-2). These data show vidicon S/N as a function of faceplate illumination for a specific bandwidth. The basic function is approximately

$$\frac{\text{peak-to-peak signal}}{\text{noise (rms)}} = 100\ E \tag{E-21}$$

where E is faceplate illumination in LUX. The noise equivalent signal is (signal input that just equal noise)

$$NEM = \frac{noise}{signal} = \frac{1}{100E} \qquad \text{(E-22)}$$

assuming that the noise is proportional to the square root of the bandwidth (Δf) of $4(10^8)$ Hz. For data given:

$$NEM = \frac{\Delta f}{100E\sqrt{4X\ 10^6}} = 5\ X\ 10^{-6}\frac{\sqrt{\Delta f}}{E}\ \text{(E in LUX)} \qquad \text{(E-23)}$$

For E in footcandles:

$$NEM = \frac{4.64 \times 10^{-7}\ \sqrt{\Delta f}}{E}\ \text{(E in Foot-Candles)} \qquad \text{(E-24)}$$

The faceplate illumination can be calculated from system geometry as follows:

$$E_f = \frac{BT_aT_o}{4\ F^2_{No}} \qquad \text{(E-25)}$$

Where

B=Scene brightness in footlamberts

T_a= Atmospheric transmission

T_a= Optical transmission within sensor

F_{no}= The equivalent F/number or F/number actually supplying the vidicon. This is the lens F/number modified by the relay and from basic geometrical optical theory is:

$$F_{noe} = F_{no}\frac{L_D}{L_c} \qquad \text{(E-26)}$$

If the sensor employs an automatic light level control which operates on vidicon target current, E will be accurately maintained. Therefore, Equation (E-24) applies as written for the level of E which is preset. For the silicon vidon under study, best performance is obtained when the level is about 0.1 lumens/ft^2. Equation(E-23)then becomes:

$$NEM = 4.64\ X\ 10^{-6}\ \sqrt{\Delta f} \qquad \text{(E-27)}$$

E.3 MRM CALCULATIONS

The following MRM equation modifications are required so that the computation may be performed in linear spatial frequency terms. First, in the NVL MRT equation, Δy must be replaced by the apparent detector size at the foveal lens image plane, i.e., it must be the Δh defined on Figure E-2. As previously demonstrated in Equation (E-11).

$$\Delta h_y = a_y \frac{L_C}{L_D} \qquad \text{(E-28)}$$

Also, in the MRM equation, it is best to compute the Q integral in terms of temporal frequency. This eliminates the velocity term in the MRT equation and makes the Q integral easier to compute. The Q integral is therefore

$$Q(f,\theta) = \int_o^\infty \frac{S(f)}{S(f_o)} H_N^2(f) H_w\left(\frac{f}{V_x}\right)^2 H_{Eye}\left(\frac{f}{V_x}\right) df \qquad \text{(E-29)}$$

Of these terms, only H_w, the transfer function for a rectangular bar of width w, has not been defined. This transfer function is in linear rather than angular dimensions, i.e.,

$$H_w\left(\frac{f_x}{V_x}\right) = \text{Sinc } W\left(\frac{f_x}{V_x}\right) = \text{Sinc } \left(WS_x\right) \qquad \text{(E-30)}$$

where

$$W \triangleq \frac{1}{2S_x} \qquad \text{(E-31)}$$

The MRM equation written to show the dependency of two variables is

$$MRM(S_x,\theta) = \frac{SNR\pi^2 NEM}{4\sqrt{14}\ MTF_{TOTAL}(S_x,\theta)} \left[\frac{\Delta h_y\ S_x Q(f,\theta)}{\Delta f_N F_R\ t_e\ \eta_{OVSC}}\right]^{1/2} \qquad \text{(E-32)}$$

This equation results in an MRT very weakly dependent on θ. To obtain the MRM for any field angle θ, we convert the spatial frequency term S_x into an angular frequency term by using Equation(E-9) containing the focal length function:

$$f_\mu = S_x L(\theta)$$

Note this will be the angular spatial frequency in the scan direction (target bars normal to the scan direction). It could be related to f_x and f_y but this does not appear to be required at this point.

E.4 CONCLUSIONS

To conclude this effort, a block diagram of the NVL model converted to the VARVS Concept in the visual spectrum is shown in Figure E-3. This model was used in the study to compute Minimum Resolvable Modulation to predict performance.

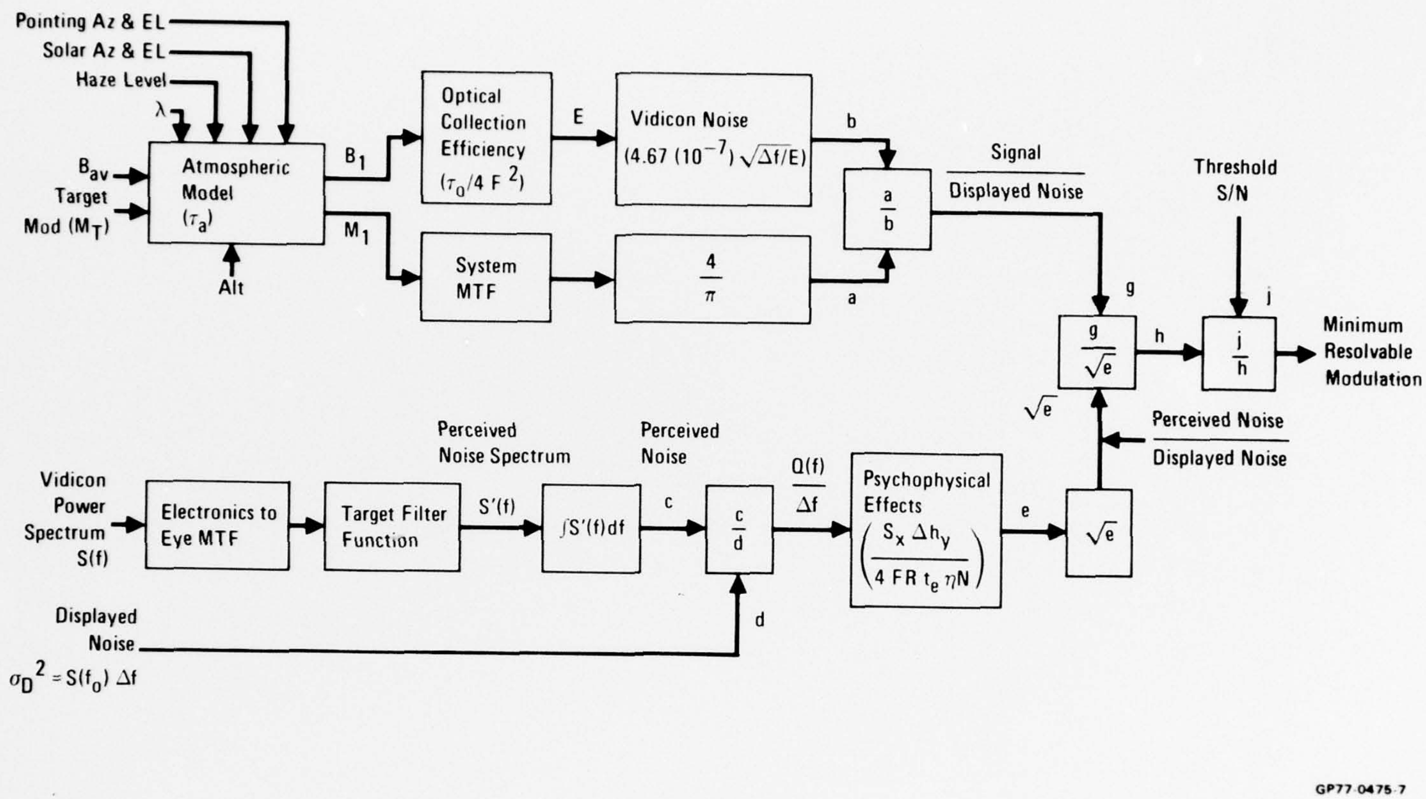

FIGURE E-3
NVL MODEL ADAPTED TO VARVS
FOR VISUAL SPECTRUM

APPENDIX

LIST OF REFERENCES

C-1 Klaiber, R.J., Physical and Optical Properties of Projection Screens; Technical Report NAVTRADEVCEN IH-63, December 1966

C-2 Single Crystal Ferroelectronics and Their Application in Light Valve Display Devices; Proceedings of the IEEE Vol. 61, No. 7, July 1973

E-1 Ratches, James, et al, Night Vision Laboratory Static Performance Model For Thermal Viewing Systems, Army Electronics Cmd., Fort Monmouth, N.J., Report No. 7043, April 1975.

E-2 RCA, Inc., 4532A Camera Tube Specification Sheet RCA Corp., Harrison, N.J., Jan. 1973

DISTRIBUTION LIST

Chief of Naval Research 800 North Quincy Street Arlington, VA 22217 ATTN: Code 221	10
455	1
421	1
Defense Documentation Center Cameron Station Alexandria, VA 23314	12
Naval Research Laboratory Washington, DC 20375 ATTN: Tech Info Division Library, Code 2039	1
Office of Naval Research Branch Office New York Area Office 715 Broadway (5th Floor) New York, NY 10003	1
Office of Naval Research Branch Office 1030 East Green Street Pasadena, CA 91106	1
Office of Naval Research Branch Office 495 Summer Street Boston, MA 02210	1
Office of Naval Research Branch Office 536 Clark Street Chicago, IL 60605	1
Director of Defense Research and Engineering Washington, DC 20350 ATTN: ODDR&E/E&PS	1
ODDR&E/E&LS	1
Chief of Naval Operations Washington, DC 20350 ATTN: OP 987	1
OP 986	1
OP 982	1
OP 596	1
OP 506	1
Naval Material Command Washington, DC 20360 ATTN: MAT 08T231	1
Headquarters, U.S. Marine Corps Washington, DC 20380 ATTN: RD-1	1
Naval Air Systems Command Washington, DC 20360 ATTN: AIR 5103F	1
5105	1
340D	1
340F	1
360E	1
PMA 247	1
Naval Sea Systems Command Washington, DC 20360 ATTN: NSEA 0341	1
NSEA 653C	1
Naval Electronic Systems Command Washington, DC 20360 ATTN: ELEX 320	1
330	1
U.S. Naval Air Development Center Warminster, PA 18974 ATTN: Code 402	1
304	1
54P3	1
30P8	3
6011	1
Naval Ocean Systems Center 271 Catalina Boulevard San Diego, CA 92152 ATTN: Code 8235	1
Naval Weapons Center China Lake, CA 93555 ATTN: Code 3925	1
Code 3175	1
Naval Weapons Center Dahlgren, VA 22448 ATTN: Mr. K. Ferris	3

Naval Training Equipment
Orlando, FL 32813
ATTN: Code N-2224 1

Naval Air Test Center
Service Test Division
Aero Medical Branch
Patuxent River, MD 20670
ATTN: Mr. Fred Hoerner 1

Naval Avionics Facility
6000 E. 21st Street
Indianapolis, IN 46218
ATTN: Technical Library 1

Dean of Research Administration
Naval Postgraduate School
Monterey, CA 93940
ATTN: Dr. J. Powers 1

U.S. Coast Guard Headquarters
400 7th Street, NW
Washington, DC 20591
ATTN: GDST/62 TRPT 1

HQS Army Research Institute
1300 Wilson Boulevard
Arlington, VA 22209 1

Headquarters U.S. Army
Washington, DC 20350
ATTN: DAMA-WSA 1
DAMA-ZE 1
DAMA-WSM 1
DAMA-ARZ 1

U.S. Army Avionics Laboratory
U.S. Army R&D Command
Fort Monmouth, NJ 07703
ATTN: DAVAA-F (Mr. Respass) 2
DAVAA-E (Mr. Gurman) 1

U.S. Army Material Command
Washington, DC 20315
ATTN: DRCDR-HA 1
DRCPM-AAH 1
DRCPM-GCM-WF 1

U.S. Army Night Vision Lab
Fort Belvoir, VA 22060
ATTN: DRSEL-NV-SD 1

U.S. Army Research and Development Command
P.O. Box 209
St. Louis, MO 63166
ATTN: DRSAV-EV 1

U.S. Army Aviation Center
Ft. Rucker, AL 36362
ATTN: ATQZ-D-SGA 1

Human Engineering Labs
Aberdeen Proving Grounds, MD 21105
ATTN: DRXRD-HEL 1

Headquarters Aeronautical Systems Division
Air Force Systems Command
Wright-Patterson AFB, OH 45433
ATTN: AFAL/AA 1
AFAL/CC 1
AFAL/RWI 1

Air Force Flight Dynamics Laboratory
Air Force Systems Command
Wright-Patterson AFB, OH 45433
ATTN: AFFDL/FG 1

Aero Medical Research Laboratory
Wright-Patterson AFB, OH 45433
ATTN; AMRL/HE 1

Air Force Office of Scientific Research
4100 Wilson Boulevard
Arlington, VA 22209 1

Federal Aviation Agency
NAFEC Bldg. 10
Atlantic City, NJ 03405
ATTN: Mr. D. Elliott 1

Headquarters Aeronautical Systems Division
Air Force Systems Command
Wright-Patterson AFB, OH 45433
ATTN: ASD/YRD 1
ASD/SD 1

Defense Advanced Research
Project Agency
1400 Wilson Blvd.
Arlington, VA 22209
ATTN: Dr. Strom 1

National Aeronautical and
Space Administration
Langly Research Center
Mail Stop 1574
Hampton, VA 23665
ATTN: Mr. R. Morris 1

National Aeronautical and
Space Administration
Ames Research Center
Mail Stop 200-10
Moffett Field, CA 94035
ATTN: Mr. J. Dusterberry 1

Institute for Defense Analysis
400 Army-Navy Drive
Arlington, VA 22204
ATTN: Mr. L. Biberman 1
Dr. A. Schnitzler 1